Ege-Serpkenci, Deniz

ELECTROCHEMISTRY OF METHYLATED PTERINS: I. ELECTROCHEMICAL OXIDATION OF 6,7-DIMETHYLTETRA HYDROPTERIN. II. ELECTROCHEMICAL OXIDATION OF 2-DIMETHYLAMINO-3,6,7-TRIMETHYL TETRAHYDROPTERIN. III. COMPARISON OF ELECTROCHEMICAL AND SPECTROELECTROCHEMICAL BEHAVIOR OF VARIOUS METHYLATED PTERINS

The University of Oklahoma PH.D. 1982

PLEASE NOTE:

In all cases this material has been filmed in the best possible way from the available copy. Problems encountered with this document have been identified here with a check mark __√__.

1. Glossy photographs or pages _____
2. Colored illustrations, paper or print _____
3. Photographs with dark background _____
4. Illustrations are poor copy _____
5. Pages with black marks, not original copy _____
6. Print shows through as there is text on both sides of page _____
7. Indistinct, broken or small print on several pages _____
8. Print exceeds margin requirements _____
9. Tightly bound copy with print lost in spine _____
10. Computer printout pages with indistinct print _____
11. Page(s) _____ lacking when material received, and not available from school or author.
12. Page(s) __287__ seem to be missing in numbering only as text follows.
13. Two pages numbered __286__. Text follows.
14. Curling and wrinkled pages _____
15. Other _____

THE UNIVERSITY OF OKLAHOMA

GRADUATE COLLEGE

ELECTROCHEMISTRY OF METHYLATED PTERINS

I. ELECTROCHEMICAL OXIDATION OF 6,7-DIMETHYLTETRAHYDROPTERIN

II. ELECTROCHEMICAL OXIDATION OF 2-DIMETHYLAMINO-3,6,7-TRIMETHYL-TETRAHYDROPTERIN

III. COMPARISON OF ELECTROCHEMICAL AND SPECTROELECTROCHEMICAL BEHAVIOR OF VARIOUS METHYLATED PTERINS

A DISSERTATION

SUBMITTED TO THE GRADUATE FACULTY

in partial fulfillment of the requirements for the degree of

DOCTOR OF PHILOSOPHY

By

DENIZ EGE-SERPKENCI

Norman, Oklahoma

1982

ELECTROCHEMISTRY OF METHYLATED PTERINS

I. ELECTROCHEMICAL OXIDATION OF 6,7-DIMETHYLTETRAHYDROPTERIN

II. ELECTROCHEMICAL OXIDATION OF 2-DIMETHYLAMINO-3,6,7-TRIMETHYL-TETRAHYDROPTERIN

III. COMPARISON OF ELECTROCHEMICAL AND SPECTROELECTROCHEMICAL BEHAVIOR OF VARIOUS METHYLATED PTERINS

APPROVED BY

DISSERTATION COMMITTEE

ACKNOWLEDGEMENTS

I would like to express my gratitude to Dr. Glenn Dryhurst who suggested these interesting and challenging research problems, for his guidance and support during the course of study.

Financial assistance in the form of research assistantships from Dr. Glenn Dryhurst and teaching assistantships from the Chemistry Department of the University of Oklahoma is greatly acknowledged.

The author would also like to thank Dr. John Carden and Dr. Hadi Ozbal for initiating interest in graduate research in analytical chemistry. Early days in graduate school were made much easier with the help and friendship of Mike Cleary, Henry Marsh and Arnold Conway.

I would like to acknowledge Dr. Raghavan Rajagopalan who has synthesized three of the methylated pterins and let me use his results obtained from 2-dimethylamino-6,7,8-trimethylpterin.

Correspondence and discussions with Dr. Wolfgang Pfleiderer have been very useful for the progress made in this work.

Dr. and Mrs. E. R. Cunningham deserve special thanks

for their love and support, especially in the early days of graduate school.

It is not possible to adequately thank my parents for their love, encouragement and support throughout my education.

I would also like to thank Ms. Nancy Burnett for the beautiful typing of this manuscript.

Without the love, understanding and moral support of my husband, Ray Resit, it would have been difficult to complete this work.

TABLE OF CONTENTS

TABLE OF CONTENTS (continued)

LIST OF TABLES

List of Tables (continued)

List of Tables (continued)

List of Tables (continued)

LIST OF ILLUSTRATIONS

List of Illustrations (continued)

List of Illustrations (continued)

List of Illustrations (continued)

List of Illustrations (continued)

List of Illustrations (continued)

List of Illustrations (continued)

List of Illustrations (continued)

List of Illustrations (continued)

List of Illustrations (continued)

Figure Page

List of Illustrations (continued)

ELECTROCHEMISTRY OF METHYLATED PTERINS

CHAPTER 1

INTRODUCTION

Pteridines (1) are formed by fusing a pyrazine ring with a pyrimidine ring. A large number of pteridines may be found in plants and animals as well as microorganisms but only in trace amounts. These heterocyclic compounds usually have highly fluorescent properties. Pteridines which have a (2)-amino- and a (4)-oxo-substituent are called pterins (2).

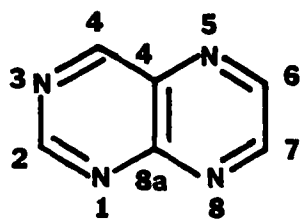

1

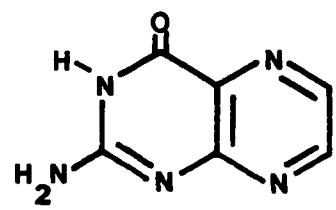

2

The history of pteridines started in 1889, when Hopkins[1] found a group of natural pigments present in butterfly wings. In the next fifteen years Wieland, Schöpf and coworkers[2-4] investigated the pteridine chemistry involved

in butterfly wings. A climax in these investigations was reached when Purrman[1] determined the chemical structures of three of the most common butterfly pigments: leucopterin (3), xanthopterin (4), and isoxanthopterin (5).

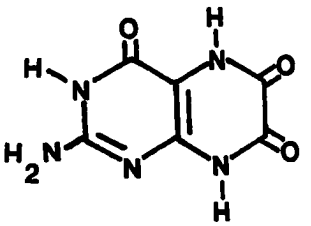

3

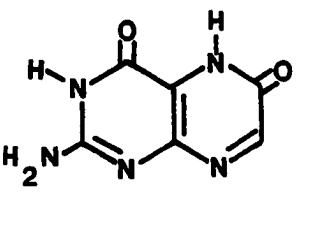

4

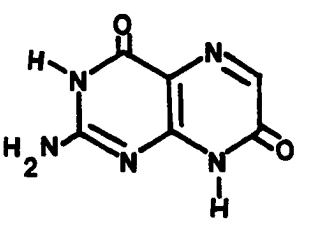

5

Naturally occurring pteridines can be recognized directly as pigments in the wings of insects and in the eyes and skin of fish, amphibia and reptiles.[5] Potentially productive isolation, purification and identification of pteridines from natural sources are limited by the small quantities of material available. Nevertheless, over the years methods for isolation, purification and separation of pteridines have improved. Initial studies for the characterization of pteridines involved paper[6] and thin-layer chromatography.[7,8] Later, ion exchange[9] and high-pressure liquid chromatography (HPLC)[10-12] were applied to analyze pteridine samples. Several powerful methods have been developed for the determination and separation of unconjugated pteridines occurring in biological fluids and tissue

culture media.[13-19] The most effective and convenient method for analysis of biological samples proves to be HPLC employing a cation exchange or a reverse phase column with fluorescence detection.[14,16,19]

^{3}H, ^{13}C and ^{15}N nuclear magnetic resonance spectra of several pteridines have been studied by Schwotzer et al.[20] Mass spectra of pteridines have also been reported.[21-24] Gas chromatography coupled to mass spectrometry (GC-MS) results in successful separation and identification of pteridines.[25,26]

One of the first pteridines isolated from mammalian sources was a fluorescent, yellow pterin which was found in human urine by Koschara in 1936.[27] Later Koschara determined the molecular formula of this compound and named it urethione (6). The structure of urethione has been determined by Tschesche.[28]

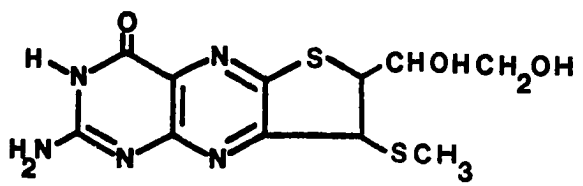

6

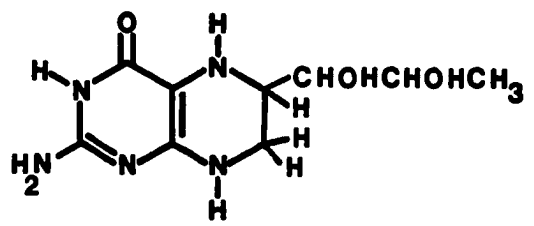

7

In 1963 Kaufman[29] observed that tetrahydrobiopterin (THBP) (7) is the natural cofactor for phenylalanine hydroxylase in the hydroxylation reaction of phenylalanine to tyrosine. It is suspected that other enzymes that utilize molecular oxygen to introduce a hydroxyl group into amino acids such as tyrosine and tryptophan also require THBP as the natural cofactor.[30-32]

Disorders of tryptophan metabolism may play an important role in affective disturbances, for example, mania, endogenous depression, schizophrenia and neurological diseases.[33] The enzymic hydroxylation of tyrosine and tryptophan represent the rate-limiting steps in the biosynthesis of catecholamines (norepinephrine and dopamine) and the indoleamine serotonin, respectively, in the central nervous system.

Kaufman[13] has shown that a deficiency in THBP will cause hyperphenylalaninemia, a varient form of phenylketonuria (PKU) which may lead to mental retardation. Hyperphenylalaninemia may be caused by absent or deficient dihydropteridine reductase activity or deficient THBP synthesis. Classical PKU is due to a deficiency in phenylalanine hydroxylase and patients with PKU may be treated by a low phenylalanine diet. Hyperphenylalaninemia patients show neurological deterioration in spite of dietary control of the elevated blood phenylalanine levels. Therefore, early diagnosis of the cause of hyperphenylalaninemia is important

to ensure correct treatment. Assessment of pterins in biological samples is a rapid method for recognition of the variants of hyperphenylalaninemia.[18] In recent years a considerable amount of emphasis has been put on the analysis of pterins in biological samples.[13-19]

Elevated levels of pteridines may be found in tissue of cancer patients, as well as in the urine of mice carrying tumors.[14]

Tetrahydropterins are also involved in hydroxylation of steroids and in the formation of melanin.[1] It has also been shown that enzymic oxidation of glyceryl ethers in the liver requires a tetrahydropterin substituted at the C(6) position.[33]

Tetrahydrofolic acid (8) is recognized to be part of the vitamin B complex[34] and is essential for the growth of many organisms.

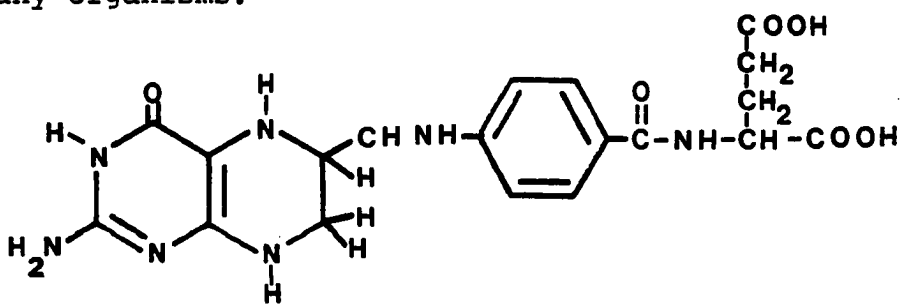

8

Folic acid occurs as its dihydro derivative in nature and its function is to insert a carbon atom wherever needed during biosynthesis. Dihydro folic acid is reduced to tetrahydrofolic acid by the enzyme dihydrofolate reductase which is

then united with an appropriate one-carbon fragment. This fragment is then inserted into the molecule undergoing biosynthesis.[1]

Methotrexate (9), introduced into the clinic in 1958, has proved to be an excellent and reliable drug in the treatment of certain forms of cancer. Methotrexate, alone or in combination with other inhibitors of deoxyribonucleic acid (DNA) synthesis, provides the standard treatment for the leukemia of young adults.[1]

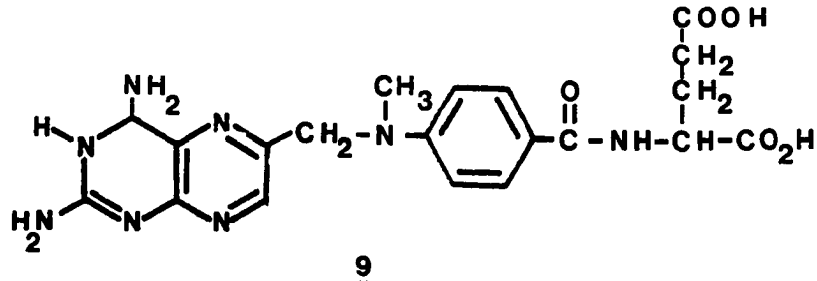

9

Formyl-N-tetrahydrofolic acid (10) is important as a carrier of a formate unit which is utilized in the biosynthesis of purines and other biologically important molecules.[35]

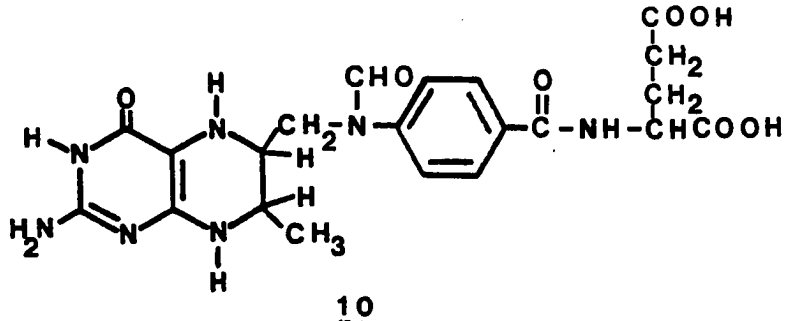

10

Because of their unusual redox properties and very wide distribution in nature various pteridines have been proposed to be involved in cellular electron transport [36,37] and as one electron acceptors in the photosynthetic apparatus of plants.[38,39]

There have been several schemes proposed for the cofactor function of THBP in enzymic hydroxylation reactions.[40] The scheme, initially proposed by Kaufman[29,43,44] (Fig. 1) was quite generally accepted until recently. According to Kaufman's first scheme phenylalanine is oxidized in the presence of phenylalanine hydroxylase and oxygen to tyrosine. Coupled to this reaction is the oxidation of the THBP cofactor to a quinonoid-dihydro form. A second enzyme, dihydropterin reductase catalyzes the reduction of the quinonoid-dihydropterin back to the tetrahydro level using the reduced form of nicotinamide adenine dinucleotide (NADH) as the reductant. But in this scheme, there is clearly no detailed explanation for how O_2 is involved in the overall process. Following his observation of a transient intermediate (λ_{max} 250 nm and 290 nm) during hydroxylation of phenylalanine at pH 8-8.2 in the presence of low concentration of THBP and high hydroxylase concentrations Kaufman proposed that the active hydroxylating agent is a hydroperoxide (Fig. 2).[45-47]

Mager and Berends[48,49] have proposed an autooxidation scheme which involves a 8-a-hydroperoxide intermediate rather than the 4a-hydroperoxide proposed by Kaufman for the bio-

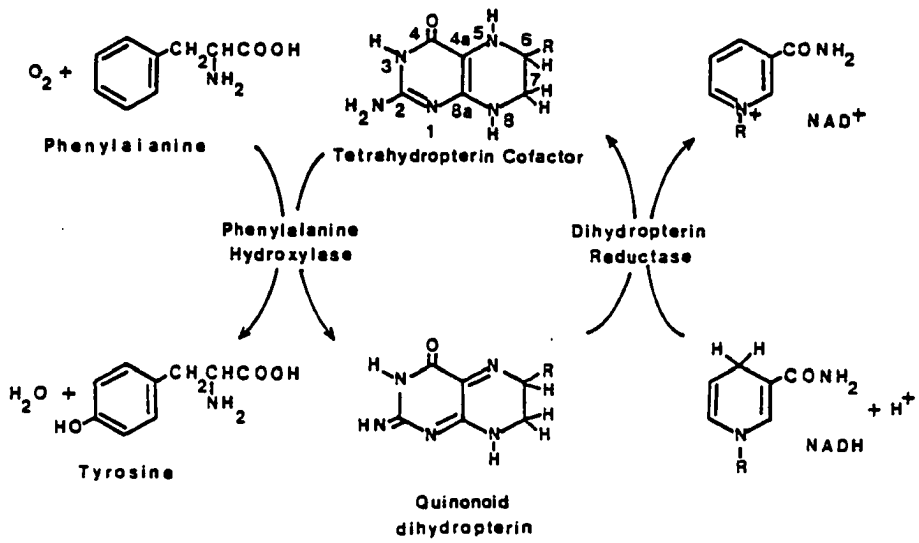

Figure 1. Initial scheme proposed by Kaufman for the hydroxylation of phenylalanine.

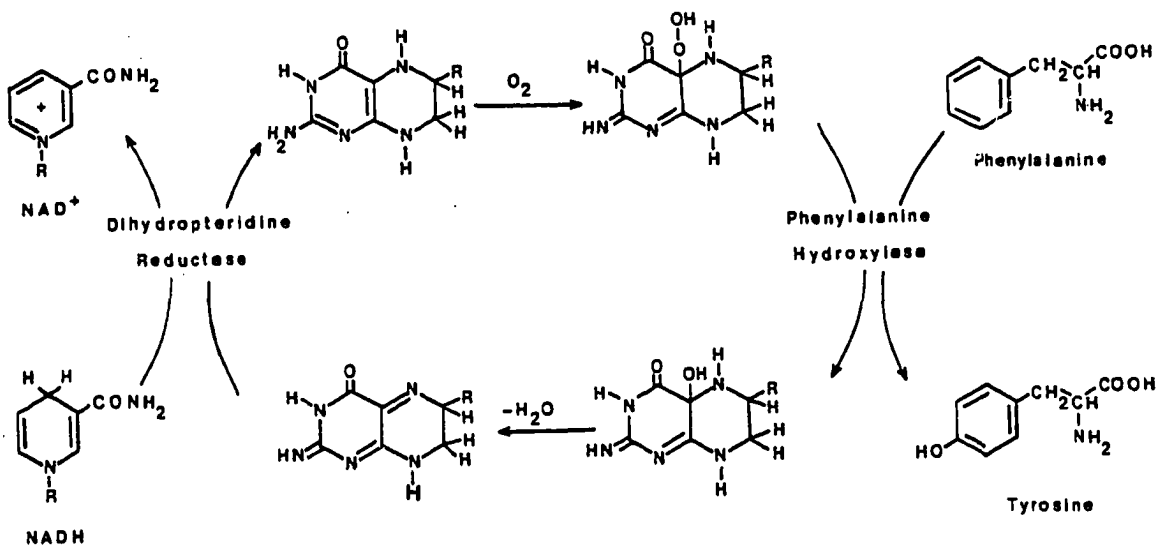

Figure 2. Scheme proposed by Kaufman explaining how O_2 is involved in the hydroxylation of phenylalanine.

logical oxidation.

Pearson and coworkers have been unable to detect the presence of any hydroperoxides formed during the oxidation of THBP by molecular oxygen.[50-53] Woolf et al. suggested that phenylalanine was attacked by a peroxide of the THBP during the hydroxylation reaction.[54] In another recent study it was shown that $O_2^{-\bullet}$ plays an important role in the overall process of THBP oxidation by O_2.[55] Hamilton has proposed that an oxenoid reagent is created by addition of oxygen to C(4a) of THBP followed by a cleavage of the C(4a)-N(5) bond[40] (Fig. 3).

Two pyrimidine cofactors for phenylalanine hydroxylase, 2,5,6-triamino-4-pyrimidone and 5-benzylamino-2,6-diamino-4-pyrimidone were shown to be permanently cleaved into two fragments, an oxidized pyrimidine and an amine, by the substrate-dependent action of the enzyme.[40] The scission of the pyrimidine bond, equivalent to the C(4a)-N(5) bond of the natural cofactor THBP, supports ring cleavage as a mechanism for oxygen activation by the THBP-dependent aromatic amino acid hydroxylases[40] (Fig. 4).

A number of reports have suggested that a radical intermediate is formed during the chemical oxidation of THBP.[36,39,41,42] Also, a radical similar to that observed in chemical oxidation reactions of THBP was detected by a photoinduced reaction with chlorophyl II_a.[38]

A number of tetrahydropterins, other than THBP may

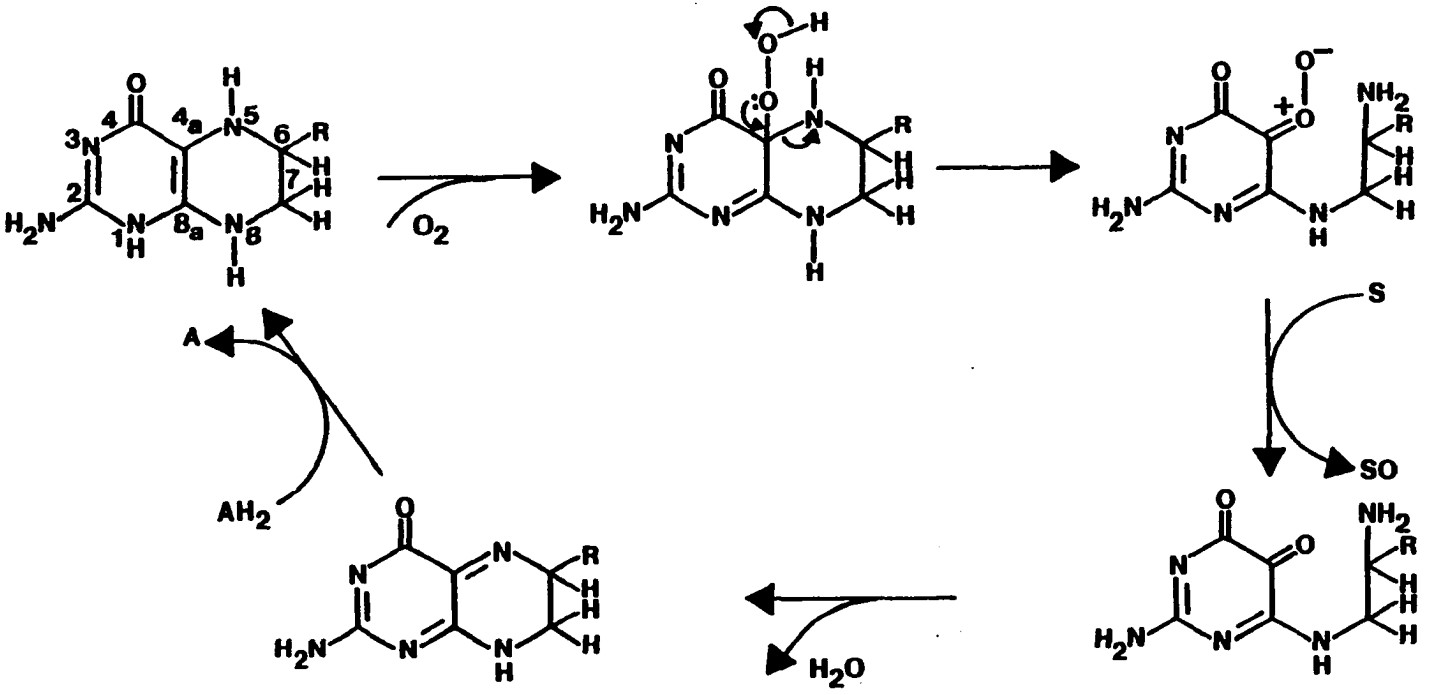

Figure 3. Hamilton's scheme for enzymic hydroxylation of phenylalanine.

S = substrate

SO = oxidized (hydroxylated) substrate

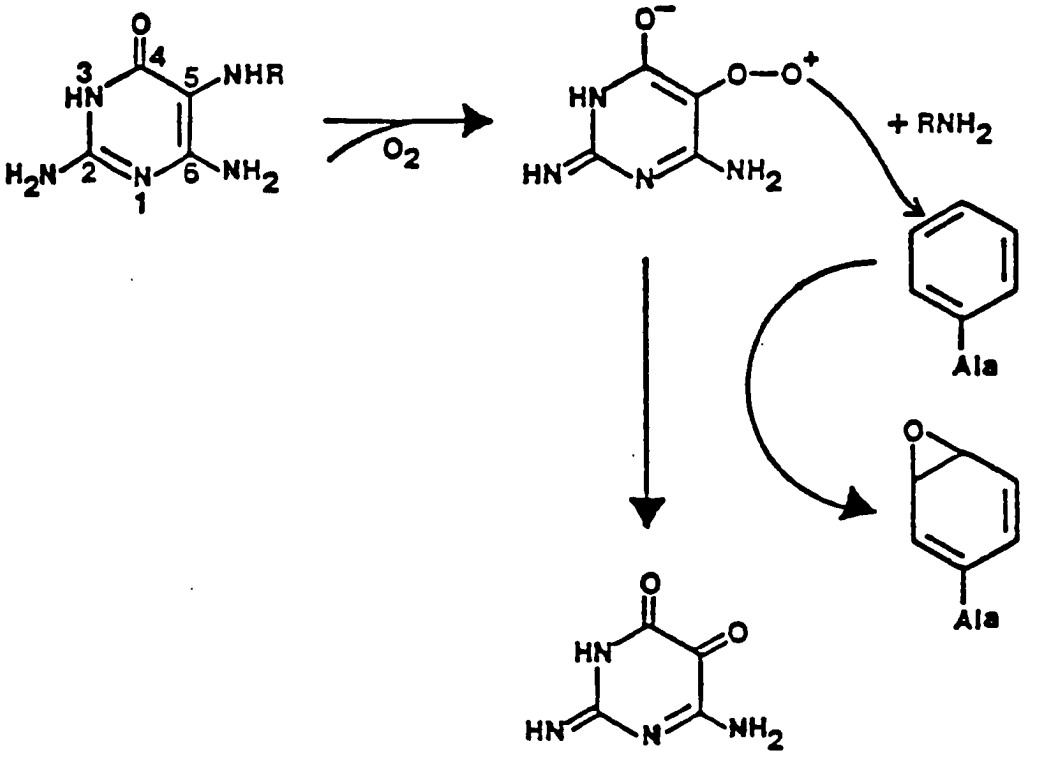

Figure 4. Bailey-Ayling scheme to account for the cofactor properties of pyrimidines.

Ala = alanine

function as a cofactor for phenylalanine hydroxylase and other hydroxylating enzymes. Non-reduced pteridines have no activity.[56] A 2-amino group or possibly a similar electron donor is essential for cofactor activity.

A keto or an amino group at C(4) position produces an equally effective cofactor.[56] Pteridines with a keto group at C(2) are inactive.[56,57] Alkylation of the 2-amino group or N(8) leads to a severe or total loss in cofactor activity. 2-Methylamino-4-hydroxy-6,7-dimethyltetrahydropteridine (11) has only one-third of the cofactor activity of THBP.

Tetrahydrofolate was found to be highly active in replacing the natural cofactor. Anhydroleucoverin (5,10-formyltetrahydrofolate) showed slight activity. Folic acid, leucovorin and pteroic acid were completely inactive.[57]

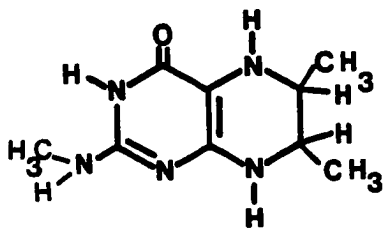

11

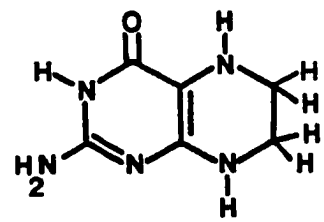

12

Although the unsubstituted compound 5,6,7,8-tetrahydropterin (THP (12)) has some cofactor activity. alkylation of either the C(6) or C(7) greatly enhances the cofactor activity. For example, among the so-called pseudo cofactors

6-methyl-5,6,7,8-tetrahydropterin (6-MTHP) has the highest activity, followed by 6,7-dimethyl-5,6,7,8-tetrahydropterin (6,7-DMTHP), 7-methyl-5,6,7,8-tetrahydropterin (7-MTHP) and THP in decreasing order of cofactor activity.

Either diasteroisomer of THBP is active with identical K_m values although the natural isomer ((L-erthro)-2-amino-4-hydroxy 6(R) [1,2-dihydroxypropyl]-pteridine) has a four-fold greater velocity.[29] 6,7-DMTHP, a pseudo cofactor, is one-fourth as reactive as THBP.[29]

The orientation and nature of the side chain at C(6) does not affect K_m. This observation is also supported by K_m values and activities exhibited by 2,5,6-triamino-4-pyrimidone and 5-benzylamino-2,6-diamino-4-pyrimidone. The K_m values and activities exhibited by these latter compounds were similar to those observed with corresponding pterin analogs.[58] However, substitution at C(6) appears to be necessary for tetrahydropterins to bind to the enzyme in a highly selective way.[35,36]

Electrochemical methods are very useful in providing biologically significant information on electron transfer reactions. The nature of certain electrochemical and enzymic electron transfer reactions are similar. For example, the electrochemical and enzymic reactions of certain purines proceed by similar, if not identical mechanisms.[68,69] Both electrochemical and enzymic processes involve heterogeneous electron transfers; the former taking place at an

electrode solution interface and the latter at an enzyme solution interface. The pH, ionic strength of the inert electrolyte and type of solution (aqueous) in which these reactions take place are comparable. In both cases, the orientation of the substrate molecule is important for an electron transport to take place.

Although the unique selectivity of an enzyme cannot be duplicated by an electrode, there is at least a superficial similarity between electrochemical and biological reactions. Therefore, biologically important molecules may be studied using electrochemical techniques and mechanistic information may be obtained about their behavior in biological systems.

Pteridines, in general appear to be rather readily reduced electrochemically. Reducible pteridines are reduced in the pyrazine ring and not in the pyrimidine ring. The more recent detailed investigations of pteridine,[70] various 2-amino-4-hydroxypteridines,[65] and folic acid[71-73] appear to support the view that these compounds are reducible in an initial $2\underline{e}$-$2H^+$ process to an unstable 5,8-dihydro derivative, when formation of such a product is structurally possible. For pteridines that are able to form a 5,8-dihydro-derivative, the reduction is reversible. Once formed the 5,8-dihydro derivative rapidly rearranges to the more stable 7,8-dihydro-derivative. The detailed mechanism of such electrochemical reductions and the kinetics of the follow-

up reaction have not been studied. The spectral and other physical properties of the 5,8-dihydropteridine derivatives are also unknown.

The only definitive study of such electrochemical reductions using modern electrochemical techniques coupled with product isolation and identification is that of McAllister and Dryhurst[70] who studied the reduction of pteridine.

The polarographic reduction of a number of pterin and lumazin derivatives structurally "locked" into a quinonoidal form in dilute acid medium suggests, on the basis of polarographic wave height data, that the 6,7-unsubstituted compounds undergo 1e reductions to form radicals which subsequently dimerize.[74]

There have been a number of studies on the d.c. polarographic reduction of folic acid such as those by Hrdý,[75] Ashai[76] and Kretschmar and Jaenicke.[71,72] However, the results by these authors are often contradictory.

There have been a few reports of the electrochemical oxidation of pteridines. Archer and Scrimgeour[63] have reported that THP, 6-MTHP and 6,7-DMTHP are electrochemically oxidized at a dropping mercury electrode. Polarographic data indicate that the oxidation proceeds by an ee mechanism (electrode process where an initial electrochemical reaction is followed rapidly by a further electrochemical reaction); the first step being the removal of 1e to give a radical

which is then further oxidized (1e, $2H^+$) to give a quinonoid-dihydropterin.

Preliminary cyclic voltammetric experiments have demonstrated that some tetrahydropterins give a reversible or quasi-reversible couple at pH 9 at a mercury electrode.[65] The oxidation process has been presumed to be a $2e$-$2H^+$ electrooxidation of the tetrahydropterin to quinonoid-6,7-dihydropterin and the reverse reaction is the reduction of the quinonoid back to tetrahydropterin.

Kretzchmar and Jaenicke[71,72] have reported that 5,6,7,8-tetrahydrofolic acid at pH 6.8 exhibits an anodic d.c. polarographic wave indicative of a $1e$-$1H^+$ oxidation reaction to give a neutral radical which could either dimerize or undergo further electrooxidation to the quinonoid-6,7-dihydrofolic acid. According to these workers the latter compound cannot only rearrange to the more stable 7,8-dihydro-derivative but also cleaves the side chain from C(6).

Braun and Pfleiderer[71,72] have reported some simple electrochemical studies. At a rotating platinum electrode some 7,8-dihydropterins are apparently electrooxidized in a 1e reaction. The 1e processes were proposed to result in formation of radical species, although this was not confirmed by cyclic voltammetry or EPR spectroscopy.

McAllister and Dryhurst[79] have studied the electrochemical oxidation of 6- and 7-hydroxypteridine at the

pyrolytic graphite electrode.

Electrochemical oxidation of 6,7-DMTHP at a Pt electrode was investigated by Pradac et al.[80] but only over a very limited pH range and in buffers of different composition and ionic strength. A double potential-step chronocoulometric method was employed to study the first-order reaction of the intermediate generated from 6,7-DMTHP following charge transfer. The rate of this chemical step was found to be pH-dependent and different for various THP derivatives.[81]

A detailed and systematic investigation of the redox chemistry of tetrahydropterins (5,6,7,8-THP, 7,8-DHP and pterin) and 6-methyltetrahydropterin and 6-methyl-7,8-dihydropterin) has been reported.[82,83] The initial electrooxidation of both THP and 6-MTHP involves a $2e^{-}2H^{+}$ reaction giving an unstable quinonoid-dihydropterin which rearranges to the corresponding 7,8-DHP in a pH-dependent fashion. THP is the simplest of all the fully reduced pterins, but its electrochemistry is rather complex. THP can also function as a pseudo-cofactor for the hydroxylation of phenylalanine in the presence of phenylalanine hydroxylase and oxygen.[56] However, THP leads to formation of only about one-half of the amount of tyrosine formed when THBP or the other common pseudo-cofactors are used. In comparison to THP the electrochemistry of 6-MTHP appears to be rather straightforward.

Conventional studies of hydroxylation reactions

which utilize THP cofactors and chemical and polarographic studies of the THP have not provided the required understanding of the chemistry of these cofactor species. It is clear from the mechanisms shown in Figures 1 and 2, that in order to understand the roles of reduced pterins in normal and abnormal biological reactions to understand the fundamental redox and related chemistry of these compounds. Accordingly, an investigation into the redox and related chemistry of biologically-significant reduced pterins was initiated to hopefully increase our knowledge of the biological function of these compounds in enzymic hydroxylation reactions and other processes.

REFERENCES

1. A. Albert in, Chemistry and Biology of Pteridines, W. Pfleiderer (ed.), W. de Gruyter, Berlin, 1975.

2. C. Schöpf and H. Wieland, Chem. Ber., 59 (1926), 2067.

3. H. Wieland and C. Schöpf, Chem. Ber., 58 (1925), 2178.

4. H. Wieland and P. Decker, Justus Lieligs Ann. Chem., 547 (1941), 180.

5. W. Pfleiderer, Angew. Chem., 75 (1963), 993.

6. H. Kwietny and F. Bergmann, J. Chrom., 2 (1959) 162.

7. B. R. J. Nicolaus, J. Chrom., 4 (1960) 384.

8. H. Descimon and M. Barial, Bull. Soc. Chim. France, 1 (1973), 87.

9. H. Rembold, Methods in Enzymology, 18B (1971) 652.

10. S. W. Bailey and J. E. Ayling in, Chemistry and Biology of Pteridines, W. Pfleiderer (ed.), W. de Gruyter, Berlin (1975) 633.

11. S. W. Bailey and J. E. Ayling, Anal. Biochem., (1980) 107.

12. S. W. Bailey and J. E. Ayling, J. Biol. Chem., 253 (1978) 1598.

13. J. C. Nixon, C.-L. Lee, S. Milstien, S. Kaufman and K. Bartholome, J. Neurochem., 35 (1980) 898.

14. B. Stea, R. M. Halpern, B. C. Halpern and R. A. Smith, J. Chrom., 188 (1980) 363.

15. B. Stea, R. M. Halpern and R. A. Smith, J. Chrom., 168 (1979) 385.

16. F. Röthler and M. Karobath, Clin. Chim. Acta, 69 (1976) 456.

17. H. Rokos, K. Rokos, H. Frisius and H.-J. Kirstaedter, Clin. Chim. Acta, 105 (1980) 275.

18. J.-L. Dhondt, C. Langilliere, P. Andouin, J.-P. Farriaux and M. Dautrevaux, Clin. Chim. Acta, 110 (1981) 205.

19. T. Fukushima and J. C. Nixon, Anal. Biochem., 102 (1980) 176.

20. W. Schwotzer, J. H. Bieri, M. Viscontini and W. von Philipsborn, Helv. Chim. Acta, 61 (1978) 2108.

21. K. Koboyashi and M. Goto in, Chemistry and Biology of Pteridines, Iwai (ed.), Intl. Acad. Print Co., Tokyo, 1970, 57.

22. J. W. Serum, P. Haug, T. Urischibara and H. S. Forrest, Z. Anal. Chem., 262 (1972) 110.

23. T. Gato, A. Tatematsu and S. Matsuura, J. Org. Chem., 30 (1965) 1844.

24. J. A. Blair and C. D. Foxall, Org. Mass Spect. 2 (1969) 923.

25. T. Lyoyd, M. Sanford and N. Weiner, Anal. Biochem., 42 (1971) 108.

26. R. Weber, W. Frick and M. Viscontini, Helv. Chim. Acta, 57 (1974) 1485.

27. W. Koschara, Z. Physiol. Chem., 240 (1936) 127.

28. R. Tschesche, F. Korte and G. Heuschkel, Chem. Ber., 88 (1955) 1251.

29. S. Kaufman, PNAS USA, 50 (1963) 1085.

30. H.-Ch. Curtius, H. Farner and F. Rey, J. Chrom. 199 (1980) 171.

31. T. Kato, T. Yamaguchi, T. Nagatsu, T. Sugimoto and S. Matsuura, Biochim. Biophys. Acta, 611 (1980) 241.

32. T. Kato, K. Oka, T. Nagatsu, T. Sugimoto and S. Matsuura, Biochim. Biophys. Acta, 612 (1980) 226.

33. A. Tietz, M. Lindberg and E. P. Kennedy, J. Biol. Chem., 239 (1964) 4081.

34. H. K. Mitchell, E. E. Snell and R. J. Williams, JACS, 63 (1941) 2284.

35. M. Osanai and H. Rembold, Z. Physiol. Chem., 352 (1971) 1359.

36. A. Ehrenberg, P. Hemmerich, F. Müller and W. Pfleiderer, Eur. J. Biochem., 16 (1970) 584.

37. H. Rembold and G. Hein, Z. Physiol. Chem., 352 (1971) 1271.

38. R. C. Fuller and N. A. Nugent, PNAS USA, 63 (1969) 1311.

39. A. M. Bobst, PNAS USA, 68 (1971) 541.

40. S. W. Bailey and J. E. Ayling, J. Biol. Chem. 255 (1980) 7774.

41. A. Ehrenberg, P. Hemmerich, F. Müller, T. Okada and M. Viscontini, Helv. Chim. Acta, 50 (1967) 411.

42. A. Bobst, Helv. Chim. Acta, 51 (1968) 607.

43. S. Kaufman, J. Biol. Chem., 234 (1959) 2677.

44. S. Kaufman and B. Levenberg, J. Biol. Chem. 239 (1964) 332.

45. S. Kaufman in, Chemistry and Biology of Pteridines, W. Pfleiderer (ed.), W. de Gruyter, Berlin, 1975, 291-304.

46. C. Huang, E. E. Max and S. Kaufman, J. Biol. Chem., 248 (1973) 4233.

47. S. Kaufman, Adv. Exp. Med. Biol., 74 (1976) 91.

48. H. I. X. Mager and W. Berends, Rec. Trav. Chim., 84 (1965) 1329.

49. H. I. X. Mager and W. Berends, Rec. Trav. Chim., 91 (1967) 1137.

50. J. A. Blair and A. J. Pearson, J. Chem. Soc. Perkin II (1974) 80.

51. A. J. Pearson, Chem. Ind., (1974) 233.

52. J. A. Blair, A. J. Pearson and A. J. Robb, J. Chem. Soc. Perkin II (1975) 18.

53. J. A. Blair and A. J. Pearson, J. Chem. Soc. Perkin II (1975) 245.

54. L. J. Woolf, A. Jakubovic and E. C. Henry, Biochem., 125 (1971) 569.

55. M. Nikishimi, Arch. Biochem. Biophys., 166 (1975) 273.

56. J. E. Ayling, G. R. Boehm, S. C. Textor and R. A. Pirson, Biochem., 12 (1973) 2045.

57. S. Kaufman and B. Levenberg, J. Biol. Chem., 234 (1959) 2683.

58. S. Kaufman, Biochim. Biophys. Acta, 27 (1958) 428.

59. S. J. Benkovic, Ann. Rev. Biochem., 49 (1980) 227.

60. P. Hemmerich in, Pteridine Chemistry, W. Pfleiderer and E. C. Taylor (eds.), Pergamon, London, 1964, pp. 143, 323.

61. S. Kaufman in, Pteridine Chemistry, W. Pfleiderer and E. C. Taylor (eds.), Pergamon, London, 1964, p. 307.

62. M. Viscontini and A. Bobst, Helv. Chim. Acta, 48 (1965) 816.

63. M. C. Archer and K. G. Scrimgeour, Can. J. Biochem., 48 (1970) 278.

64. M. C. Archer, D. J. Vonderschmitt and K. G. Scrimgeour, Can. J. Biochem., 50 (1972) 1174.

65. S. Kwee and H. Lund, Biochim. Biophys. Acta, 297 (1973) 285.

66. S. Kaufman, J. Biol. Chem., 236 (1961) 804.

67. D. J. Vonderschmitt and K. G. Scrimgeour, Biochem. Biophys. Res. Commun., 28 (1967) 302.

68. A. Brajter-Toth, R. N. Goyal, M. Z. Wrona, T. Lacava, N. T. Nguyen and G. Dryhurst, Bioelectrochem. Bioenergetics, 8 (1981) 413.

69. M. Z. Wrona, R. N. Goyal and G. Dryhurst, Bioelectrochem. Bioenergetics, 7 (1980) 433.

70. D. L. McAllister and G. Dryhurst, J. Electroanal. Chem., 59 (1975) 75.

71. K. Kretzschmar and W. Jaenicke, Z. Naturforsch. Teil B, 26 (1971) 225.

72. K. Kretzschmar and W. Jaenicke, Z. Naturforsch. Teil B, 26 (1971) 999.

73. S. Kwee and H. Lund, Bioelectrochem. Bioenergetics, 6 (1979) 441.

74. H. Braun and W. Pfleiderer, Justus Liebigs Ann. Chem., (1973) 1099.

75. O. Hrdý, Coll. Czech. Chem. Comm., 24 (1959) 1180.

76. Y. Asahi, Yakugaku Zasshi, 79 (1959) 1548, Chem. Abst., 54 (1960) 10592.

77. H. Braun and W. Pfleiderer, Justus Liebigs Ann. Chem., (1973) 1082.

78. H. Braun and W. Pfleiderer, Justus Liebigs Ann. Chem., (1973) 1091.

79. D. L. McAllister and G. Dryhurst, J. Electroanal. Chem., 55 (1974) 69.

80. J. Pradác, J. Pradácová, D. Homolka, J. Koryta, J. Slavik, J. Weber and R. Cihar, J. Electroanal. Chem., 74 (1976) 205.

81. J. Weber, K. Holub, D. Homolka and J. Pradác, J. Electroanal. Chem., 73 (1976) 151.

82. R. Raghavan and G. Dryhurst, J. Electroanal. Chem., 129 (1981) 189.

83. L. G. Karber and G. Dryhurst, J. Electroanal. Chem., 136 (1982) 271.

CHAPTER 2

ELECTROCHEMICAL OXIDATION OF 6,7-DIMETHYL-5,6,7,8-TETRAHYDROPTERIN

INTRODUCTION

In order to obtain more information relating to the electrochemistry of tetrahydrobiopterin, the natural cofactor in many biological hydroxylation reactions, 6,7-dimethyl-5,6,7,8-tetrahydropterin (6,7-DMTHP, $\underset{\sim}{1}$), was chosen as a model system because of its wide use and effectiveness as a pseudo cofactor for <u>in vitro</u> enzymic hydroxylation reactions.

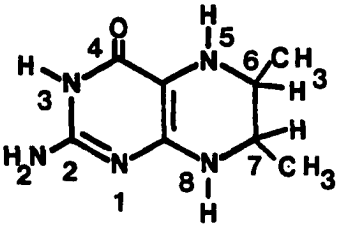

$\underset{\sim}{1}$

Previous work has shown that 6,7-DMTHP undergoes a $2\underline{e}$-$2H^+$ electrooxidation reaction to form a stable

product[1,2,3,4] after undergoing a chemical reaction. The rates of this chemical reaction have been determined by Archer et al.[5] and Weber et al.[6]

The first oxidation product of 6,7-DMTHP can further be oxidized to form a rather insoluble, stable product by a 2e-$2H^+$ reaction.

The present study was directed toward a detailed and systematic investigation of the electrochemical oxidation of 6,7-DMTHP over a wide pH range using a variety of sophisticated techniques.

RESULTS AND DISCUSSION

Physical properties of 6,7-DMTHP

In aqueous solution 6,7-DMTHP can exist as a dication, monocation, neutral or anionic species. The pK_a values have been determined[7,8] and are shown below. Solu-

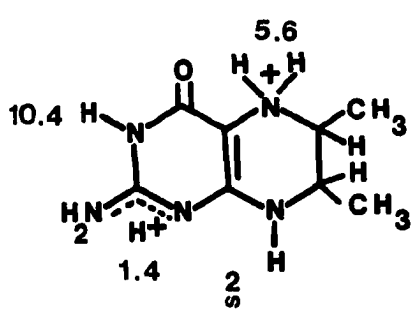

tions of 6,7-DMTHP are stable provided they are completely deaerated and maintained under an inert atmosphere. However,

with increasing pH the susceptibility of 6,7-DMTHP to attack by oxygen greatly increases. The oxidation state of 6,7-DMTHP may be determined by analyzing 6,7-DMTHP samples using a high pressure liquid chromatographic method.[9] As soon as solutions of 6,7-DMTHP are exposed to air oxidation takes place. Figure 1 shows liquid chromatograms obtained with samples of 6,7-DMTHP exposed to air, as a function of time.

A solution of stabilized 6,7-DMTHP is colorless and possesses no fluorescence. As soon as oxidation begins, the solution becomes faintly yellow colored and a blue fluorescence immediately appears.[10]

Linear scan and cyclic voltammetry

In linear sweep voltammetry a stationary micro electrode is immersed in a quiet, unstirred solution of electroactive material containing a large excess of supporting electrolyte. The applied potential is varied linearly with time at sweep rates varying between 0.005V/sec and 1000V/sec. The current is recorded as a function of potential. Non-faradaic currents flow if the potential scan is started at a point negative (positive) of the oxidation (reduction) potential of the electrochemically active species. When the electrode potential reaches the vicinity of the oxidation (reduction) potential of the electroactive species, oxidation (reduction) begins and current starts

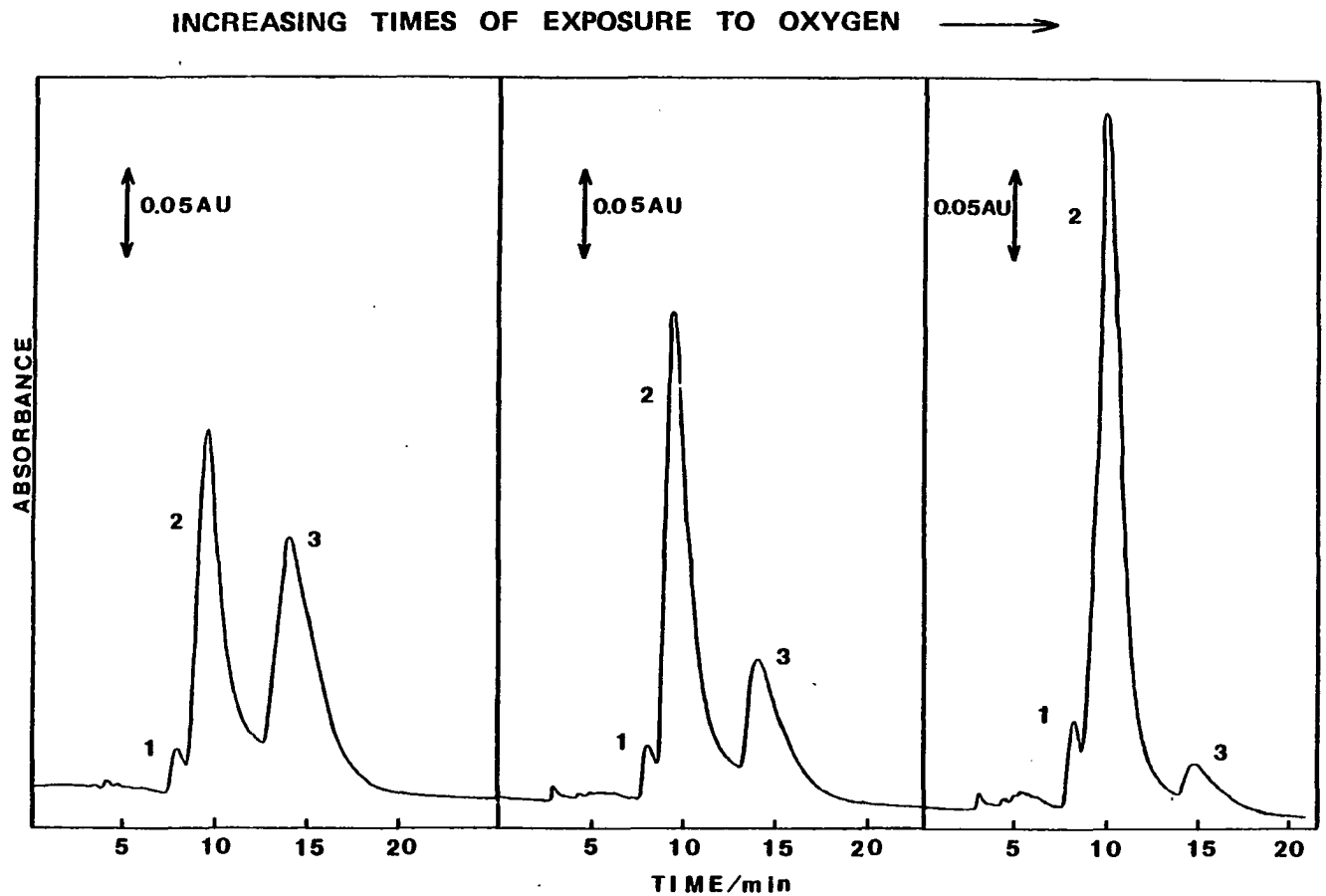

Figure 1. Liquid chromatograms obtained using a high pressure liquid chromatograph in phosphate buffer pH 6.5, ionic strength of 0.1 M during air oxidation of 6,7-DMTHP. Peak (1) 6,7-DMP, (2) 6,7-DHDHP and (3) 6,7-DMTHP. A partisil strong cation exchange column was used at a flow rate of 0.8 ml min^{-1}.

to flow. As the applied potential increases in positive (negative) direction, the surface concentration of the electroactive species drops causing the flux to the surface to increase which causes an increase in current. As the applied potential moves past the oxidation (reduction) potential of the electroactive species, the surface concentration drops to almost zero and the mass transfer to the surface reaches a maximum rate and then it declines. The observed current as a function of potential forms a peak (Fig. 2). The Nernst equation (1) may be used to characterize the electrode potential for a reversible electrochemical reaction

$$E = E^{\circ\prime} + \frac{RT}{nF} \ln \frac{C_O^*}{C_R^*} \qquad (1)$$

where

E = observed cell potential in volts

$E^{\circ\prime}$ = formal potential characteristic of a particular half reaction, in volts

R = the gas constant (8.314 volt·coulombs $^{\circ}K^{-1}$ $mole^{-1}$)

T = absolute temperature, $^{\circ}K$

n = number of electrons involved in the reaction as defined by the half-cell reaction (equivalents)

F = the Faraday's constant (96487 coulombs/equivalents)

C_O^* = bulk concentration of oxidized species

C_R^* = bulk concentration of reduced species

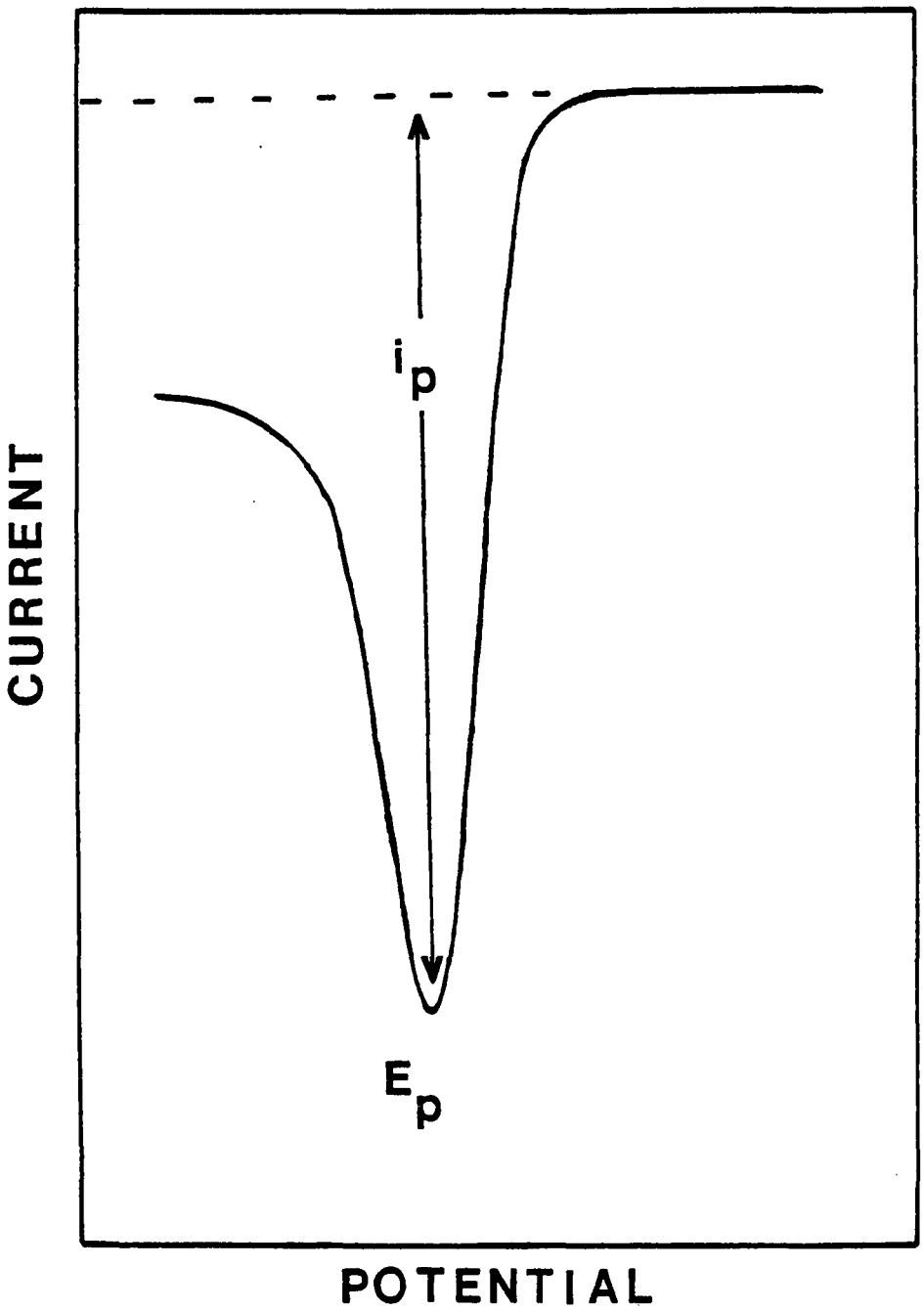

Figure 2. Theoretical single sweep voltammogram.

The peak current, i_p, for a reversible reaction may be defined by the Randles-Sevcik[11] equation (2).

$$i_p = 2.687 \times 10^5 n^{3/2} A D^{1/2} C V^{1/2} \quad (2)$$

where

i_p = peak current in μA

C = concentration of electroactive species in the bulk solution in mM

A = area of the electrode in cm^2

n = number of electrons involved in the electrochemical reaction

V = scan rate of the applied linear voltage in volts sec^{-1}

D = diffusion coefficient of the electroactive species in cm^2 sec^{-1}

The peak current is dependent on the scan rate of the potential sweep and varies linearly with $V^{1/2}$. However, the sensitivity can be increased only up to a limited value by increasing the scan rate of the applied potential. The charging current (i_c) is directly proportional to V, so that i_c becomes relatively more important at faster scan rates. Severe distortion of the linear sweep voltammograms occur at high V and low concentrations. This effect often sets the limit of the maximum useful scan rate.[12]

Between pH 2.0 and 11.0 6,7-DMTHP exhibits up to

four voltammetric oxidation peaks at the pyrolytic graphite electrode (PGE) (Fig. 3). The most positive of these peaks occurs very close to background discharge and is due to electrooxidation of 6,7-dimethylpterin (6,7-DMP) formed in the peak II_a and peak III_a reactions. Thus, this positive peak gave the same peak potential vs. pH relationship ($E_{p_{(pH\ 2\text{-}11)}}$ = [1.51-0.052 pH]V) as the single oxidation peak observed for 6,7-DMP. This peak will not be further discussed.

The variation of the peak potential with pH for the remaining three oxidation peaks is given by the following equations and is shown in Fig. 4:

Peak I_a (pH 2.0-11.0): E_p = [0.309-0.053 pH]V

Peak II_a (pH 2.0-4.1): E_p = [0.442-0.055 pH]V

Peak III_a (pH 2.0-4.1): E_p = [0.847-0.078 pH]V

(pH 4.1-10.6): E_p = [0.630-0.021 pH]V

Below pH 4.1 three voltammetric oxidation peaks may be observed, whereas above pH 4.1 only two peaks may be observed (peaks I_a and III_a).

The potential for the first electrooxidation process (peak I_a in this study) has been reported by two other groups (Table 1). The agreement between the various groups for the potential of peak I_a is modest due, probably, to the different electrode materials and buffer systems employed.

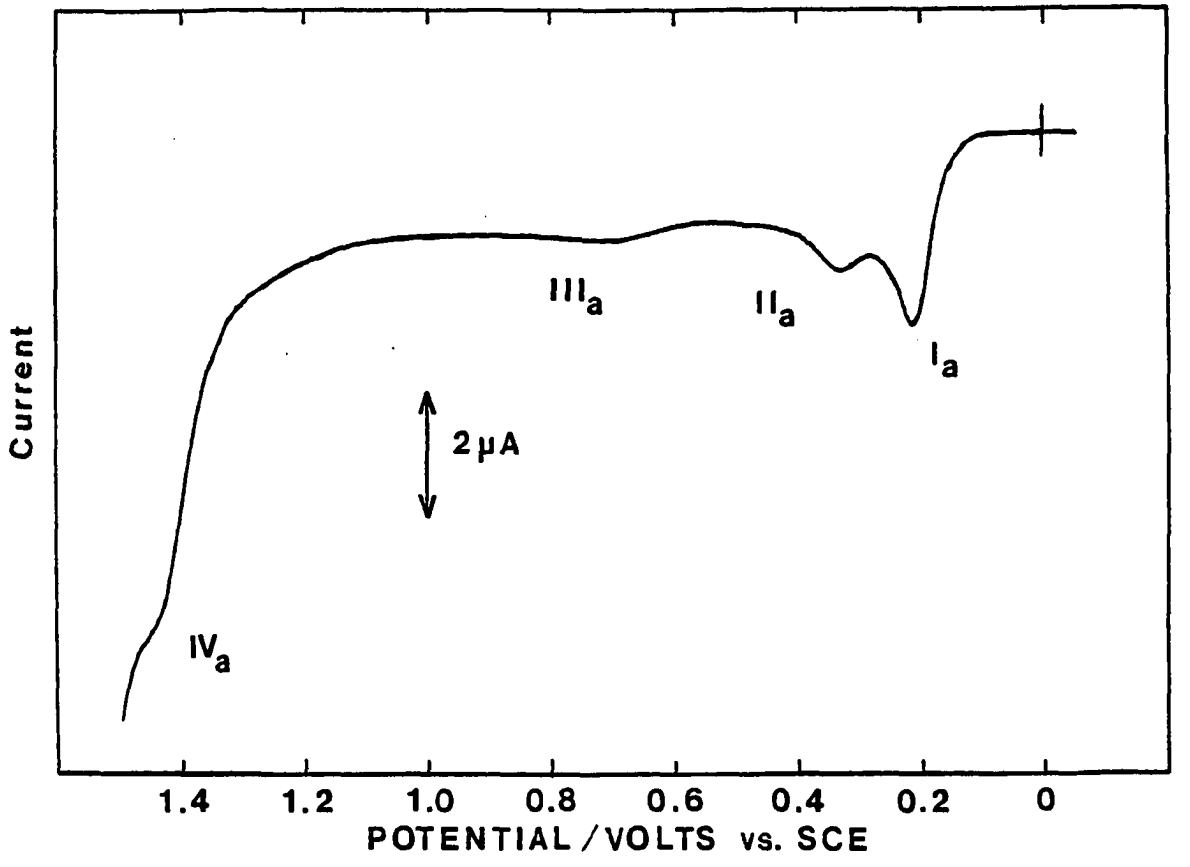

Figure 3. Single sweep voltammogram of 1 mM 6,7-DMTHP at the PGE in phosphate buffer pH 2 at a scan rate of 5 mV s^{-1}.

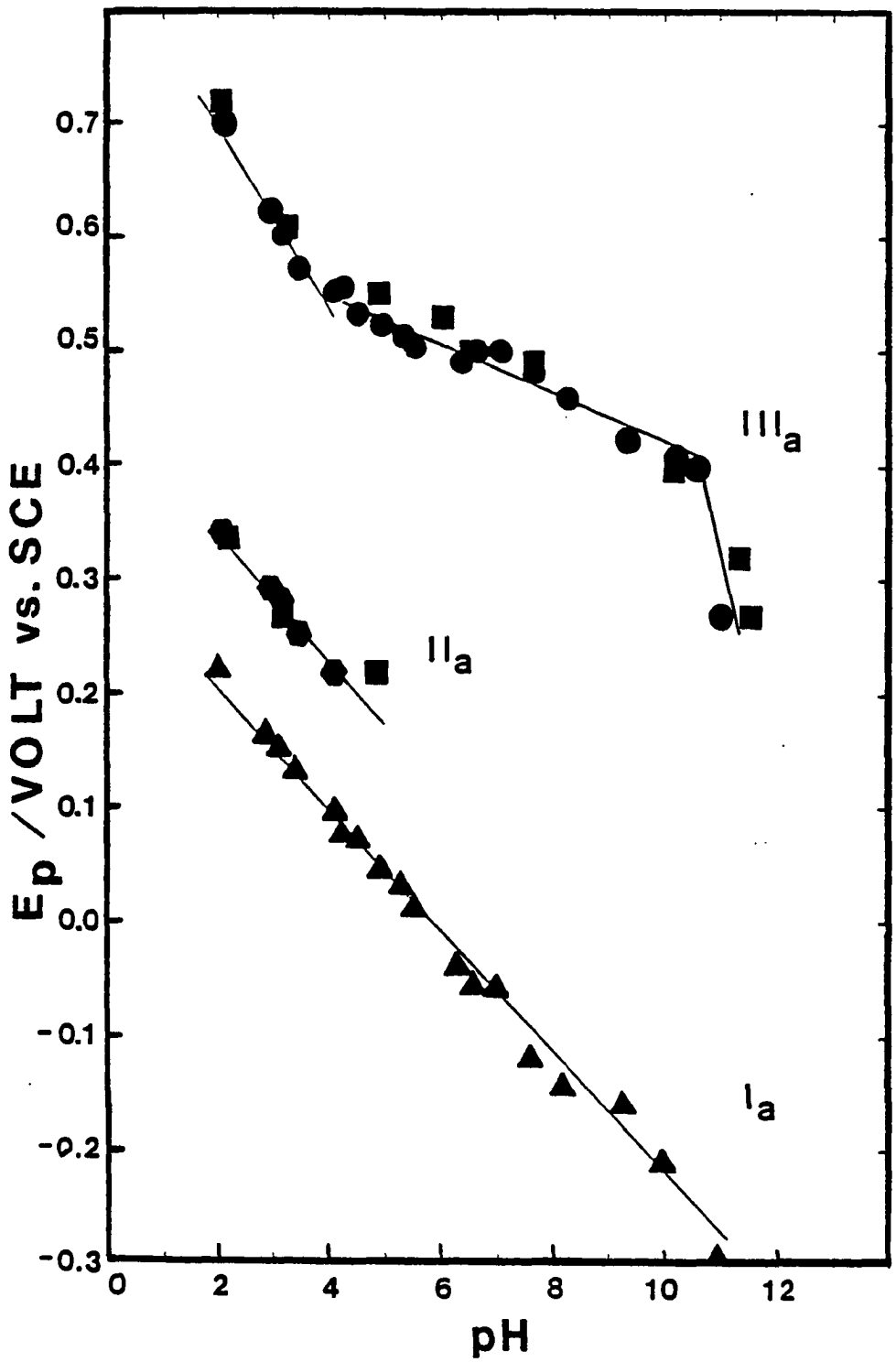

Figure 4. Dependence of peak potential, E_p on pH for 6,7-DMTHP, E_p values obtained at a scan rate of 5 mV s^{-1}. (■) correspond to E_p values obtained from 6,7-DMDHP.

Table 1. Comparison of E_p for peak I_a with literature values

pH	E_p/Volt vs. SCE		
	Archer et al.[a]	Pradac et al.[b]	This study[c]
3.0	0.172		0.150
4.0	0.107		0.097
4.7		0.100	
5.0	0.042		0.044
6.0	0.023		0.009
7.0	0.118	0.030	0.062
8.0	0.153		0.115
9.0	0.218		0.168
9.2		0.045	

[a] Polarographic $E_{1/2}$ data corrected to volt vs. SCE and then E_p calculated using $E_p = (E_{1/2} + \frac{0.029}{n})V$, setting n=2.

[b] Obtained at a platinum electrode; pH 4.7 was an acetate buffer, ionic strength 0.05 M; pH 7 was a phosphate buffer, ionic strength 0.3 M and pH 9.2 was a borate buffer ionic strength 0.1 M.

[c] Phosphate buffers having an ionic strength of 0.5 M.

In cyclic voltammetry, a triangular voltage waveform is applied to a stationary electrode, and the resulting current is monitored during the entire voltage sweep. Voltage sweep rates from 5 mV s^{-1} to 100V s^{-1} or greater are usually employed, and the amplitude of the triangular wave is in the range of 0.5-3.0V. The data are recorded on an x-y recorder or an oscilloscope. Cyclic voltammetric experiments are very useful in obtaining mechanistic information. Since in cyclic voltammetry the time interval between reverse sweeps may be short, then some of the products produced during the initial scan are still in the vicinity of the electrode surface when the sweep direction is reversed. These products can, if electroactive, give rise to voltammetric peaks. For a reversible reaction the oxidation and reduction peak potentials are separated by a small potential increment defined in the following equation (3):

$$(E_p)_a - (E_p)_c = \frac{0.058}{n} V \qquad (3)$$

where

E_{p_a} = anodic peak potential, volts

E_{p_c} = cathodic peak potential, volts

n = number of electrons involved in the electrochemical step

Equation (3) holds for single-sweep voltammograms

of individual solutions of oxidizable and reducible solutions. Conditions in the actual cyclic voltammograms are slightly different. The switching potential E_λ becomes an important factor. If E_λ is too close to the peak potential, the separation of peak potentials will be slightly greater than predicted by equation (3). Provided that the sweep is carried far enough that $(E_{1/2}-E_\lambda)n$ is of the order of 2-300 mV, the position of the reverse peak is relatively unaffected for sweep rates as low as 50 mV s^{-1}.[11] If the electrode reaction is quasi-reversible (intermediate between reversible and totally irreversible) then even at slow scan rates the peak potentials will be separated by more than the value predicted by equation (3).

In the presence of weakly adsorbed material, voltammograms obtained may show an increase in peak currents because of electron transfer involving adsorbed material at nearly the same potential as the "normal" uncomplicated diffusion-controlled electron transfer. However, if the product or reactant is strongly adsorbed, a separate adsorption peak may be observed prior to or after the peak due to the diffusion controlled process.[13]

The presence or absence of adsorption may be determined by varying the concentration and the scan rate. In cases where a prepeak or a postpeak appears, the presence of adsorption is usually more or less obvious. In other cases the presence of adsorption may not be easily detected

because of simultaneous oxidation or reduction of both the adsorbed and diffusion controlled species at the same potential. If the adsorption process contributes significantly to the total current at the concentrations and scan rates studied, three quick tests can be applied. The first one of these tests is to observe the shape of the resulting voltammetric peak. If the voltammetric peaks are more symmetrical than those obtained for uncomplicated nernstian charge transfer reactions, or if their symmetry increases with increasing sweep rate or decreasing concentrations, adsorption is probably involved. The second test involves varying the scan rate to measure the experimental peak current function, $i_p/CV^{1/2}$. If adsorption is present the experimental peak current function increases with increasing scan rate, while i_p/VC may remain nearly constant.

The third test is to study the effect of concentration. While i_p/C is constant for a number of electrode processes, i_p/C usually increases with decreasing concentration in the presence of adsorption.

Cyclic voltammograms of 6,7-DMTHP at pH 3.1 exhibit no reduction peaks if the initial sweep is towards negative potentials, but three oxidation peaks (I_a, II_a and III_a) are observed on the first sweep to positive potentials (Fig. 5). Having scanned these three peaks, four reduction peaks are observed on the reverse sweep. Reduction peak

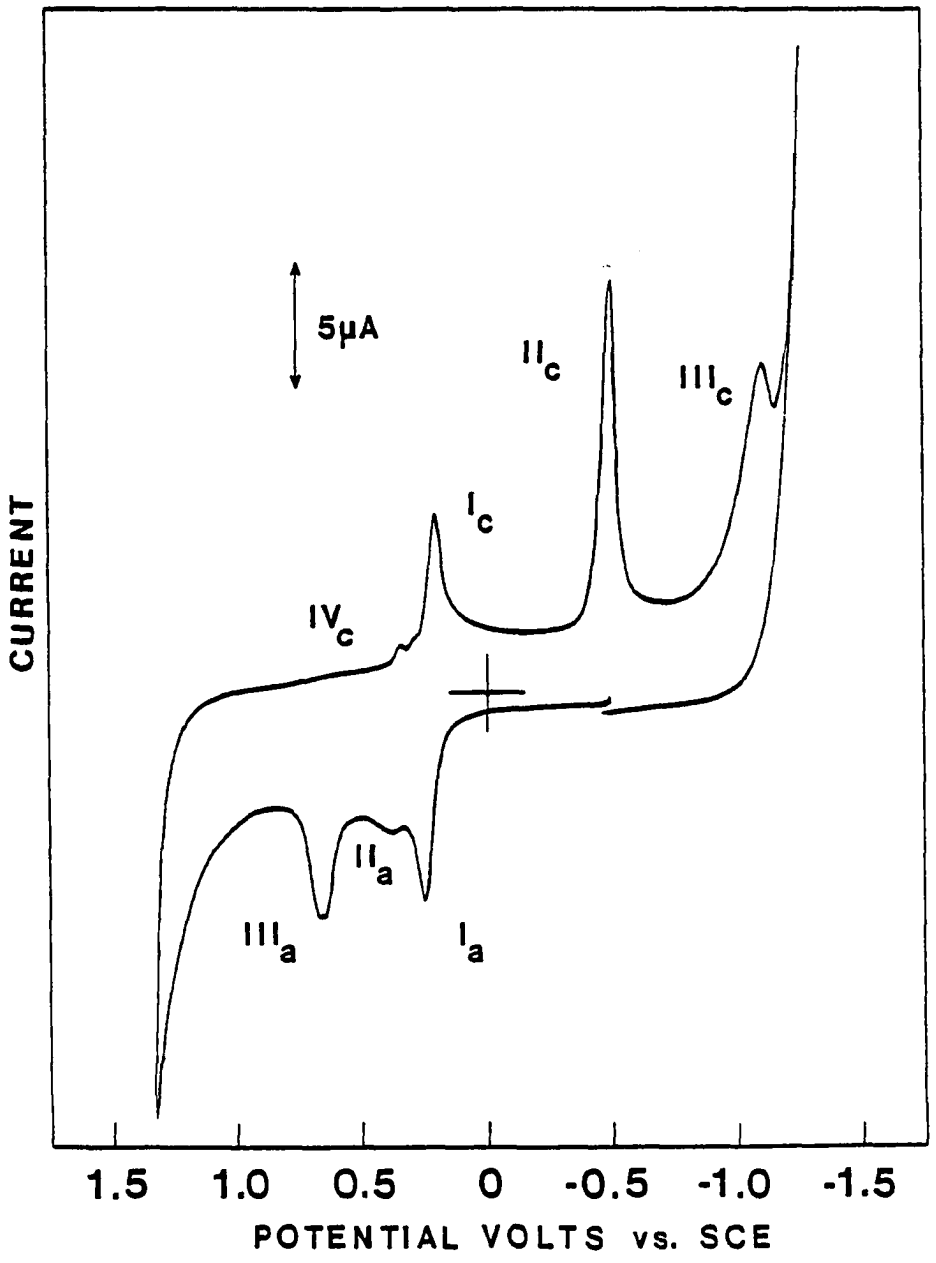

Figure 5. Cyclic voltammogram of 2 mM 6,7-DMTHP in phosphate buffer pH 3.0 at a scan rate of 200 mV s^{-1}.

I_c forms an almost reversible (quasi-reversible) couple with peak I_a. Indeed, at sweep rates between 50-200 mV s^{-1} and between pH 2.0-6.3 the ΔE_p value between peaks I_a and I_c averaged 38±13 mV; the ΔE_p values at different pH values are summarized in Table 2.

The ΔE_p value observed for peaks I_a and I_c is close to the 29 mV theoretically expected for a 2e reversible reaction.[11] As the sweep rate increases, the rate of electron transfer becomes slow relative to the scan rate, therefore peak separation increases.

At relatively slow sweep rates (e.g., <200 mV s^{-1}) the peak current for peak I_c was smaller than that for peak I_a particularly between pH 5-7 (Fig. 6). This indicates that the primary peak I_a electrooxidation product is not stable, particularly around pH 5-7, and disappears via a chemical follow-up reaction.

The various possibilities that were considered to explain the decrease in the peak current for I_c with decreasing scan rate were: 1. a chemical reaction followed by a second electrochemical reaction (overall an e.c.e. reaction), 2. reaction of the electrode product with solvent or supporting electrolyte, 3. dimerization of the electrode product and, 4. reaction of the electrode product with starting material.

The possibility of an overall e.c.e. reaction was eliminated by a study of the variation of the peak current

Table 2. Difference in peak potentials for the redox couple peaks I_a and I_c at various pH[a] values and scan rates

pH	scan rate (mV s^{-1})	$\triangle E_p$ (mV)
2.0	200	25
2.8	200	50
3.4	50	30
4.0	200	50
4.0	50	25
5.3	100	50
5.3	50	30
5.5	50	50
5.9	200	35
6.3	50	35

[a]Phosphate buffers having an ionic strength of 0.5 M was used.

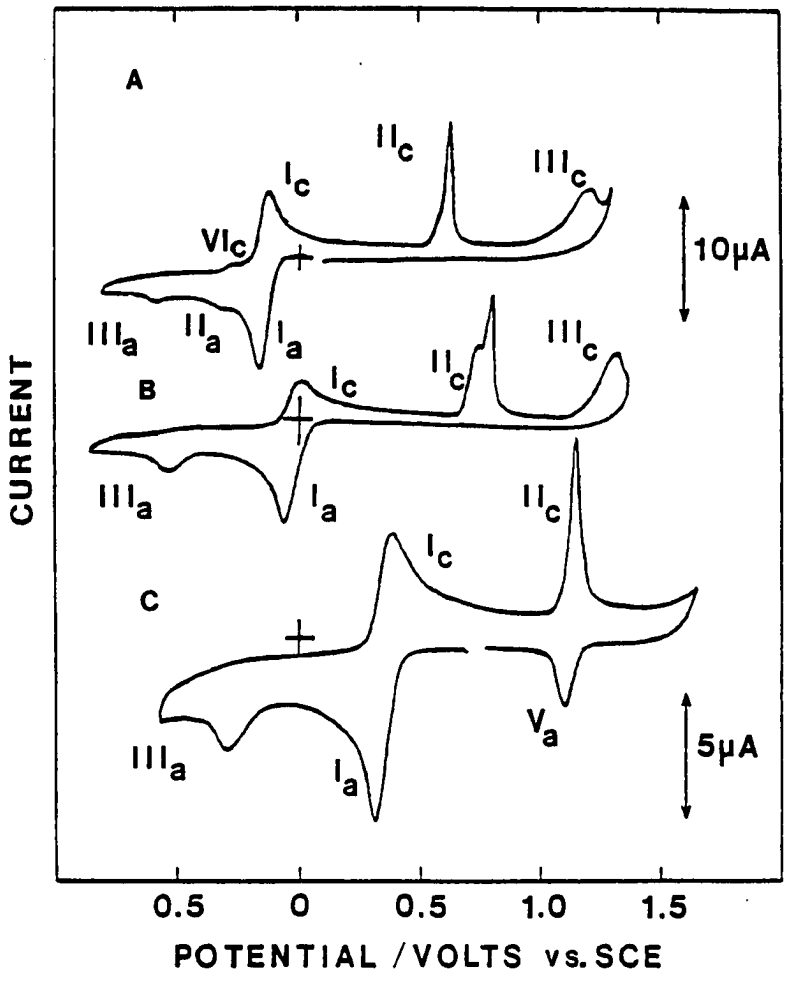

Figure 6. Cyclic voltammograms of 1.1 m<u>M</u> 6,7-DMTHP at the PGE at (A) pH 3.1, (B) pH 5.0 and (C) pH 11.0 at a sweep rate of 50 mV s^{-1}.

for peak I_c with voltage sweep rate. The Randles-Sevcik equation (2) shows that the ratio $i_p/v^{1/2}$ should be constant as a function of sweep rate in the case of an uncomplicated electrochemical reaction. If there were a chemical reaction followed by a second electrochemical reaction, the ratio $i_p/v^{1/2}$ would decrease with increasing voltage sweep rate. The results obtained at pH 7 (Table 3) indicate that the quantity $i_p/v^{1/2}$ increases with increasing sweep rate instead of decreasing which would be the case for an e.c.e. reaction.

The increase in $i_p/v^{1/2}$ with increasing sweep rate is indicative of an e.c. mechanism (electrochemical reaction followed by a chemical reaction). Previous work reported on 6,7-DMTHP also indicates that there is a chemical reaction following the electron transfer reaction.[1-6]

On the basis of coulometric evidence (see later discussion), reactions that are second order in 6,7-DMTHP (possibilities 3 and 4) were eliminated.

The possibility of the electrode product reacting with solvent or supporting electrolyte was assumed not to take place, because of the similar nature of electrochemical results reported on 6,7-DMTHP in different electrolyte solutions.[5,14]

The mechanism for a reaction taking place in the peak I_a process can be written as:

Table 3. Change in peak current, i_p for the I_a/I_c redox couple of a 5.6 mM 6,7-DMTBP solution in phosphate buffer pH 7 as a function of sweep rate

V $mV\ s^{-1}$	i_{p_a} (μA)	i_{p_c} (μA)	$i_{p_a}/V^{1/2}$ ($\mu A/mV^{1/2}$)	$i_{p_c}/V^{1/2}$ ($\mu A/mV^{1/2}$)	i_{p_c}/i_{p_a}
500	53.5	42.5	2.40	1.90	0.80
200	27.6	26.0	1.95	1.84	0.94
	14.2	7.9	2.00	1.10	0.56

$$Red \rightleftarrows Ox_1 + ne$$

$$Ox_1 \overset{k}{\rightleftarrows} Ox_2$$

where the electron transfer reaction is quasi-reversible and the Ox_1, Ox_2 and Red are soluble in the solution phase. The homogeneous chemical reaction is irreversible and characterized by a rate constant k. The rate of this chemical reaction changes with pH as can be observed from cyclic voltammetric data (Fig. 6).

Sweep rate studies indicate that the peak current function ($i_p/ACV^{1/2}$) for oxidation peak I_a is constant over a fairly large range of sweep rates (Table 4), whereas the peak current function for reduction peak I_c increases with increasing sweep rate until peak I_c becomes equal in height to peak I_a. It was also noted that with increasing sweep rate oxidation peaks II_a and III_a and reduction peaks II_c and III_c decrease, and at sufficiently high sweep rates almost disappear (Fig. 7). This behavior clearly implies that the species responsible for peaks II_a, III_a, II_c and III_c are dependent on formation of the product(s) formed in the chemical reaction of the peak I_a primary product.

Peaks II_a and III_a of 6,7-DMTHP are due to the electrooxidation of 6,7-DMDHP since the peak potentials observed with the latter compound agree with those for peaks II_a and III_a (Fig. 4). This information strongly supports the view that the peak I_a electrooxidation product

Table 4. Variation of $i_p/C_o v^{1/2}$ for peak I_a over a wide range of sweep rates for a 1.88 mM 6,7-DMTHP solution in phosphate buffer pH 4.5

V ($V\ s^{-1}$)	i_p (μA)	$i_p/C\ v^{1/2}$ ($\mu A\ mM^{-1} V^{-1/2}$)
0.050	12.86	0.967
0.100	14.29	0.760
0.200	24.29	0.914
0.500	34.29	0.816
1.000	51.43	0.865
5.000	128.57	0.967
10.000	171.43	0.912
20.000	214.29	0.806

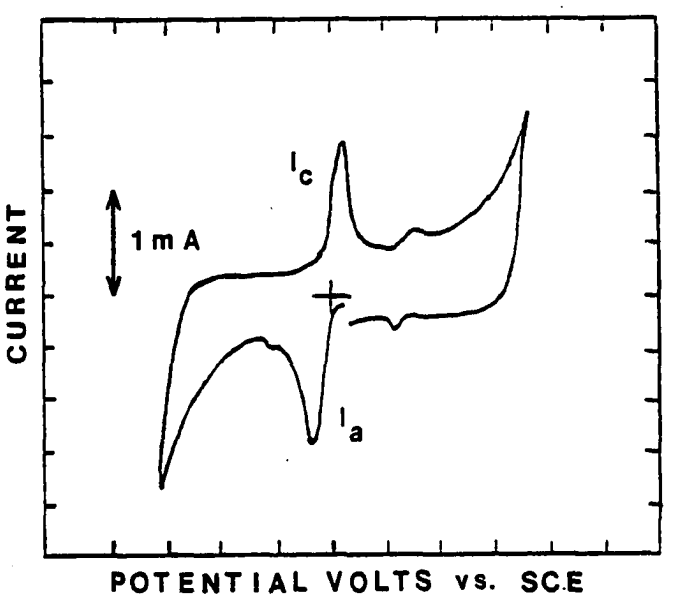

Figure 7. Cyclic voltammogram of 1 mM 6,7-DMTHP in phosphate buffer pH 4.2 at a scan rate of 20 V s^{-1}.

undergoes a chemical reaction to yield 6,7-DMDHP which then gives peaks II_a and III_a. At fast sweep rates in cyclic voltammetry there is insufficient time for the latter chemical reaction to occur so that peaks II_a and III_a cannot be observed (Fig. 7).

Cyclic voltammetry of 6,7-DMTHP below pH 4.2 results in formation of reduction peak IV_c (Fig. 8). This peak is observed clearly only at low concentrations of 6,7-DMTHP (<2 m$\underline{M}$) and it is necessary only to sweep past peak II_a for it to be observed. From single sweep and cyclic voltammetric experiments it may be inferred that peaks II_a and III_a are due to two electroactive species which are in equilibrium in aqueous solution. Thus, at low pH values, $\underline{e.g.}$, pH 2, and at a sweep rate of 5 mV s^{-1} peak II_a is larger than peak III_a. However, as the pH and/or the sweep rate is increased peak III_a grows relative to peak II_a. Above pH 4.5, peak II_a is no longer observed.

Switching potential experiments in cyclic voltammetry of 6,7-DMTHP reveal that it is necessary to sweep only oxidation peak I_a in order for reduction peak III_c to be observed on the reverse cycle. In order to observe reduction peak II_c it is necessary to sweep oxidation peak II_a and/or III_a (Fig. 9). Holding the applied potential past peak II_a and/or peak III_a resulted in an increase in the peak current for peak II_c, which suggests that 6,7-DMP is formed in the peak II_a and III_a electrode process.

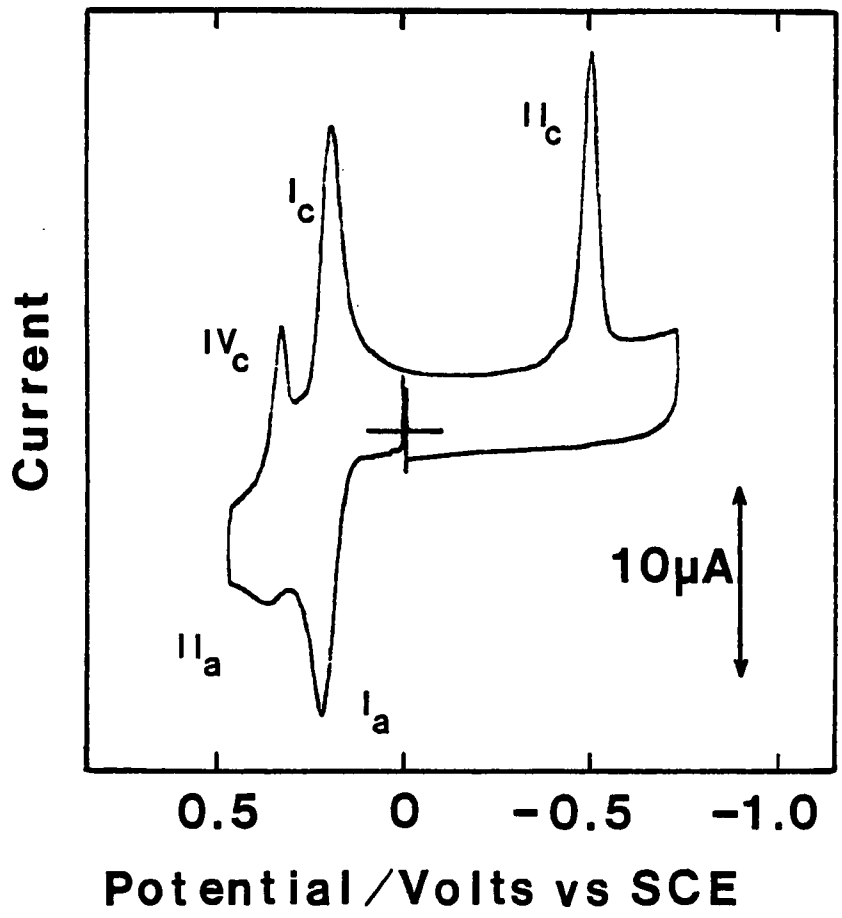

Figure 8. Cyclic voltammogram of 0.2 mM 6,7-DMTHP in phosphate buffer pH 2 at a sweep rate of 200 mV s^{-1}.

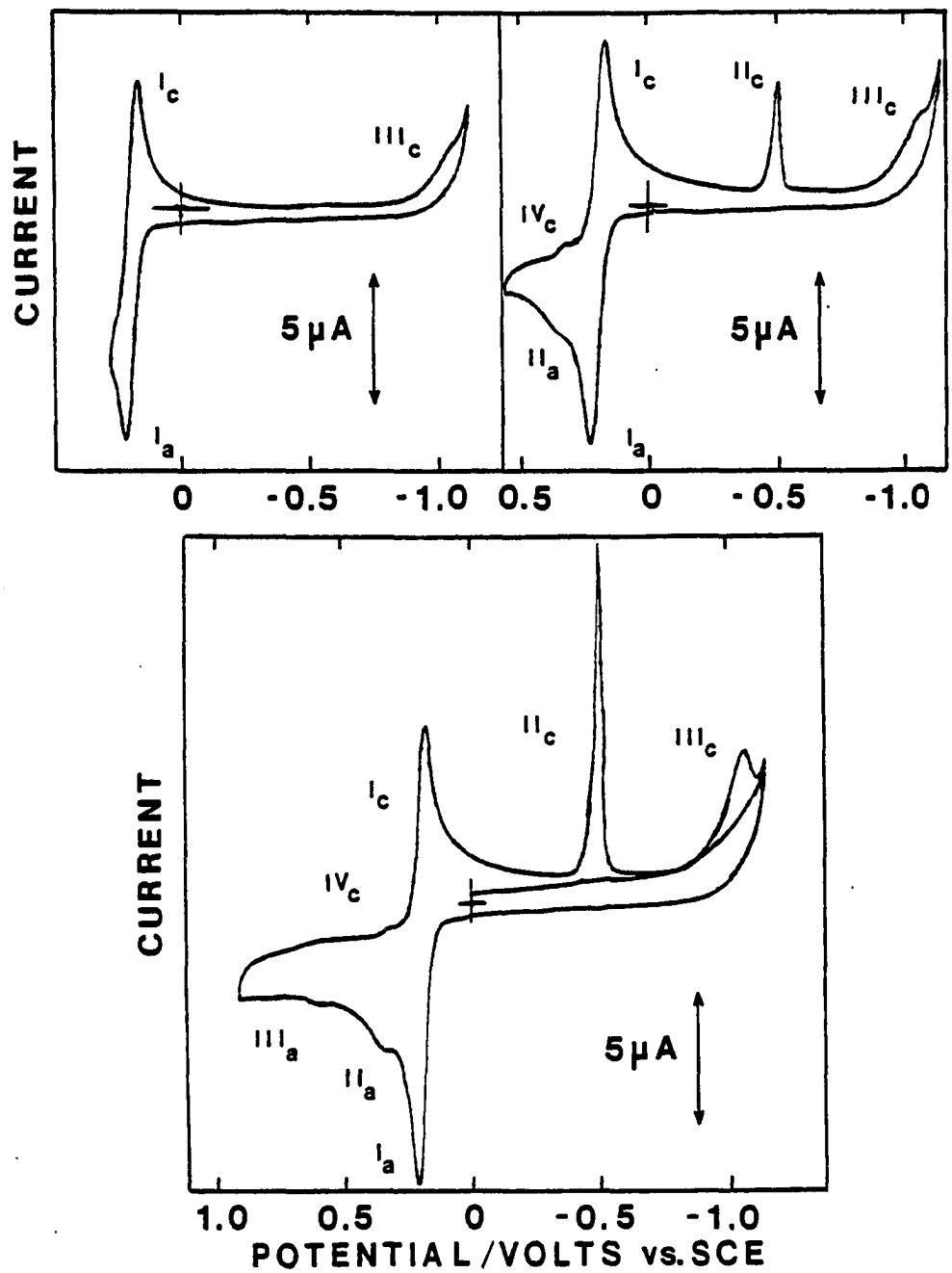

Figure 9. Effect of positive switching potential on the cyclic voltammetric behavior of 1.0 mM 6,7-DMTHP in phosphate buffer pH 2 using a sweep rate of 200 mV s^{-1}. (A) switching potential slightly positive of peak I_a, (B) switching potential positive of peak II_a, (C) switching potential positive of peak III_a.

At 6,7-DMTHP concentrations greater than 1 m$\underline{M}$ peak II_c observed under cyclic voltammetric conditions was often split into two very closely spaced peaks. Because of the very low solubility of 6,7-DMP[15] it is likely that this compound is adsorbed resulting in the formation of an adsorption post peak.

Changing the concentration of 6,7-DMTHP gives rise to voltammograms which are slightly different. For example, at pH 2 single sweep voltammograms of 6,7-DMTHP show only two oxidation peaks (I_a and II_a) of comparable size at a sweep rate of 5 mV s^{-1}. When the concentration is doubled or increased an order of magnitude a third oxidation peak (III_a) may be observed and the peak height for peak I_a is almost double that of peak II_a (Fig. 10). The peak height for peak I_a increases linearly with increasing concentration, whereas the peak current for peak II_a shows a non-linear dependency on concentration. A similar observation may be made at pH 4. However, at pH values where peak II_a is no longer observed, both peak I_a and peak III_a show a linear increase with increasing concentration. Table 5 summarizes the changes in peak current for peak I_a as a function of concentration and scan rate at pH 9.3. At concentrations higher than 2 m$\underline{M}$ the peak current function for peak I_a is no longer directly proportional to concentration (i.e., i_p is usually smaller than predicted by theory). The peak current function for peak III_a shows a slight increase

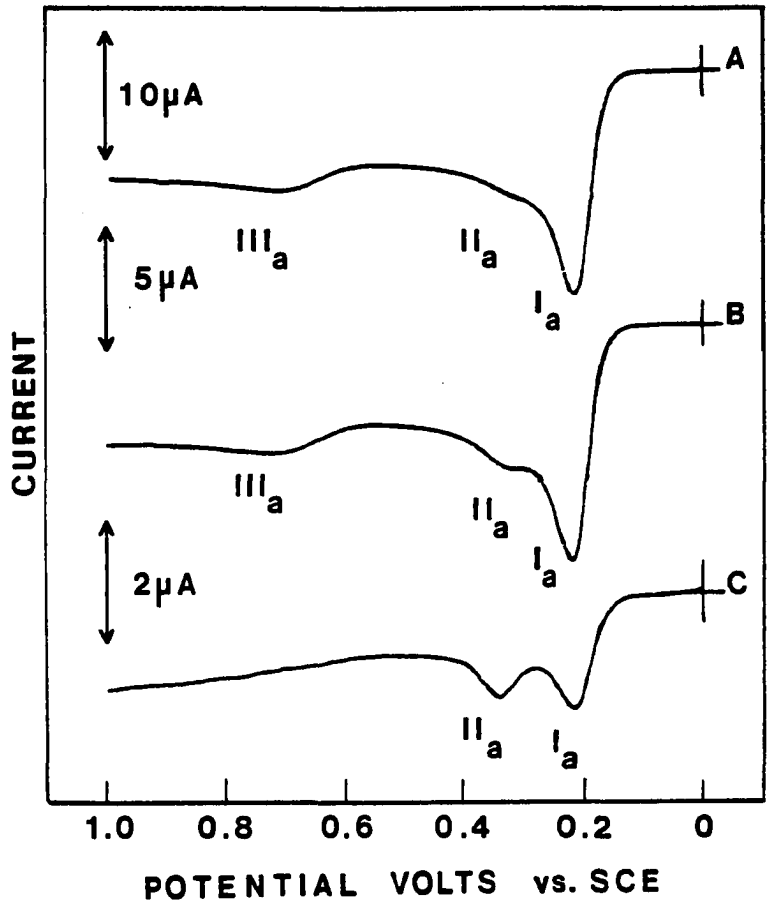

Figure 10. Effect of concentration on the linear sweep voltammograms of 6,7-DMTHP in phosphate buffer pH 2 at a concentration of (A) 5.0 m$\underline{M}$, (B) 2.5 m$\underline{M}$, and (C) 0.5 m$\underline{M}$. The scan rate is 5 mV s^{-1}.

Table 5. Change in i_p for peak I_a of 6,7-DMTHP as a function of concentration and sweep rate in phosphate buffer pH 9.3

Concn (mM)	V ($mV\ s^{-1}$)	i_p (μA)	$i_p/C\ V^{1/2}$ $\mu A\ mM^{-1}\ (mV\ s^{-1})^{-1/2}$
0.66	5	1.3	1.1
	20	3.4	1.2
	50	8.0	1.7
	200	18.3	2.0
0.81	5	1.6	0.9
	20	-	-
	50	4.8	0.8
	200	8.7	0.8
1.62	5	5.4	1.5
	20	-	-
	50	14.5	1.3
	200	29.3	1.3
3.34	5	10.0	1.3
	20	16.0	1.1
	50	25.0	1.1
	200	47.5	1.0

with increasing sweep rate (Table 6). Considering the fact that the species responsible for this peak is formed in a chemical reaction, one would expect that increasing the sweep rate would result in a decrease in the peak current for peak III_a. Hence, the increase has to be due to oxidation of some adsorbed material on the electrode surface.

Cyclic voltammograms of 6,7-DMTHP at high concentrations (i.e., 3 mM) exhibit different behavior in comparison to solutions at lower concentrations (i.e., 0.6 mM). The most pronounced difference is that the peak height for peak III_a decreases with increasing concentration relative to the peak height for peak I_a (Fig. 11). At a scan rate of 50 mV s^{-1} reduction peak II_c splits into two and an adsorption post peak may be observed.

Besides the quasi-reversible redox couples I_a, I_c and II_a, IV_c, reduction peak II_c has a reversible oxidation peak (peak V_a) associated with it. This reduction process may be observed at high pH values (pH >5) and/or fast scan rates (2V s^{-1} or higher) (Fig. 12). The fact that this peak is not observed at slow scan rates indicates that the reduction product of peak II_c undergoes a chemical reaction.

The reduction of 6,7-DMP has been studied[1] and it is reported that the first step in the reduction of 6,7-DMP involves formation of a 5,8-dihydro species. This species

Table 6. Change of experimental i_p values for peak III_a of 1.88 m$\underline{M}$ 6,7-DMTHP in phosphate buffer pH 4.5 as a function of sweep rate

V ($V\ s^{-1}$)	i_p (μA)	$i_p/C\ V^{1/2}$ ($\mu A\ m\underline{M}^{-1}\ V^{-1/2}$)
0.050	4.3	0.32
0.100	8.6	0.46
0.200	12.7	0.48
0.500	24.3	0.58
1.000	38.6	0.65
5.000	100.0	0.75
10.000	150.0	0.80
20.000	171.4	0.65

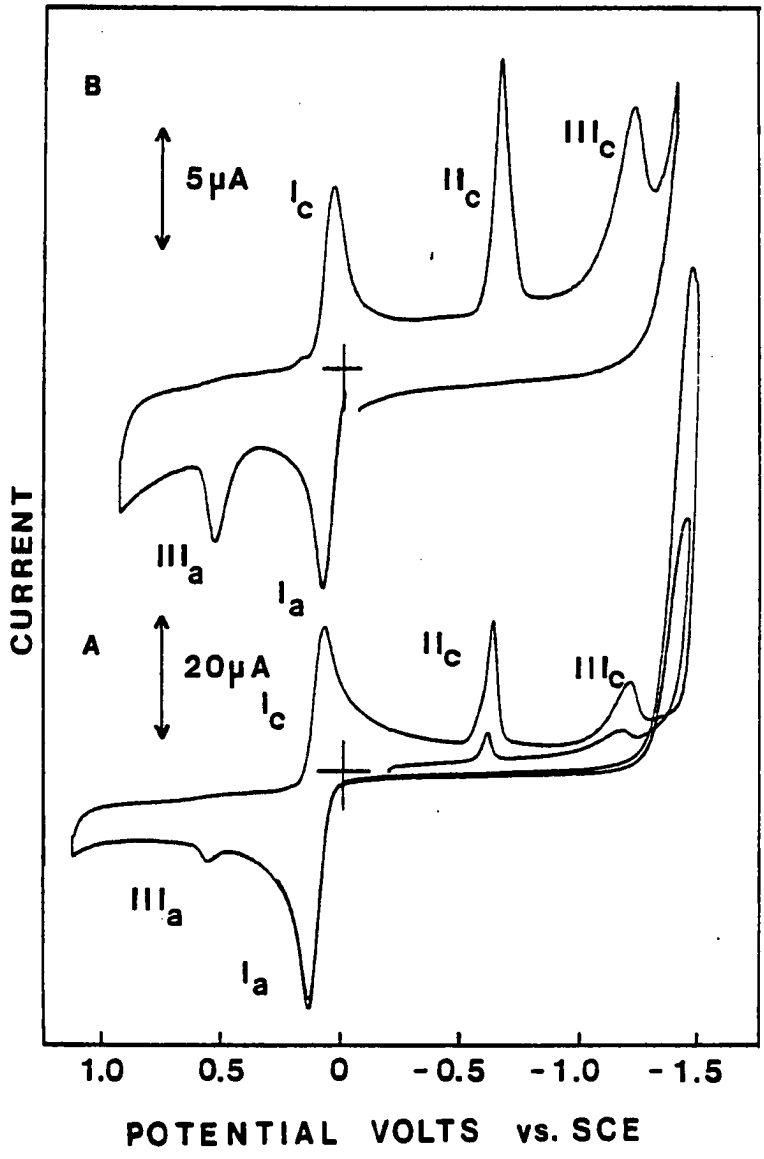

Figure 11. Cyclic voltammograms of 6,7-DMTHP in phosphate buffer pH 4, at a sweep rate of 200 mV s^{-1}, (A) 3 m<u>M</u>, (B) 0.6 m<u>M</u>.

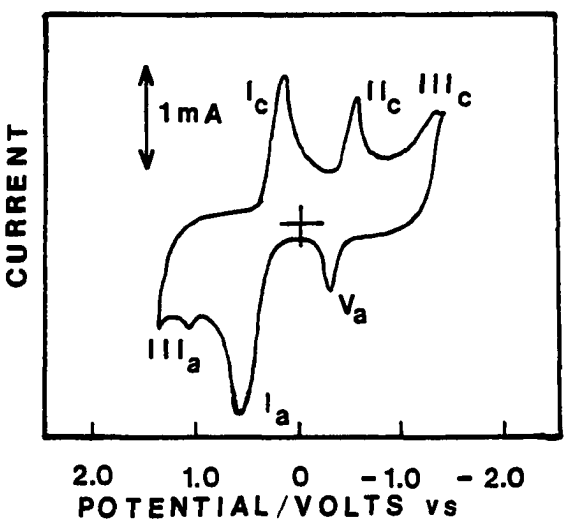

Figure 12. Cyclic voltammogram of 5 m<u>M</u> 6,7-DMTHP in phosphate buffer pH 3.1 at a scan rate of 20 V s^{-1}.

is not very stable and rearranges to the more stable 7,8-dihydropterin, which may be further reduced to the tetrahydro-derivative in the peak III_c reduction process.

Voltammetry at a gold electrode

Since the initial spectroelectrochemical studies were carried out using optically transparent thin-layer gold mini-grid electrodes, brief voltammetric studies at a gold electrode were carried out. Gold foil electrodes (area ≈9 mm^2) were fabricated as described by Adams.[16]

The electrooxidation of 6,7-DMTHP was studied as a function of pH. Two electrooxidation peaks, peaks I_a and III_a, were observed between pH 3-11.2. Another electrooxidation peak, peak II_a, may be observed at pH <5 as a shoulder. Peak potential vs. pH relationship for these electrooxidation peaks may be represented by the following equations:

$$\text{Peak } I_a \quad (\text{pH } 3\text{-}5.4) \quad [E_p = 0.34\text{-}0.060 \text{ pH}]\text{V}$$

$$\text{pH } (6.3\text{-}11.2) \quad [E_p = 0.112\text{-}0.015]\text{V}$$

$$\text{Peak } III_a \quad (\text{pH } 3\text{-}5.4) \quad [E_p = 0.82\text{-}0.060 \text{ pH}]\text{V}$$

$$\text{pH } (6.3\text{-}11.2) \quad [E_p = 0.67\text{-}0.010 \text{ pH}]\text{V}$$

The oxidation potentials at the gold foil electrode are slightly more positive than those observed at the PGE. Correspondingly, the reduction potentials observed occur at slightly more negative values. These differences in peak potentials are no doubt attributable to the different

type of electrode materials used.[17] Based on such single sweep and cyclic voltammetric studies at a gold foil electrode, it was concluded that the basic electrochemistry of 6,7-DMTHP is very similar to that at PGE.

Controlled potential coulometry

Controlled potential coulometry experiments are performed at a constant potential under uniform stirring of the solution which contains the electroactive species reaching the electrode surface by convection. The number of coulombs that is passed during the electrochemical reaction is determined and may be used to calculate the number of electrons per molecule involved in the electrode reaction. Controlled potential coulometric experiments may be employed to accomplish separations, electrochemical syntheses, electrochemical analyses and to investigate mechanisms of voltammetric redox processes.

Controlled potential coulometric oxidation of 6,7-DMTHP at large PGE at potentials corresponding to peak I_a between pH 2 and 9.3 indicates that 1.9±0.2 electrons per molecule are transferred (Table 7). At pH values below ca. 4.5 it was necessary to use an applied potential corresponding to the rising portion of peak I_a to minimize interference from the peak II_a process. Above pH 4.5, peak II_a is no longer present and potentials more positive than peak I_a could be applied without significant interference from the peak III_a process. After completion

Table 7. Coulometric n-values observed upon electrooxidation of 6,7-DMTHP at peak I_a potentials[a]

pH[b]	Initial Concentration of 6,7-DMTHP/mM	$E_{applied}$/Volt vs. SCE	Experimental n-value
2.0	1.7	0.2[c]	2.1
	2.6	0.2	2.0
	2.9	0.2	2.0
3.1	0.1	0.2[c]	1.9
	0.5	0.2	2.1
	1.0	0.2	2.2
	7.0	0.2	1.6
4.0	0.4	0.1[c]	2.0
	1.5	0.1	2.0
	2.4	0.1	1.9
6.0	0.2	0.0	1.8
	2.0	0.1	1.6
	27.4	0.2	1.9
7.0	0.5	0.2	2.1
	0.8	-0.1	1.7
	0.9	-0.1	2.0
9.3	0.5	0.1	1.9
	0.7	0.1	1.8

[a]Data obtained using a large PGE working electrode.

[b]Phosphate buffers having an ionic strength of 0.5 M.

[c]Potential corresponds to the rising portion of peak I_a to minimize interference by the peak II_a process.

of the electrolysis at peak I_a, potentials below ca. pH 4.5 peaks II_a and III_a are observed on the first sweep towards positive potentials (Fig. 13B) whereas peak III_c is observed if the first voltammetric sweep is towards negative potentials (Fig. 13C). Single sweep voltammograms were recorded to monitor the electrolysis of 6,7-DMTHP. Figure 14 shows the change in the single sweep voltammograms during the course of an electrolysis at pH 3. If, after completing the sweep in a negative direction, the sweep direction is changed and swept towards positive potentials, a new oxidation peak, peak III_a' is observed at slightly less positive potentials than peak III_a. Concentration and sweep rate studies suggest that peak III_a' is due to adsorption of the product of the electrooxidation of 6,7-DMDHP (Fig. 15).

Following complete electrooxidation of 6,7-DMTHP at peak I_a potentials at pH values >4.5, voltammetry of the resulting product solution shows only oxidation peak III_a on the first positive sweep and only reduction peak III_c on the first negative sweep (Fig. 16). The U.V.-absorption spectrum of the product formed by controlled potential electrooxidation of 6,7-DMTHP at peak I_a potentials is identical to that of 6,7-DMDHP (Fig. 17). For example, at pH 7 three U.V. bands are observed at λ_{max} = 321 nm, 280 nm and 227 nm which agree well with the literature spectrum of 6,7-DMDHP[14]. This spectrum differs

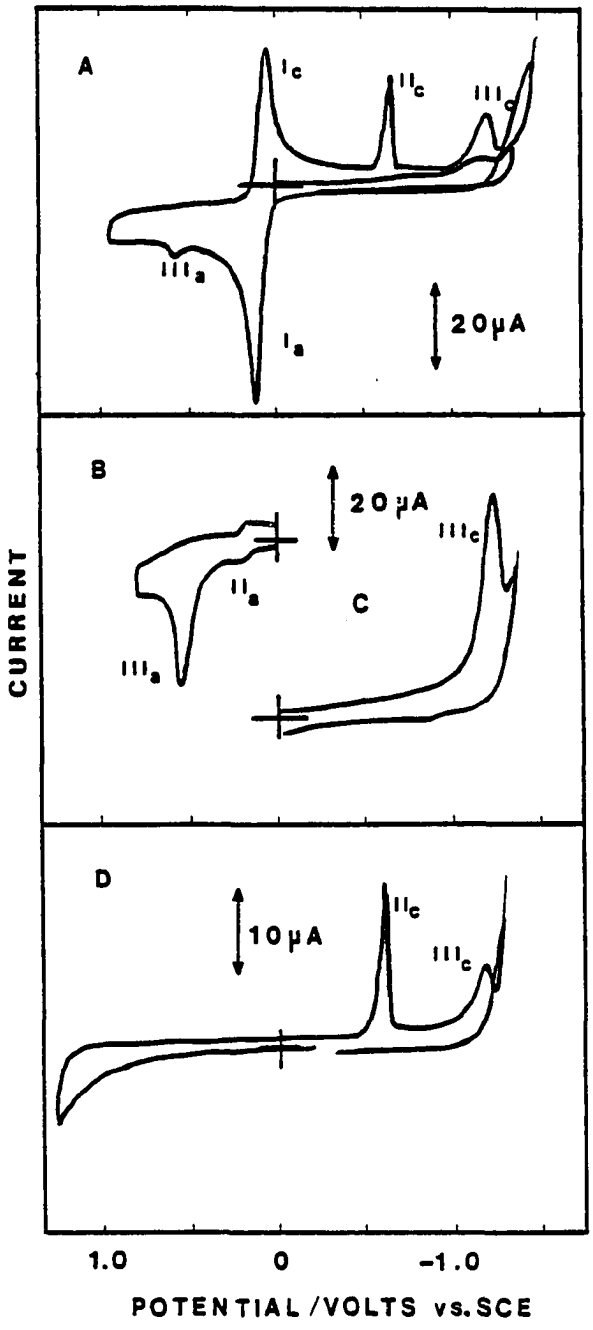

Figure 13. (A) Cyclic voltammogram of 0.34 mM 6,7-DMTHP in phosphate buffer pH 4.0 before electrolysis at +0.1V (peak I_a); (B) first positive sweep at completion of the electrolysis; (C) first negative sweep and (D) cyclic voltammogram of product after electrolysis at +0.4V (peak II_a). Sweep rate 200 mV s^{-1}.

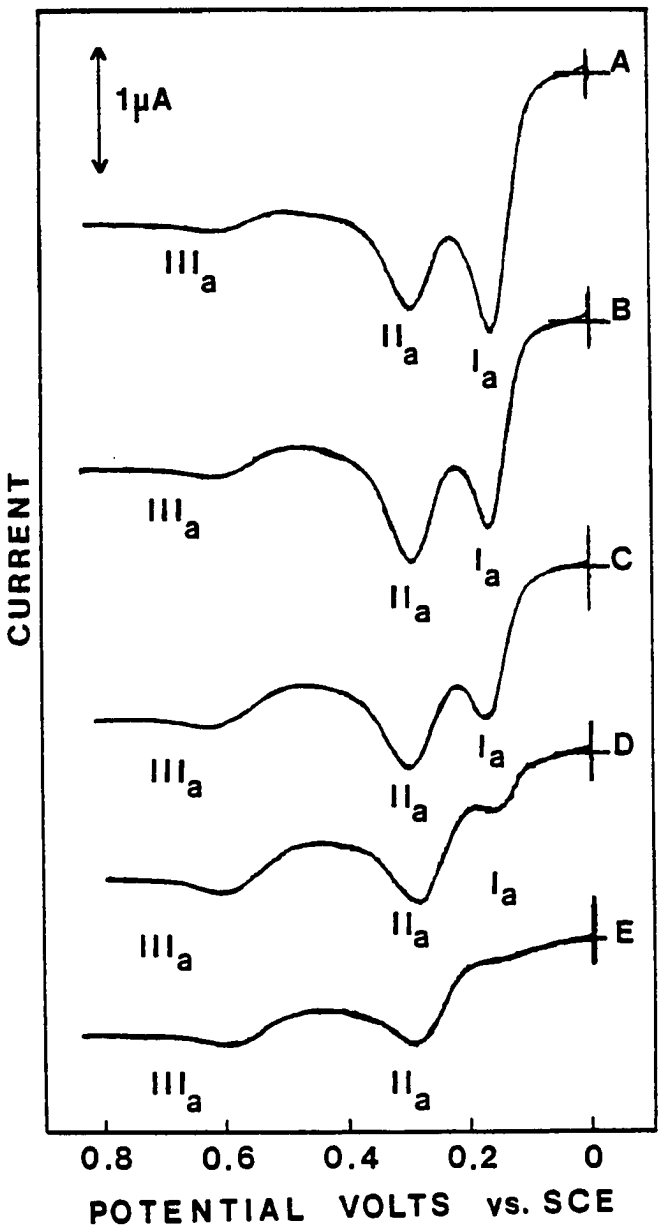

Figure 14. Single sweep voltammograms of 0.23 mM 6,7-DMTHP in phosphate buffer pH 3.1 recorded during the electrolysis (A) t=0, (B) at 2 hrs, (C) at 3.5 hrs, (D) at 9 hrs, (E) at 16 hrs of electrolysis. Scan rate 5 mV s^{-1}.

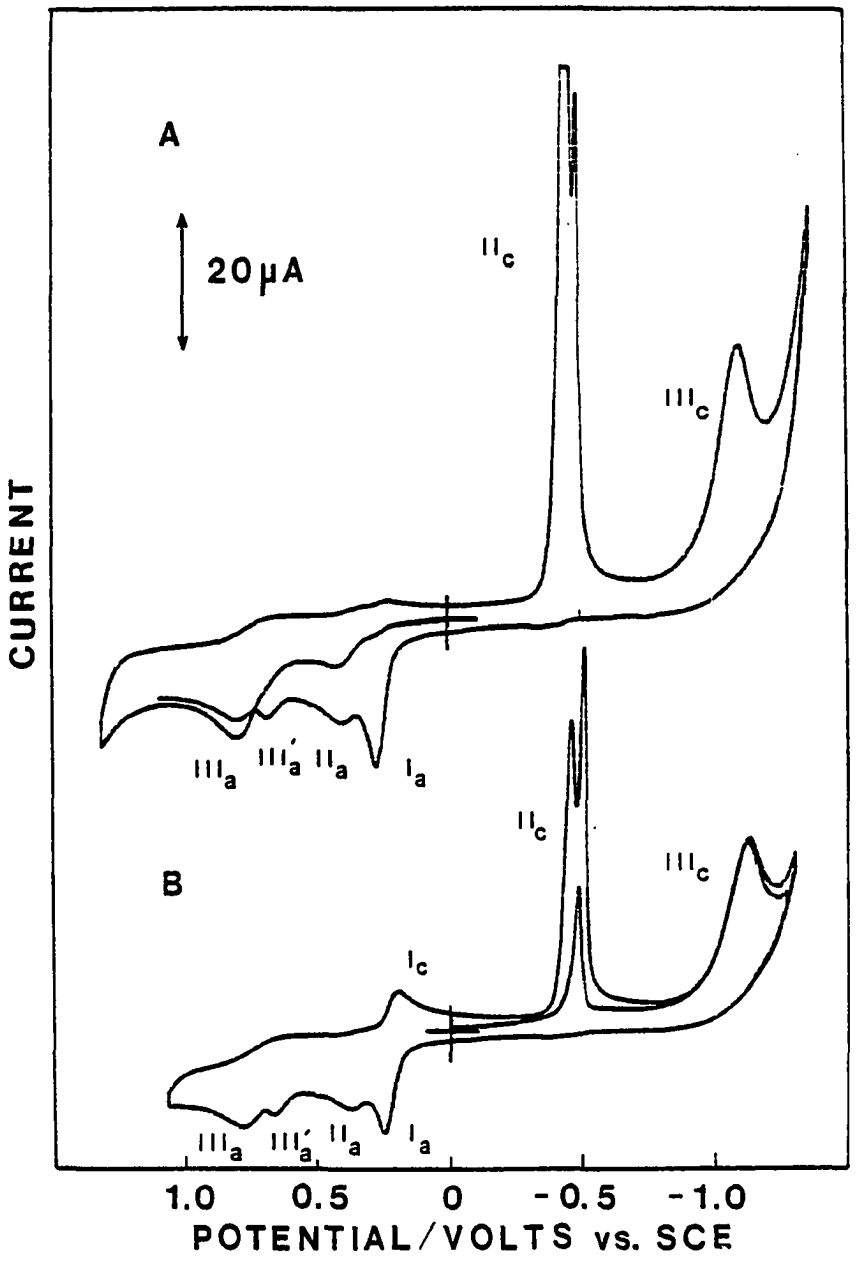

Figure 15. Cyclic voltammograms of 3.34 mM 6,7-DMTHP in phosphate buffer pH 2 at the end of electrolysis at peak I_a potentials. (A) initial sweep towards increasing positive potential, (B) initial sweep towards increasing negative potential.

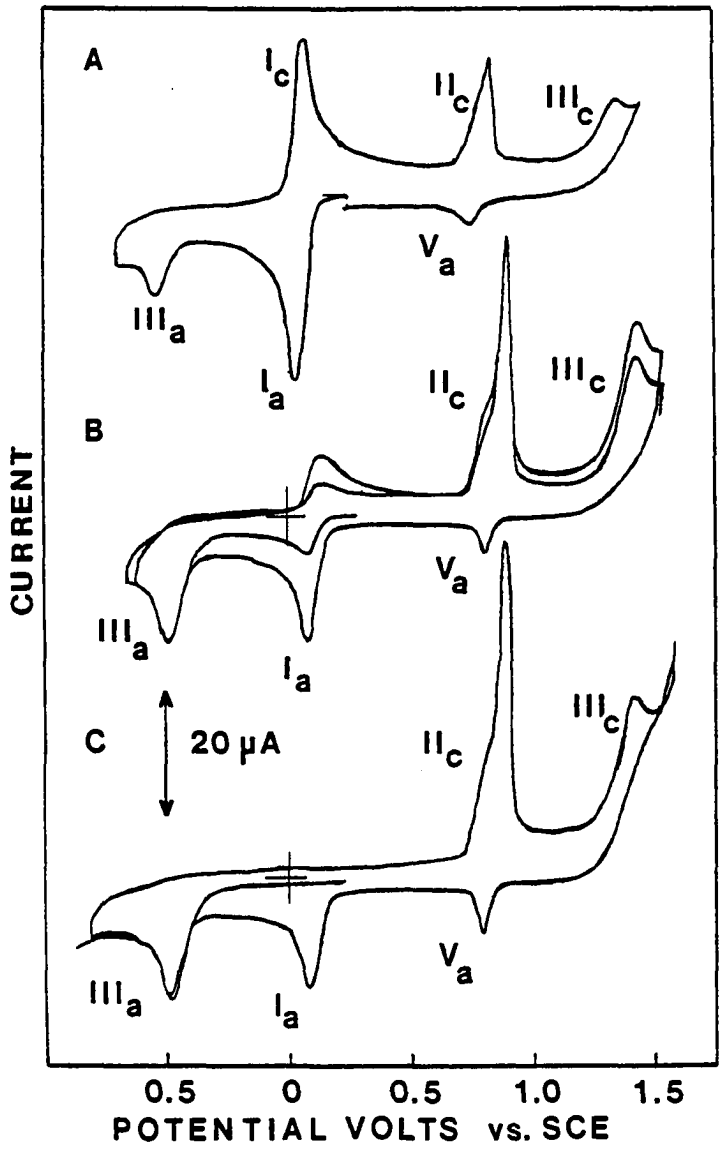

Figure 16. Cyclic voltammograms of 0.1 mM 6,7-DMTHP in phosphate buffer pH 7 (A) before electrolysis, (B) during electrolysis and (C) at the end of electrolysis at -0.1V (Peak I_a). Scan rate is 200 mV s^{-1}.

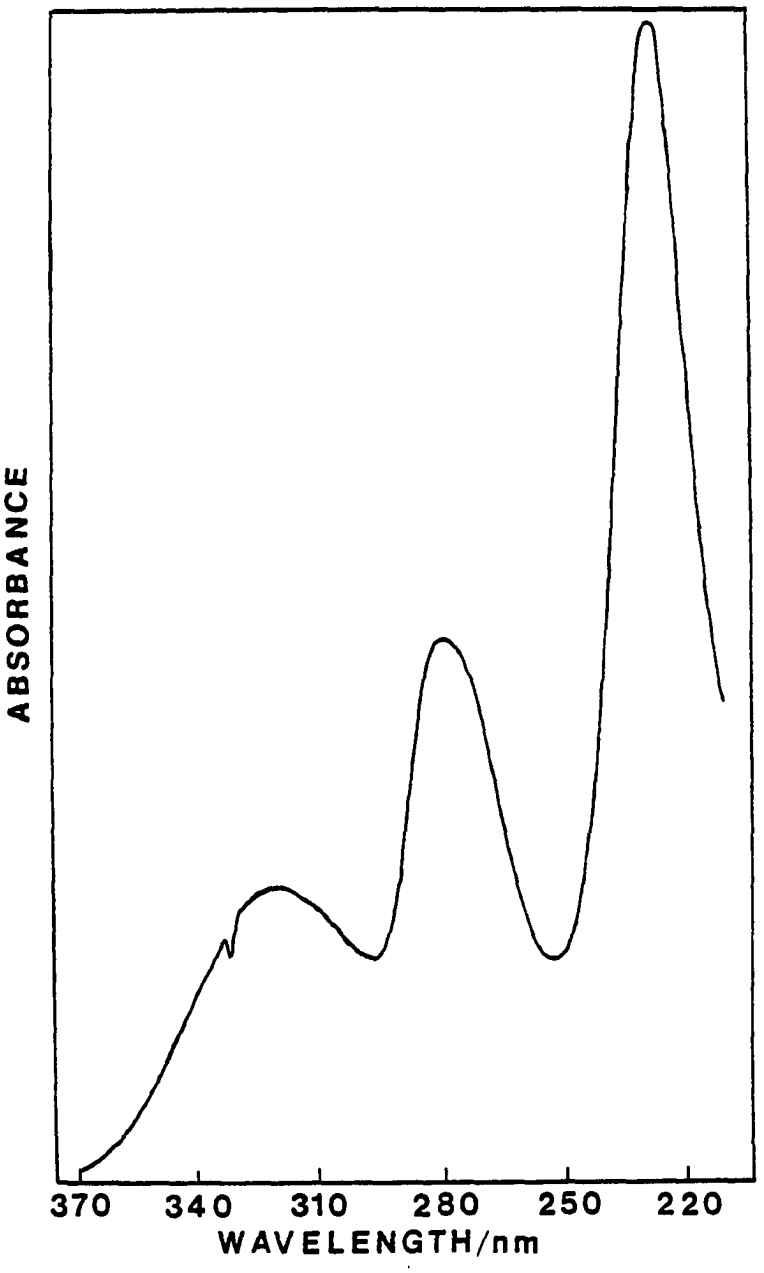

Figure 17. U.V. spectrum of the electrolysis product of 0.1 mM 6,7-DMTHP in phosphate buffer pH 7 at -0.1V.

significantly from that of 6,7-DMTHP (λ_{max} = 298 nm and 223 nm at pH 7).

Below ca. pH 4 coulometric oxidation of 6,7-DMTHP at potentials positive of peak II_a gave n-values close to four (3.8±0.2, Table 8). Voltammetry of the product revealed that peak III_a was also eliminated and that reduction peaks II_c and III_c were present (Fig. 13D). The U.V.-spectrum of the product of electrooxidation of 6,7-DMTHP at peak II_a or peak III_a potentials was identical with that of 6,7-DMP. For example, at pH 3.0 three U.V. bands were observed for the oxidation product at λ_{max} = 328 nm, 260 nm, and 212 nm which agreed with the spectrum of 6,7-DMP at the same pH. The voltammetric peak potentials observed for the product solution were also identical to those observed for 6,7-DMP.

The results of controlled potential coulometry clearly support the view that the peak I_a process of 6,7-DMTHP is a 2e reaction and that the peak II_a and peak III_a processes also involve overall, 2e. Since oxidation peak III_a is eliminated following electrooxidation at peak II_a potentials, it is clear that the species responsible for these peaks are in some sort of equilibrium, one form of the compound being oxidized in the peak II_a reaction, another in the peak III_a reaction. Voltammetric and spectrophotometric results reported earlier support the view that peaks II_a and III_a are due to electrooxidation

Table 8. Coulometric n-values obtained upon electrooxidation of 6,7-DMTHP at peak II_a and peak III_a potentials[a]

pH[b]	Initial Concentration of 6,7-DMTHP/mM	Applied Potential/ Volt vs. SCE	Experimental n-value
2.0	0.77	0.4 (peak II_a)	3.5
2.0	0.55	0.4	3.7
4.0	0.50	0.3 (peak II_a)	3.7
4.0	0.30	0.4	4.0
7.0	0.31	0.4 (peak III_a)	4.0
7.0	0.50	0.5	4.1
7.0	0.70	0.5	3.8
9.3	0.61	0.5 (peak III_a)	3.4
9.3	0.44	0.5	3.7
9.3	0.20	0.5	3.8

[a]Electrolyses carried out at a large PGE.

[b]Phosphate buffers having an ionic strength of 0.5 M.

of 6,7-DMDHP. Since oxidation peak II_a disappears between pH 4-5 it may be concluded that the species responsible for this peak is formed only at low pH. One way to account for these experimental observations is to assign peak II_a to the electrooxidation of a covalently hydrated form of 6,7-DMDHP (6,7-DMDHP·H_2O) (3) and peak III_a to the electrooxidation of the nonhydrated form of 6,7-DMDHP (4). The

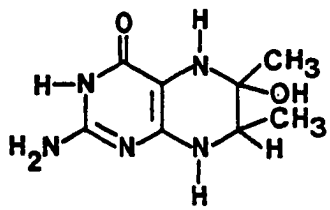

3

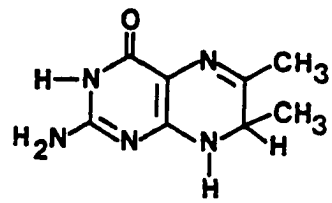

4

structure of the hydrated dihydro species (3) is very similar to that of 6,7-DMTHP which may explain why the oxidation potentials of peak I_a and II_a are so close.

In the coulometric experiments when a potential was applied corresponding to the rising portion of peak I_a at low pH values an additional reduction peak besides peak III_c was observed at the end of the electrolysis. This additional reduction peak appeared at potentials corresponding to peak II_c. The presence of this peak was puzzling. Since at low pH values peaks II_a and I_a are at very close potentials, it was possible that some of the

peak II_a species may have been oxidized to form 6,7-DMP. On the other hand, it has been reported that 6-methyl-5,6,7,8-tetrahydropterin (6-MTHP) and 5,6,7,8-tetrahydropterin (THP) may undergo reactions of the type shown in equation (4)[2] upon oxidation by chemical oxidants such as potassium ferricyanide.

$$QDHP + 7,8\text{-}DHP \rightarrow P + THP \qquad (4)$$

where

QDHP = quinonoid-dihydropterin

7,8-DHP = 7,8-dihydropterin

P = pterin

Therefore the possibility of such a reaction was considered. Scheme 1 shows the proposed reaction mechanism for the oxidation of 6,7-DMTHP in the presence of such a coupled reaction as was shown in equation (4).

k_1 = rate of rearrangement of the intermediate to 6,7-DMDHP

k_2 = rate constant for the reaction of 6,7-DMDHP with the intermediate (6,7-DMQDHP) to give 6,7-DMTHP and 6,7-DMP.

If $k_2 >> k_1$, then it would be expected that at high concentrations of 6,7-DMTHP controlled potential coulometric experiments would result in transfer of four electrons whereas at low concentrations of 6,7-DMTHP should give

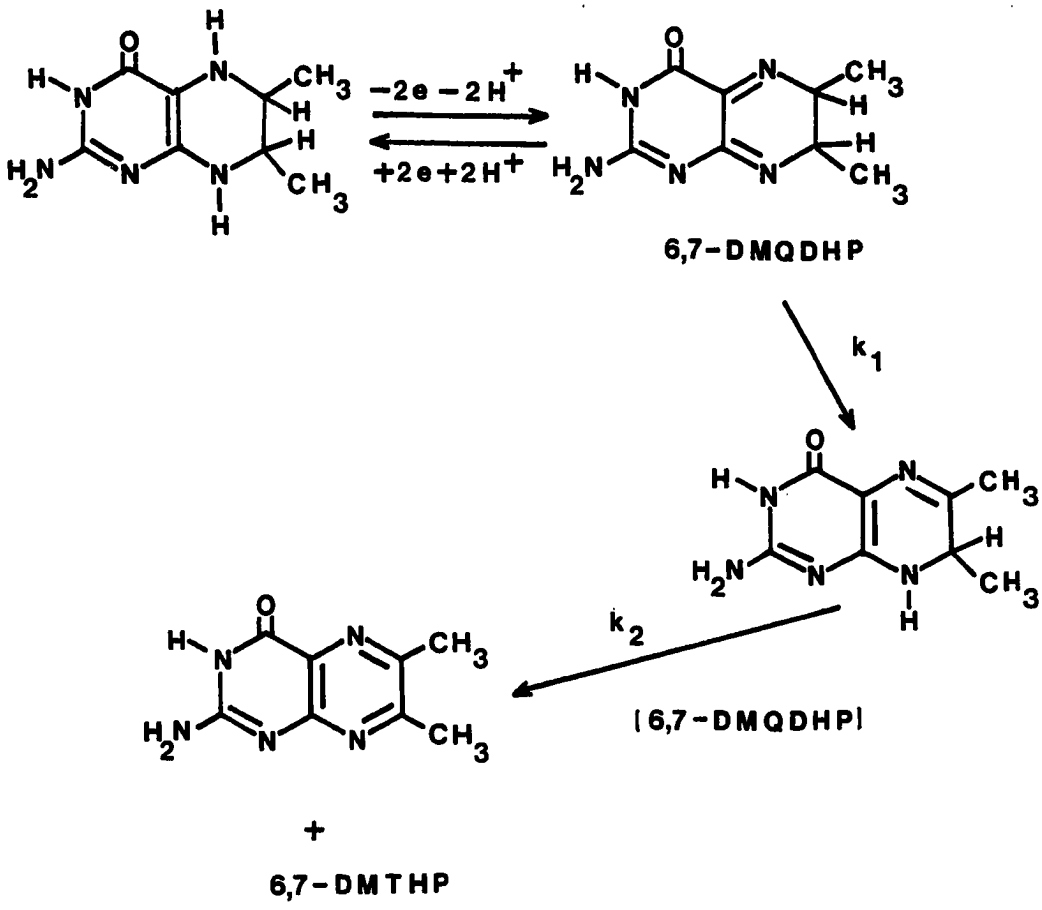

SCHEME 1

transfer of two electrons. The above statement would hold true only if the applied potential is kept at values which would oxidize the peak I_a species.

It was first believed that the increase in peak height of reduction peak II_c was due to the type of reaction mentioned above. But the experimental n-values obtained by oxidation at peak I_a potentials were always less than or equal to two. Cyclic voltammograms showed that peak II_a and peak III_a were still present at the end of the electrolysis, the spectra obtained were that of the peak II_a and III_a species. The fact that polarographic experiments done by Archer and Scrimgeour did not show any accumulation of the 6,7-DMP product, which would be the only product at the end of the electrolysis if the proposed reaction was taking place, made it clear that there had to be another explanation. It was decided that the increase in peak height of peak II_c when 6,7-DMTHP was electro-oxidized at peak I_a potentials was due to further oxidation of peak II_a. Since the increase in peak height of peak II_c, during the oxidation of peak I_a, occurs only at low pH values where peak I_a and II_a peak potentials are very close, the above explanation seemed to be more reasonable.

Further experiments were done to make certain whether there was an interaction between the intermediate species produced during the oxidation of peak I_a and the

first stable oxidation product. Thus, mixtures of the starting material 6,7-DMTHP and the first stable oxidation product (6,7-DMDHP) were electrolyzed at peak I_a potentials and coulometric n-values determined. If in fact there were a reaction of type (1), the n-value obtained would be between 2-4. Experimental n-values obtained with a 6,7-DMTHP:6,7-DMDHP mixture (1:1, 1:1.5 and 0.5:1) were less than 2 in all cases, thus indicating that there is no reaction between the unstable intermediate species and the first stable oxidation product, 6,7-DMDHP.

The experimental controlled potential coulometry results obtained with the 6,7-DMTHP:6,7-DMDHP mixture are summarized in Table 9. The results shown in Table 9 show that there is no reaction of 6,7-DMTHP of the type shown in equation (4). There is also no evidence for an interaction between 6,7-DMTHP and 6,7-DMDHP. The 0.5:1 6,7-DMTHP, 6,7-DMDHP mixture was injected on a HPLC column before and after electrolysis and as individual samples of 6,7-DMTHP and 6,7-DMDHP before mixing. Chromatograms obtained indicate that 6,7-DMDHP is the only oxidation product at the end of the controlled potential coulometric experiment. The chromatograms also showed that the starting materials were not pure and contained some 6,7-DMP (Fig. 18).

Coulometric experiments were carried out at high and low concentrations of 6,7-DMTHP to make certain that

Table 9. Coulometric n-values obtained upon electrooxidation of a 6,7-DMTHP: 6,7-DMDHP mixture at peak I_a potentials[a] (+0.2V) in phosphate buffer pH 3.1[b]

6,7-DMTHP:6,7-DMDHP (mM:mM)	n[c]
1:1	1.20[d]
1.5:1	1.86
0.5:1	1.82

[a]Data obtained using a large PGE working electrode.

[b]Phosphate buffers had an ionic strength of 0.5 M.

[c]Number of electrons involved in the electrooxidation process.

[d]This value is lower than expected, some of the 6,7-DMTHP may have been air oxidized thus resulting in low n.

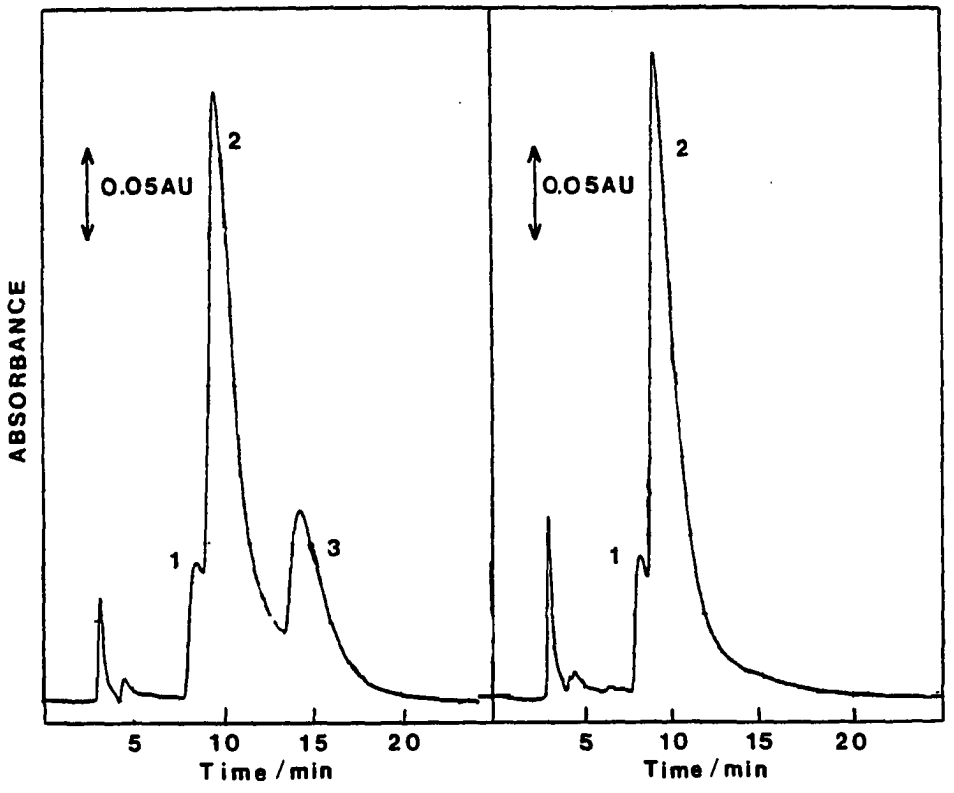

Figure 18. HPLC chromatograms of (A) 6,7-DMTHP:6,7-DMDHP mixture (0.5:1.0), (B) electrolysis product phosphate buffer pH 3.1, flow rate 0.83 ml/min. Peak (1) corresponds to 6,7-DMP, (2) to 6,7-DMDHP and (3) to 6,7-DMTHP.

there were no second order reactions such as dimerization. Applying a potential corresponding to the rising portion of peak I_a at low pH values, and a potential just positive of peak I_a at high pH values resulted in transfer of 1.9±0.2 electrons. Highly concentrated solutions (>15 m$\underline{M}$) turned yellow during the electrolysis and a very insoluble yellow product precipitated. At medium concentrations (5-10 m$\underline{M}$) solutions turned yellow but without any precipitate whereas at low concentrations (<5 m$\underline{M}$) no apparent change was observed. The coulometric $\underline{n}$-values obtained are given in Table 10.

Potentiostatic studies

Cyclic voltammetric evidence coupled with coulometric $\underline{n}$-value measurements indicated that the peak II_a/III_a process is a further 2$\underline{e}$ electrooxidation of 6,7-DMDHP formed by chemical reaction of the primary peak I_a product. If this is the case then electrolysis of 6,7-DMTHP at peak II_a or peak III_a potentials should be an e.c.e. reaction (equation 5).

$$\text{6,7-DMTHP} \xrightarrow[E]{-2e} \text{INTERMEDIATE} \xrightarrow[C]{k_1} \text{6,7-DMDHP} \xrightarrow[E]{-2e} \text{6,7-DMP} \qquad [5]$$

In order to verify this mechanism the potentiostatic method of Alberts and Shain[19] was employed.

In this method the potential of a stationary micro-

Table 10. Coulometric n-values obtained upon electro-oxidation of 6,7-DMTHP at peak I_a in phosphate buffer

pH	concn. (mM)	n	E (V)
3.1	0.1	1.9	+0.2
	0.5	2.1	+0.2
	1.0	2.2	+0.2
	7.0	1.6	+0.2
6.0	0.2	1.8	0.0
	2.0	1.6	+0.1
	27.4	1.9	+0.2
7.0	0.5	2.1	+0.2

electrode is stepped to a value at which all of the electroactive substance which reaches the electrode surface is immediately oxidized. The resulting current is then monitored as a function of time. At short times the observed current corresponds to the first electron transfer step. But at longer times there is a transition to a current corresponding to both electron transfer reactions. The time at which the transition occurs depends upon the rate of the intervening chemical reaction.

The equation describing the instantaneous current for an uncomplicated electrochemical reaction of a substrate at a planar electrode under semi-infinite linear diffusion control is known as the Cottrell equation[11] (equation (6).

$$i_t = \frac{nFAD^{1/2}C}{\pi 1/2 t^{1/2}} \qquad (6)$$

where

i_t = current at time (t) in amperes

n = total number of electrons involved in the electrochemical step

A = electrode area, cm^2

D = diffusion coefficient of the electroactive species, $cm^2\ s^{-1}$

C = concentration of electroactive species in moles ml^{-1}

For a given value of concentration, the value of

$it^{1/2}$ should remain constant, if the system is diffusion controlled. In the case of 6,7-DMTHP for periods of up to 6.0 seconds, the product $it^{1/2}$ increased somewhat (as much as 10-15%) with increasing time at the PGE. At times less than 10 seconds, linear diffusion to a planar electrode, i.e., equation 6, can be used with little error.[11] At times greater than 8-10 seconds, linear diffusion is no longer the only mode of mass transport. Because the electrodes used are not shielded there is convection and hence the Cottrell equation (6) is no longer applicable.[11]

The theoretical equation relating current to time for an e.c.e. process[18] is:

$$i_t = \frac{FAD^{1/2}[n_1+n_2(1-e^{-k_f t})]}{\pi^{1/2} t^{1/2}} \qquad (7)$$

where

i_t = instantaneous current at time t (μA)

n_1 = number of electrons involved in the first electron transfer step

n_2 = number of electrons involved in the second electron transfer step

t = time elapsed since the application of potential (s)

k_f = homogeneous rate constant for the chemical reaction, s^{-1}

The remaining terms have their usual meaning.

The number of electrons transferred in the first and second electrode processes have been determined coulometrically and $n_1=n_2=2$. There are two limiting cases for equation (7), i.e., when $k_f=\infty$ and when $k_f=0$. When $k_f=\infty$, the interposed chemical reaction is so rapid that a Cottrellian n_1+n_2 electron transfer is observed. When k_f is close to zero the rate of the chemical reaction is very slow so that only an n_1 electron transfer process takes place. For each limiting case, equation (7) reduces to the Cottrell equation for a (n_1+n_2) electron and n_1 electron process, respectively. Theoretical normalized current $(i_t/FAD^{1/2}C)$ vs. $t^{-1/2}$ curves were calculated for n=2 and n=4 for $k_f=0$ and $k_f=\infty$, respectively. Experimental curves revealed that at very short times the normalized current was close to that expected for a 2 electron diffusion controlled reaction, while at longer times the curve deviated from a 2 electron process and approached the theoretical 4 electron curve (Fig. 19).

The value of k_f can be obtained from the theoretical curves by comparing the experimental curve with theoretical ones using different k_f values. The experimental curve obtained for a 0.24 mM solution of 6,7-DMTHP in phosphate buffer pH 5.6 agreed very well with the theoretical curve which was calculated with $k_f = 4.05 \times 10^5\ s^{-1}$. Table 11 summarizes the experimental data at various times after application of the applied potential. The theoretical

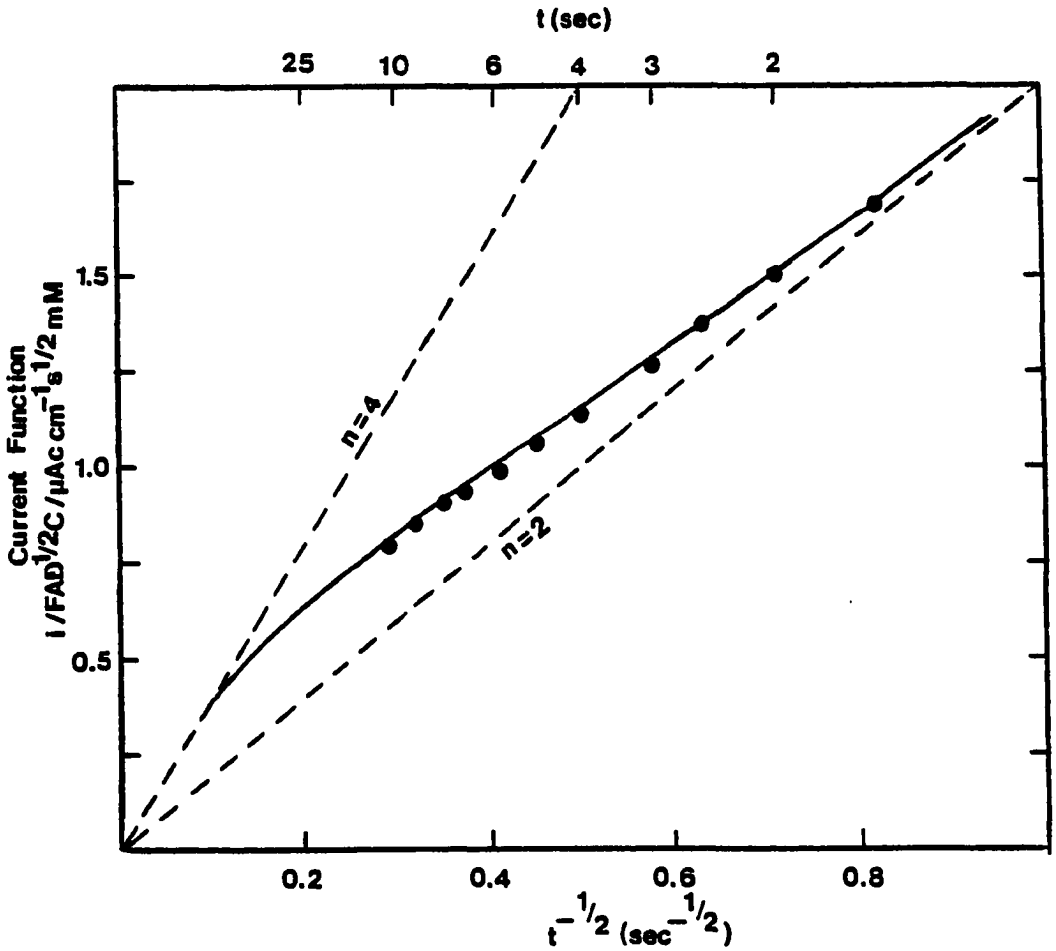

Figure 19. Comparison of theoretical and experimental current vs. time curves for the electrochemical oxidation of 0.25 mM 6,7-DMTHP at the PGE in phosphate buffer pH 5.6. Experimental values (●); theoretical curve calculated for a solution rate constant, k, of 4.05×10^{-2} s^{-1} (-); and theoretical curves for uncomplicated 2e and 4e transfer processes (----).

Table 11. Experimental and theoretical data for potentiostatic studies of 1 mM 6,7-DMTHP in phosphate buffer pH 5.6

t (s)	i_t (μA)	$i_{exp}{}^a/FAD^{1/2}C^b$	$i_{th}{}^b/FAD^{1/2}C^b$
6.00	5.16	0.56	0.56
5.50	5.30	0.58	0.58
5.00	5.50	0.60	0.60
4.50	5.70	0.62	0.62
4.00	5.90	0.64	0.65
3.50	6.20	0.67	0.69
3.00	6.60	0.72	0.73
2.50	7.20	0.78	0.78
2.00	7.80	0.85	0.86
1.50	9.10	0.99	0.98
1.00	10.60	1.15	1.17
0.80	11.40	1.24	1.30
0.60	14.30	1.55	1.49
0.50	15.30	1.66	1.62
0.40	16.90	1.83	1.81
0.30	20.00	2.17	2.09
0.25	21.40	2.32	2.55
0.20	24.20	2.63	2.93
0.15	32.70	3.55	3.58

[a] Experimentally measured i_t using $A = 3.7 \times 10^{-2}$ cm^2

$D^{1/2} = 2.58 \times 10^{-3}$ cm^{-1} s$^{-1/2}$

[b] Theoretically calculated i_t using $\frac{n_1+n_2\ (1-e^{-k_f t})}{t^{1/2}\ \pi^{1/2}}$

$n_1 = n_2 = 2$

$k_f = 4.05 \times 10^{-2}$ s^{-1}

normalized current values are also listed in Table 11. The potentiostatic studies were carried out only at pH 5.6 which appears to be the pH at which the rearrangement reaction is fastest. At other pH values the rate of the chemical reaction is too slow for diffusion controlled conditions to be maintained at the electrode. The value for $it^{1/2}$ is not constant at times longer than 10s probably due to processes such as convection caused by build up of concentration gradients in solution. Therefore, the Cottrell equation cannot be used for the evaluation of k_f at other pH values.

Experimental current-time curves revealed that at very short times the current was close to that expected for a 2 electron reaction (Fig. 19). At longer times the curve deviated and became close to the theoretical 4 electron curve (Fig. 19). These results are in good agreement with the coulometric n-values determined and they verify the e.c.e. mechanism proposed for the electro-oxidation of 6,7-DMTHP.

Thin-layer spectroelectrochemistry

Cyclic voltammetry of 6,7-DMTHP indicated that the peak I_a process involved a 2e oxidation to form an unstable intermediate species which undergoes a chemical follow-up reaction leading to 6,7-DMDHP. In order to gain some additional insights into the behavior of the intermediate

species, thin-layer spectroelectrochemical studies first proposed by Murray et al.[18] were carried out.

Several proposed spectra of the quinonoid-dihydropterin have been reported from studies of enzymic and chemical oxidation reactions.[5,20-22]

Because of the unstable nature of the quinonoid-dihydro intermediate it has not been possible to isolate this species and determine its structure. In fact there are five possible quinonoid structures which can be assigned to this intermediate. These possible structures will be discussed in a later chapter.

Since the intermediate species formed in the primary peak I_a electrooxidation process has a quinonoid structure, its U.V. spectrum was expected to be different to that of the parent 6,7-DMTHP or its stable chemical reaction product 6,7-DMDHP.

It was anticipated that by monitoring the U.V.-visible spectrum of an electrolyzing solution of 6,7-DMTHP any transient but absorbing intermediate could be detected and characterized by its absorption spectrum.

Initial spectroelectrochemical measurements were carried out in optically transparent thin-layer cells with a gold minigrid sandwiched in between two quartz slides.

Electrolysis potentials for thin-layer spectroelectrochemical studies at the gold minigrid electrode were chosen from linear sweep voltammograms run at a gold foil

electrode. Freshly deaerated sample solutions were used for each run at each pH value studied. A special sample holder was used, as described in the experimental section. Nitrogen was passed over the solution during the experiment to prevent air oxidation of the sample.

At pH 3, 6,7-DMTHP in a gold-minigrid thin-layer cell shows two absorption peaks (λ_{max} = 218 nm and 266 nm). The compound at this pH is a singly charged cation, the positive charge being located at N(5). Upon application of a potential corresponding to peak I_a both of the absorption bands decrease and a new absorption band at about 338 nm starts to grow in. When the applied potential is turned off the band at 338 nm continues to increase and another absorption band at ca. 246 nm starts to grow in. When the applied potential is turned off no electrochemical products may be produced, hence the change in absorption after the system has been open-circuited must be due to a chemical reaction. Although it was not possible to definitely identify a spectrum due solely to the intermediate, the quinonoid-dihydro species generated clearly absorbs at 338 nm and 294 nm, because after the potential is turned off the band at 338 nm shifts to longer wavelengths (λ_{max} $\sim$346 nm) and the absorbance at 294 nm decreases.

At pH 7.6, 6,7-DMTHP is in a neutral form and has two absorption bands (λ_{max} = 300 nm and 234 nm). Upon

application of a potential corresponding to peak I_a the absorption band at 300 nm decreases and splits into two new bands (λ_{max} = 305 nm, 283 nm). There is also a broad absorption band between 360-400 nm. When the potential is turned off, the absorbance at 234 nm and between 360-400 nm decreases and a new absorption band at 320 nm grows in. Two additional absorption bands at λ_{max} = 282 nm and 240 nm are also observed. The absorbance at 300 nm subsequently decreases. The final spectrum obtained after there is no longer any changes in absorbance corresponds to that of 6,7-DMDHP. The observed spectra suggest that the intermediate species generated absorbs between 360-400 nm and at 300 nm. Although several approaches were tried to obtain a definitive spectrum of the intermediate species (e.g., a very positive potential was applied for a few seconds so that the electrochemical generation of the intermediate was much faster than its chemical reaction, and cooled N_2 was passed over and around the solution to slow down the rearrangement reaction), it was not possible to record a spectrum of only the intermediate. It was concluded therefore that the absorption characteristics of the intermediate were not very different from those of 6,7-DMTHP.

The potential window at a gold minigrid electrode is relatively narrow compared to that of a reticulated vitreous carbon electrode. Also the thickness of a gold

minigrid thin-layer cell is much smaller than a reticulated vitreous carbon (RVC) thin-layer cell which, therefore, does not require the use of highly concentrated solutions. Because of numerous advantages of RVC thin-layer electrodes over gold minigrid electrodes, further work was carried out in a specially designed RVC thin-layer cell (see experimental section). It was observed that the spectro-electrochemical behavior of 6,7-DMTHP at the RVC electrode was very similar to that noted at the gold minigrid electrode.

A spectrum of 6,7-DMTHP at pH 3.0 (λ_{max} = 264 nm and 212 nm) in a thin-layer cell containing an optically-transparent RVC electrode is shown in curve 1 of Fig. 20. Upon application of a potential such that the peak I_a oxidation occurs, both U.V. bands of 6,7-DMTHP decrease while the absorbance around 240 nm and 340 nm increases. Curve 2 in Fig. 20A corresponds to the spectrum observed about 40s after initiation of the electrooxidation of 6,7-DMTHP. Curve 1 in Fig. 20B is the spectrum of 6,7-DMTHP; curve 2 is the spectrum observed when essentially all of the 6,7-DMTHP has been oxidized and the applied potential is turned off. With time the shoulder at ca. 266 nm continues to increase as does the absorbance centered at ca. 212 nm and the band at $\lambda_{max} \approx 300$ nm decreases, a new band grows in at λ_{max} = 250 nm. It was also noticeable that the broad band which originally grew in at λ_{max} = 340

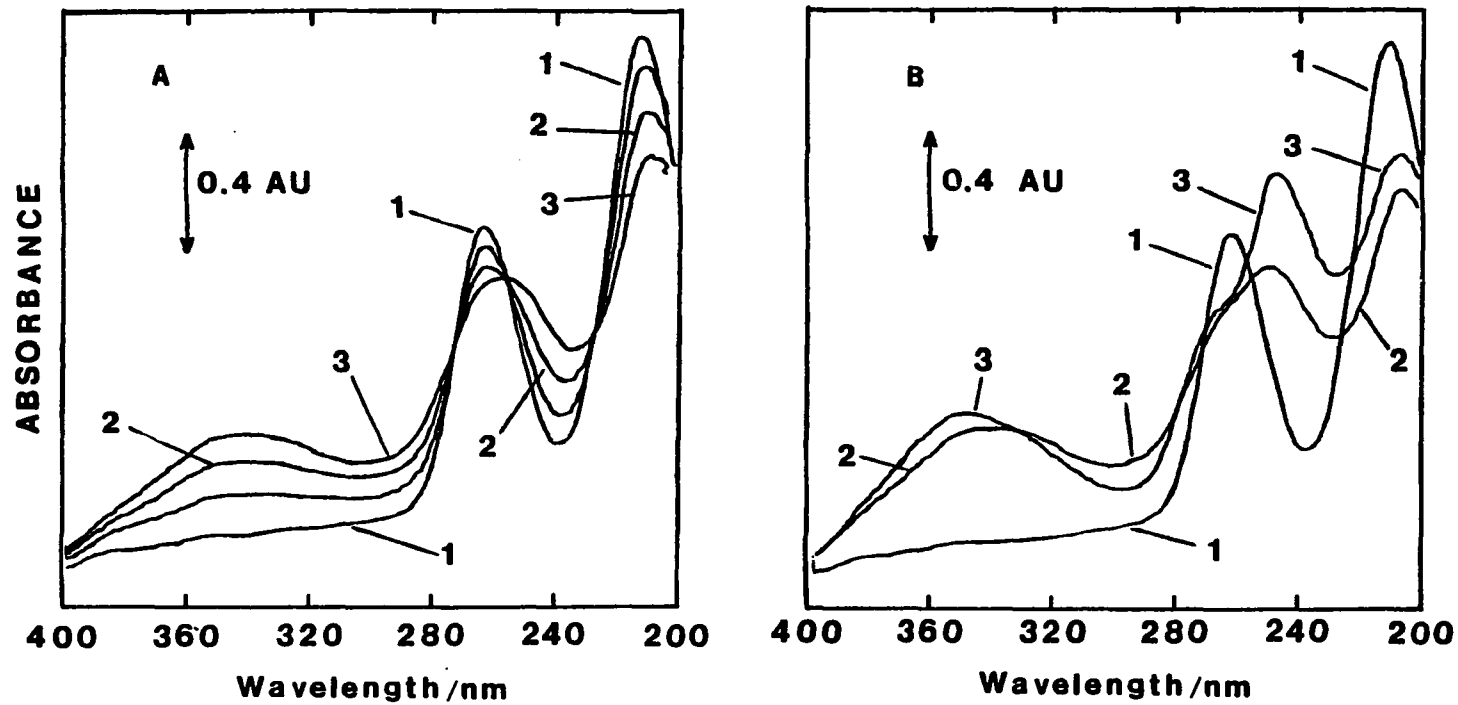

Figure 20. Spectrum of 1.26 mM 6,7-DMTHP electrolyzing at 0.3V in phosphate buffer pH 3.0 at a reticulated vitreous carbon electrode in a thin-layer cell. (A) Curve 1 is 6,7-DMTHP before electrolysis, curve 2 is the spectrum after 40s of electrolysis and curve 3 after 60s of electrolysis. (B) Curve 1 is the spectrum before electrolysis, curve 2 is the spectrum after 60s electrolysis at a point where all 6,7-DMTHP has been oxidized, curve 3 is the spectrum after complete decay of the intermediate species and corresponds to 6,7-DMDHP.

nm shifts towards longer wavelengths with time (Fig. 20B). Curve 3 in Fig. 20B is the spectrum of the final product formed upon electrooxidation of 6,7-DMTHP at peak I_a potentials and corresponds to that of 6,7-DMDHP.

Somewhat different spectroelectrochemical behavior was observed at higher pH. For example, at pH 9.3 6,7-DMTHP exhibits two absorption bands (λ_{max} = 220 nm and 300 nm, Fig. 21A, curve 1). Upon application of a potential corresponding to oxidation peak I_a both bands decrease but the absorbance between 320-400 nm and at ca. 226 nm increases (Fig. 21A curves 2 and 3). If, after all of the 6,7-DMTHP has been electrooxidized, the applied potential is turned off, absorption bands at λ_{max} = 226 nm and λ_{max} = 280 nm begin to grow in and, correspondingly, the absorbance between about 340-400 nm and 325-290 nm decreases. The spectrum of the final product obtained following such changes is identical to that of 6,7-DMDHP (Fig. 21B, curve 3).

Such spectroelectrochemical results indicate that electrooxidation of 6,7-DMTHP at peak I_a potentials generates an intermediate species which disappears in a chemical follow-up reaction to give 6,7-DMDHP. Selected absorbance vs. time curves are shown in Fig. 22.

A first order rate law can be written for the change in concentration of the intermediate with time as follows:

$$-\frac{d[I]}{dt} = k[I] \qquad (8)$$

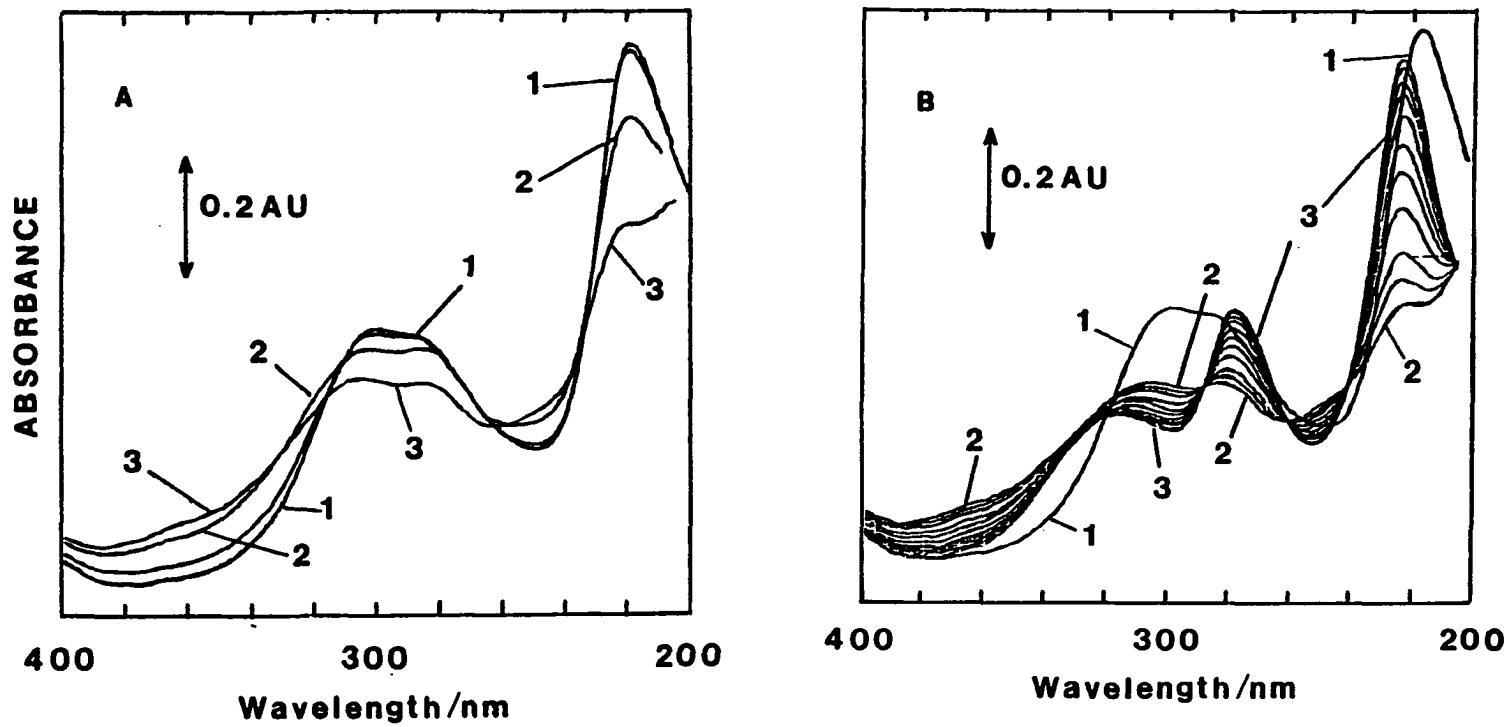

Figure 21. Spectrum of 1.68 mM 6,7-DMTHP electrolyzing at -0.03V in phosphate buffer pH 9.3 at an RVC electrode in a thin-layer cell. (A) Curve 1 is 6,7-DMTHP before electrolysis, curve 2 is the spectrum after 188s and curve 3 after 282s of electrolysis at a point where all 6,7-DMTHP has been electrolyzed, and curve 3 is the spectrum after complete decay of the intermediate species. Curve 3 is identical to the spectrum of 6,7-DMDHP. Repetitive scans of 94s are shown.

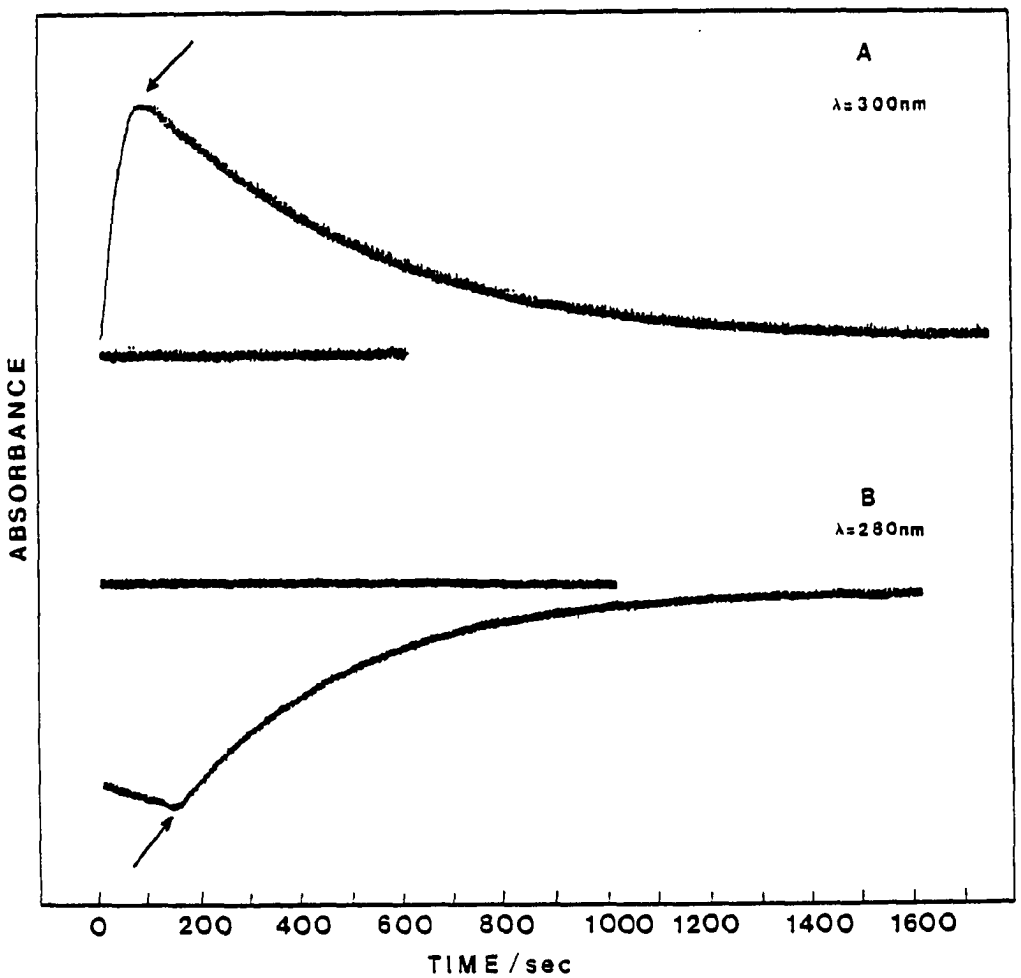

Figure 22. Typical absorbance vs. time curves obtained in an optically transparent RVC thin-layer cell (A) 1.0 mM 6,7-DMTHP electrolyzed in phosphate buffer pH 9.3, (B) 1.24 mM 6,7-DMTHP electrolyzed in phosphate buffer pH 8.0. The arrows indicate the point at which the potential was turned off.

where

[I] = concentration of the intermediate

The rate constant is then a positive quantity and has units of the reciprocal of time. Thus, experimental results were obtained by comparing absorbance, which is related to concentration, at various times. Such data can better be compared with the integrated form of the first order rate law. If the initial absorption, at time t=0, is A_o, and if at some later time t, the absorption changes to A, integration results in

$$-\int_{A_o}^{A_t} \frac{dA}{A} = k\int_{o}^{t} dt \qquad (9)$$

and

$$-\ln \frac{A_t}{A_o} = \ln \frac{A_o}{A_t} = kt \qquad (10)$$

a more convenient form is

$$\log A_t' = \frac{k}{2.303} t + \log A_o \qquad (11)$$

where

$$A_t' = A_t - A_\infty$$

If a plot of A_t' vs. t gives a straight line, the reaction is first order. The slope of this line can be used to calculate k. For 6,7-DMTHP, under all conditions studied, plots of log A_t' vs. t were linear. Thus the rearrangement

of the intermediate follows first-order kinetics.

The kinetics of the follow-up reaction at the RVC electrode were studied between pH 3-9.3 by a thin-layer spectroelectrochemical method by either monitoring the decay of the U.V. absorbance of the intermediate species or the increase in absorbance of 6,7-DMDHP, i.e., the reaction product. At all pH values the follow-up reaction was found to be first order. Values of the observed rate constants (k_{obs}) at the RVC electrode are presented in Table 12 and in Fig. 23.

The curve describing the dependence of the observed rate constant on pH is bell shaped, reaching a maximum at around pH 6. A bell shaped curve can usually be accounted for in terms of two acid-base dissociations of the substrate.[23] Archer and Scrimgeour[5] assume the pK_a values for the 6,7-dimethylquinonoid-dihydropterin as being equal to 4.2 (presumably for N(5)) and 10.4 (for the amide nitrogen). It is expected that the conjugate acid and conjugate base forms will undergo reactions at different rates.[23] Archer and Scrimgeour[5] explain the bell-shaped rate constant profile as a function of pH as a general acid-base catalysis of the breakdown of the quinonoid intermediate. Base catalysis is explained by attack of the base at position 6 (5) followed by a rapid transfer of a proton, probably from a water molecule, in a step that would not be detected kinetically.[5] Acid catalysis is explained by

Table 12. Observed first-order rate constant for reaction of the primary peak I_a electrooxidation product 6,7-DMTHP as a function of pH

pH	k_{obs}/s^{-1}[a]	$\sigma x10^2$[b]
2.0	0.014	0.08
3.1	0.023	0.12
4.0	0.029	0.25
5.6	0.030	0.57
6.0	0.043	0.19
6.8	0.048	0.44
7.0	0.020	
8.0	0.0074	0.19
9.3	0.0054	0.02

[a]Mean of at least three determinations.

[b]Standard deviation. Data was obtained using a thin-layer spectroelectrochemical method in an optically transparent reticulated vitreous carbon electrode.

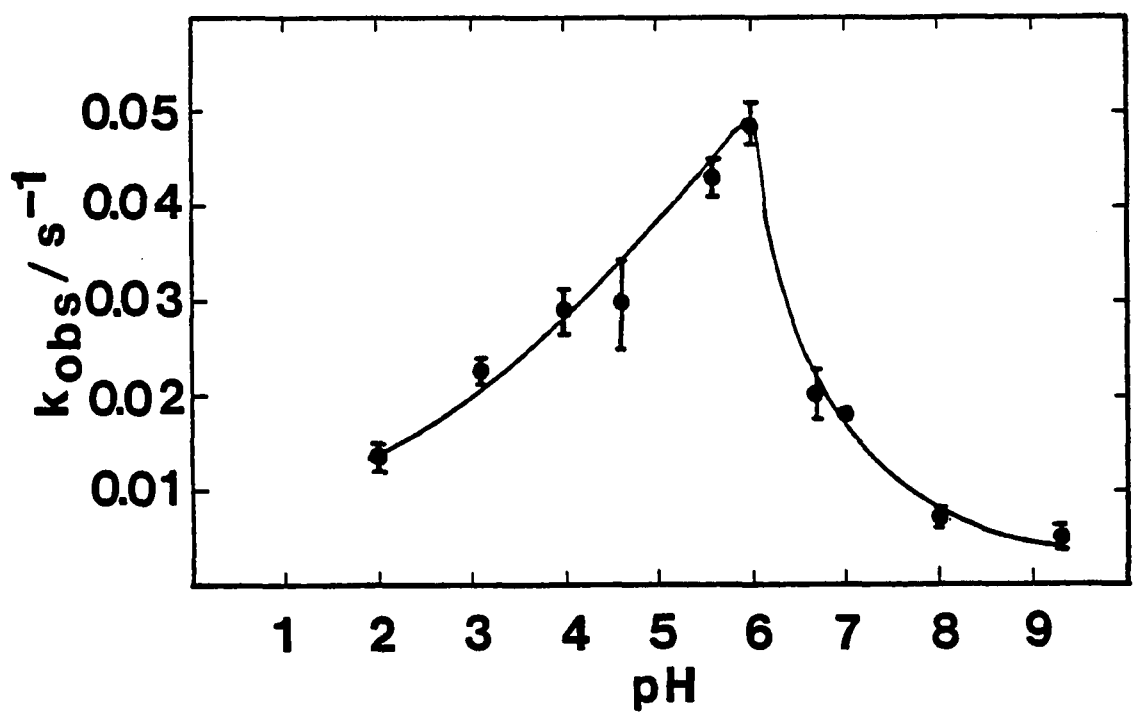

Figure 23. Variation of the observed first-order rate constant for the chemical reaction of the peak I_a electro-oxidation product of 6,7-DMTHP to give 6,7-DMDHP as a function of pH. Data obtained by a thin-layer spectroelectrochemical method using an optically transparent reticulated vitreous carbon electrode. Phosphate buffers were used at all pH values which had an ionic strength of 0.5 M.

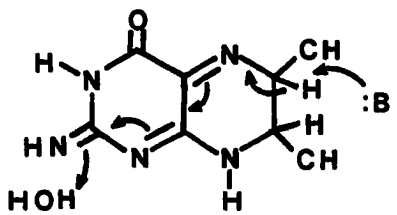

5

donation of a proton either to the imino nitrogen or to N(5), though they claim that the former is more likely. Because it is observed from deuterium isotope effect that breaking of the carbon-hydrogen bond at C(6) is rate limiting the scheme shown in equation (12) is favored.[5]

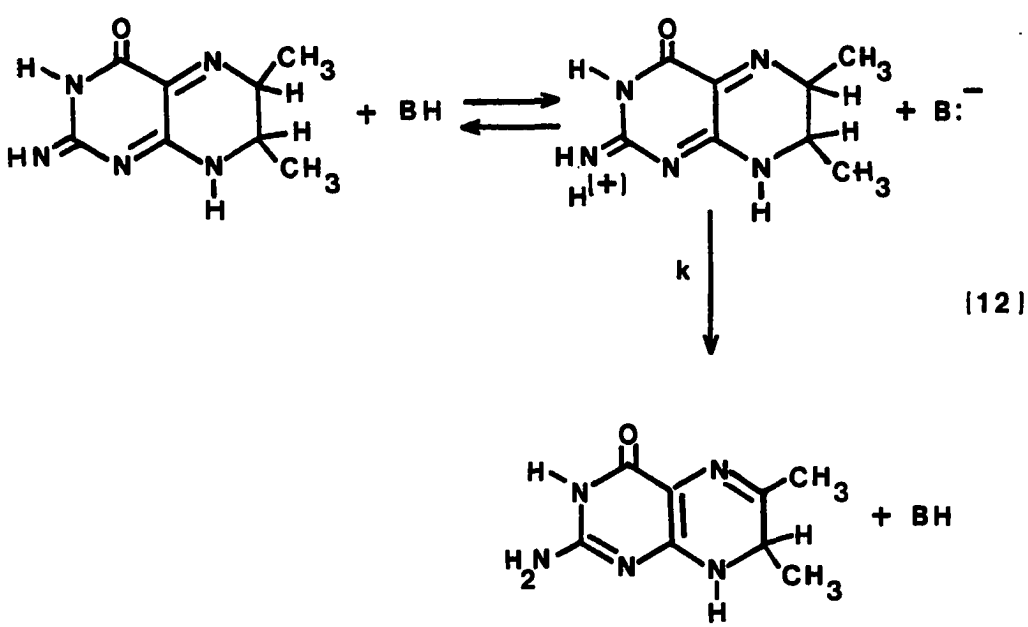

[12]

It has been reported that changing the buffer constituents used causes a change in the observed rate constants.[5] The rate constant has also been reported to be dependent on the concentration of buffer used.

The effect of ionic strength on the rate of the follow-up reaction was investigated at pH 3.1 and 5.6. It was observed that decreasing the ionic strength decreased the rate of the rearrangement reaction. The observed first-order rate constants as a function of ionic strength are summarized in Table 13.

It is also clear that there is a direct relationship between the ionic strength of the buffer and the observed pseudo first-order rate constant. As the ionic strength increases, the rate of rearrangement reaction also increases in almost direct proportion. Archer and Scrimgeour[5] reported that a direct relationship exists between the buffer concentration and the measured rate constant.

6,7-Dimethyl-7,8-dihydropterin

The pK_a values of 6,7-DMDHP are reported to be 4.16[15] and 10.4.[5] At pH <4, 6,7-DMDHP may potentially exist in four different forms which are in equilibrium with one another as shown in equation 13. Although these four species may exist in equilibrium in aqueous solution, only two oxidation peaks (II_a and III_a) are observed at

Table 13. Effect of ionic strength on the observed first-order rate constant for the chemical reaction of the peak I_a electrooxidation in phosphate buffer pH 5.6

μ (M)	concn. (mM)	$k_{obs} \times 10^2$ (s^{-1}) [b]
0.1	0.96	1.24±0.14
0.2	0.60	1.84±0.26
0.5	1.07	4.73±1.24

[a] Ionic strength

[b] Rate constants were measured at λ = 280, 284, 300, 372 and 380 nm.

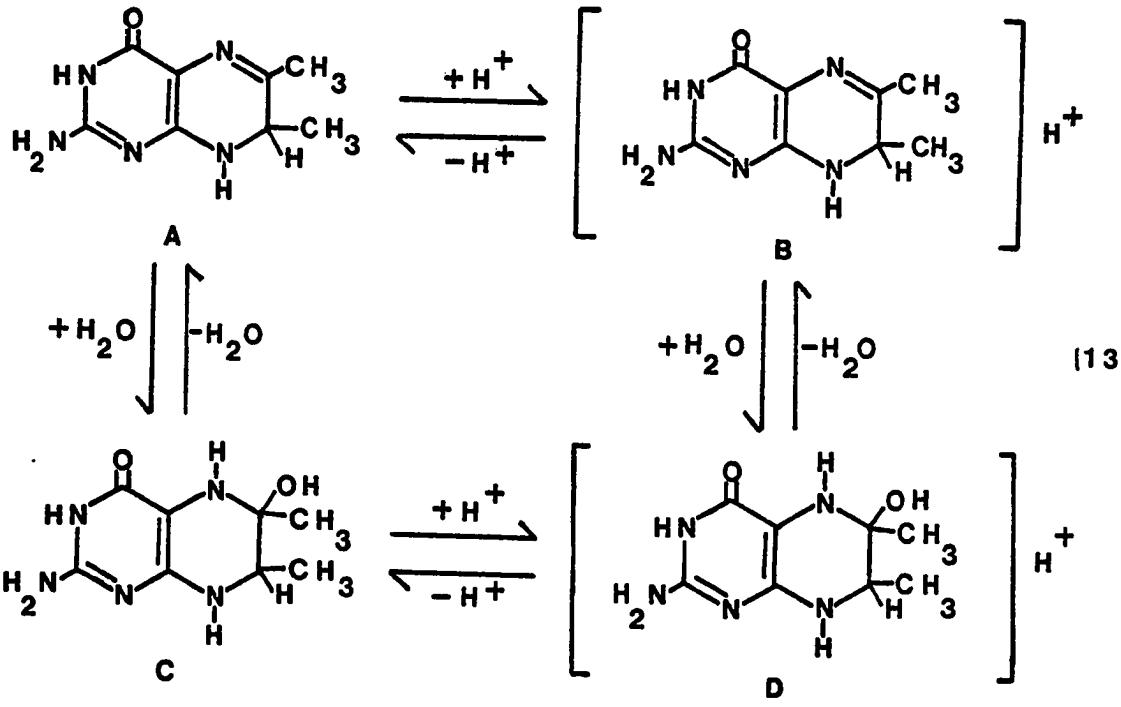

[13]

low pH values at the PGE at a sweep rate of 5 mV s^{-1}. A third oxidation peak very close to the background discharge current may be observed occasionally due to oxidation of 6,7-DMP. The variation of peak potential with pH for peaks II_a and III_a are given by the following equations (Fig. 4):

Peak II_a (pH 2.0-4.9): E_p =[0.48-0.054 pH]V

Peak III_a (pH 2.0-4.0): E_p =[0.86-0.076 pH]V

(pH 4.0-10.0): E_p =[0.66-0.024 pH]V

(pH 10.0-11.6): E_p =[1.35-0.092 pH]V

The peak potentials for peak II_a and peak III_a of 6,7-DMDHP are in good agreement with the peak potentials observed for peaks II_a and III_a of 6,7-DMTHP.

Below pH 4.8 and at slow sweep rates (5 mV s^{-1}), 6,7-DMDHP normally gives rise to peaks II_a and III_a, whereas above pH 4.8 only peak III_a is observed. At slow scan rates and below pH 4.8 peak II_a is much larger than peak III_a, but with increasing scan rates peak III_a becomes larger than peak II_a. Under certain conditions (e.g., pH 2 and at sweep rates $\geq$50 mV s^{-1}) an additional oxidation peak III_a' may be observed at potentials slightly negative of peak III_a. With increasing sweep rate peaks III_a' becomes larger than peak III_a and, as discussed before, it has all the characteristics of an adsorption peak according to the diagnostic criteria of Wopschall and Shain.[12]

At pH 4, peak II_a is the only oxidation peak observed for 6,7-DMDHP at a concentration of 0.1 mM and a sweep rate of 5 mV s^{-1}. However, at a sweep rate of 10 mV s^{-1} peak III_a' appears. At a concentration of 0.25 mM both peaks II_a and III_a may be observed at a sweep rate of 5 mV s^{-1}. Again, with increasing sweep rate peak III_a' grows in and at a sweep rate of 50 mV s^{-1} only peaks II_a and III_a' may be observed.

Cyclic voltammograms of 6,7-DMDHP at pH $\leq$4.8 exhibit two oxidation peaks (II_a and III_a) if the initial sweep is towards positive potentials (Fig. 24). Having scanned these peaks four reduction peaks are observed on the reverse sweep. Reduction peak IV_c forms a quasi reversible couple with peak II_a, the peak separation being 25±8 mV between

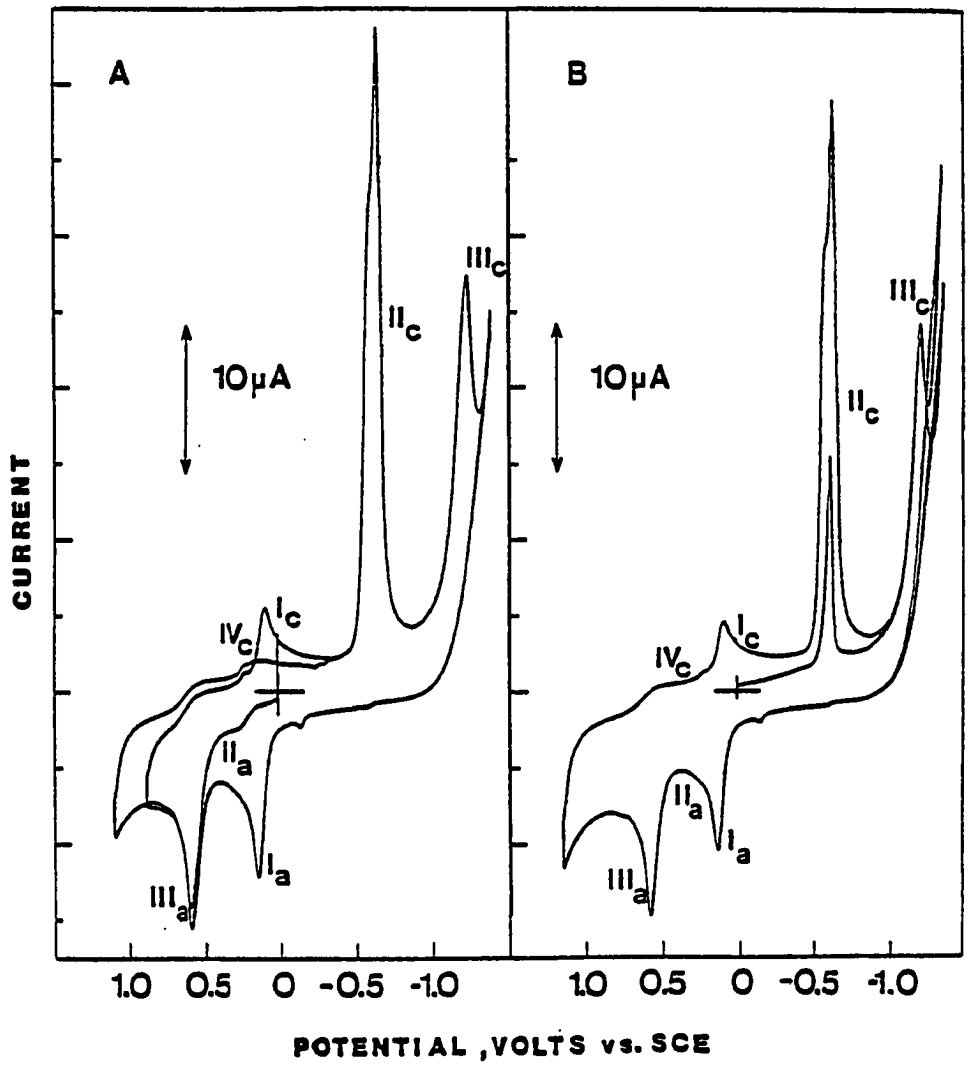

Figure 24. Cyclic voltammogram at the PGE of 0.9 mM 6,7-DMDHP in phosphate buffer pH 2 at a sweep rate of (A) 200 mV s^{-1}, (B) 100 mV s^{-1}, (C) 50 mV s^{-1}.

pH 2-4 and at scan rates between 50-200 mV s^{-1}. At slow scan rates the peak current for peak IV_c is smaller than that for peak II_a.

Below about pH 4.8, careful inspection reveals that reduction peak IV_c is composed of two very closely spaced peaks (peaks IV_c and IV_c', Fig. 25). At relatively fast sweep rates peak IV_c is the largest of these two peaks (Fig. 25A) but with decreasing sweep rate peak IV_c decreases and peak IV_c' grows (Fig. 25C). Potential holding experiments also indicated that the peak height of peak IV_c decreased with increasing length of potential holding time. These observations suggest that an unstable product is formed in the peak II_a electrooxidation of 6,7-DMDHP which is responsible for reduction peak IV_c. This product then apparently undergoes a chemical reaction forming a second transient species which is reduced in the peak IV_c' process. The species responsible for peak IV_c' is not very stable and undergoes further decomposition. There is additional evidence for the existence of these two intermediate species which will be discussed later. When the potential is scanned in positive direction for the second time a new oxidation peak, peak I_a, may be observed (Fig. 24). This peak appears at the same peak potential as peak I_a of 6,7-DMTHP. If the initial sweep is towards negative potentials, one major reduction peak III_c is observed (Fig. 24B).

Usually, a small reduction peak for the initially

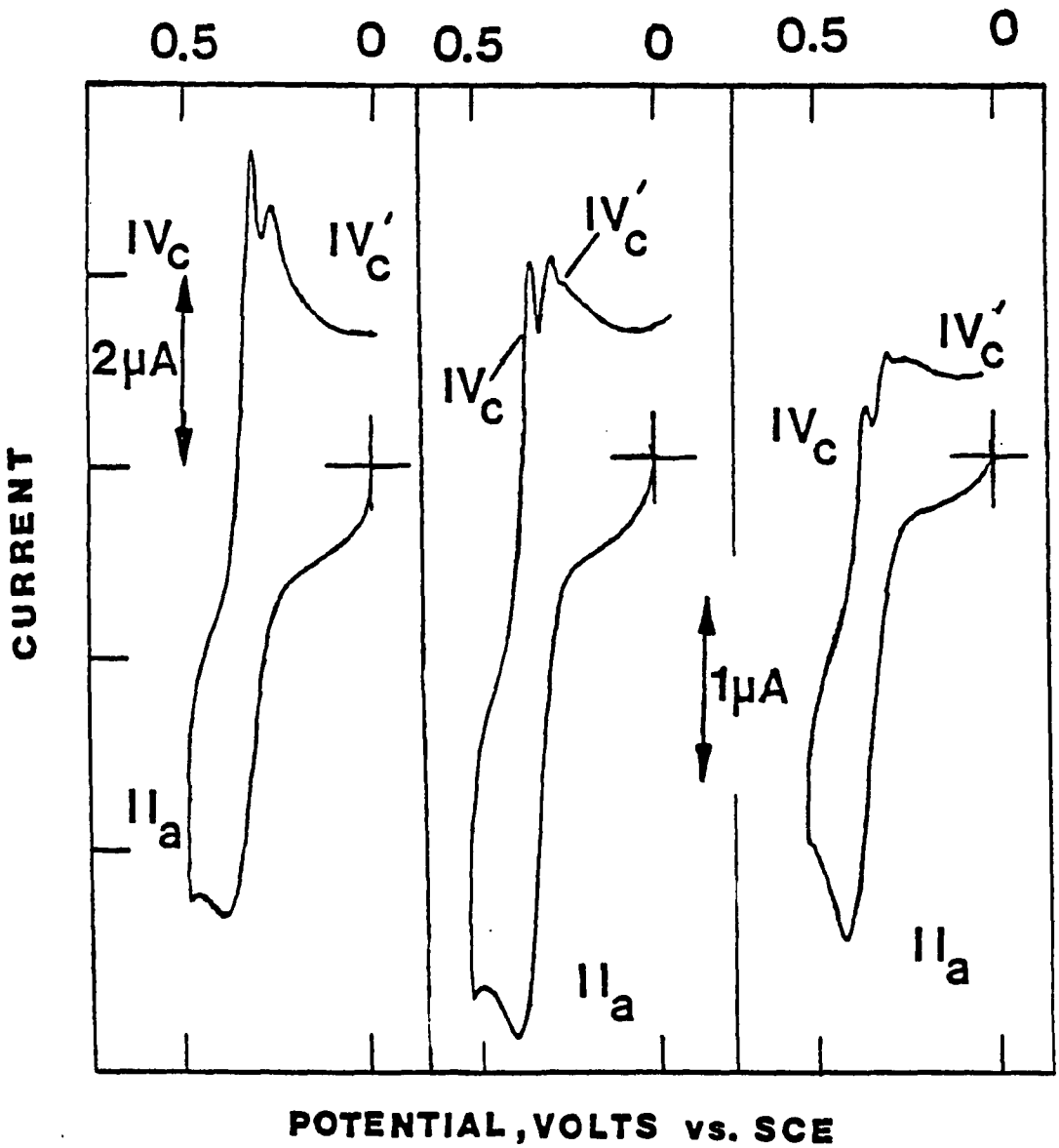

Figure 25. Cyclic voltammograms at the PGE of 1.0 mM 6,7-DMDHP in phosphate buffer pH 2 at a sweep rate of (A) 200 mV s^{-1}, (B) 100 mV s^{-1}, (C) 50 mV s^{-1}.

present 6,7-DMP impurity is also seen as peak II_c (Fig. 24B). Peak II_c grows significantly as the potential is scanned past peak III_a and then reversed.

Cyclic voltammograms of 6,7-DMDHP are somewhat different above pH 4.8 (Fig. 26). Oxidation peak II_a is no longer present nor are peaks IV_c and IV_c'. Peak II_c is reversibly coupled to peak V_a which is due to the oxidation of 6,7-dimethyl-5,8-dihydropterin.[1] This compound is not very stable and rearranges to form 6,7-DMDHP in a pH dependent reaction.

Controlled potential coulometry

Controlled potential electrolysis of 6,7-DMDHP at both peak II_a and peak III_a potentials at pH 3 indicated that 1.8±0.4 electrons per molecule are transferred. The final electrolysis product showed no voltammetric oxidation peak up to +1.0V. However, reduction peaks II_c and III_c were observed. The U.V. spectrum of the electrolysis product was identical to that of 6,7-DMP. In order to verify the cyclic voltammetric and spectrophotometric results, solutions of 6,7-DMDHP at a concentration of 0.5-1 mM were electrolyzed in a thin-layer cell and the resultant product, after freeze drying, was silylated and studied by GC-MS (see experimental). The GC-MS results confirmed that at both pH 3 and pH 7.5 the peak II_a and peak III_a electrooxidation product was 6,7-DMP.

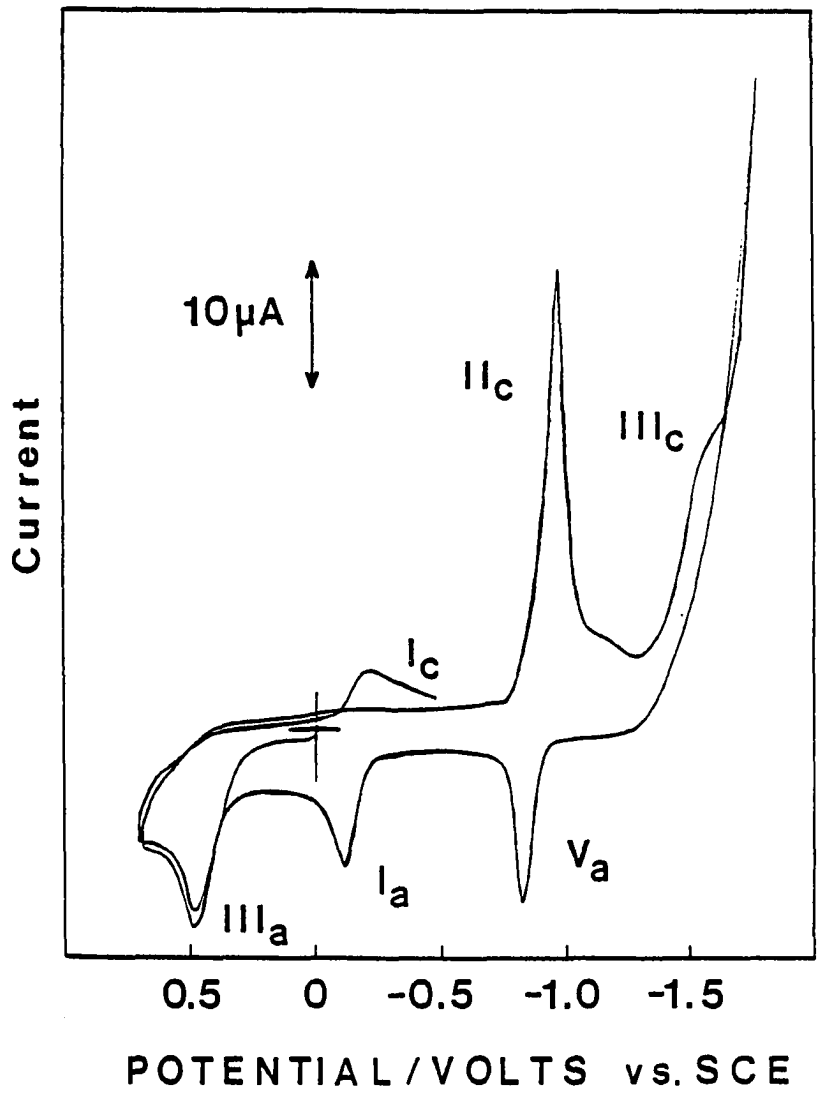

Figure 26. Cyclic voltammogram at the PGE of 0.6 mM 6,7-DMDHP in phosphate buffer pH 6.8 at a scan rate of 200 mV s^{-1}.

Thin-layer spectroelectrochemistry

Cyclic voltammetric experiments on 6,7-DMDHP suggested that the $2\underline{e}$-$2H^+$ electrooxidation of 6,7-DMDHP·H_2O at peak II_a gives at least two short-lived intermediate species (Fig. 25). Thin-layer spectroelectrochemical studies were carried out between pH 3 and 7.3 to more completely characterize such intermediates and their reactions. At pH 3, for example, 6,7-DMDHP shows four absorption bands (λ_{max} = 352, 272, 252 and 213 nm).

Application of a potential corresponding to oxidation peak II_a causes the absorbance at all wavelengths, except at ca. 300 nm, to decrease; the band at 352 nm shifts to slightly shorter wavelengths (∿8 nm). The absorbance at ca. 300 nm initially increases slightly but after 10s of electrolysis it then also decreases. If the electrolysis is terminated after ca. 10-30s the entire spectrum continues to decrease for about 7 min. The spectrum of the final oxidation product formed in the thin-layer cell agreed well with that of 6,7-DMP (Fig. 27). Electrolysis of 6,7-DMDHP at pH 3 at peak III_a potentials brings about the same changes as at peak II_a potentials except that during the course of the electrooxidation the absorbance decreases more rapidly. In addition, upon termination of the electrolysis the subsequent absorbance changes were somewhat smaller than were observed following oxidation at peak II_a potentials.

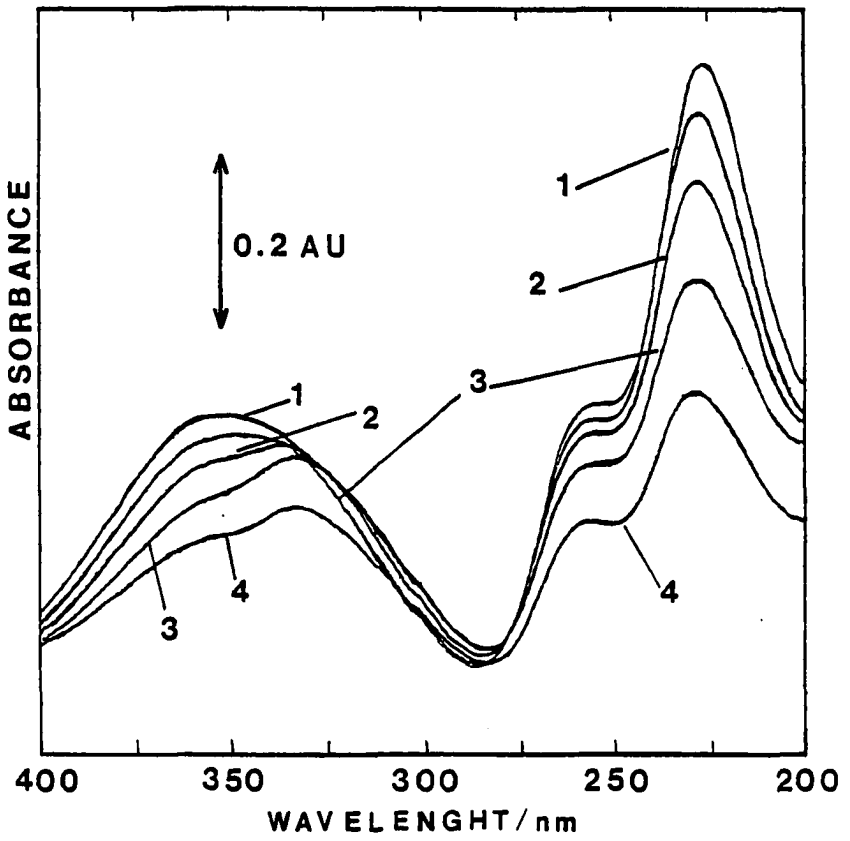

Figure 27. Spectrum of 1.0 mM 6,7-DMDHP electrolyzing at +0.45V in phosphate buffer pH 3 at a reticulated vitreous carbon electrode in a thin-layer cell. (1) Before electrolysis (2) 60s of electrolysis (3) 120s of electrolysis (4) 170s of electrolysis.

Similar thin-layer spectroelectrochemical behavior was noted at pH 4.8. However, although peak II_a cannot be observed by voltammetry at a PGE at pH 4.8 it is possible to oxidize 6,7-DMDHP at potentials where peak II_a might be expected to occur. Thus, when a potential corresponding to peak II_a (0.35V) is applied to a solution of 6,7-DMDHP the entire spectrum ($_{max}$ = 313, 267, 206 nm) very slowly decreases. If the electrooxidation is carried out at peak III_a potentials and terminated after, for example, 50s, the absorbance continues to decrease with time for about 8 min but during the electrolysis the rate of decrease of the absorbance is much more rapid. The fact that 6,7-DMDHP may be slowly electrooxidized at peak II_a potentials even above pH 4.8 where voltammetric peak II_a cannot be observed indicates that the hydrated form must exist to a very small extent. Presumably, the rate of electrooxidation at peak II_a potentials at pH $\geq$4.8 largely reflects the rate of conversion of 6,7-DMDHP to 6,7-DMDHP·H_2O.

The thin-layer spectroelectrochemical results clearly support the view that electrooxidation of 6,7-DMDHP at peak II_a or peak III_a potentials generates an intermediate that absorbs in the U.V. region. Unfortunately, the spectrum of this intermediate is not significantly different from that of 6,7-DMDHP or 6,7-DMP for it to give any distinguishing bands.

The kinetics of the reactions of the intermediate species was studied by a thin-layer spectroelectrochemical method. 6,7-DMDHP was electrooxidized in a thin-layer cell to generate the intermediate. The electrolysis was then terminated and the resulting absorbance vs. time (A vs. t) changes were monitored at a preselected wavelength. Kinetic measurements were taken between pH 3-7.3. At each pH value analysis of A vs. t curves indicated that two first-order processes took place. The calculation procedure used to analyze A vs. t curves will be described in detail in the experimental section. Kinetic results obtained are summarized in Table 14.

6,7-Dimethylpterin

6,7-Dimethylpterin (6,7-DMP) shows only one oxidation peak (peak IV_a) between pH 2-11 at relatively high oxidation potentials. The peak potential, E_p for this peak, shifts to more negative potentials with increasing pH. The E_p vs. pH dependence is represented by the following equation and in Fig. 28:

Peak IV_a pH (2-11) $E_p = [1.51-0.052\ pH]V$

6,7-DMP exhibits two reduction peaks (peaks II_c and III_c) if the initial sweep is in negative direction. The E_p dependence of these peaks on pH may be given as follows:

Table 14. Observed first-order rate constant for reaction of the primary peak II_a and peak III_a electro-oxidation product of 6,7-DMDHP as a function of pH[a]

pH[b]	λ/nm[c]	$k_2 x^d 10^2/s^{-1}$	$k_3 x^d 10^3/s^{-1}$
3.0	254,356	2.86±0.8[e]	5.62±1.2[e]
		4.17±0.8[f]	5.41±0.3[f]
4.2	313,260,228	1.80±0.7[e]	4.86±2.0[e]
4.6	263	7.86[e]	5.34±0.3[e]
		6.22±2.5[f]	5.84±0.1[f]
5.6	262	7.41±0.01[e]	1.66±0.5[e]
		3.38±1.60[f]	4.98±0.1
6.8	262	3.82[e]	4.32±2.7[e]
		3.53±0.4[f]	2.97±0.9[f]
7.3	204,266,313	9.0±2.9[f]	10.6±2.9[f]

[a]Data obtained by a thin-layer spectroelectrochemical method using an optically transparent reticulated vitreous carbon electrode.

[b]Phosphate buffers having an ionic strength of 0.5 M.

[c]Wavelengths employed to monitor absorbance vs. time.

[d]k values obtained by fitting absorbance vs. time data of at least three runs with a non-linear least-squares program.

[e]Rate constants obtained by applying peak II_a potentials.

[f]Rate constants obtained by applying peak III_a potentials.

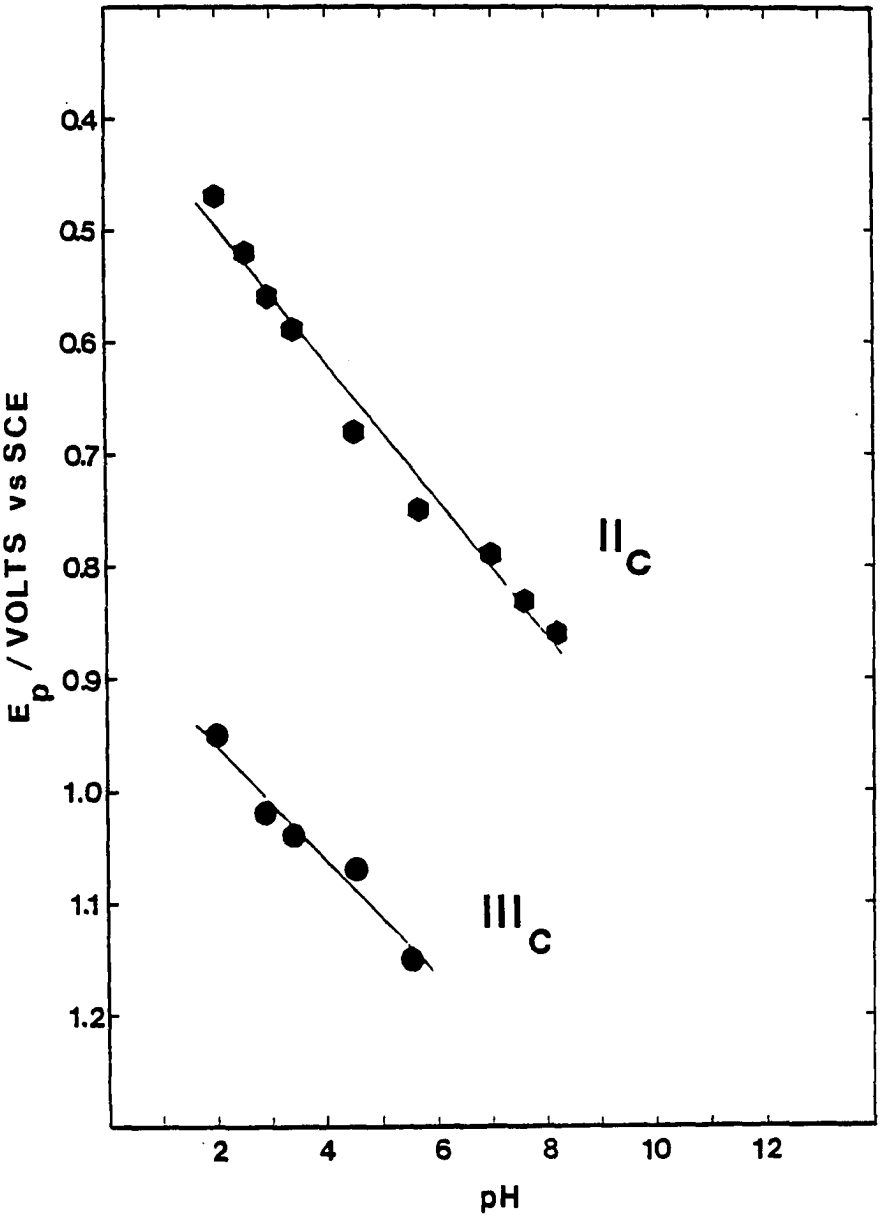

Figure 28. E_p vs. pH relationship for 6,7-DMP at PGE.

Peak II_c pH (2-11) $[E_p = -0.41-0.056\ pH]V$

Peak III_c pH (2-11) $[E_p = -0.94-0.032\ pH]V$

The electroreduction of 6,7-DMP has been studied.[1] It has been shown that peak II_c is due to reduction of 6,7-DMP to a 5,8-dihydro species which is not very stable and rearranges to form 6,7-DMDHP in a pH-dependent chemical reaction. The peak III_c process is due to electroreduction of 6,7-DMDHP to 6,7-DMTHP.

After scanning first in a negative direction if the sweep direction is changed oxidation peaks (peaks I_a, II_a and III_a) (pH = 2) may be observed at the same potentials as for peaks I_a, II_a and III_a of 6,7-DMTHP. If the sweep direction is changed at potentials past peak II_c the only electrooxidation peaks observed upon a positive sweep are peaks II_a and III_a (pH = 2). Figure 29 shows typical voltammograms of 6,7-DMP at different pH values.

DISCUSSION

Linear sweep voltammetry and coulometry indicate that the peak I_a electrooxidation of 6,7-THP is a 2e process. Cyclic voltammetry supports the view that the peak I_a/peak I_c couple is almost reversible. The shift of the peak potential of peak I_a with pH (-0.054V per pH unit) is in approximate accord with that expected for a reversible $2e-2H^+$ electrode reaction. Therefore the peak I_a

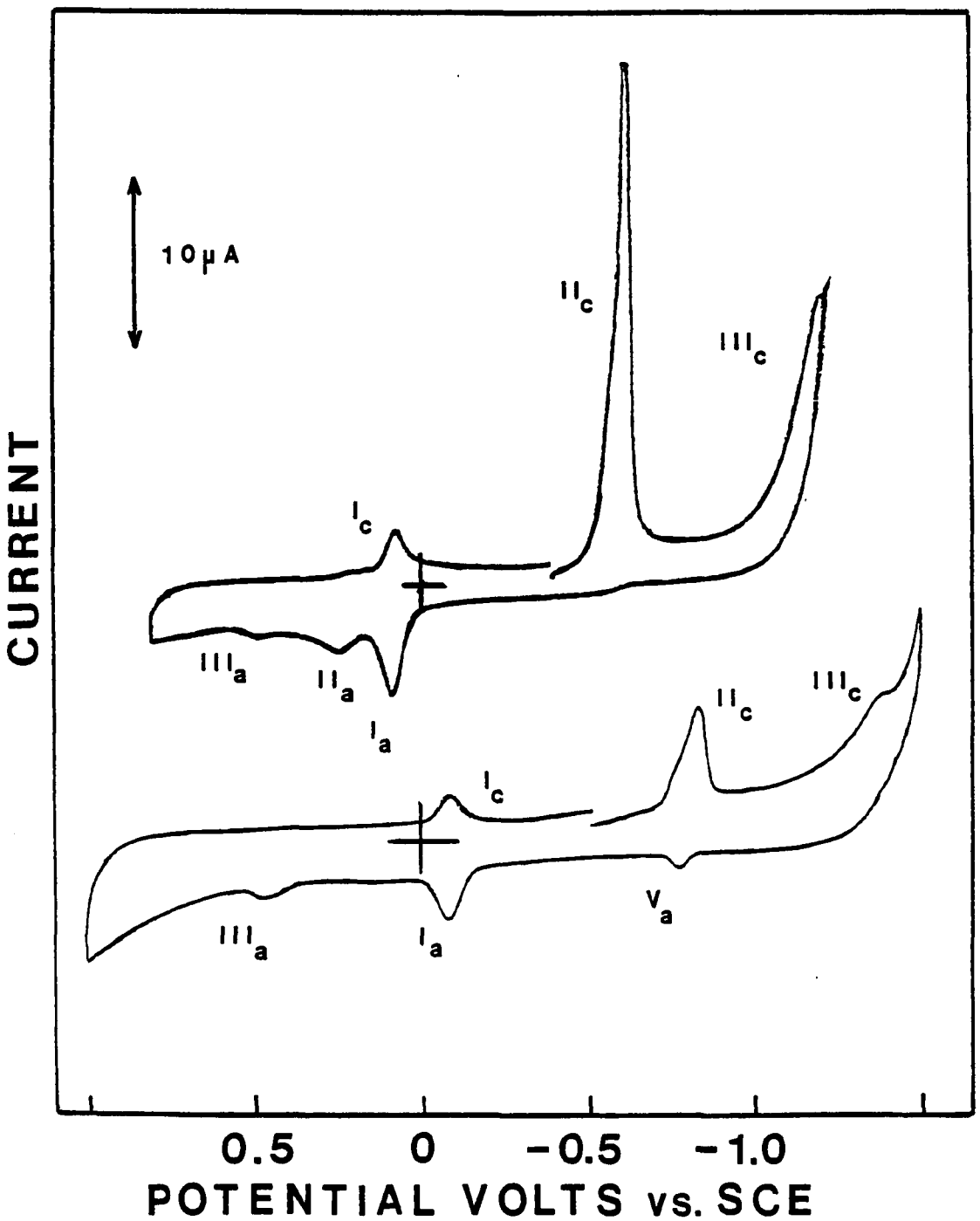

Figure 29. Cyclic voltammograms of 6,7-DMP in phosphate buffer (A) pH 2 at a concentration of 0.56 m$\underline{M}$, sweep rate 100 mV s^{-1} (B) pH 7 at a concentration of 0.5 m$\underline{M}$, sweep rate 200 mV s^{-1}.

process must e due to a $2\underline{e}$-$2H^+$ electrooxidation of 6,7-DMTHP (Fig. 30) to a quinonoid-dihydropterin species; no structure will be assigned to this species at this time.

Sweep rate studies indicate that the peak current function ($i_p/ACv^{1/2}$) for oxidation peak I_a is constant over a fairly large range of sweep rates, whereas the peak current function for reduction peak I_c increases with increasing sweep rate until it becomes equal in value to that for peak I_a. It was also noted that with increasing sweep rate oxidation peaks II_a and III_a and reduction peaks II_c and III_c decrease, and at sufficiently high sweep rates disappear. This behavior implies that the species responsible for peaks II_a, III_a, II_c and III_c are dependent on formation of the product(s) formed in the chemical reaction of the peak I_a primary product.

The quinonoid-dihydropterin species is not stable as demonstrated by cyclic voltammetry, thin-layer spectroelectrochemistry and potentiostatic experiments and disappears in a first-order process to give 6,7-DMDHP (Fig. 30). A bell-shaped relationship exists between k_{obs} for this process and pH with the maximum value of k_{obs} occurring at close to pH 6. Archer and Scrimgeour[5] have studied the kinetics of appearance of 6,7-DMDHP from an intermediate generated when 6,7-DMTHP is chemically oxidized with ferricyanide between pH 6 and 7. These workers utilized a

lower ionic strength buffer (0.1 M) than in the work reported here. For comparative purposes some electrochemical studies were carried out in phosphate buffers having an ionic strength of 0.1 M and pH values of 5.6, 6.24 and 7.0. The first-order rate constants observed by Archer and Scrimgeour[5] were 1.28×10^{-2}, 9.82×10^{-3} and 4.67×10^{-3} s^{-1} at pH values of 6.0, 6.45 and 7.11, respectively. Spectroelectrochemically the observed rate constants were 1.04×10^{-2}, 7.66×10^{-3} and 4.5×10^{-3} s^{-1}, respectively. Weber et al.[14] have determined the rate of the follow-up reaction by a chronocoulometric method. The first-order rate constants reported were 0.02 s^{-1} in pH 7 phosphate buffer, ionic strength 0.3 M and 0.03 s^{-1} in pH 4.7 acetate buffer of ionic strength 0.05 M.

It seems reasonable to conclude that at least around pH 6-7 the same unstable intermediate is generated on both electrochemical and chemical oxidation of 6,7-DMTHP.

The peak I_c process observed on cyclic voltammetry is due to the electrochemical reduction of the intermediate quinonoid-dihydropterin back to 6,7-DMTHP. Since there is no obvious break in the E_p vs. pH plot for oxidation peak I_a of 6,7-DMTHP it must be concluded that both the monocation and neutral form of the compound are electrooxidized in quasi-reversible $2e$-$2H^+$ reactions. Archer and Scrimgeour[5] have suggested that the pK_a of the putative quinonoid-dihydropterin corresponding to dissociation of the mono-

cation to a neutral species is almost identical to that of 6,7-DMDHP, i.e., pK_a = 4.16. Thus, at pH values below pK_a the monocation of 6,7-DMTHP would be electrooxidized in the peak I_a process in a $2e^-2H^+$ reaction to the monocation of the quinonoid-dihydropterin. At pH values above the pK_a neutral 6,7-DMTHP would be electrooxidized to neutral quinonoid-dihydropterin.

Oxidation peaks II_a and III_a of 6,7-DMTHP are due to the electrooxidation of 6,7-DMDHP. This information strongly supports the view that the peak I_a electrooxidation product undergoes a chemical reaction to yield 6,7-DMDHP which in turn gives peaks II_a and III_a. At fast sweep rates in cyclic voltammetry there is insufficient time for the latter chemical reaction to occur so that peaks II_a and III_a cannot be observed.

For the reasons outlined previously, peak II_a is due to electrooxidation of the hydrated form of 6,7-DMDHP (i.e., 6,7-DMDHP·H_2O, Fig. 30). The latter compound has a structure which is very similar to that of 6,7-DMTHP and hence it seems reasonable to expect that 6,7-DMDHP·H_2O is electrooxidized at potentials very close to those for 6,7-DMTHP. Owing to the shift of the equilibrium between 6,7-DMDHP and 6,7-DMDHP·H_2O, peak II_a is the only oxidation peak observed at slow sweep rates.

The shift of the peak potential with pH (-0.054V per pH unit) for peak II_a is in accord with that expected

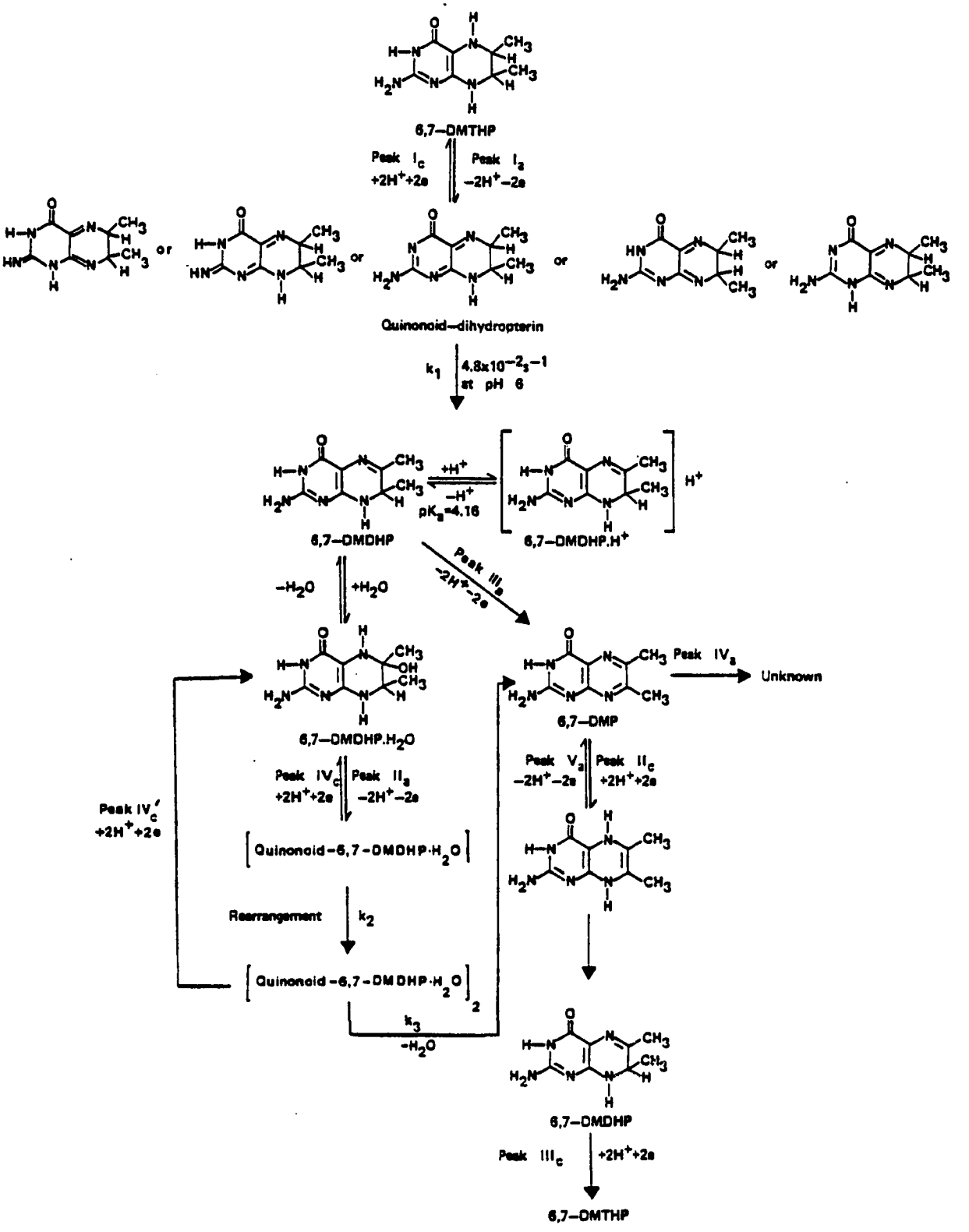

Figure 30. Proposed reaction scheme to account for the voltammetric redox peaks of 6,7-DMTHP at the PGE.

for a reversible reaction involving an equal number of electrons and protons. It has been concluded, therefore, that peak II_a corresponds to the $2\underline{e}$-$2H^+$ electrooxidation of 6,7-DMDHP·H_2O to an intermediate quinonoid species. Both cyclic voltammetry and thin-layer spectroelectrochemical studies indicate that this intermediate disappears in a two-step process. It is thus proposed that the initially formed intermediate, ([quinonoid-6,7-DMDHP·H_2O]$_1$, Fig. 30) characterized by k_2 in Table 3 rearranges to a second, more stable quinonoid ([quinonoid-6,7-DMDHP·H_2O]$_2$, Fig. 30) characterized by k_3 in Table 14, which then finally dehydrates to give 6,7-DMP (Fig. 30) as the final product.

Alternatively, two intermediates might be formed simultaneously which decompose at different rates. In either case, the final stable product generated by the chemical follow-up reactions is 6,7-DMP. The voltammetric and thin-layer spectroelectrochemical results support the conclusion that it is the 6,7-DMDHP·H_2O species which gives rise to the transient intermediates. Non-hydrated 6,7-DMDHP appears to be directly electrooxidized to 6,7-DMP without formation of any detectable intermediates. Two plausible reaction pathways followed upon $2\underline{e}$-$2H^+$ electrooxidation of 6,7-DMDHP·H_2O are shown in equations 14 and 15.

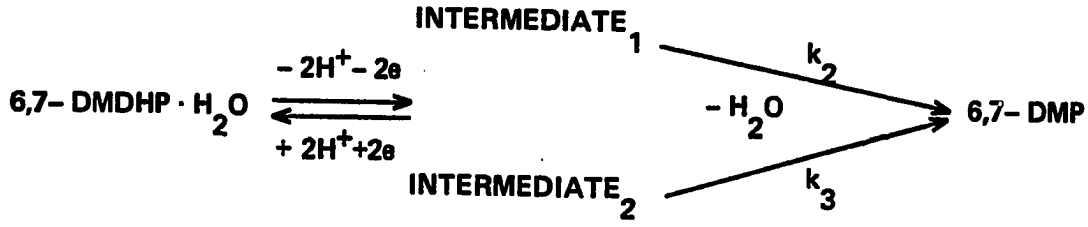

[14]

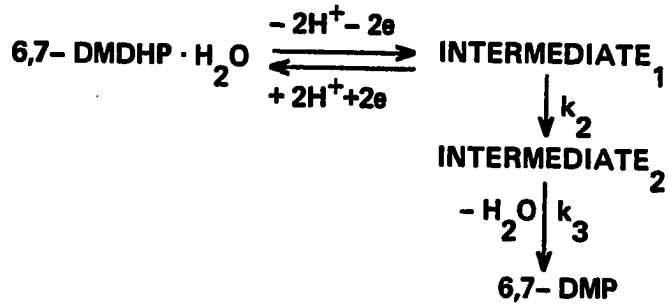

[15]

Cyclic voltammetric experiments favor the scheme shown in equation 15 (see Fig. 25). Cyclic voltammetric evidence suggests that [quinonoid-6,7-DMDHP·H_2O]$_1$, may be reduced to 6,7-DMDHP <u>via</u> peak IV_c (Fig. 25) while [quinonoid-6,7-DMDHP·H_2O]$_2$, may be reduced to the same product <u>via</u> peak IV'_c (Fig. 25).

It is apparent from the results shown in Table 14 that there is no systematic effect of pH on the values of k_2 and k_3. A study of the effect of phosphate concentration at pH 4.2 on k_2 and k_3, where the total ionic strength of the solution was maintained at 2.0 <u>M</u> with NaCl and the phosphate concentration was varied from 0.04-0.4 <u>M</u>, was carried out. It was found that k_2 and k_3 were unaffected

by phosphate concentration.

Peak III_a corresponds to the electrochemical oxidation of the non-hydrated form of 6,7-DMDHP in a $2\underline{e}$-$2H^+$ irreversible reaction to give 6,7-DMP (Fig. 30).

Reduction peaks II_c and III_c have not been studied in great detail since earlier work by Kwee and Lund[1] at mercury electrodes has established the electrode processes. Thus, peak II_c is due to the quasi-reversible $2\underline{e}$-$2H^+$ voltammetric reduction of 6,7-DMP, formed in the peak II_a and/or peak III_a process, to 6,7-dimethyl-5,8-dihydropterin which rapidly rearranges to 6,7-DMDHP. Peak III_c is a further, irreversible $2\underline{e}$-$2H^+$ reduction of 6,7-DMDHP to 6,7-DMTHP. Under fast sweep cyclic voltammetric conditions or at pH >6 a voltammetric peak (peak V_a) due to oxidation of 6,7-dimethyl-5,8-dihydropterin may be observed.

CONCLUSIONS

This electrochemical study of 6,7-DMTHP and its oxidized derivatives has provided information over a wide pH range and has given useful insights into the spectral properties of the quinonoid-dihydropterin intermediate formed in the initial $2\underline{e}$-$2H^+$ electrooxidation. There is no evidence in this study for an initial $1\underline{e}$ oxidation of 6,7-DMTHP as proposed by other workers.[2] For example, at pH 3 and at a sweep rate of 200 mV s^{-1} the experimental peak current for peak I_a of 6,7-DMTHP is 17 μA. The

theoretical peak current for a 1e reaction may be calculated to be 8.7 μA using an electrode area of 2.8×10^{-2} cm^2, a diffusion coefficient of 6,7-DMTHP of 6.66×10^{-6} cm^2 s^{-1} and a concentration of 1.0 mM.

The quinonoid intermediate species can clearly be rapidly and easily generated in a thin-layer cell by electro-oxidation and its spectrum readily observed. Although the U.V. spectrum for the intermediate quinonoid has been reported by several workers[5,20,21] it has not been as well defined as in this study. Thus, Kaufman[20] has indicated that in 0.1 M potassium phosphate λ_{max} = 302-304 nm, while in tris buffer pH 8 λ_{max} = 303 nm has been reported.[5] In spectroelectrochemical experiments this study has shown that the quinonoid spectrum can be readily observed. For example, in phosphate buffer pH 9.3 the quinonoid exhibits two sharp bands at λ_{max} = 307 nm and 290 nm and a broad band between 340-400 nm. At pH 6.0 the intermediate absorbs at λ_{max} = 300 nm along with a broad band between 340-400 nm. Ayling et al.[21] have reported a partial spectrum of a supposed quinonoid intermediate (λ_{max} = 307 nm, 281 nm and a broad band between 370-400 nm). However, the latter spectrum was obtained in a very complex mixture containing 0.1 M tris-HCl pH 7.4, H_2O_2, peroxidase and catalase. In addition, the observed first-order rate constant for conversion of the quinonoid dihydropterin to 7,8-DMDHP was 11.3 min^{-1} (which indicates a half-life of the intermediate

of 3.7s, i.e., much shorter than observed in this study).

EXPERIMENTAL

Chemicals

6,7-DMTHP as the mono- or dihydrochloride salt was obtained from Aldrich. 6,7-DMDHP was synthesized by the method of Viscontini[10] using a hydrogenation apparatus at atmospheric pressure. 6,7-DMP was obtained from Sigma. The tetrahydro compound was always contaminated with dihydropterin and pterin. Similarly, the dihydro compound was always contaminated with pterin. The contaminant in each species could be detected by voltammetric techniques and measured quantitatively by a high performance liquid chromatography method [see later discussion]. Because the samples of 6,7-DMTHP were always contaminated with 6,7-DMDHP and 6,7-DMP, most test solutions were reduced by controlled potential electrolysis at a mercury pool electrode at potentials more negative than peak III_c. After 1-2 hours of electrolysis at such potentials, most of the 6,7-DMDHP and 6,7-DMP were reduced to the tetrahydro compound. However, it proved to be exceedingly difficult to eliminate the last traces of 6,7-DMP.

Phosphate buffers having an ionic strength of 0.5 M were used for all experiments, except when products were examined by gas chromatography-mass spectrometry (GC-MS). Samples subjected to GC-MS analysis were prepared in 0.5 M

NaCl containing 5 mM Na_2HPO_4, the pH being adjusted to the desired value by addition of NaOH or HCl.[24]

Apparatus

Linear sweep voltammetry, and cyclic voltammetry were performed with an instrument of conventional operational amplifier design.[25,26] Voltammograms were recorded on a Hewlett-Packard Model 7001A or a Houston Instruments Model 2000 X-Y recorder. Fast-sweep voltammograms were recorded on a Tektronix Model 5031 Dual Beam Storage Oscilloscope and photographed with a Tektronix Model C-70 camera. Potentiostatic experiments utilized a Princeton Applied Research Corporation Model 175 universal programmer.

A water jacketed one compartment cell maintained at a known and constant temperature (25°±0.1 C) was used for most electrochemical measurements. Contact with the reference electrode was made with a capillary tube used as a salt bridge. This salt bridge was prepared by dissolving 4 g of agar (Difco, Detroit, Michigan) in 90 ml of buffer solution. The salt bridge in direct contact with the reference electrode was prepared according to the procedure described by Meites.[17] A saturated calomel electrode (SCE) served as the reference electrode and a mercury pool as a counter electrode. All potentials are referred to the SCE at 25°C. The temperature of the one-compartment cell and water jacketed bubbling chamber was maintained by a water

bath (Lauda, Brinkman).

Pyrolytic graphite electrodes were machined from small rods of graphite (Super-Temp Company, Santa Fe Springs, California) to a diameter of 2 mm and a length of ca. 5 mm and were sealed into lengths of 6 mm bore glass tubing with Hysol Epoxi-Patch 1 C White (Hysol Corporation, Olean, New York). The electrodes were ground flush with the end of the glass tube, and were resurfaced, prior to running each voltammogram, with 600-grit silicon carbide paper (Buehler Ltd., Evanston, Illinois) mounted on a rotating disc. The electrode then was sprayed with a fine stream of dionized water to remove the graphite powder from the surface, and dried by gently touching the surface with an absorbant paper tissue.

Controlled potential electrolyses were carried out in a three compartment cell using a Princeton Applied Research Corporation Model 173 or a Wenking LT 73 Potentiostat. Current integration during electrolysis was performed with a Koslow coulometer Model 541. Controlled potential electroreductions were carried out at a stirred mercury pool electrode whereas for oxidation reactions a large (12 cm^2) PGE was used. The compartments of the electrochemical cell were separated by a Nafion (Du Pont) membrane. The counter electrode was a Pt gauze, a SCE was used for a reference electrode. Argon or nitrogen were passed through the solution during electrolysis. Solutions

were stirred magnetically with a teflon-covered magnetic stirrer.

A Corning Model 10 and an Orion Model 501 digital pH meter were used for pH measurements. Ultraviolet spectra were recorded using a Perkin-Elmer Hitachi Model 124 and a Hitachi 100-80 computerized spectrophotometer.

A Harrick Rapid Scanning Spectrometer (RSS) and signal processing module (Harrick Scientific Company, Ossining, New York) were utilized for spectroelectrochemical and kinetic measurements.

Construction of the thin-layer cell

The optically transparent reticulated vitreous carbon (RVC) thin-layer electrode was made by placing an RVC slice of 0.7 mm thickness and 31x9 mm dimensions between two quartz slides about 8 mm from one end of the slides. One side of the RVC slice was allowed to stick out to make electrical contact. The quartz slides were held together by epoxy. A fine copper wire was looped into the portion of RVC slice sticking out from the slides and was attached to the RVC using liquid organic silver (Engelhard, Inc., East Newark, New Jersey). The spot covered with liquid organic silver was coated with a layer of Tygon paint. The counterelectrode was platinum foil which was held between the slides by epoxy cement. Electrical contact with the counter electrode was made through a platinum wire which

was spotwelded onto the platinum foil. The quartz slides were sealed with epoxy all around except the parts where sample solution was introduced into or transferred out of the cell and where contact was made with the reference electrode. The bottom of the cell was sealed with a glass tube which was cut in such a fashion that the quartz slides would fit the opening. Surgical tubing was attached to the open end of this glass tube and a Hamilton IMMI valve was connected to the other end of the tubing. Electrical contact with the RVC electrode was made through a copper wire which was soldered to the fine copper wire looped onto the RVC. A Luer outer taper and a IMMI Hamilton valve was used to connect the cell to vacuum or to a nitrogen line. This joint was glued onto the quartz cell and epoxied to avoid leakage. The connection with the reference electrode was made with a bent outer Luer taper with a IMMI Hamilton valve. A second outer Luer taper which had a reference tube in it was placed on top of the Hamilton valve. A silver wire which was soldered on a 7/25 shortened ground glass joint extended in this reference tube. An air-tight syringe was used to fill the RVC cell with sample solution. Before filling the cell with sample solution, large quantities of doubly distilled water were passed through the cell by suction to get rid of any air bubbles present in the RVC electrode. Flushing with buffer solution followed. To fill the cell valves 1 and 3 (Fig. 31)

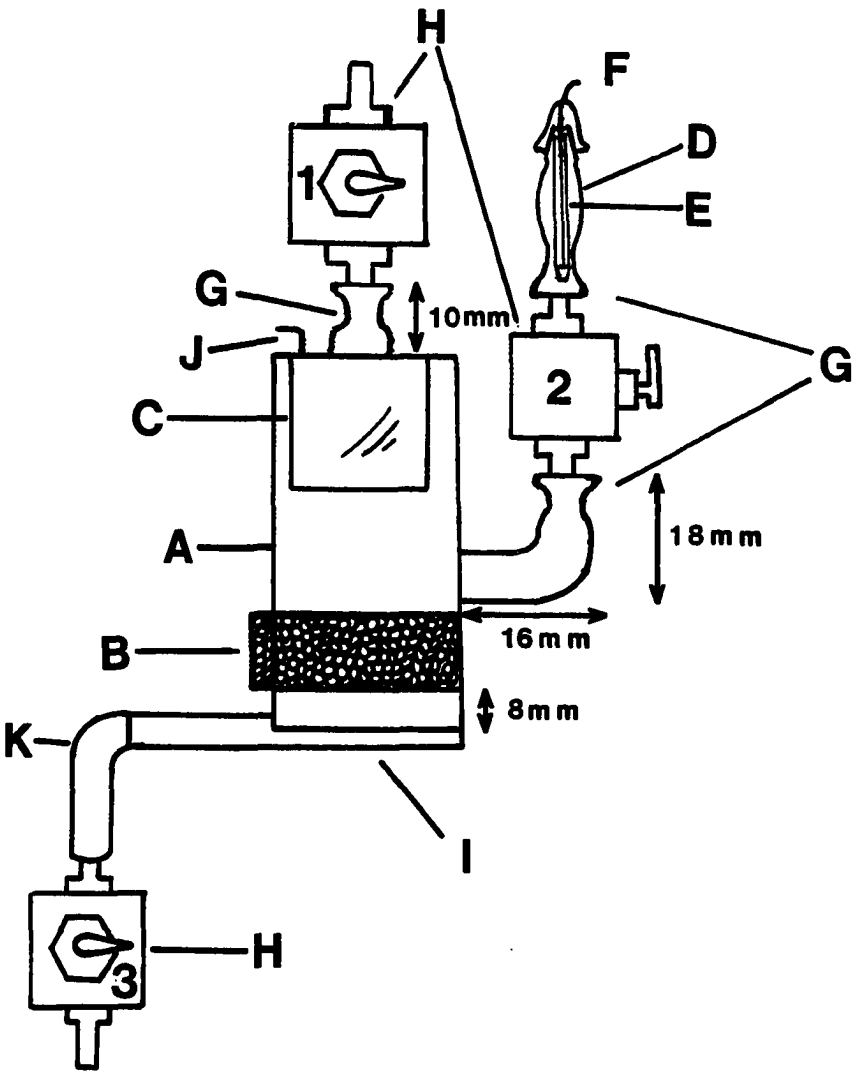

Figure 31. Design of the RVC thin-layer cell (A) Quartz microscope slide (2"xl"xl/16"), (B) RVC electrode (100 ppi, 9 mm x 31 mm x 0.7 mm), (C) Platinum foil counter electrode (18 mm x 23 mm), (D) Ag/AgCl reference electrode, (E) Reference tube, (F) Copper wire for electrical contact, (G) Luer outer taper, (H) Valves, (I) Glass tubing, (J) Electrical contact to platinum foil, (K) surgival tubing.

were opened with the air-tight syringe attached to valve 1 and solution was pushed into the cell, the excess coming out through valve 3. In order to fill the reference arm with sample solution, valve 3 was closed and valve 2 was opened and the reference electrode was removed. Again solution was pushed into the cell. The excess solution came out of valve 2. The reference electrode was put back and it was ensured that there were no air bubbles in the reference electrode tube. At the end of each experiment, valves 1 and 3 were opened and new sample solution was introduced into the cell from the syringe. A 1.0 M KCl solution was used for the reference electrode electrolyte. The potential difference between the AgCl reference electrode and SCE was measured before and after electrochemical experiments. This value was usually around 10 mV.

The construction of the gold minigrid electrode has been reported elsewhere.[18,27,28] In the thin-layer spectroelectrochemical experiments carried out using a thin-layer gold minigrid electrode the sample solution was put into a 5 ml cylinder glass "cup" with a slit at the top wide enough for the thin-layer cell to fit in. Nitrogen could be bubbled through the sample solution through a glass tube connected to the bottom of the cylindric sample holder. A platinum foil shaped to fit the sample holder was used as the counter electrode.

In order to calculate the rate constant for the fast step it was first necessary to subtract the contribution of the slow step to the absorbance at the times where the fast step occurs. To do this the slope and intercept of the ln $|A-A_\infty|$ versus time plot for the slow step are calculated. Knowing these it is possible to calculate the ln $|A-A_\infty|$ values for the slow step at times where the fast step is occurring. By taking the anti-ln of the ln $|A-A_\infty|$ one obtains the absorbance contribution of the slow step at that time. Then the absorbance due to the slow step is subtracted from the total absorbance to obtain the absorbance arising from the fast step. The log is then taken of this fast step absorbance to obtain ln $|A-A_\infty|$ for the fast step. This is done at a series of times to generate a ln $|A-A_\infty|$ versus time plot. From the slope of this plot the rate constant is then calculated.

Voltammetric procedure

Test solutions were prepared prior to each experiment. These solutions were made by dissolving the appropriate solid compound in a deaerated solution of 1:1, buffer: doubly distilled water mixture yielding an ionic strength of 0.5 M. Water-saturated nitrogen was passed over the sample solution during each experiment.

Test solutions of 6,7-DMTHP were analyzed for 6,7-DMDHP and 6,7-DMP by a high pressure liquid chromatographic method.[9] In this method phosphate buffer pH 6.5 having an ionic strength of 0.1 M was used as the eluent at a flow

rate of 0.8 ml min^{-1}. A partisil strong cation exchange column was used along with a Water Associates pump, Model UGK Injector and Model 400 absorbance detector. A Hewlett-Packard Model 5985B gas chromatographic-mass spectrometer was used for the analysis of electrolysis products.

Summary

Electrochemical Oxidation of 6,7-Dimethyl-5,6,7,8-tetrahydropterin

6,7-Dimethyl-5,6,7,8-tetrahydropterin (6,7-DMTHP) is an effective and widely used pseudo cofactor for phenylalanine hydroxylase. 6,7-DMTHP gives rise to three voltammetric oxidation peaks at the pyrolytic graphite electrode. Peak I_a is an almost reversible $2\underline{e}$-$2H^+$ oxidation reaction to an unstable quinonoid-dihydropterin. The actual structure of this unstable species has not been established but cyclic voltammetry, thin-layer spectroelectrochemistry and potentiostatic experiments reveal that the quinonoid-dihydropterin undergoes a pH-dependent, first-order reaction to give 6,7-dimethyl-7,8-dihydropterin (6,7-DMDHP). Peak II_a is due to a $2\underline{e}$-$2H^+$ quasi-reversible electrooxidation of covalently hydrated 6,7-DMDHP (6,7-DMDHP·H_2O) giving rise to two unstable quinonoid-dihydropterins which in turn react chemically to give 6,7-dimethylpterin (6,7-DMP). Nonhydrated 6,7-DMDHP is oxidized to 6,7-DMP in the peak III_a process.

REFERENCES

1. S. Kwee and H. Lund, Biochim. Biophys. Acta, 297 (1973) 285.

2. M. C. Archer and K. G. Scrimgeour, Can. J. Biochem., 48 (1970) 526.

3. M. C. Archer, D. Vonderschmitt, and K. G. Scrimgeour, Can. J. Biochem., 50 (1972) 1174.

4. J. Pradác, J. Pradácová, D. Homolka, J. Koryta, J. Slavík, J. Weber and R. Cihar, J. Electroanal. Chem., 74 (1976) 205.

5. M. C. Archer and K. G. Scrimgeour, Can. J. Biochem., 48 (1970) 278.

6. J. Weber, K. Holub, D. Homolka, and J. Pradác, J. Electroanal. Chem., 73 (1976) 151.

7. W. Schwotzer, J. H. Bieri, M. Viscontini and W. von Philipsborn, Helv. Chim. Acta, 61 (1978) 2108.

8. R. G. Kallen and W. P. Jencks, J. Biol. Chem., 241 (1966) 5845.

9. S. W. Bailey and J. E. Ayling in, Chemistry and Biology of Pteridines, W. Pfleiderer (ed.), W. de Gruyter, Berlin (1975) 633.

10. M. Viscontini, Methods in Enzymology, 18B (1971) 678.

11. R. N. Adams in, Electrochemistry at Solid Electrodes, Marcel Dekker, New York, 1969.

12. A. J. Bard and L. R. Faulkner in, Electrochemical Methods, John Wiley, N.Y., 1980. p. 220.

13. R. H. Wopschall and J. Shain, Anal. Chem. 39 (1967) 1514.

14. J. Pradáč, J. Pradácová, D. Homolka, J. Koryta, J. Slavík, J. Weber and R. Cihar, J. Electroanal. Chem., 74 (1976) 205.

15. R. L. Blakley in, The Biochemistry of Folic Acid and Related Pteridines, A. Neuberger and E. L. Totum (eds.), North-Holland, Amsterdam, 1979, p. 58.

16. R. N. Adams in, Electrochemistry at Solid Electrodes, Marcel Dekker, Inc., N.Y., 1969, p. 276.

17. L. Meites in, Polarographic Techniques, 2nd edn., Wiley, N.Y., 1965, p. 441.

18. R. W. Murray, W. R. Heineman and G. W. O'Dom, Anal. Chem., 39 (1967) 1666.

19. G. S. Alberts and T. Shain, Anal. Chem., 35 (1963) 1859.

20. S. Kaufman, J. Biol. Chem., 239 (1964) 332.

21. J. Ayling, R. Pirson, W. Pirson and G. Boehm , Anal. Biochem., 51 (1973) 80.

22. J.-L. Dhondt, M. Dautrevaux and G. Bioerte, J. Heterocyclic Chem., 16 (1979) 1489.

23. K. A. Connors, in Reaction Mechanisms in Organic Analytical Chemistry, John Wiley, N.Y., 1973.

24. A. Brajter-Toth and G. Dryhurst, J. Electroanal. Chem., 122 (1981) 205.

25. G. Dryhurst, M. Rosen and P. J. Elving, Anal. Chim. Acta, 42 (1968) 143.

26. D. L. McAllister and G. Dryhurst, Anal. Chim. Acta, 64 (1973) 121.

27. J. L. Owens and G. Dryhurst, J. Electroanal. Chem., 80 (1977) 171.

28. W. R. Heineman, B. J. Norris and I. F. Goelz, Anal. Chem., 47 (1975) 79.

CHAPTER 3

ELECTROCHEMICAL OXIDATION OF 2-DIMETHYLAMINO-3,6,7-TRIMETHYL-TETRAHYDROPTERIN

INTRODUCTION

It is a well established fact that tetrahydrobiopterin (THBP) acts as the natural cofactor for phenylalanine hydroxylase and a number of other enzymes.[1] Kaufman initially proposed that the primary oxidation product of THBP in enzymic hydroxylation reactions is a dihydropterin. However, it was first suggested by Hemmerich[2] that this product is a quinonoid-dihydropterin, based on observations he made on the autooxidation of a tetrahydropteridine alkylated at the C(8) position (equation 1).

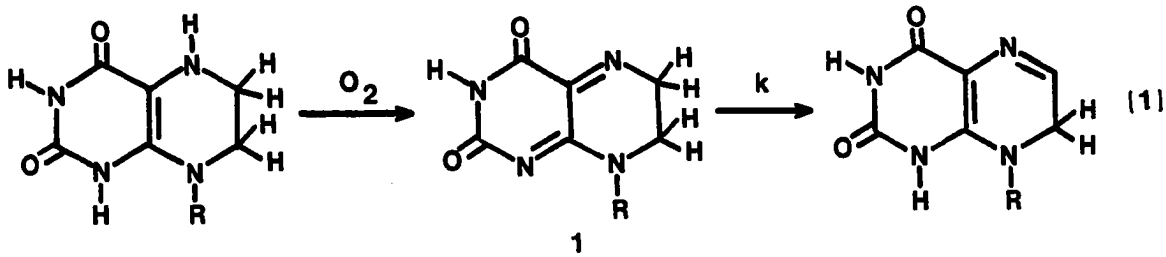

1 [1]

The spectral properties of this intermediate (1)

were quite similar to those of an intermediate generated by Kaufmann in the oxidation of THBP with a dye.[3]

There is a substantial amount of evidence that this intermediate is labile and that it rapidly rearranges to the more stable 7,8-dihydropterin as shown in equation (2).

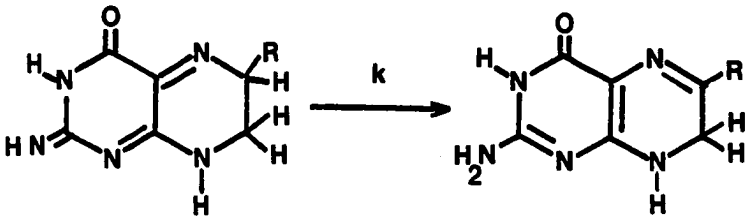

(2)

Quinonoid-dihydropterin 7,8-dihydropterin

There are at least five possible forms of the intermediate quinonoid species ($\underset{\sim}{2}$, $\underset{\sim}{3}$, $\underset{\sim}{4}$, $\underset{\sim}{5}$, $\underset{\sim}{6}$).

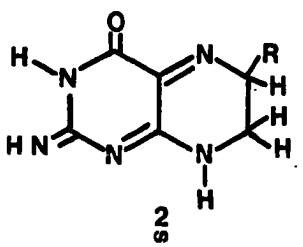

$\underset{\sim}{2}$

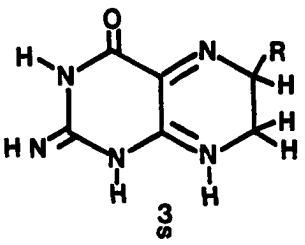

$\underset{\sim}{3}$

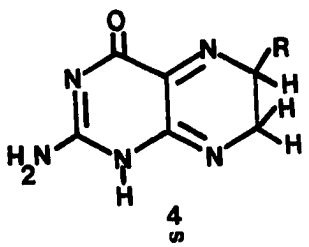

$\underset{\sim}{4}$

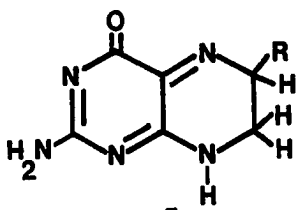

5

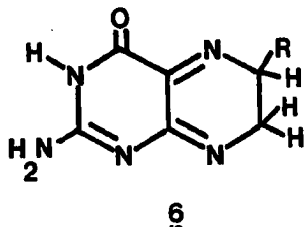

6

Based on kinetic and spectroscopic data the parallel para quinonoid structure (2) has been favored.[4-6] Theoretical molecular orbital calculations were against (5). Electrochemical studies of several methylated pterins suggested that the ortho structure (6) was formed.[7] However, there is no conclusive literature evidence concerning the structure of the quinonoid intermediate.

The available experimental data indicates that the same quinonoid species is generated in enzymic, chemical and electrochemical oxidation reactions.

The structure of the quinonoid-dihydro species that forms during the oxidation of THBP may play an important role in determining the cofactor activity. Therefore it is important to know which of these structures is formed during the oxidation of the natural cofactor THBP. This knowledge may enable us to explain why some pterins are better cofactors than others and how they are involved in biological reactions. It is known that different substituents on the pyrimidine or pyrazine ring result in different cofactor activities. Even the stereochemistry of the substituent groups is very important in determining the effectiveness of cofactors. A study of methylated tetrahydropterins was therefore initiated to determine

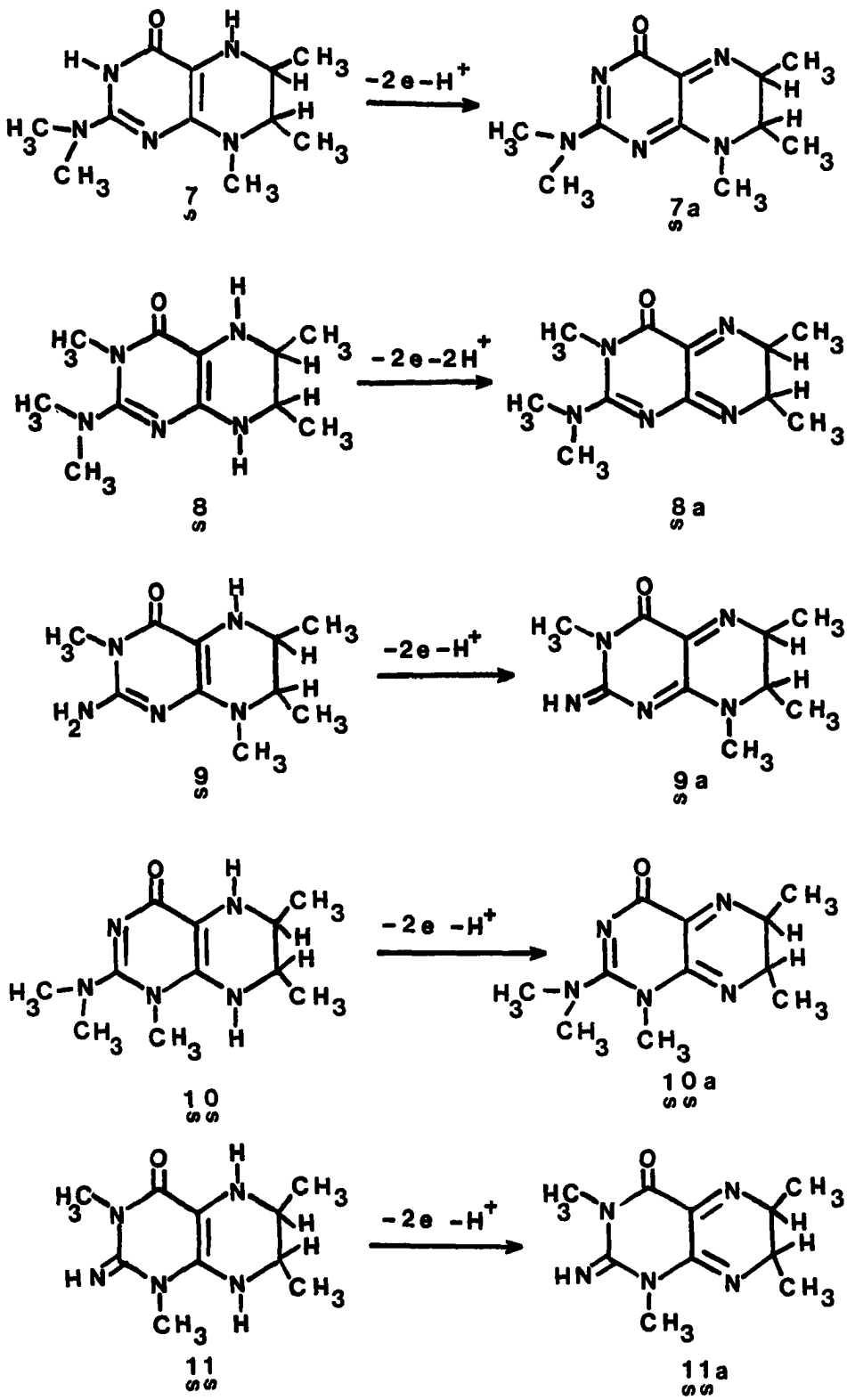
-2e-H+
7 ss
7a ss
-2e-2H+
8 ss
8a ss
-2e-H+
9 ss
9a ss
-2e -H+
10 ss
10a ss
-2e -H+
11 ss
11a ss

information concerning the structure of the putative quinonoid-dihydro species. There are several methylated pterins which may form locked quinonoid-dihydropterins as shown on the previous page (7-11).

It was thought that a comparison of electrochemical, spectroelectrochemical and kinetic data obtained upon electrooxidation of these methylated pterins might lead to an understanding of the putative quinonoid structure.

The present study involves the electrochemical oxidation of 2-dimethylamino-3,6,7-trimethyl-5,6,7,8-tetrahydropterin (2-DMTHP (8), 2-dimethylamino-3,6,7-trimethyl-7,8-dihydropterin (2-DMDHP) (12) and 2-dimethylamino-3,6,7-trimethylpterin (2-DMP) (13).

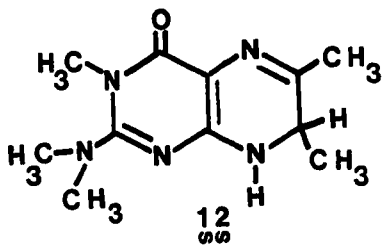

12

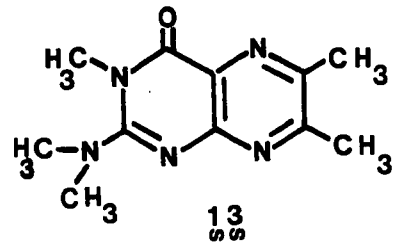

13

RESULTS

Physical properties of 2-DMTHP

In aqueous solution, 2-DMTHP can exist as a cation and neutral species. The shift in λ_{max} as a function of

pH is shown in Fig. 1. It is obvious that there is a big change in λ_{max} between pH 6 and 8. There is no pK_a reported for this compound in the literature. However, from the behavior of its U.V. spectrum as a function of pH, the pK_a for 2-DMTHP may be assumed to be close to 7, which corresponds to protonation at N(5).

Solutions of 2-DMTHP are extremely air sensitive. Air oxidation of 2-DMTHP may be eliminated by completely deaerating the solutions used to prepare 2-DMTHP samples and maintaining them under an inert atmosphere. The susceptibility of 2-DMTHP to attack by oxygen increases with increasing pH and a yellow colored solution results upon oxidation.

Linear and cyclic sweep voltammetry

Between pH 1.5 and 9.2, 2-DMTHP exhibits up to four voltammetric oxidation peaks at the pyrolytic graphite electrode (PGE). The most positive of these peaks occurs very close to background discharge current (E_p > 1.2V) and is due to electrooxidation of 2-DMP formed in the peak II_a and peak III_a reactions. This peak was not very well defined at any pH value. Its oxidation potential agrees well with that observed for the single oxidation peak of 2-DMP. This peak will not be further considered in this report.

The variation of the peak potential with pH for

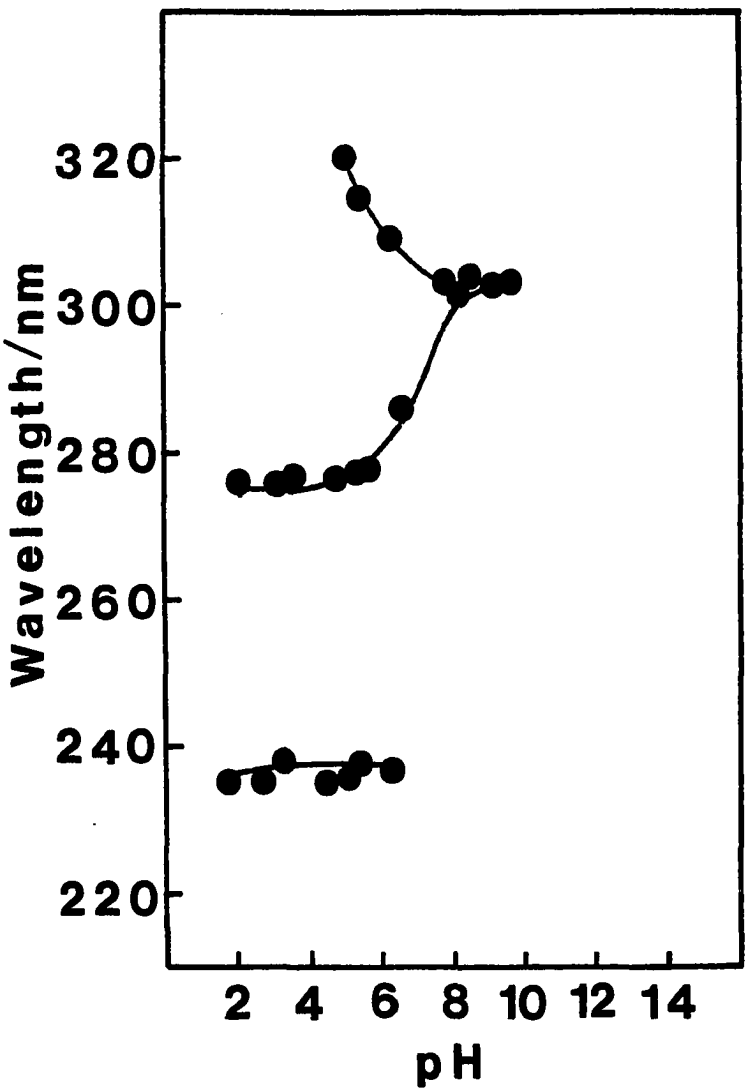

Figure 1. Change in λ_{max} for 2-DMTHP as a function of pH.

the remaining three oxidation peaks is shown in Fig. 2 and are represented by the following equations:

Peak I_a (pH 1.5-9.2): E_p = [0.30-0.048 pH]V

Peak II_a (pH 1.5-5.0): E_p = [0.42-0.043 pH]V

Peak III_a (pH 1.5-5): E_p = [0.89-0.067 pH]V

(pH 5.0-9.2): E_p = [0.66-0.018 pH]V

Below pH 5 three voltammetric oxidation peaks may be observed, whereas above pH 5 only two peaks may be observed (peaks I_a and III_a).

Cyclic voltammograms of 2-DMTHP at pH 2.0 exhibit no reduction peaks if the initial sweep is towards negative potentials, but three oxidation peaks (I_a, II_a and III_a) are observed on the first sweep to positive potentials (Fig. 3). Having scanned these peaks, four reduction peaks (I_c, II_c, III_c and IV_c) are observed on the reverse sweep. Reduction peak I_c forms an almost reversible couple with peak I_a. At sweep rates between 50-200 mV s^{-1} and between pH 1.5 and 7 the ΔE_p value between peaks I_a and I_c averaged 48 ± 19 mV. At relatively slow scan rates (e.g., 200 mV s^{-1}) the peak current for peak I_c was smaller than that for peak I_a particularly between pH 6-8 (Fig. 4) but with increasing scan rate i_p for peak I_c increased. The change in peak current for peak I_c as a function of scan rate is shown in Table 1. The increase in peak current for peak I_c with increasing scan rate indicates that the primary peak I_a electrooxidation product is not very stable and

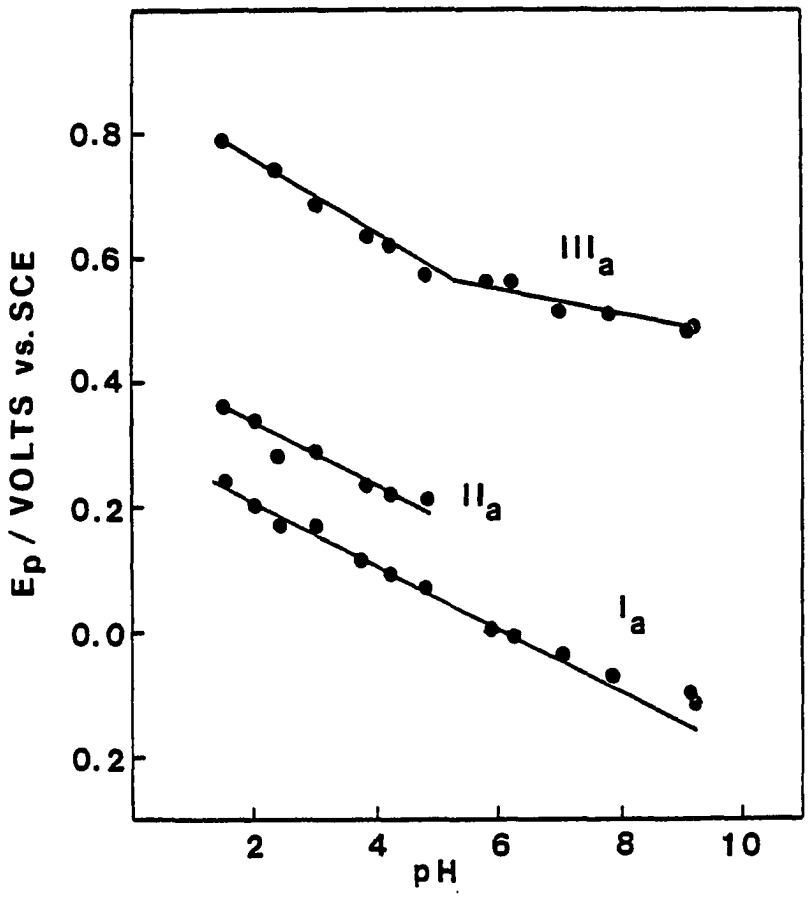

Figure 2. Dependence of E_p on pH at a concentration of 1 mM of 2-DMTHP and at a scan rate of 5 mV s^{-1}.

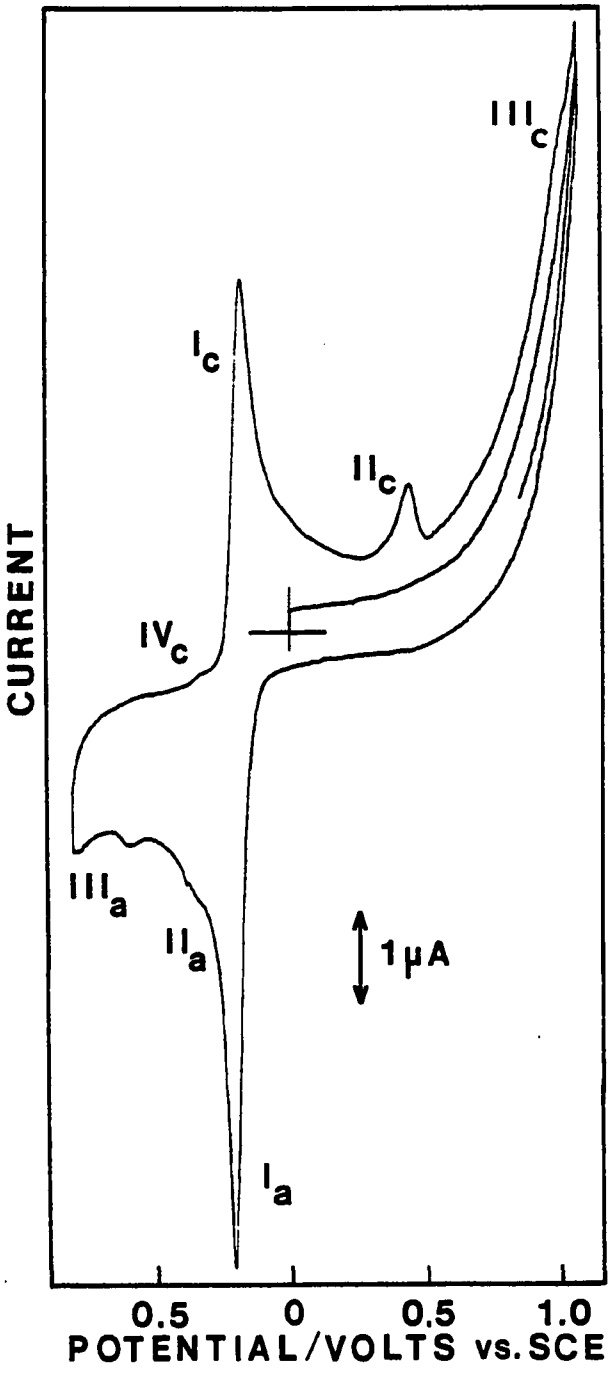

Figure 3. Cyclic voltammogram of 1 m$\underline{M}$ 2-DMTHP at pH 2.0 at a scan rate of 50 mV s^{-1}.

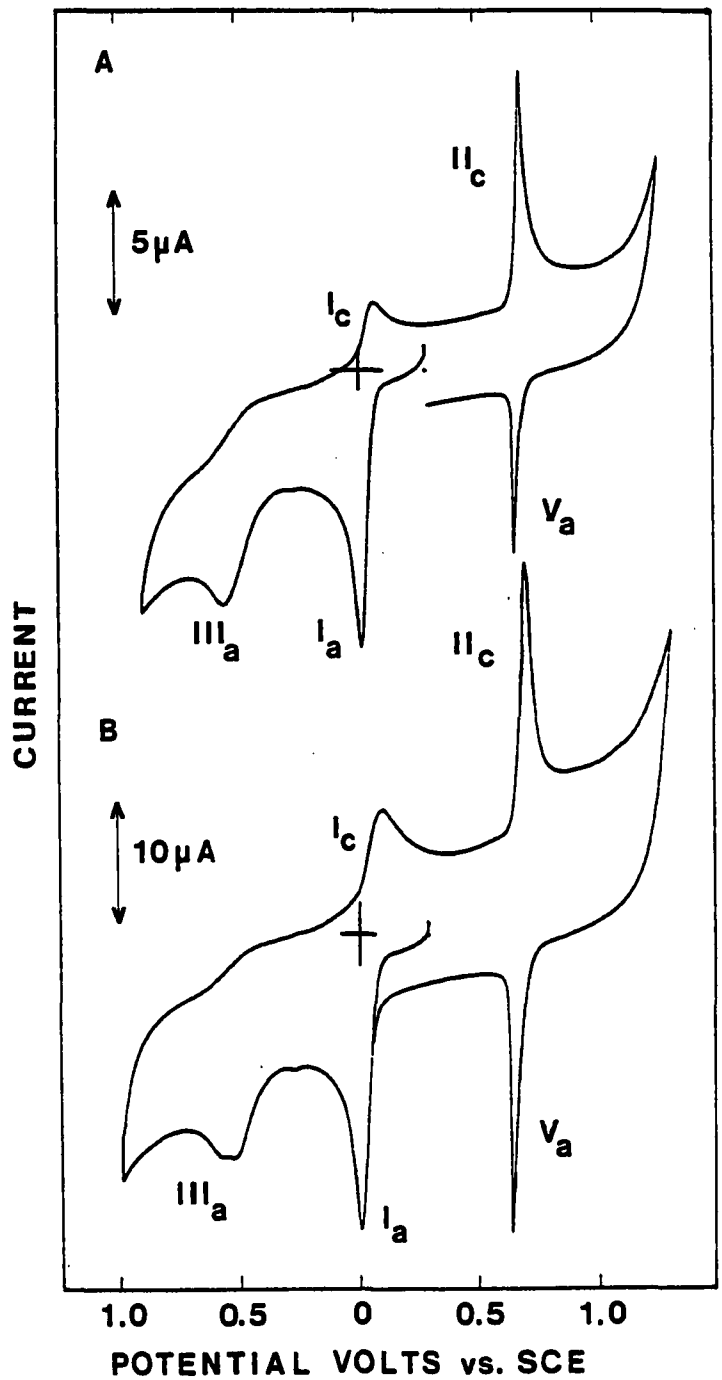

Figure 4. Cyclic voltammogram of 1 mM 2-DMTHP in phosphate buffer pH 7.0 at a scan rate of A) 50 mV s^{-1}, B) 200 mV s^{-1}.

Table 1. Peak current dependence of peak I_c of 2-DMTHP as a function of scan rate at a PGE in phosphate buffer of 0.5 M ionic strength

pH	scan rate/mV s^{-1}	$(i_p)_c$/mV s^{-1}
4.7	50	1.25
	100	1.56
	200	1.61
9.1	50	1.36
	100	1.52
	200	1.88

undergoes a chemical follow-up reaction. The peak current ratio $(i_p)_c/(i_p)_a$, where $(i_p)_c$ is the peak current due to peak I_c reduction and $(i_p)_a$ is the peak current due to peak I_a oxidation, decreases with increasing pH up to about pH 6. At pH values higher than 6 this ratio stays almost constant (Fig. 5) and at higher scan rates it is closer to one.

Sweep rate studies indicate that the experimental peak current function for peak I_a increases by about 35% at pH 3 and 4.7 between scan rates 5 mV s^{-1} to 200 mV s^{-1}. At higher pH values the experimental peak current function for peak I_a increases only slightly with increasing scan rate. For example at pH 7.8 the increase in the experimental peak current function is 15% for an increase of scan rate from 5 mV s^{-1} to 200 mV s^{-1}. Table 2 summarizes the observed peak currents and the experimental peak current functions at different scan rates and pH values.

For a diffusion controlled electrochemical reaction without complications the peak current function stays constant when the scan rate is varied. However when there is adsorption the peak current increases linearly with sweep rate. In the presence of weakly adsorbed material voltammetric peaks may exhibit an increase in the peak currents because of electron transfer involving both the weakly adsorbed material and the electroactive species diffusing to the electrode surface.[8] Therefore it may be concluded that

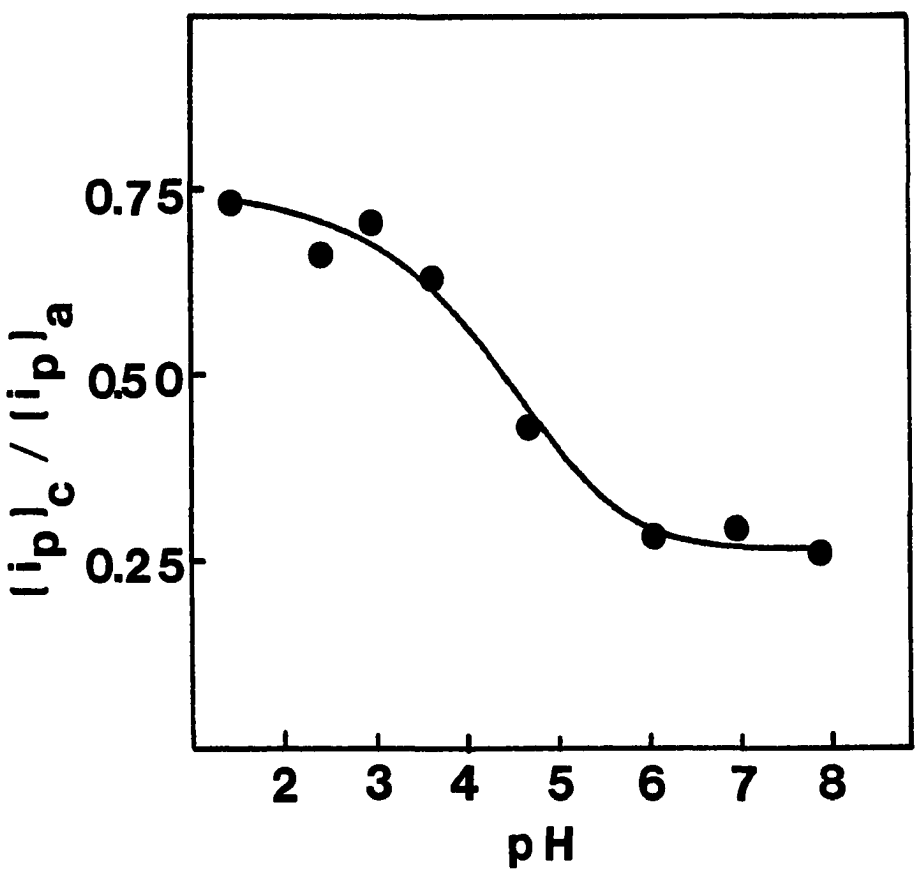

Figure 5. Dependence of peak current ratio $(i_p)_c/(i_p)_a$ on pH at a scan rate of 200 mV s^{-1} for a 1 m$\underline{M}$ solution of 2-DMTHP in phosphate buffer.

Table 2. Variation of peak current[a] for peak I_a as a function of scan rate and pH[b]

pH	i_p (μA)	$i_p (V)^{-1/2}$ μA $(mV^{-1/2})$	scan rate (mV s^{-1})
3.0	2.30	1.03	5
	3.19	1.01	10
	4.29	0.96	20
	7.50	1.06	50
	11.40	1.14	100
	19.00	1.34	200
4.7	2.87	1.28	5
	3.96	1.25	10
	5.35	1.20	20
	8.11	1.15	50
	13.20	1.32	100
	22.60	1.60	200
7.8	3.88	1.73	5
	5.14	1.62	10
	6.95	1.55	20
	13.00	1.84	50
	19.90	1.99	100
	27.00	1.91	200

[a]Concentration of pH 3 solution was 0.75 m$\underline{M}$, at other pH values concentration was approximately 1 m$\underline{M}$.

[b]Phosphate buffers of ionic strength 0.5 $\underline{M}$.

at low pH peak I_a involves electrooxidation of weakly adsorbed 2-DMTHP as well as electrooxidation of 2-DMTHP diffusing to the electrode surface. At higher pH values (i.e., pH >5) there is almost no adsorption of electroactive species involved in peak I_a process. At pH 3 the peak current function for peak II_a increases only slightly (ca. 10%) with increasing sweep rate (5 mV s^{-1} - 200 mV s^{-1}). This slight increase in peak current function with increasing sweep rate is not very significant to be considered as to be due to adsorption (Table 3). At higher pH values the peak current function for peak II_a decreases between a scan rate of 5 mV s^{-1} and 50 mV s^{-1}. Above a scan rate of 50 mV s^{-1} peak II_a may not be observed at pH values higher than 3. The peak current function for peak III_a decreases with increasing sweep rate as does the peak current function for peak II_a. The decrease in the peak current function with increasing scan rate is probably due to the chemical reaction that the peak I_a primary oxidation product has to undergo in order to form the electrochemically active species giving rise to peaks II_a and III_a. At slow scan rates and at pH values around 6 more of the electroactive species may be formed. But at faster scan rates and at lower and higher pH values (e.g., pH 3, pH 9) the concentration of species giving rise to peaks II_a and III_a is low, thus the peak current function goes down with increasing scan rate. At high scan rates there is not enough time for the chemical reaction

Table 3. Variation of peak current[a] for peaks II_a and III_a as a function of scan rate and pH[b]

pH	i_p (μA)		$i_p (V)^{-1/2}$ / μA (mV$^{-1/2}$)		scan rate
	II_a	III_a	II_a	III_a	
3.0	1.61		0.72		5
	2.21		0.70		10
	2.91		0.65		20
	4.67		0.66		50
	6.66		0.66		100
	9.62		0.68		200
4.7	1.75	1.71	0.78	0.76	5
	2.12	1.91	0.67	0.60	10
	2.59	2.35	0.58	0.53	20
	-	4.45		0.62	50
	-	5.77		0.58	100
	-	9.51		0.67	200
7.8		2.63		1.18	5
		3.15		1.00	10
		3.76		0.84	20
		5.41		0.76	50
		8.86		0.86	100
		11.12		0.79	200

[a]Concentration of pH 3 solution was 0.75 m$\underline{M}$, the other solutions were 1 m$\underline{M}$ in 2-DMTHP.

[b]Phosphate buffers of ionic strength 0.5 $\underline{M}$ were used.

to take place.

The appearance of single sweep voltammograms changes with increasing sweep rate. For example a 0.1 mM solution of 2-DMTHP in phosphate buffer pH 3 shows only two oxidation peaks at low scan rates (i.e., 5 mV s^{-1}). However as the scan rate is increased additional oxidation peaks appear (peaks III_a and III_a') (Fig. 6). At a scan rate of 200 mV s^{-1} peak II_a is much smaller than peak I_a and peak III_a' forms an adsorption prepeak.

Cyclic voltammograms of 2-DMTHP at low pH show that with increasing scan rate oxidation peak II_a disappears, peaks III_a, II_c and III_c decrease and become very small (Fig. 7). This behavior suggests that peaks II_a, III_a, II_c and III_c are dependent on formation of a species by a chemical reaction the concentration of which decreases with increasing scan rate. The redox couple characterized by peak I_a/I_c are the major peaks observed at very high scan rates (i.e., 50V s^{-1}).

Concentration studies show that the peak current dependence on concentration for peak I_a is almost linear between 0.1 mM and 1.0 mM at pH 3 (Fig. 8). All adsorption systems show a marked non-linear influence on the current with variations in the bulk concentration, C*. As the concentration is increased, the surface of the electrode ultimately becomes nearly saturated and the total charge flowing during reduction due to adsorbed material becomes

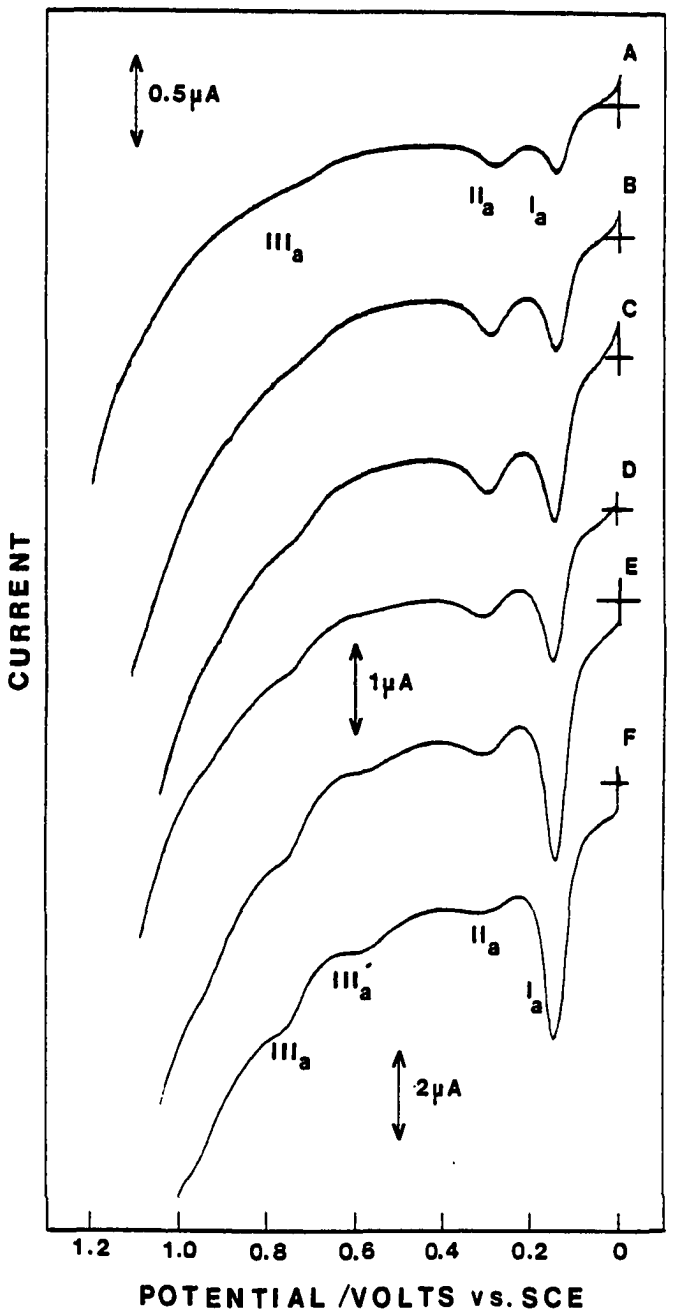

Figure 6. Single sweep voltammograms of 0.1 mM 2-DMTHP in phosphate buffer pH 3, at different scan rates A) 5 B) 10 C) 20 D) 50 E) 100 and F) 200 mV s^{-1}.

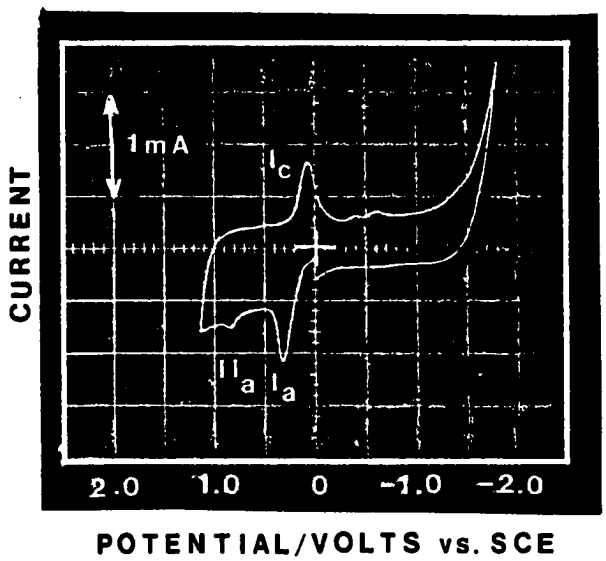

Figure 7. Cyclic voltammogram of 1 mM 2-DMTHP in phosphate buffer pH 2.0 at a scan rate of 50V s^{-1}.

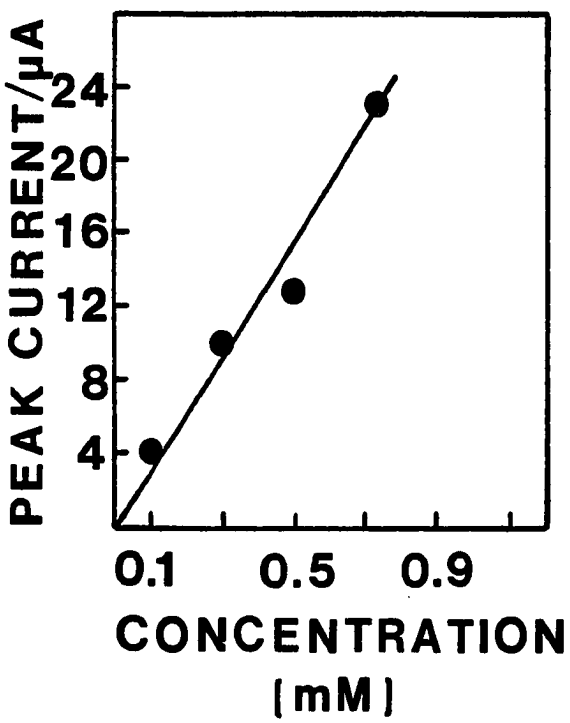

Figure 8. Dependence of peak current for peak I_a on concentration at pH 3; i_p values obtained at a scan rate of 5 mV s^{-1}.

constant, while the total change due to diffusing material continues to increase with concentration.[8] Since 2-DMTHP shows an almost linear dependence on concentration between 0.1 m$\underline{M}$ and 1.0 m$\underline{M}$, it may be concluded that adsorption over this concentration range is only slight. This conclusion is in accord with the results obtained from voltammetric scan rate studies. Figure 9 shows single sweep voltammograms of 2-DMTHP in phosphate buffer pH 3 as a function of concentration. At low concentration peak I_a and II_a are almost the same size. However, as the concentration increases the relative heights of these two peaks change. For example, at a concentration of 1 m$\underline{M}$ of 2-DMTHP peak I_a is twice as high as peak II_a (Fig. 9).

Peak(s) II_a and/or III_a have to be scanned in order to observe peak II_c. Peak III_c may be observed by only scanning past peak I_a. Peak II_c appears to have adsorption characteristics which will be discussed in a later section.

Below pH 5, peak IV_c may be observed (Fig. 3) coupled to peak II_a. This peak is better defined at low concentrations of 2-DMTHP and low pH values. As the pH approaches 5, the potential sweep has to be reversed immediately beyond peak II_a in order to observe peak IV_c. This may indicate that peak IV_c is due to a short lived species which is formed in the peak II_a process and that this species disappears in a pH dependent chemical reaction.

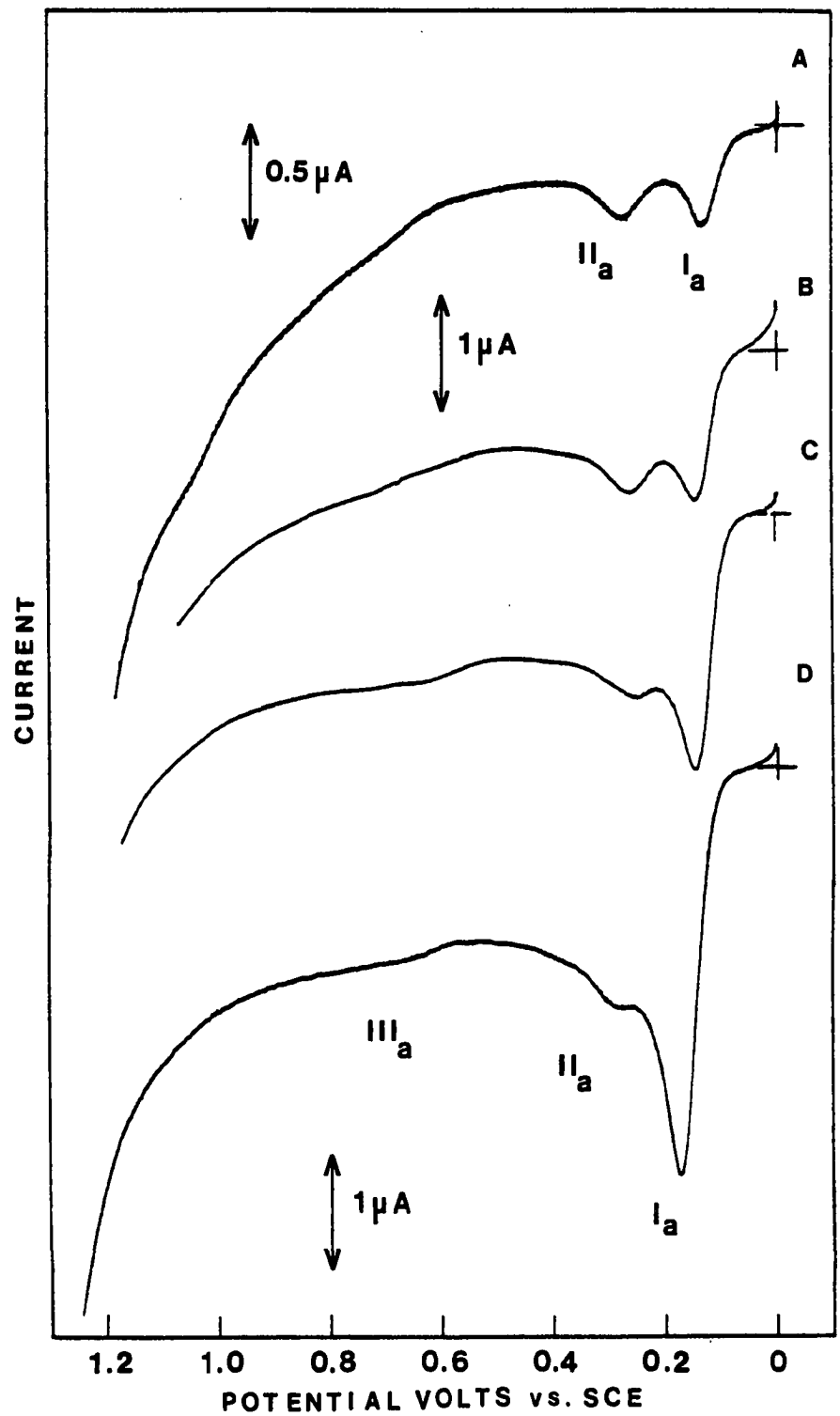

Figure 9. Single sweep voltammograms of 2-DMTHP in phosphate buffer pH 3 at different concentrations A) 0.1 B) 0.5 C) 0.75 D) 1.0 mM, at a scan rate of 5 mV s^{-1}.

At pH values higher than 5 cyclic voltammograms of 2-DMTHP exhibit different behavior. For example peak II_a is no longer observed. An additional oxidation peak, peak V_a, may be observed which forms a quasi-reversible couple with peak II_c (Fig. 10). The peak separation between peaks II_c and V_a averages 37.5±15 mV between pH 6.1-9.1 at a scan rate of 200 mV s^{-1}.

Controlled potential coulometry

Controlled potential coulometric experiments show that upon oxidation of 2-DMTHP in a thin-layer cell at potentials corresponding to peak I_a, over the pH range 1.8 to 7.7, 1.95±0.28 e per molecular are transferred. Application of peak III_a potentials results in the transfer of 3.74±0.36 e between pH 1.8 and 7.7. Figure 11 shows voltammograms recorded before and after electrolysis. Upon application of a potential corresponding to peak I_a at low pH (pH <5), peaks II_a and III_a are the only oxidation peaks observed at the end of the electrolysis (Fig. 11B). When a potential is applied past peak III_a, no oxidation peaks may be observed upon the completion of electrolysis (Fig. 11C). At higher pH values, for example at pH 6.7, electrolyzing at peak I_a potentials results in voltammograms showing only peak III_a (Fig. 12).

Large-scale controlled potential electrolyses were carried out between pH 2-7.3. At pH 2 2-DMTHP shows three

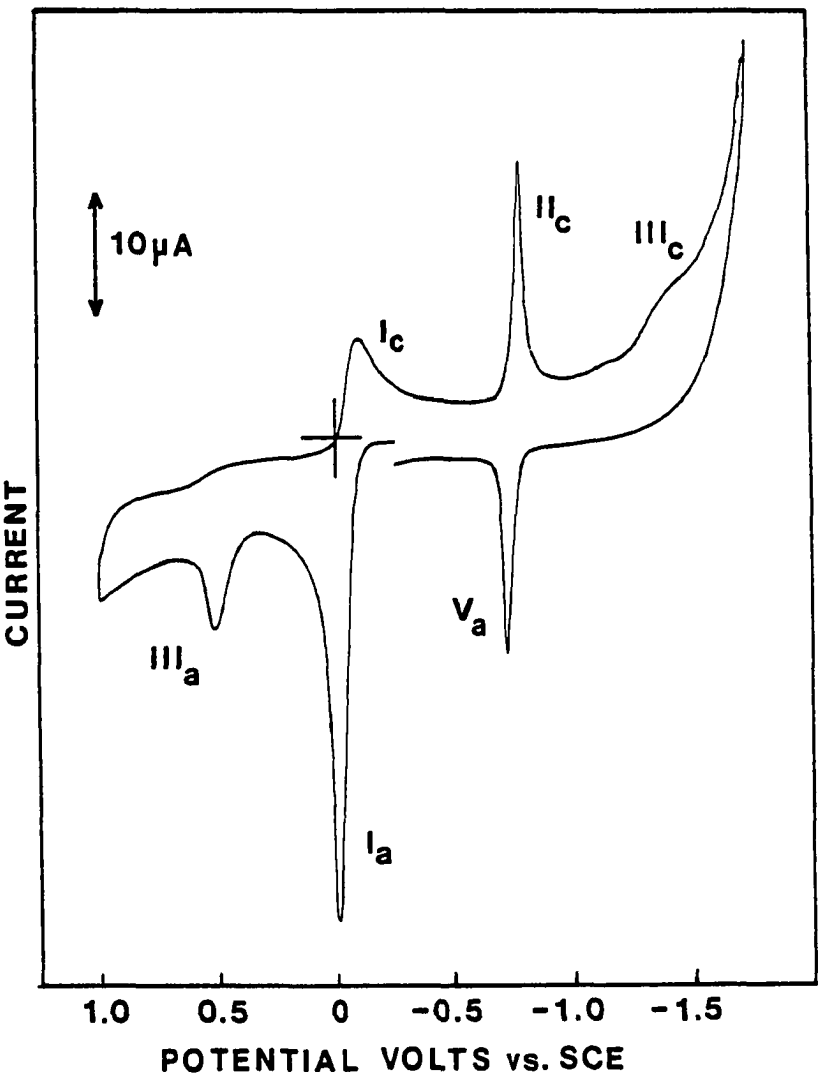

Figure 10. Cyclic voltammogram of 1 m$\underline{M}$ 2-DMTHP in phosphate buffer pH 7.3 at a scan rate of 200 mV s^{-1}.

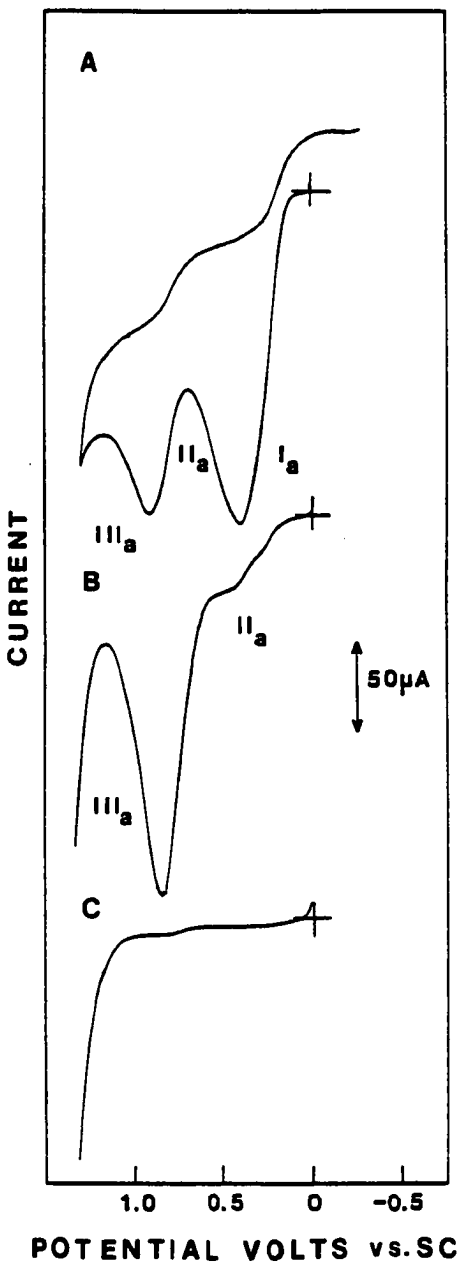

Figure 11. Voltammograms of 1 mM 2-DMTHP in a thin-layer reticulated vitreous carbon cell A) Before applying any potential B) After applying a potential of +0.2V, C) After applying a potential of 1.0V in phosphate buffer pH 3, at a scan rate of 5 mV s^{-1}.

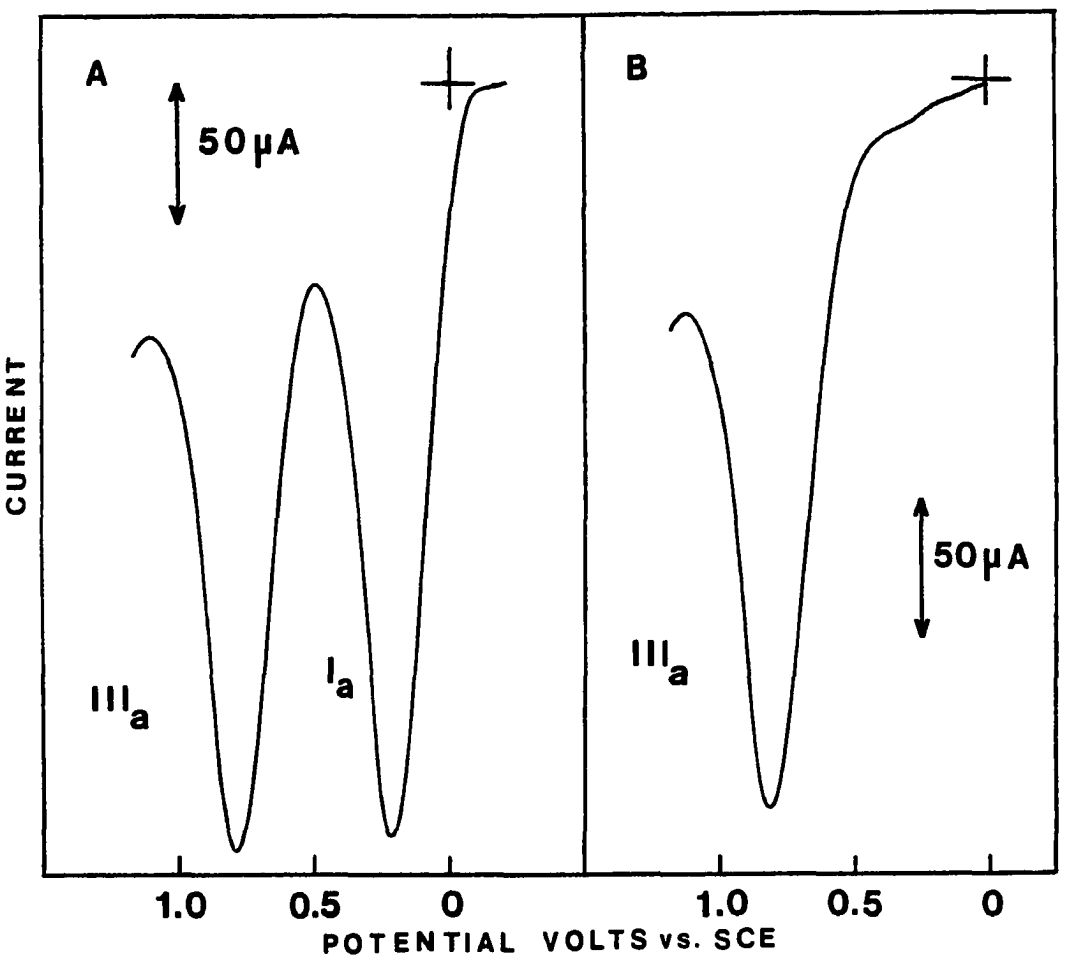

Figure 12. Voltammograms of 1 m$\underline{M}$ 2-DMTHP in a thin-layer reticulated vitreous carbon cell A) before electrolysis B) at the end of the electrolysis (0.2V) in phosphate buffer pH 6.7, at a scan rate of 5 mV s^{-1}.

electrooxidation peaks (Fig. 13A) and three U.V. absorption bands (Fig. 14, curve 1) before application of any potential. Upon application of a potential corresponding to peak I_a, peak I_a decreases in height and eventually disappears leaving peaks II_a and III_a (Fig. 13B). When scanned in a negative direction, peak III_c may be observed (Fig. 13C). The peak I_a oxidation product has an U.V. spectrum with λ_{max} = 354, 251, 223 nm and a shoulder at about 283 nm (Fig. 14, curve 2). When the electrolysis is carried on at potentials past peak II_a and/or III_a, no oxidation peaks may be observed at the end of the electrolysis (Fig. 13D). However, reduction peaks II_c and III_c may be observed if the potential is first scanned in a negative direction. The peak II_a and/or III_a product has λ_{max} = 336, 288, 245 and 203 nm (Fig. 14, curve 3) - identical to the U.V. spectrum of 2-DMP at pH 2. The product obtained upon oxidation of 2-DMTHP at peak III_a potentials in a pH 3 low phosphate buffer (0.5 M NaCl, 5 mM Na_2HPO_4) was identified as 2-DMP by gas chromatography-mass spectrometry (GC-MS).

At higher pH values, for example at pH 7.3, following complete electrooxidation of 2-DMTHP at peak I_a potentials the resulting product shows only peak III_a (Fig. 15B). Peak III_c may be observed on the first negative sweep. No oxidation peaks are observed at the end of an electrolysis at peak III_a potentials (Fig. 15C). Both peaks II_c and III_c are observed on the initial scan in a negative direction.

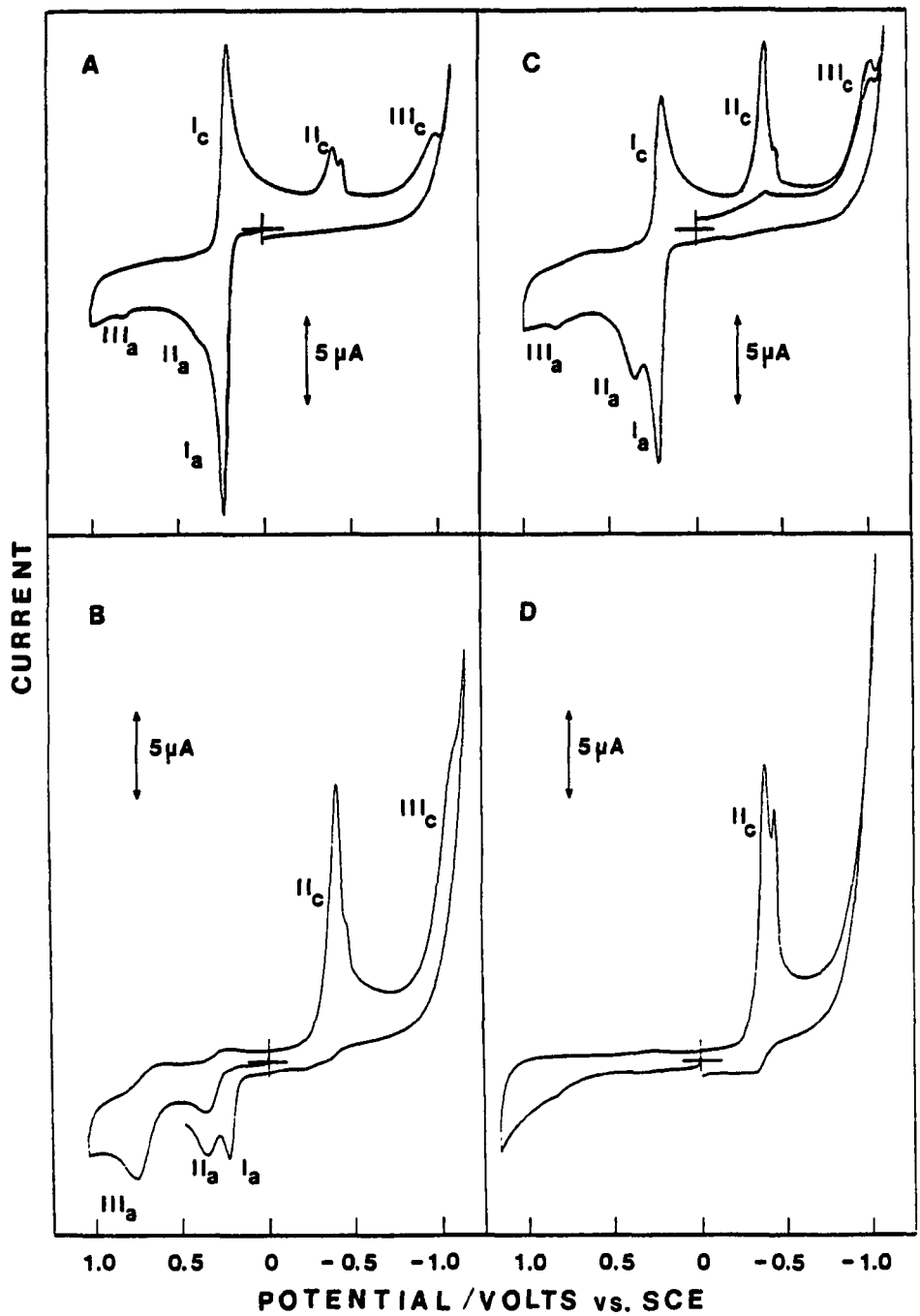

Figure 13. Cyclic voltammograms of 1 mM 2-DMTHP in phosphate buffer pH 2 at a scan rate of 200 mV s^{-1}, A) before applying a potential, B) after electrolysis at +0.25V, scanning in positive direction first, C) after electrolysis at 0.25V initial scan in negative direction, D) after applying a potential of +0.5V.

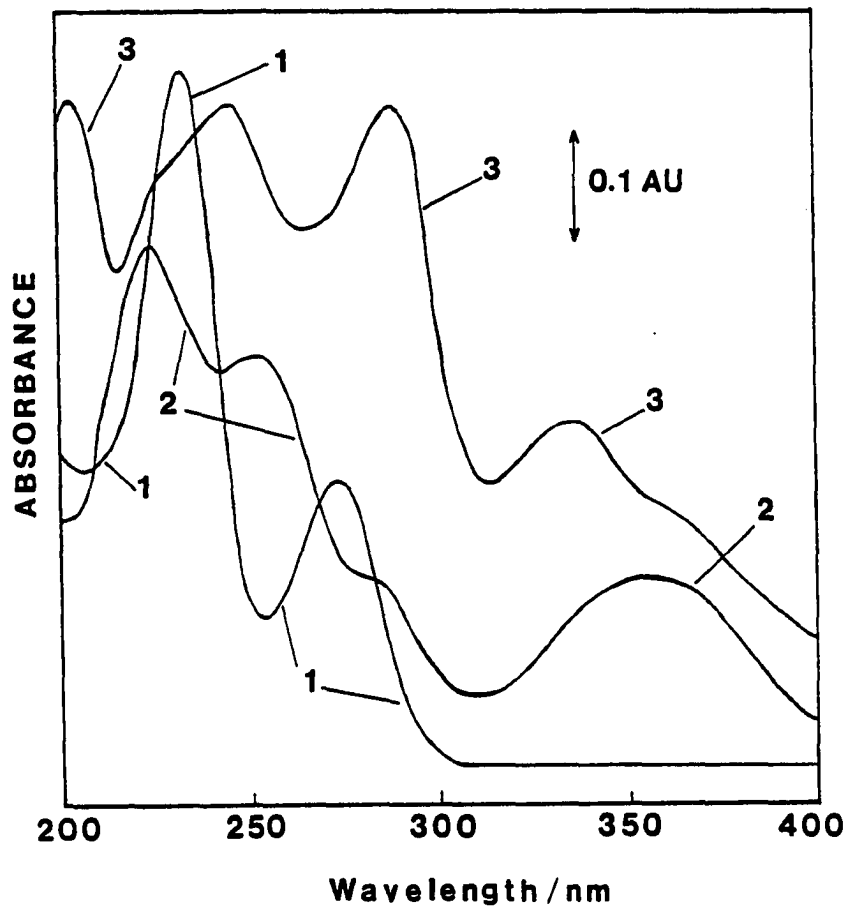

Figure 14. U.V. spectrum of 2-DMTHP in phosphate buffer pH 2, 1) before electrolysis, 2) after completing the electrolysis at peak I_a potentials (+0.25V), 3) after completing the electrolysis at peak III_a potentials, wavelength scanning rate 200 nm min^{-1}, response time 0.5 sec.

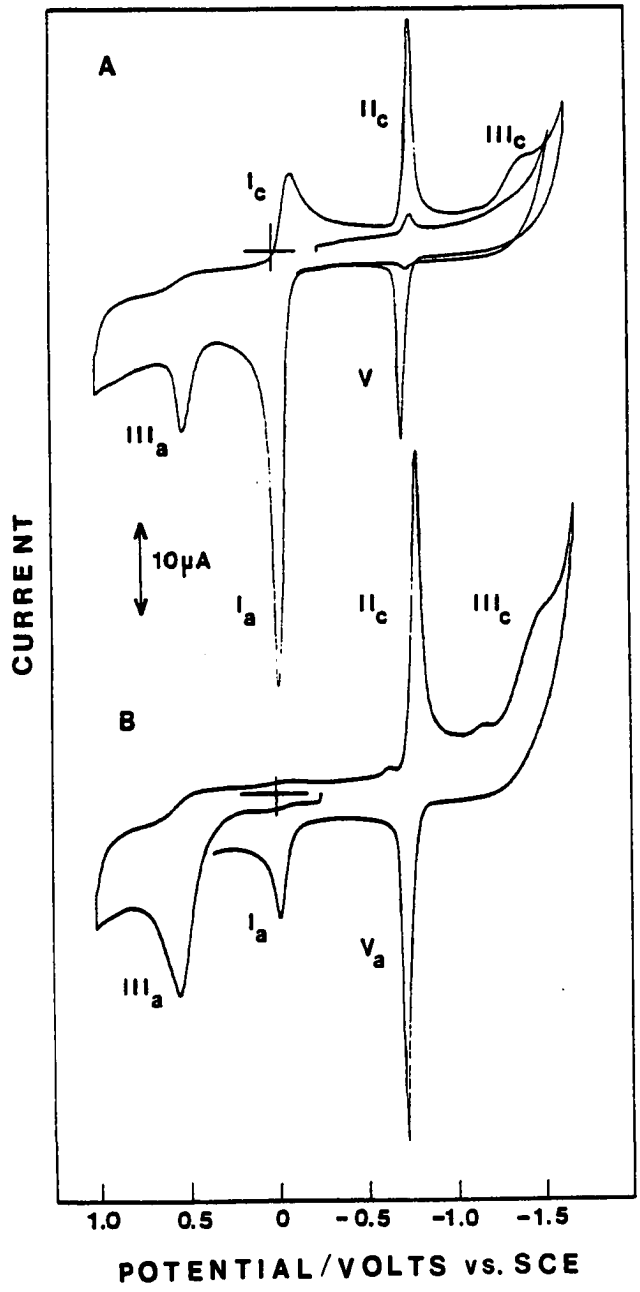

Figure 15A,B. Cyclic voltammogram of 1 mM 2-DMTHP in phosphate buffer pH 7.3, at a scan rate of 200 mV s^{-1}, A) before electrolysis, B) after electrolyzing at peak I_a potentials (+0.2V).

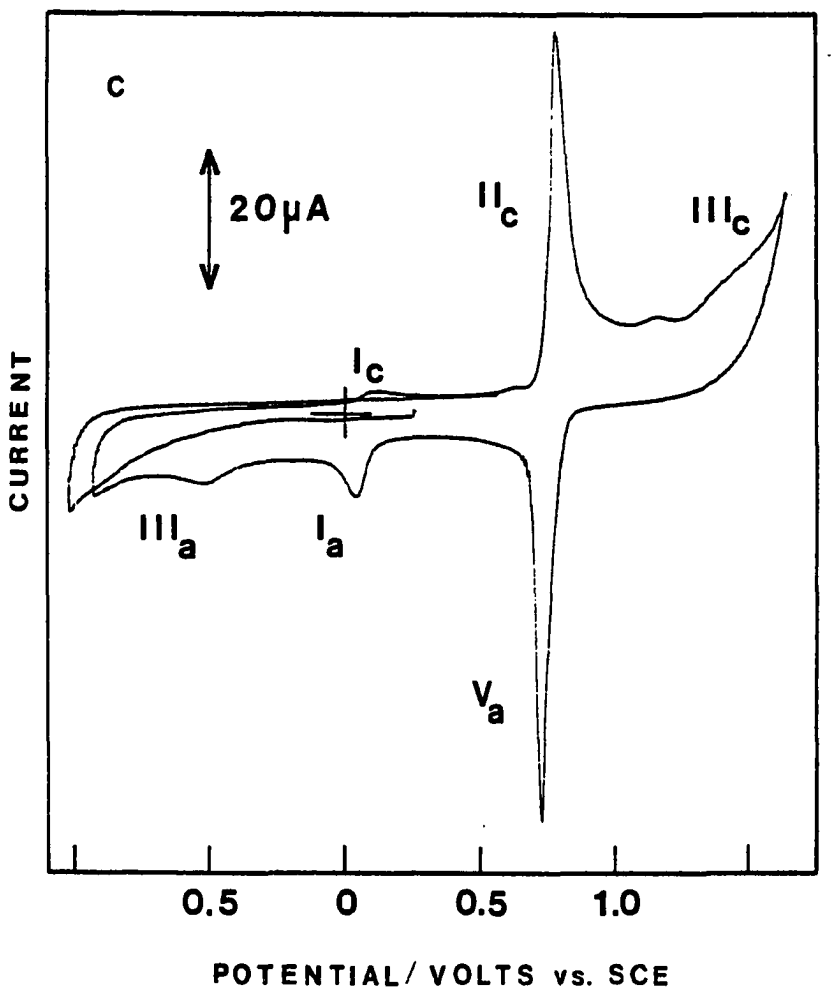

Figure 15C. Cyclic voltammogram of 1 m<u>M</u> 2-DMTHP in phosphate buffer pH 7.3, at a scan rate of 200 mV s^{-1}, C) after electrolyzing 1 m<u>M</u> 2-DMTHP at peak III_a potentials (+0.7V) in phosphate buffer pH 7.3.

The U.V. spectra of the starting material, peak I_a and III_a oxidation products may be seen in Fig. 16. The U.V. spectrum of the peak III_a product and the resulting cyclic voltammograms are identical to that of 2-DMP at pH 7.3. Product analysis on samples which were electrolyzed at peak III_a potentials at pH 7.5 in low phosphate buffers revealed formation of 2-DMP.

The results of controlled potential coulometry support the fact that peak I_a process of 2-DMTHP is a 2e reaction. When a potential was applied to a solution of 2-DMDHP corresponding to peak II_a at low pH values, two electrons were transferred and the resulting voltammogram did not show any electrooxidation peaks. The same result was obtained when a potential was applied past peak III_a. Therefore it may be concluded that the peak II_a and III_a processes involve overall two electrons. Cyclic voltammetric experiments show that at low pH and slow scan rates only voltammetric oxidation peaks I_a and II_a are observed. When the scan rate is increased an additional oxidation peak, peak III_a may be seen (Fig. 17). Based on the voltammetric and coulometric results it is clear that the species giving rise to peaks II_a and III_a are in some kind of equilibrium. Since oxidation peak II_a disappears above pH 5, formation of this species must be pH dependent. One way of explaining these experimental observations is to assign peak II_a to the electrooxidation of a covalently hydrated form of 2-DMDHP

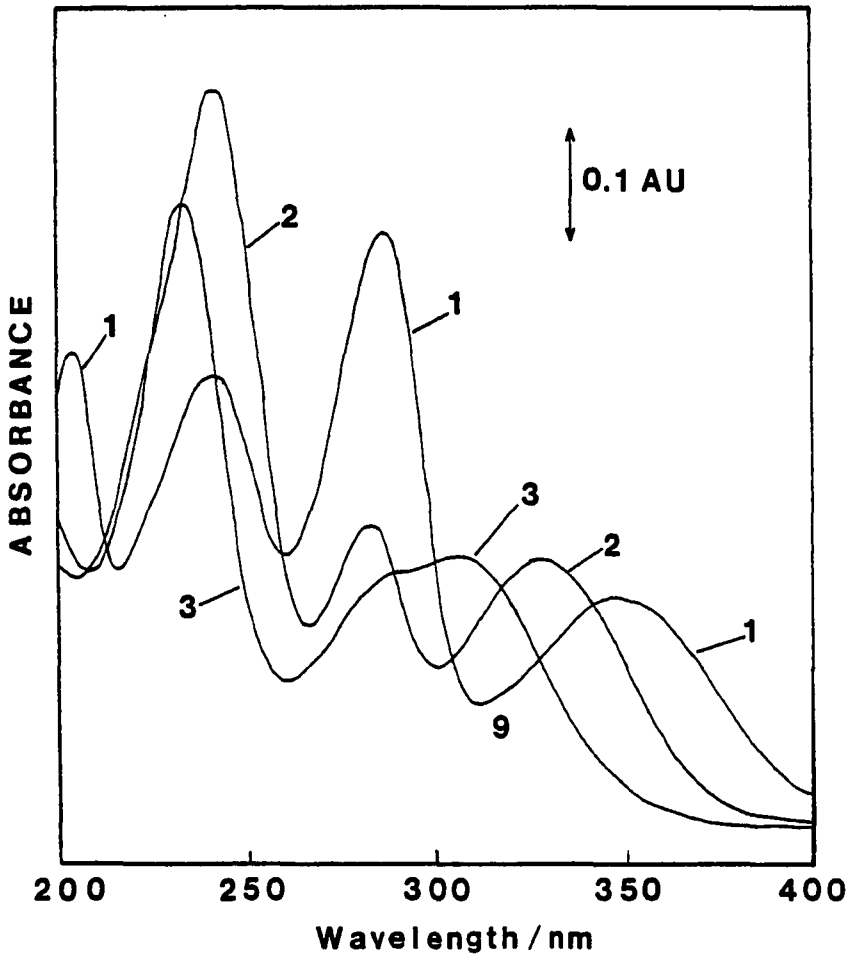

Figure 16. U.V. spectra of 2-DMTHP 1) before electrolysis, 2) peak I_a electrolysis product, 3) peak III_a electrolysis product, in phosphate buffer pH 7.3, wavelength scanning rate 200 nm min^{-1}, response time 0.5 sec.

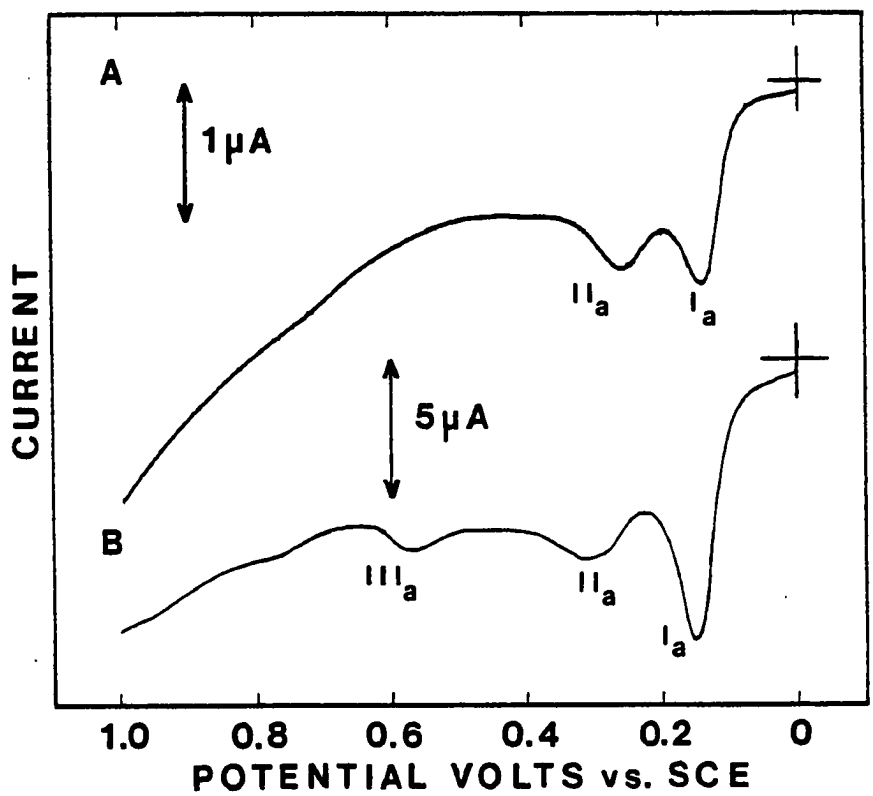

Figure 17. 2-DMTHP in phosphate buffer pH 3 at a scan rate of (A) 5 mV s^{-1} and (B) 200 mV s^{-1}.

(2-DMDHP·H_2O) (14) and peak III_a to electrooxidation of the nonhydrated form of 2-DMDHP.[9]

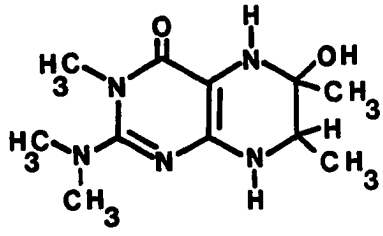

14

Thin-layer spectroelectrochemistry

As observed from cyclic voltammetric experiments an unstable intermediate species is formed in the peak I_a process of 2-DMTHP which reacts in a pH-dependent chemical reaction. It was anticipated that measurement of the rate of this chemical step might give very useful information concerning the actual structure of the quinonoid species formed.

2-DMTHP may form only one quinonoid (8a) upon a $2e^- - 2H^+$ electrooxidation. In order to gain more information on the kinetics of this intermediate species, thin-layer spectroelectrochemical experiments were carried out as a function of pH and concentration.

A spectrum of 2-DMTHP at pH 3 (λ_{max} = 232, 278 nm) in a thin-layer cell containing an optically-transparent reticulated vitreous carbon (RVC) electrode is shown in

curve 1 of Fig. 18A. Upon application of a potential corresponding to peak I_a, as determined from a single sweep voltammogram obtained in the thin-layer cell (Fig. 19), both U.V. bands of 2-DMTHP decrease while the absorbance goes up at 360 nm and around 268 nm (curves 2 and 3 in Fig. 18A). Curve 1 in Fig. 18B shows the spectrum observed about 60 seconds after initiation of the electrooxidation of 2-DMTHP. Curve 2 in Fig. 18B corresponds to the spectrum 175 seconds after termination of the electrolysis. When the applied potential is turned off the absorbance keeps increasing around 358 nm and 268 nm and decreases at 316 nm reaching a minimum in about 200 seconds. The initial and final spectra are shown in Fig. 18C. If the potential is kept on throughout the experiment the resulting product exhibits λ_{max} at 356, 288, 254 and 230 nm. This spectrum is in good agreement with the spectrum obtained after large scale electrolysis of 2-DMTHP at peak I_a potential in phosphate buffer pH 3.

The spectroelectrochemical behavior of 2-DMTHP was somewhat different at higher pH. For example, at pH 8.8 2-DMTHP exhibits two absorption bands (λ_{max} = 236 and 310 nm, Fig. 20A). Upon application of a potential corresponding to peak I_a, both absorption bands decrease. Correspondingly, another band starts to grow in at 248 nm (curve 2, Fig. 20B). If, after almost all of the 2-DMTHP has been electrooxidized, the applied potential is turned

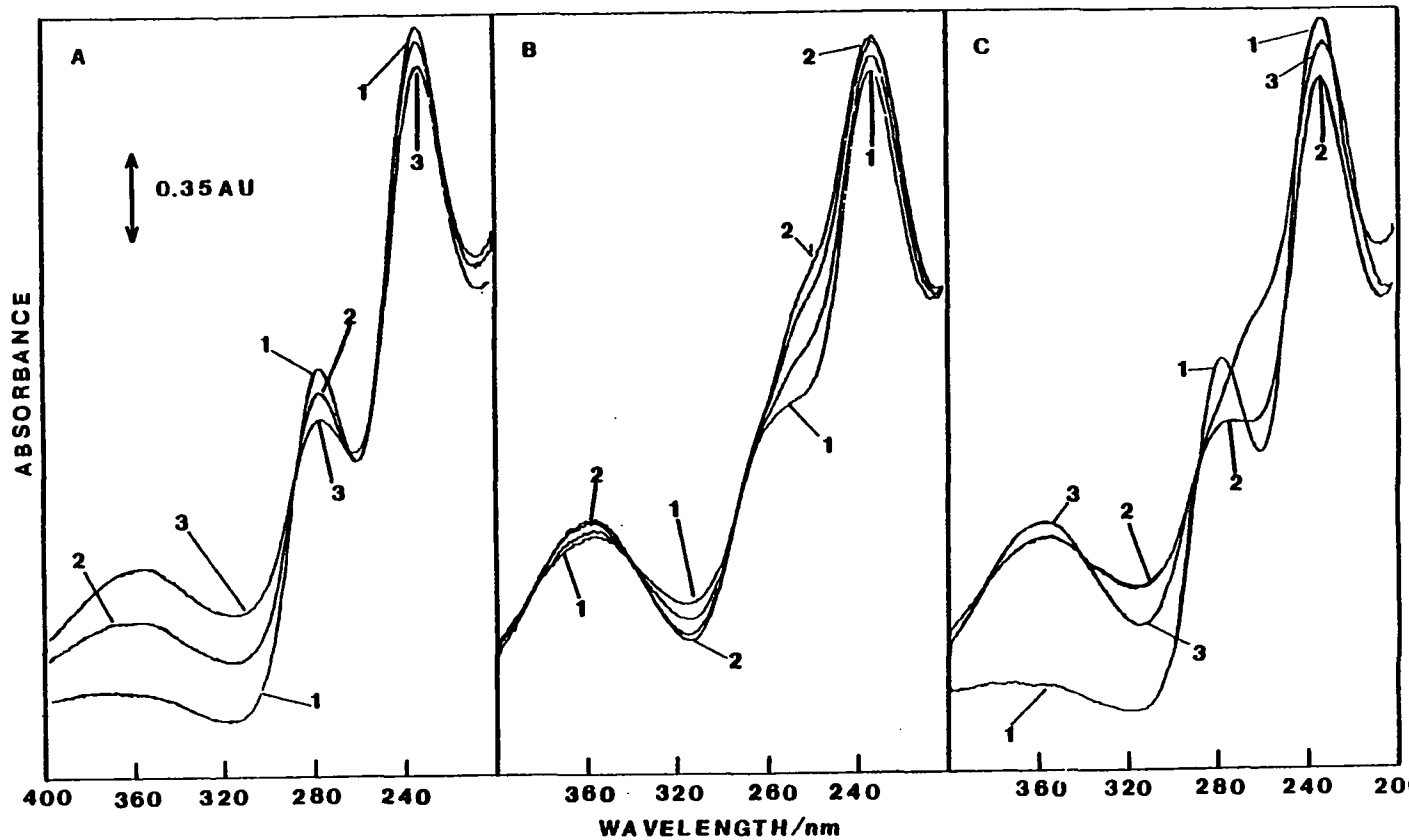

Figure 18. U.V. spectrum of 1 mM 2-DMTHP electrolyzing at 0.55V in phosphate buffer pH 3.0 at a reticulated vitreous carbon electrode in a thin-layer cell. A) Curve 1 is 2-DMTHP before electrolysis, curve 2 is the spectrum obtained after 10s, curve 3 after 30s of electrolysis; B) Curve 1 is 2-DMTHP after 40s of electrolysis at a point where most of the 2-DMTHP has been oxidized, curve 2 is the spectrum after complete decay of the intermediate species and corresponds to the u.v. spectrum of 2-DMDHP. Repetitive scans of 18.8s are shown; C) Curve 1 is 2-DMTHP before electrolysis, curve 2 is after 56s of electrolysis at which point the applied potential is turned off and corresponds to the spectrum of the intermediate generated. Curve 3 is the spectrum of the final product.

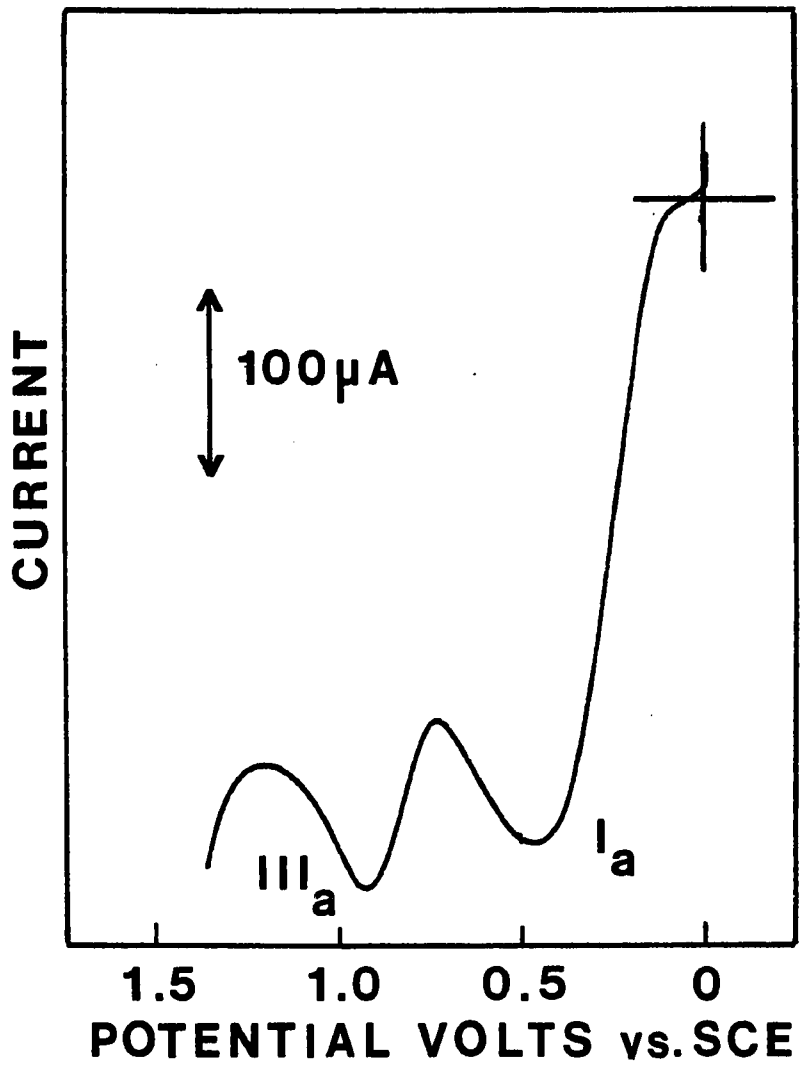

Figure 19. Single sweep voltammogram of 0.86 mM 2-DMTHP in a reticulated vitreous carbon thin-layer cell before electrolysis in phosphate buffer pH 3, at a scan rate of 5 mV s^{-1}.

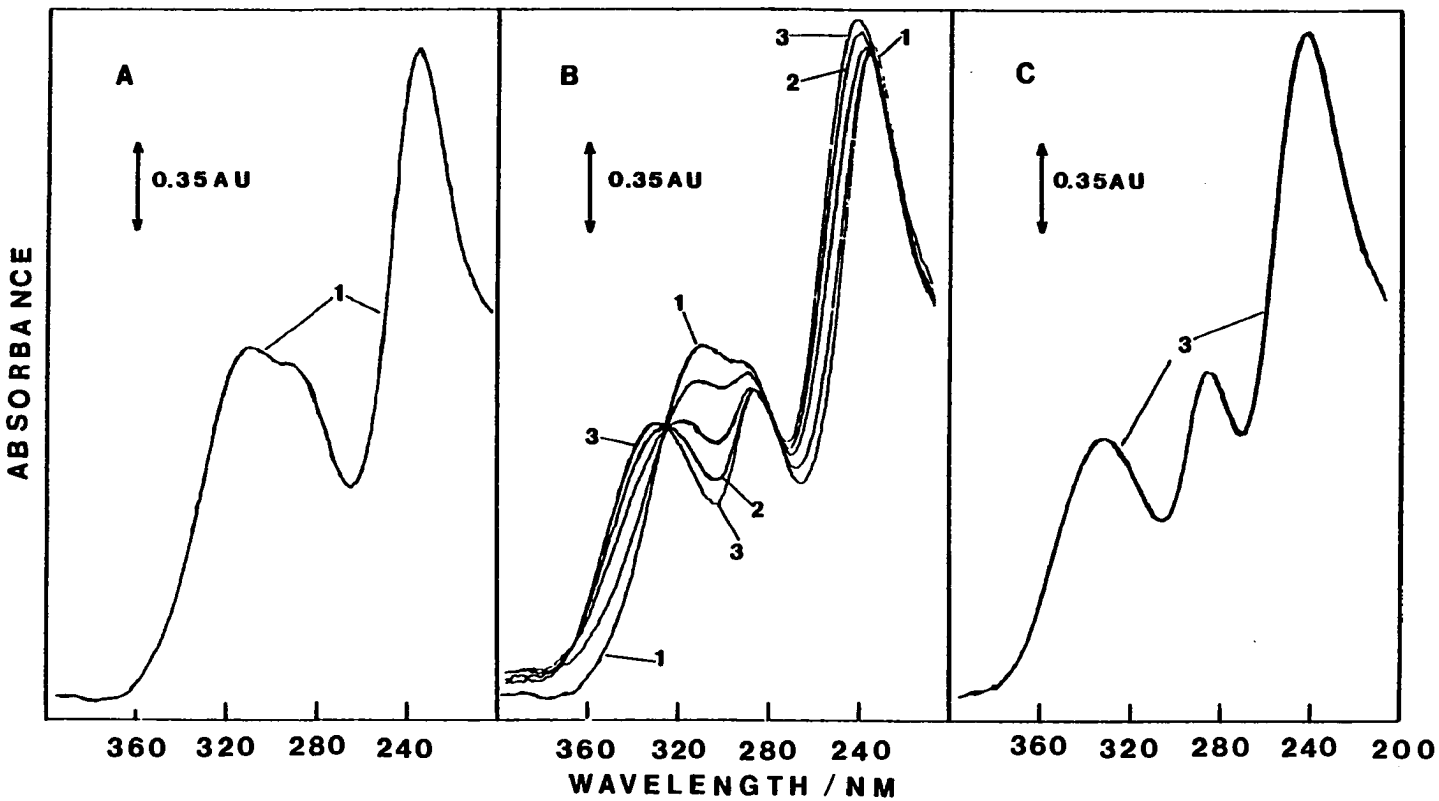

Figure 20. U.V. spectra of 1 mM 2-DMTHP in phosphate buffer pH 8.8 electrolyzing at +0.65V at a reticulated vitreous carbon electrode in a thin-layer cell. (A) Spectrum of 2-DMTHP before electrolysis, (B) Curve 1 is 2-DMTHP before electrolysis, curve 2 is spectrum after 40s and curve 3 is after 100s of electrolysis, (C) Spectrum of the electrolysis product.

off, the absorbance keep increasing at 242 nm and 330 nm and decreases at 304 nm (curve 3, Fig. 20B). Figure 20C shows the final spectrum.

These spectroelectrochemical results support the fact that an intermediate species is generated upon electro-oxidation of 2-DMTHP at peak I_a potentials. The kinetics of this reaction was studied between pH 2-9 using a thin-layer spectroelectrochemical method by either monitoring the decay of the U.V. absorbance of the intermediate species or the increase in the absorbance of 2-DMDHP, i.e., the reaction product. The dependence of the observed first order rate constant on pH is shown in Fig. 21.

Concentration studies revealed that the rate is not affected by a change in concentration of 2-DMTHP. The dependence of k_{obs} on concentration at various pH values is shown in Table 4.

2-Dimethylamino-3,6,7-trimethyl-7,8-dihydropterin

2-Dimethylamino-3,6,7-trimethyl-7,8-dihydropterin (2-DMDHP) was generated electrochemically from 2-DMP by applying a potential beyond peak II_c. 2-DMDHP could also be generated by electrooxidation of 2-DMTHP past peak I_a potentials. The U.V. spectra of 2-DMTHP obtained by electro-oxidation of 2-DMTHP past peak I_a potentials at pH 2 and 7.3 are shown in curve 2 of Figs. 14 and 16, respectively. The electrooxidation product of 2-DMTHP or the electro-

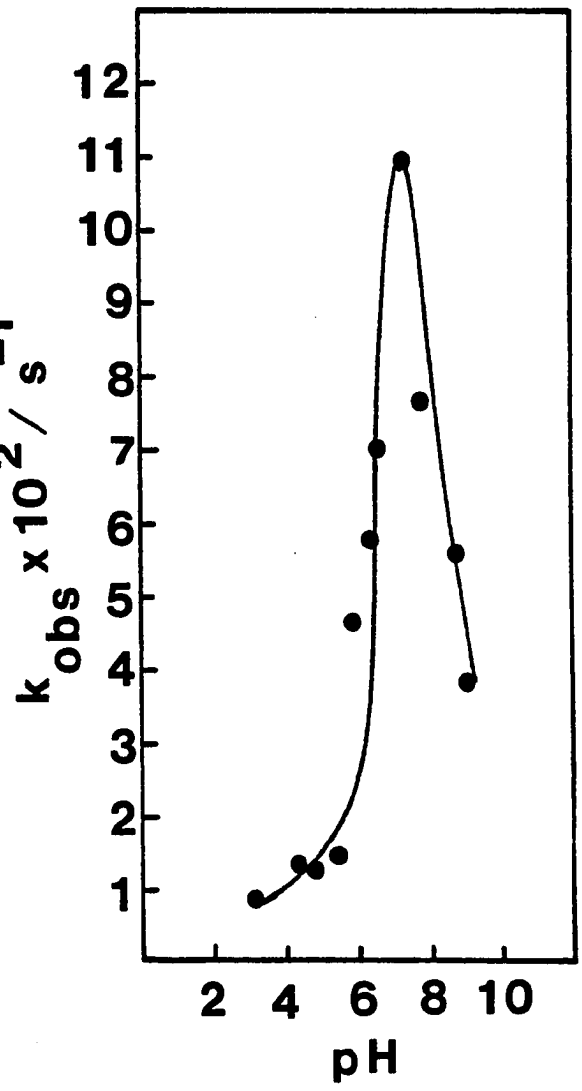

Figure 21. Variation of the observed first-order rate constant for the chemical reaction of peak I_a electrooxidation product of 2-DMTHP to give 2-DMDHP as a function of pH. Data obtained by a thin-layer spectroelectrochemical method using an optically transparent reticulated vitreous carbon electrode. Phosphate buffers were used at all pH values which had an ionic strength of 0.5 M.

Table 4. Observed first-order rate constant for reaction of the primary peak I_a electrooxidation product of 2-DMTHP as a function of concentration at various pH values[a]

pH	Initial concentration of 2-DMTHP/mM	k_{obs}/s^{-1}[b] $\times 10^3$	$\sigma \times 10^3$[c]
3.04	0.22	6.60	1.32
	0.58	6.27	0.94
	0.87	6.63	1.14
	0.98	6.58	0.31
	2.01	7.49	1.42
6.96	0.75	93.20	1.08
	1.03	91.60	1.21
	1.10	115.90	1.07
4.40	0.28	10.02	1.63
	0.50	8.67	0.54
	1.01	10.32	1.03

[a]Data obtained by a thin-layer spectroelectrochemical method using an optically-transparent reticulated vitreous carbon electrode.

[b]Mean of at least three determinations.

[c]Standard deviation.

reduction product of 2-DMP showed two oxidation peaks (II_a and III_a) below pH 5 (Fig. 13B). Only peak III_a was observed above pH 5 (Fig. 15B).

The peak potentials observed at various pH values are summarized in Table 4. At slow scan rates peak II_a is as large as or larger than peak III_a, but at faster scan rates peak III_a becomes the larger peak. Under certain conditions (e.g., pH 2 and at sweep rates >50 mV s^{-1}) an additional oxidation peak, peak III_a' may be observed at potentials slightly negative of peak III_a. This peak has the characteristics of an adsorption peak (shows more symmetry than an uncomplicated diffusion controlled reaction, increases in symmetry at fast scan rates, its peak current function increases linearly with sweep rate).

Cyclic voltammograms of 2-DMDHP at pH $\leq$5.0 exhibit two oxidation peaks (II_a and III_a) if the initial sweep is towards positive potentials. Having scanned these peaks, four reduction peaks are observed on the reverse sweep. If the initial sweep is in negative direction first, only peak III_c is observed.

At pH values $\leq$5 an additional reduction peak (peak IV_c) is observed forming a quasi-reversible couple with peak II_a. This peak appears to be split into two peaks. The relative height of these peaks change as a function of scan rate (Fig. 22).

At relatively high scan rates peak IV_c is the larger

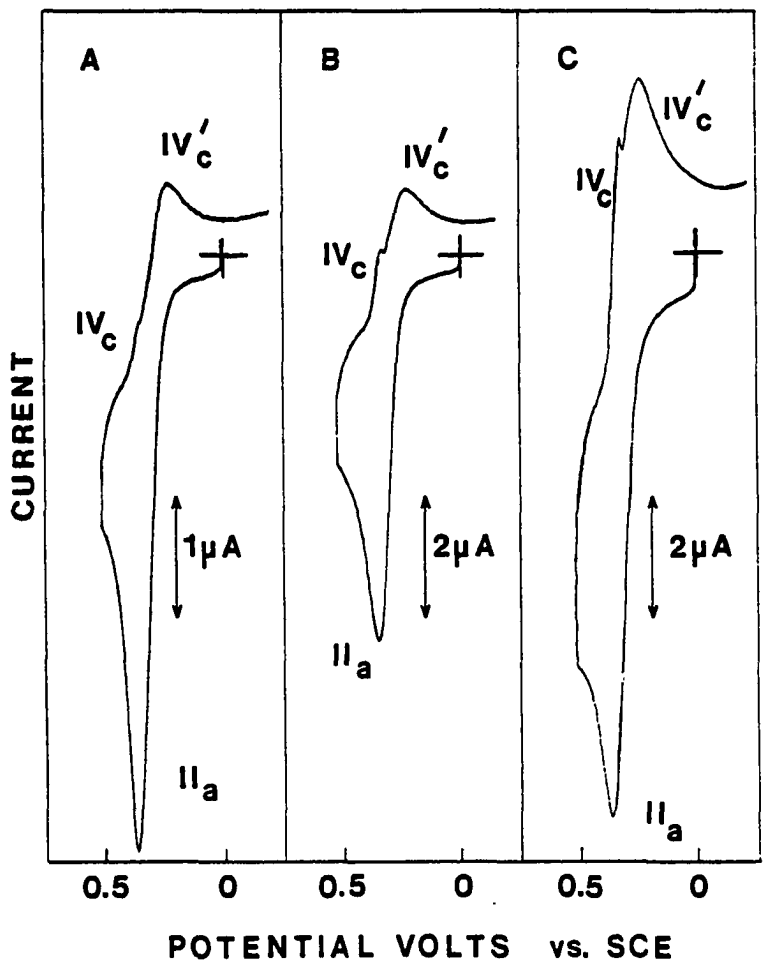

Figure 22. Cyclic voltammogram of 1 mM 2-DMDHP at PGE in phosphate buffer pH 2.0 at a sweep rate of (A) 50 mV s^{-1}, (B) 100 mV s^{-1} and (C) 200 mV s^{-1}.

one. But as the scan rate decreases IV_c becomes smaller and IV_c' grows (Fig. 22). This behavior suggests that an unstable product is formed in peak II_a electrooxidation process which can react to form a second transient species which then can be reduced at peak IV_c' potentials. The species giving rise to peak IV_c' is not very stable and further decomposes. During the second positive voltammetric sweep a new oxidation peak, peak I_a, may be observed (Figs. 13B and 15B). Peak I_a appears at the same potential as peak I_a of 2-DMTHP. On the second negative voltammetric sweep another reduction peak, peak II_c, may be observed. It is necessary to scan the potential past peak II_a in order to observe this peak. Peak II_c grows significantly as the potential is scanned past peak III_a and is reversed.

Cyclic voltammograms of 2-DMDHP have a different appearance at higher pH values (pH $\geq$5). For example, at pH 7.3 only peak III_a is observed on the first positive sweep. Peak III_c is the only reduction peak along with a small adsorption peak observed for 2-DMP. A new oxidation peak (peak V_a) may be observed coupled to peak II_c, which is due to reduction of an unstable species.

2-Dimethylamino-3,6,7-trimethypterin

2-DMP gives rise to two voltammetric reduction peaks (peaks II_c and III_c, Fig. 23) at the PGE. The peak potential (E_p) dependence on pH is represented by the following

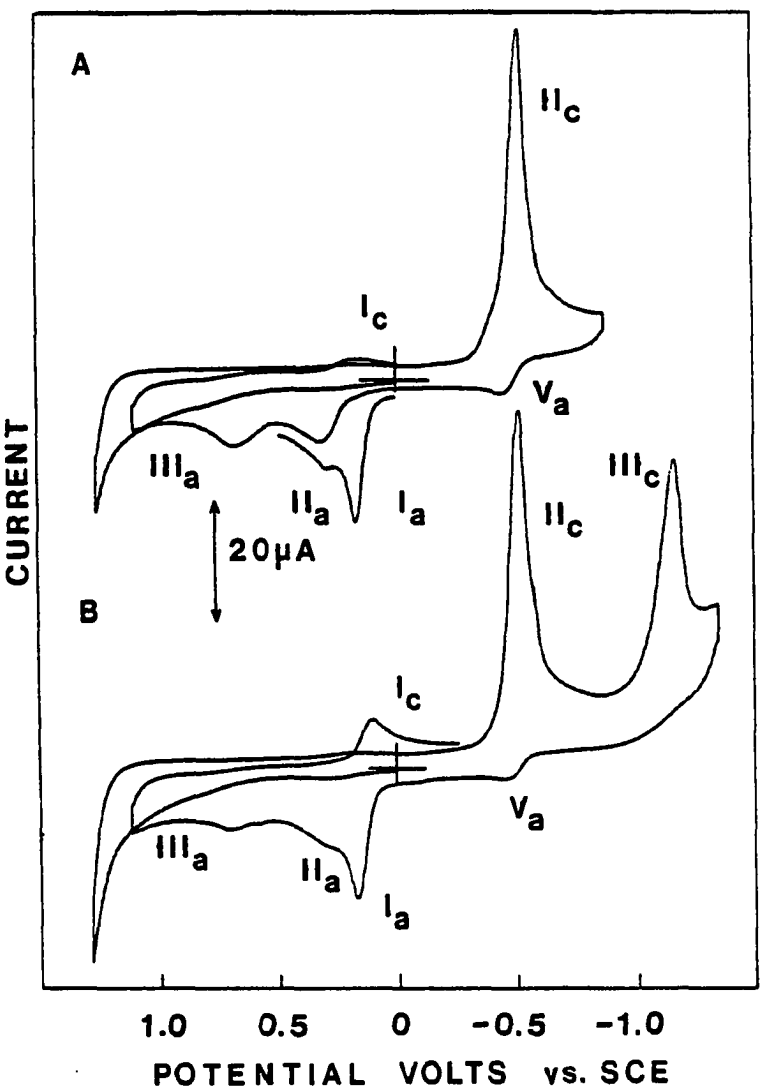

Figure 23. Cyclic voltammogram of 1 m$\underline{M}$ 2-DMP at PGE in phosphate buffer pH 3 at a sweep rate of 200 mV s^{-1}, (A) switching potential past peak II_c, (B) switching potential past peak III_c.

equations and in Fig. 24:

Peak II_c $E_p = (-0.26-0.071\ pH)V$

$pH = (1.45-9.5)$

Peak III_c $E_p = (-1.03-0.0\ pH)V$

$pH = (1.45-3.0)$

$E_p = (-0.78-0.073\ pH)V$

$pH = (3.0-7.8)$

It appears that the peak potential for peak III_c is independent of pH between pH 1.45-3.0. As the pH increases, peak III_c is harder to observe because it is very close to background discharge current. 2-DMP does not show any voltammetric oxidation peaks up to +1.2V. Cyclic voltammograms of 2-DMP show two voltammetric reduction peaks when scanned first in a negative direction. After completing the negative scan one may observe up to four voltammetric oxidation peaks (I_a, II_a, III_a and V_a) between pH 1.5-5 (Fig. 23). Peak II_a cannot be observed at pH values higher than 5. Peak V_a forms a reversible couple with peak II_c. The peak potential separation is 25 mV at sweep rates of 50 mV s^{-1} and 100 mV s^{-1}. Peak I_a is coupled to the reverse peak I_c which may be observed upon completing a second scan in a positive direction. The peak potential for peak I_a is the same as observed for peak I_a of 2-DMTHP. Peak clipping experiments show that it is necessary to sweep the potential past peak II_c in order to observe peaks II_a and III_a (Fig. 23). Both peaks II_c and III_c have to be

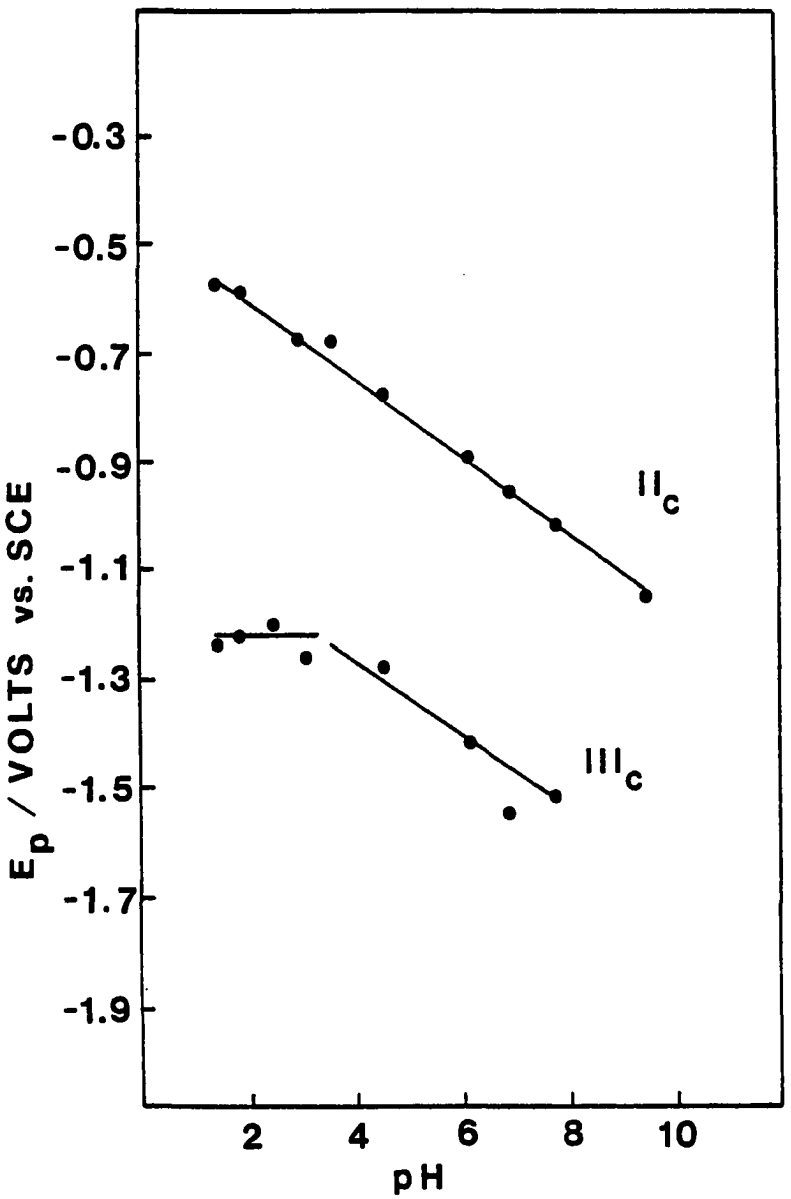

Figure 24. Variation of peak potential (E_p) with pH for the voltammetric reduction peaks of 2-DMP observed at the PGE. Data obtained at 2-DMP concentrations of 1 mM and at a sweep rate of 5 mV s^{-1}.

swept to observe peak I_a on the reverse sweep. The reverse peak for peak II_c (i.e., oxidation peak V_a) grows in peak height as the potential sweep rate and/or the pH is increased (Fig. 25). The peak height for peak V_a is higher when the potential sweep is reversed immediately after peak II_c, than when both peaks II_a and III_a are scanned. Cyclic voltammetric studies over a range of sweep rates and pH values disclose a variation in the relative magnitudes of currents observed for peak II_c and V_a. That is, at slow scan rates and low pH values, the ratio $(i_p)_c/(i_p)_a$, where $(i_p)_a$ is the peak current due to the peak V_a process and $(i_p)_c$ is the peak current due to the peak II_c process, is small. This ratio approaches unity at higher pH values and/or high sweep rates. This observation is indicative of a short lived species being formed in the peak II_c process in a pH-dependent reaction. The ratio $(i_p)/V^{1/2}$ for peak V_a increases with increasing scan rate. This also supports the conclusion that a short lived species is formed in the peak II_c process which disappears in a follow-up chemical reaction. The scheme for such a reaction can be written as:

$$Ox + ne \rightleftharpoons Red_I$$

$$Red_I \xrightarrow{k} Red_{II}$$

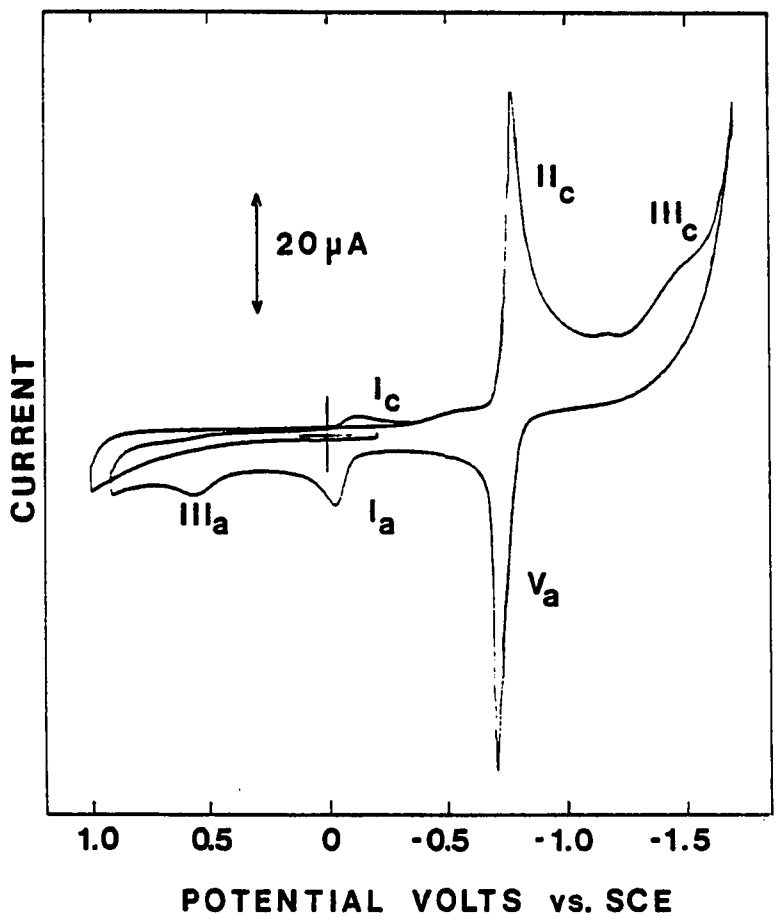

Figure 25. Cyclic voltammogram of 0.96 mM 2-DMP at PGE in phosphate buffer pH 6.95 at a sweep rate of 200 mV s^{-1}.

where the electron transfer is quasi-reversible and Red_I, Red_{II} and Ox are soluble in the solution phase. The homogeneous chemical reaction is irreversible and is characterized by a rate constant k. As observed from the cyclic voltammetric behavior of 2-DMP at various pH values, the rate of this chemical reaction is pH dependent. In fact, the rate decreases with increasing pH.

Cyclic voltammograms show that the peak current for peak II_c is enhanced by about 65% between scan rates of 5 mV s^{-1} - 200 mV s^{-1} at pH 7 upon increasing the scan rate. This is probably due to an electron transfer reaction, involving an adsorbed reactant, occurring at nearly the same potential as the diffusion-controlled electron transfer process.[8] When there is weak adsorption of the reactant, this leads generally to an enhancement of the peak current. The scan rate is one of the most important experimental parameters for differentiating between the effects due to adsorbed reactant and those due to material arising at the electrode by diffusion. This is so because the adsorbed reactant constitutes, at constant surface concentration, a fixed amount of material and charge flow, while the electrochemically active species diffusing to the electrode surface is time dependent. At sufficiently fast sweep rates, the amount of material diffusing to the electrode surface is small with respect to the amount of adsorbed material reacting at the electrode surface, while

at slow scan rates the reverse is true. Therefore, in the presence of adsorbed reactant, an increase in scan rate must cause the current function to increase.

With increasing concentration of 2-DMP there is a nonlinear increase in the peak current for peak II_c (Fig. 26). A nonlinear dependence of peak current on concentration is typical for adsorption systems.[8] At pH >5 at a sweep rate of 5 mV s^{-1} it is possible to observe a separate highly symmetrical adsorption peak at slightly more positive potentials than peak II_c (Fig. 27). At pH >7 there is an additional reduction peak at potentials about 400 mV negative of peak II_c, which appears at fast scan rates, and grows as the scan rate increases (e.g., 2V s^{-1} or higher) (Fig. 28). This process seems to be independent of the concentration of 2-DMP indicating that second order chemical reactions such as formation of a dimer are unlikely. For example, a 5 mM solution of 2-DMP showed very similar behavior to that noted for a 1 mM solution. There are two possible explanations for the presence of this additional voltammetric reduction peak. One is, that this peak is an adsorption post peak. If the reactant is strongly adsorbed, a post-peak is often observed. The peak separation ΔE_p, between the adsorption peak and the diffusion controlled peak, depends on the free energy of adsorption. As the energy of adsorption increases, the peak separation decreases.

The second approach to account for this new reduction

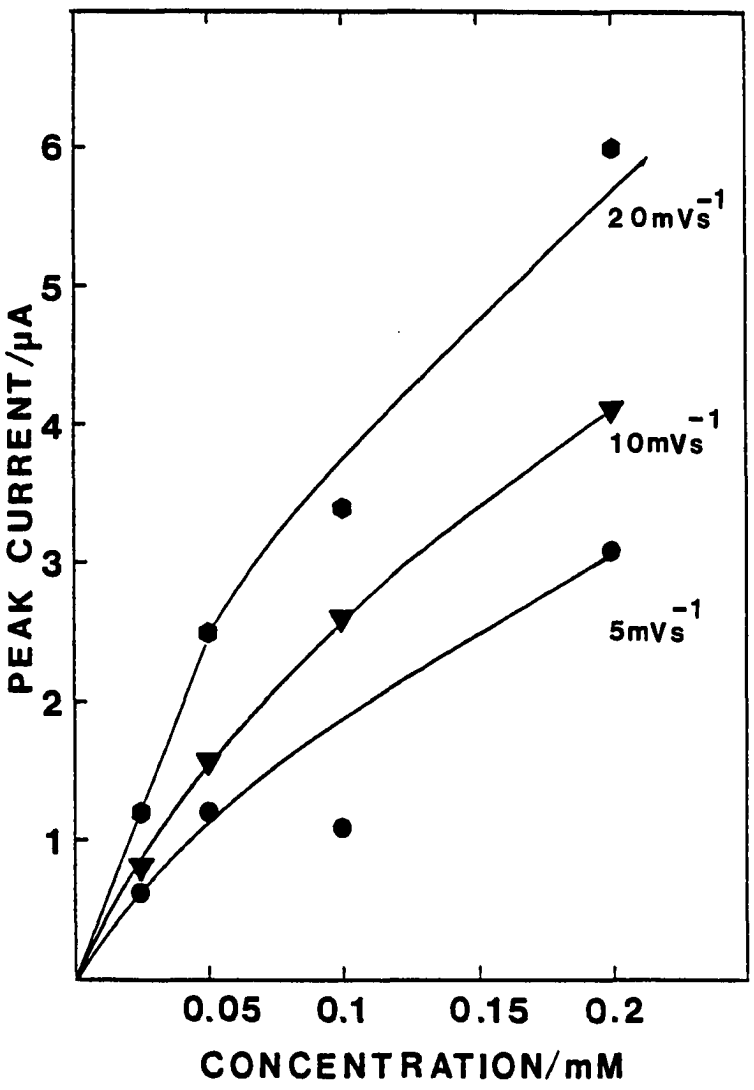

Figure 26. Change in peak current i_p as a function of concentration, for peak II_c of 2-DMP.

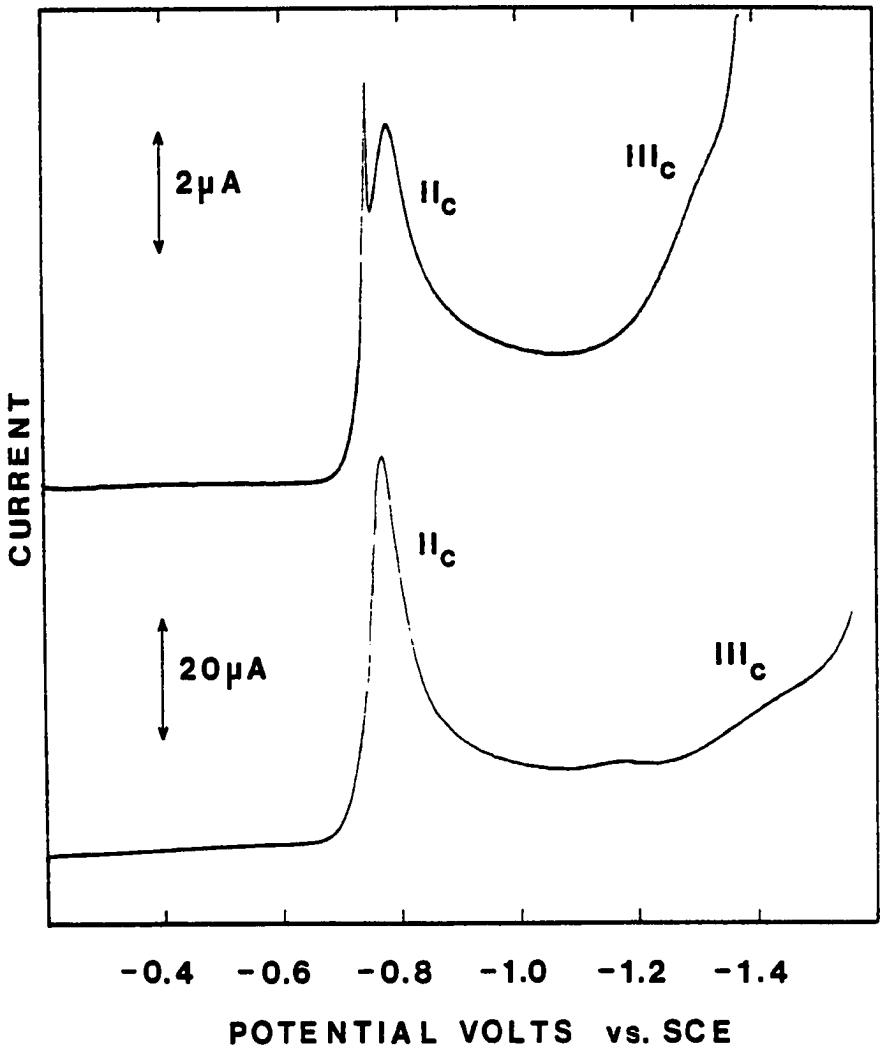

Figure 27. Single sweep voltammograms of 0.96 mM 2-DMP at PGE in phosphate buffer pH 6.95 at a sweep rate of (A) 5 mV s^{-1} and (B) 200 mV s^{-1}.

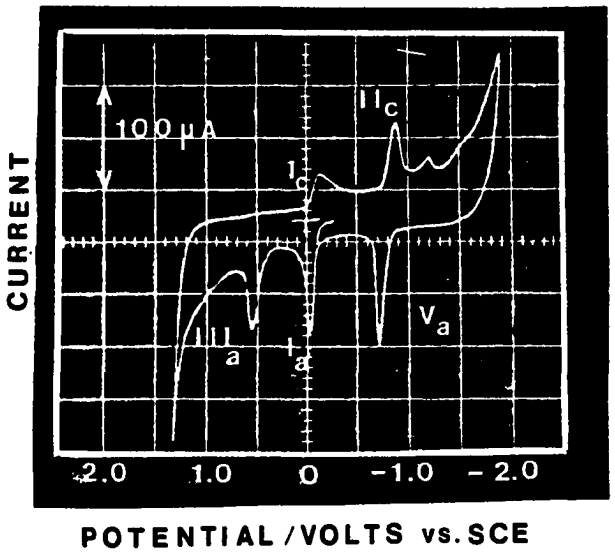

Figure 28. Cyclic voltammogram of 1 mM 2-DMTHP in phosphate buffer pH 7.8 at a scan rate of 5V s^{-1}.

peak involves formation of an electrochemically active short-lived species.

Concentration studies show that at very low concentrations peak II_c is the only reduction peak observed up to sweep rates of 200 mV s^{-1}. As the sweep rate is increased a new reduction peak starts increasing linearly with increasing sweep rate and at high sweep rates (20V s^{-1}) its peak height is almost the same as peak II_c. These studies were not sufficient to explain this new reduction peak. A surfactant (Lauryl sulfate) was added to the sample solution and the voltammetric behavior was noted. Solutions of 2-DMP with excess surfactant showed no voltammetric reduction peaks (Fig. 29A and 29B). It is believed that this behavior described above indicates that the new reduction peak observed at about 400 mV negative of peak II_c is due to an adsorption process. If this reduction peak were due to a diffusion controlled process addition of surfactant would not have effected the voltammetric results.

Controlled potential electrolysis of 2-DMP between pH 1.9-5.8 at potentials corresponding to peak II_c resulted in transfer of 1.92±0.07 electrons per molecule reduced. When the same solution was further reduced at potentials past peak III_c 1.91±0.08 additional electrons per original molecule of 2-DMP were transferred. The reduction was monitored using both cyclic voltammetry and U.V. spectrophotometry. During the first stage of reduction the forma-

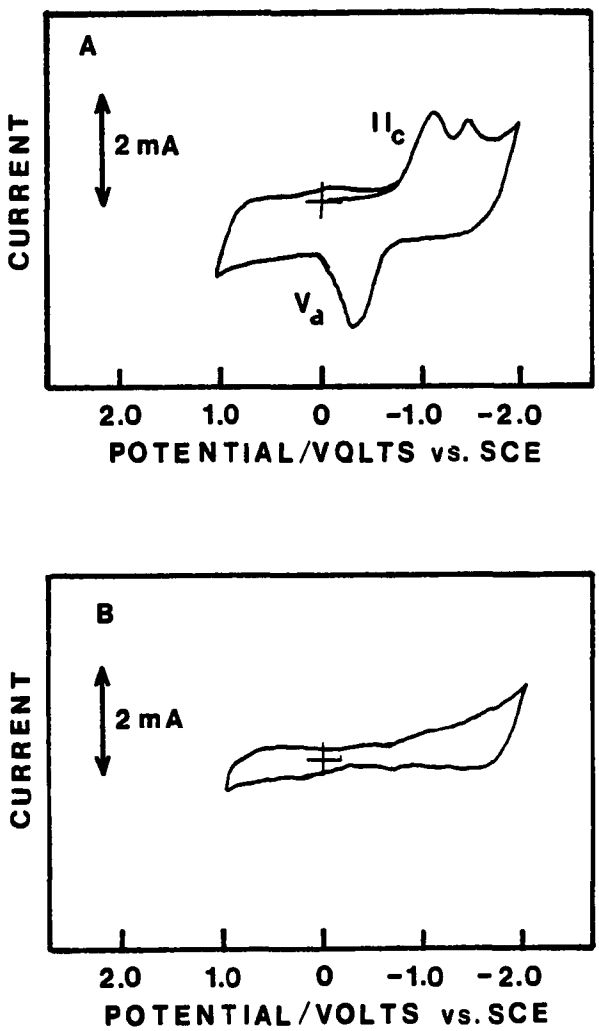

Figure 29. Cyclic voltammograms of 0.25 mM 2-DMP in phosphate buffer pH 6.94 at a sweep rate of 50V s^{-1}
A) without any surfactant, B) in the presence of excess surfactant.

tion of an intermediate species could be seen by U.V. spectrophotometry. For example, at pH 5.8 2-DMP has λ_{max} = 350 nm, 288 nm, 243 nm and 205 nm (curve 1, Fig. 30). When a potential of -0.7V (peak II_c) is applied, the absorbance increases at 350 nm, 288 nm, 243 nm and 205 nm (curve 2, Fig. 30). However, during the electrolysis (15 min) the absorbance at 288 nm and 205 nm decreases (curve 3, Fig. 30). The band at 350 nm shifts to 326 nm whereas the band at 288 nm shifts to 282 nm. The fact that the absorbance first increases (λ = 205 nm, 288 nm, and 350 nm) and then decreases during the electrolysis, indicates that a short-lived species is being formed by the electroreduction of 2-DMP which absorbs at λ_{max} = 350 nm, 288 nm and 205 nm. The final product has an U.V. spectrum with λ_{max} = 326 nm, 283 nm and 240 nm (curve 4, Fig. 30).

A 1 m<u>M</u> solution of 2-DMP in phosphate buffer pH 1.9 is dark yellow and absorbs at λ_{max} = 333 nm, 289 nm, 244 nm and 201 nm. In large-scale electrolysis, the absorbance at λ = 332 nm, 289 nm, 244 nm and 201 nm goes up during the first five minutes of electrolysis and then the absorbance decreases at 201 nm and 289 nm. The initial increase in absorbance at 201 nm and 289 nm must be due to formation of an intermediate species. This species seems to be rather unstable and disappears in a chemical reaction. New absorption peaks grow in at 225 nm, 358 nm and 254 nm later during the electrolysis. The peak II_c

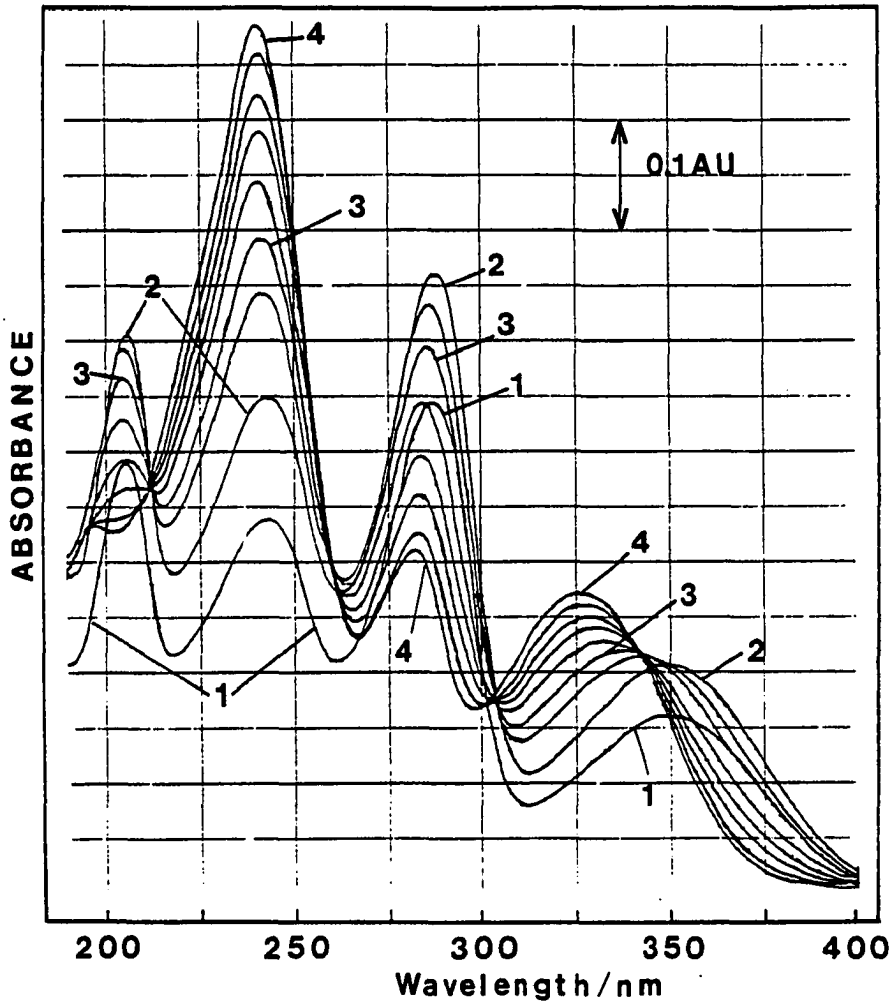

Figure 30. Spectra of 1 mM 2-DMP in phosphate buffer pH 5.8 as obtained during electrolysis at -0.7V at a mercury pool electrode (1) initial spectrum before electrolysis, (2) spectrum after 5 min of electrolysis corresponding to an unstable intermediate, (3) spectrum after 15 min of electrolysis, (4) spectrum of peak II_C reduction product. Wavelength scanning rate was 200 nm min^{-1} at a response time of 0.5s. Quartz cells of 0.1 cm pathlength were used.

electrolysis product has an U.V. spectrum with λ_{max} = 225 nm, 255 nm, 286 nm and 358 nm. Cyclic voltammograms of the electrolysis product at pH 1.9 show only peak III_c when the initial potential scan is in a negative direction. Peaks II_a and III_a are observed when the potential is swept towards more positive potentials. By applying potentials negative of peak III_c a product is obtained with an U.V. spectrum identical to that of 2-DMTHP (λ_{max} = 230 nm and 270 nm at pH 1.9, 234 nm, 280 nm and 308 nm at pH 5.8). Cyclic voltammograms of this product do not show any voltammetric reduction peaks. However, three voltammetric oxidation peaks (I_a, II_a and III_a) are observed at pH <5. Only peaks I_a and III_a are observed at pH values higher than 5. The peak potentials of these oxidation peaks are in good agreement with those observed for 2-DMTHP at the same concentration and pH.

Cyclic voltammetric and controlled potential coulometric experiments show that upon reduction of 2-DMP past peak II_c potentials an intermediate species is formed. Cyclic voltammetry reveals that the intermediate formed in peak II_c electroreduction process is more stable at high pH values.

Thin-layer spectroelectrochemistry

In order to gain more insights about the unstable species generated upon electroreduction at peak II_c potentials,

kinetic measurements were made between pH 6.9-8.3 in a thin-layer cell using an optically transparent RVC electrode.

At pH 6.9, 2-DMP shows three absorption bands (λ_{max} = 244 nm, 288 nm and 346 nm, curve 1 in Fig. 31). When a potential is applied corresponding to peak II_c the absorbance at 244 nm increases, whereas the absorbance goes down at 288 nm. The peak at 346 nm shifts to about 330 nm and increases. Curve 2 in Fig. 30 shows the spectrum of 2-DMP after 75s of electrolysis at which point most of 2-DMP is reduced (applied potential -1.3V). The absorbance at 330 nm, 288 nm and 242 nm keep increasing even after the applied potential is turned off. Since the absorbance keeps changing even though the electrolysis is terminated, there must be an unstable intermediate generated which underoges a chemical reaction to give a new product (curve 3, Fig. 31). The rate of formation of the new product was measured by following the change in absorbance with respect to time. The observed rate constant for this chemical reaction between pH 6.9-8.3 is summarized in Table 6. The half-life for the intermediate at pH 6.9, 7.8 and 8.3 is 9.7, 38.7 and 220s, respectively.

As seen from Table 6 the intermediate is more stable at higher pH (e.g., pH 8.3). The spectra shown in Fig. 32 represent 2-DMP electrolyzing at -1.4V in phosphate buffer pH 8.3 at an optically transparent RVC electrode. Formation and decay of an unstable intermediate can be clearly observed.

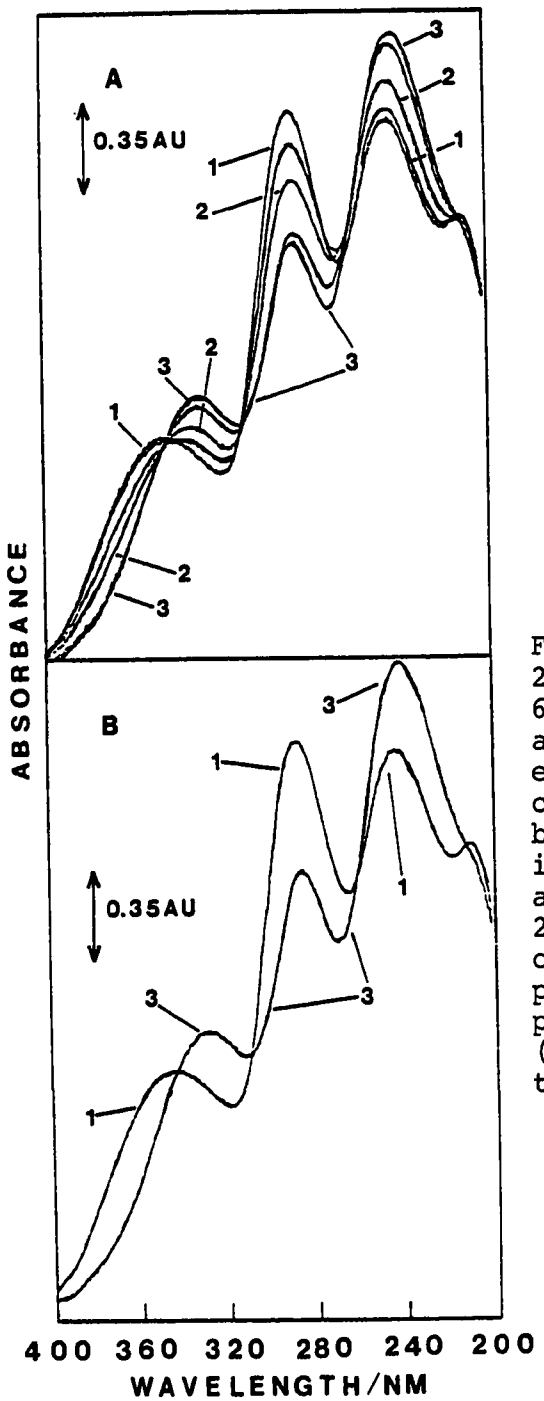

Figure 31. Spectra of 1 mM 2-DMP in phosphate buffer pH 6.9 electrolyzing at -1.3V at a reticulated vitreous carbon electrode in a thin-layer cell. (A) Curve 1 is 2-DMP before electrolysis, curve 2 is after 75s of electrolysis at a point where all of the 2-DMP has been oxidized, curve 3 is spectrum of final product after the applied potential is turned off. (B) Curve 1 and curve 3 are the same as in (A).

Table 5. E_p values for peak II_a and III_a of 2-DMDHP at various pH values at the PGE observed at a scan rate of 5 mV s^{-1}

pH	E_p/Volt vs. SCE	
	II_a	III_a
1.86	0.31	0.73
3.00	0.32	0.74
3.70	0.25	0.64
4.40	0.24	0.62
5.80		0.60
7.50		0.60

[a]Phosphate buffers of ionic strength 0.5 M were used.

[b]Data obtained by a thin-layer spectroelectrochemical method using an optically-transparent reticulated vitreous carbon electrode.

[c]Standard deviation.

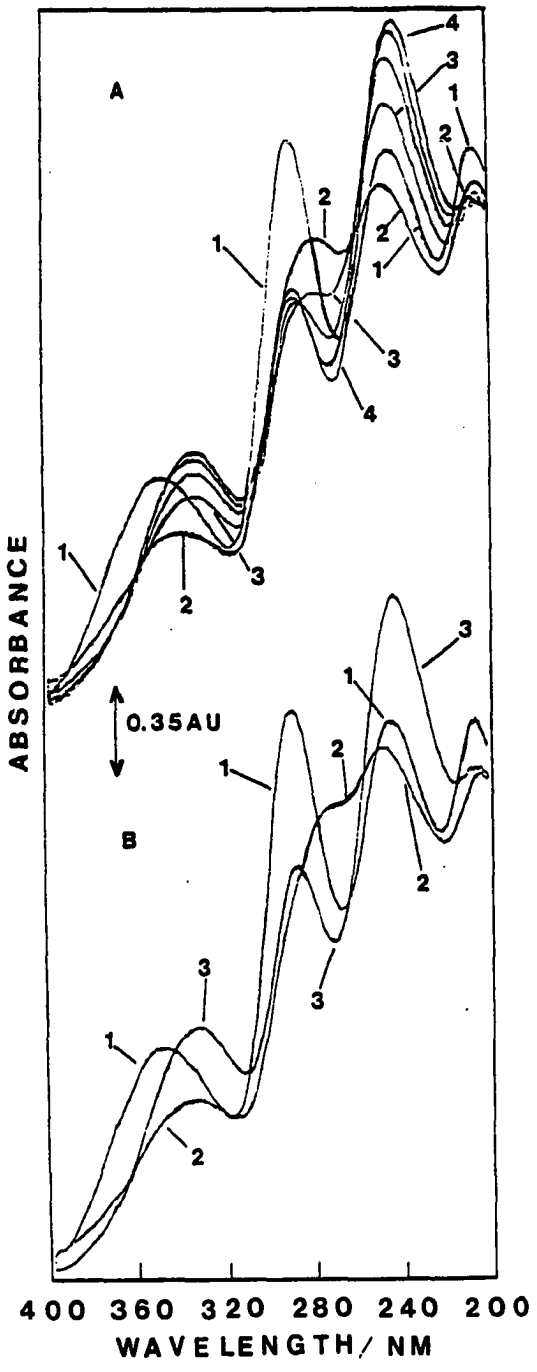

Figure 32. Spectra of 1 mM 2-DMP in phosphate buffer pH 8.3 electrolyzing at -1.4V at a reticulated vitreous carbon electrode in a thin-layer cell. (A) Curve 1 is the initial spectrum of 2-DMP before electrolysis, curve 2 is spectrum after 40s of electrolysis corresponding to the unstable intermediate generated, curve 3 is spectrum 85s after terminating electrolysis and curve 4 corresponds to the spectrum of final product. (B) Curve 1 is the initial spectrum of 2-DMP before electrolysis, curve 2 is the spectrum of the intermediate generated, curve 3 is the spectrum of the final product.

Table 6. Observed first-order rate constant for reaction of the peak II_c electroreduction product of 2-DMP as a function of pH[a]

pH	$k_{obs} \times 10^3/s^{-1}$[b]	$\sigma \times 10^3$[c]
6.87	65.0	6.6
7.80	17.9	4.9
8.34	31.5	2.8

[a]Phosphate buffers of ionic strength 0.5 M were used.

[b]Data obtained by a thin-layer spectroelectrochemical method using an optically-transparent reticulated vitreous carbon electrode.

[c]Standard deviation.

Curve 2 in Fig. 32A and 32B corresponds to the intermediate generated.

DISCUSSION

Linear sweep voltammetry and coulometry indicate that the peak I_a electrooxidation of 2-DMTHP is a 2e process. Cyclic voltammetry supports the view that the peak I_a/I_c couple is almost reversible. The shift of the peak potential of peak I_a with pH (-0.048V per pH unit) is in approximate accord with that expected for a reversible $2e\text{-}2H^+$ electrooxidation of 2-DMTHP to a quinonoid pterin which has a locked structure (8a). Sweep rate studies indicate that the peak current function ($i_p/ACV^{1/2}$) for oxidation peak I_a is constant between 5 mV s^{-1} - 100 mV s^{-1}, whereas the peak current function for reduction peak I_c increases with increasing sweep rate until peak I_c becomes equal in height to peak I_a.

The quinonoid (14) that is formed during electrooxidation of 2-DMTHP at peak I_a potentials is not very stable, as demonstrated by cyclic voltammetry and thin-layer spectroelectrochemistry. It disappears in a first-order chemical reaction to form 2-DMDHP. A bell-shaped relationship exists between k_{obs} for this process and pH with the maximum value of k_{obs} occurring at about pH 7.3 (Fig. 21). The pK_a of 2-DMTHP has been determined spectroelectrochemically to be around 7. Bell-like shaped pH-

rate profiles with two inflection points can usually be accounted for in terms of two acid-base dissociations of the substrate.[10] Thus, the pH at which the k_{obs} is highest (pH 7.3) is in reasonable agreement with the observed pK_a for 2-DMTHP.

The peak I_c process observed by cyclic voltammetry is due to the electrochemical reduction of the intermediate quinonoid-dihydropterin back to 2-DMTHP. Since there is no obvious break in the E_p vs. pH plot for oxidation peak I_a of 2-DMTHP it must be concluded that both the monocation and the neutral form of 2-DMTHP are electrooxidized in quasi-reversible $2\underline{e}\text{-}2H^+$ reactions.

Oxidation peaks II_a and III_a of 2-DMTHP are due to electrooxidation of 2-DMDHP. This means that the peak I_a electrooxidation product undergoes a chemical reaction to form 2-DMDHP, which in turn gives rise to peaks II_a and III_a.

For the reasons outlined previously, peak II_a is due to electrooxidation of the hydrated form of 2-DMDHP. Since the latter compound has a very similar structure to that of 2-DMTHP it is reasonable to expect that electrooxidation of 2-DMDHP·H_2O takes place at potentials very close to those for 2-DMTHP.

The shift of the peak potential with pH (-0.043V per pH unit) for peak II_a is close to that expected for a reversible reaction involving an equal number of electrons

and protons. It has been concluded therefore that peak II_a corresponds to the $2\underline{e}$-$2H^+$ electrooxidation of 2-DMDHP·H_2O to an intermediate quinonoid species. Cyclic voltammetric experiments indicate that the intermediate disappears in a two-step process.

No kinetic measurements were made on the electrooxidation product of 2-DMDHP·H_2O. But cyclic voltammetry clearly indicates the presence of two intermediate species. Non-hydrated 2-DMDHP appears to be directly electrooxidized to 2-DMP in the peak III_a electrooxidation process.

Reduction peak II_c is believed to be due to a $2\underline{e}$-$2H^+$ reduction of 2-DMP to form 2-dimethylamino-3,6,7-trimethyl-5,8-dihydropterin. Cyclic voltammetric and thin-layer spectroelectrochemical experiments show that this species is unstable and undergoes a pH dependent chemical reaction to form 2-DMDHP. The peak current function for peak II_c increases with increasing scan rate which is indicative of adsorption of reactant (2-DMP). The fact that the peak current function for peak V_a increases with increasing sweep rate supports the view that there is a chemical reaction taking place after the peak II_c electrochemical step. Thus, the first reduction of 2-DMP can be considered as an EC reaction.

Peak III_c is due to the reduction of 2-DMDHP which forms in the chemical step that the peak II_c product undergoes. The peak height for peak III_c decreases with in-

creasing scan rate. Thus, this observation also indicates that the species responsible for peak III_c is formed by a chemical reaction. The slower the sweep rate, the higher peak III_c (i.e., there is more time for the chemical reaction to take place).

Controlled potential coulometric experiments show that oxidation of 2-DMTHP at a large PGE and reduction of 2-DMP at a mercury pool electrode follow a similar path. Both the oxidation of 2-DMTHP and reduction of 2-DMP results in the formation of an unstable intermediate species (a quinonoid-dihydro species in the former, and a 5,8-dihydro-species in the latter). The unstable intermediates generated rearrange to form the more stable 7,8-dihydro derivative. Cyclic voltammograms and U.V. spectra recorded during oxidation of 2-DMTHP and reduction of 2-DMP are in good agreement. For example, Fig. 33 shows U.V. spectra obtained during reduction of 2-DMP in phosphate buffer pH 7.3 at a mercury pool electrode, whereas Fig. 16 shows U.V. spectra of 2-DMTHP at the same pH being oxidized at a large PGE. The proposed reaction scheme for the electro-oxidation of 2-DMTHP is summarized in Fig. 34.

CONCLUSIONS

The electrochemical results obtained from 2-DMTHP over the pH range 1.5-9.2 are in general agreement with electrochemical results obtained from 6,7-dimethyl-5,6,7,8-

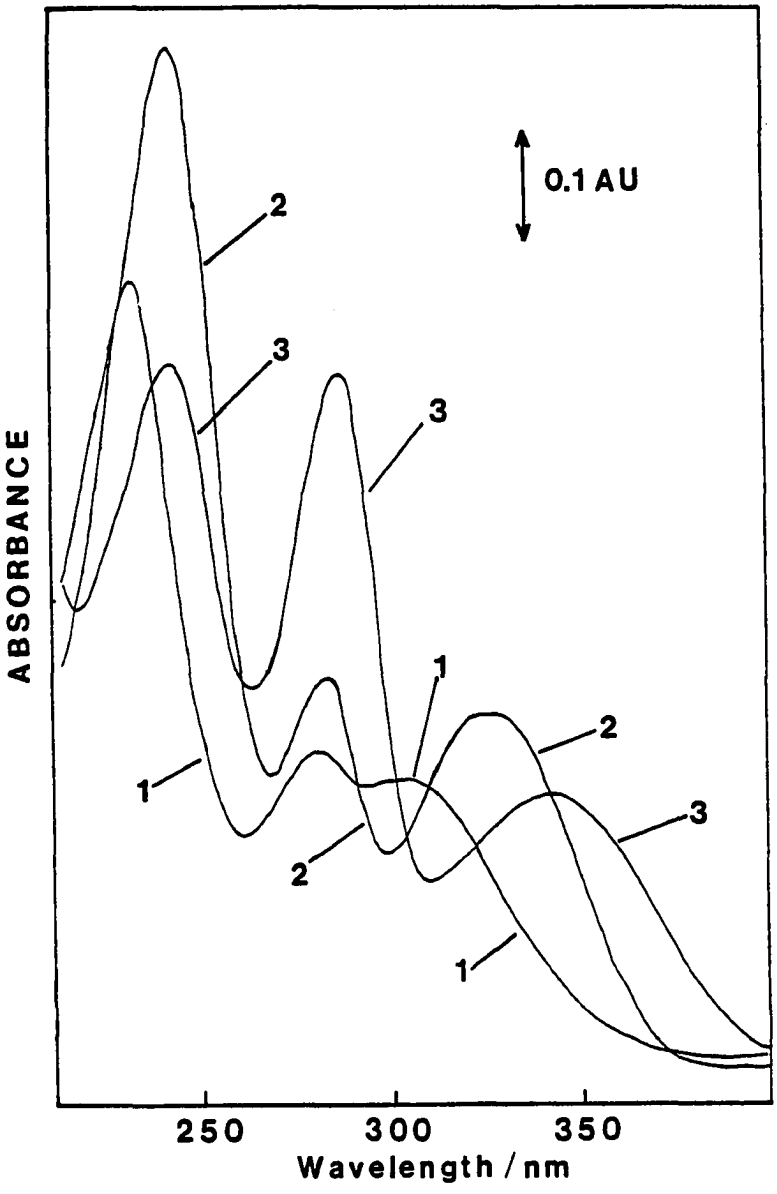

Figure 33. U.V. spectra of 1 mM 2-DMP in phosphate buffer pH 7.3 electrolyzed at -1.0V. Curve 1 corresponds to the initial spectrum of 2-DMP, curve 2 is spectrum of peak II_C electroreduction product, curve 3 represents peak III_C electrolysis product.

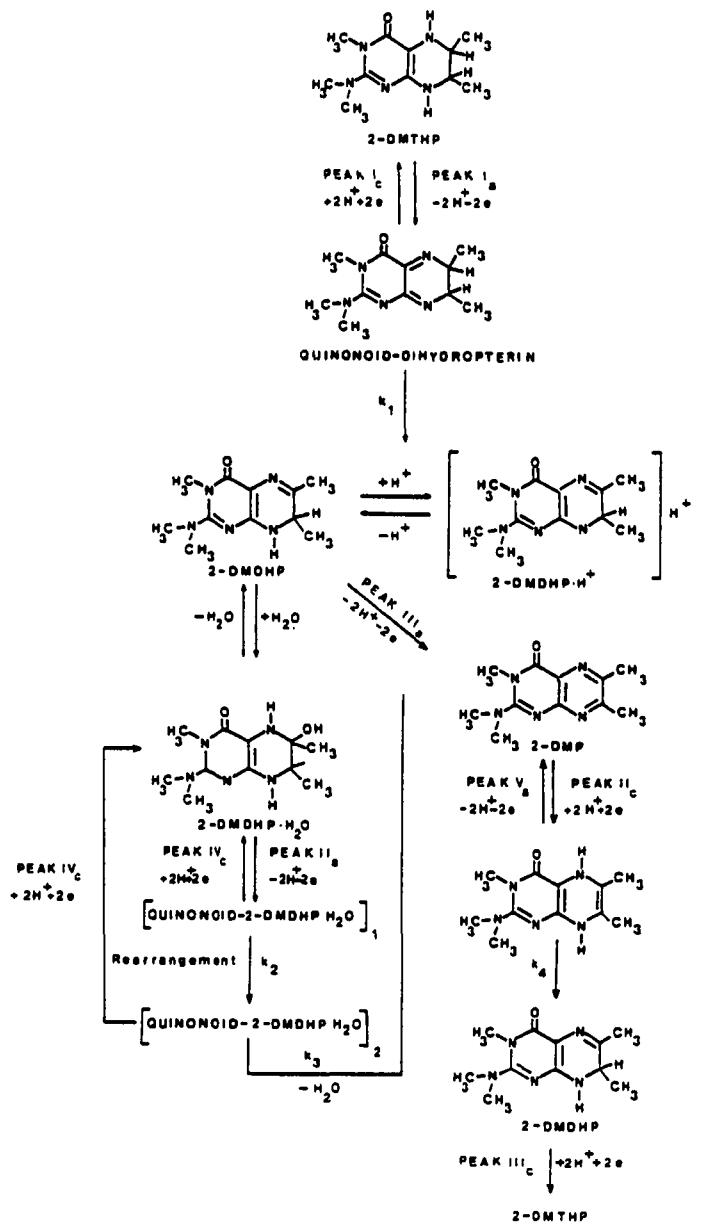

Figure 34. Proposed reaction scheme to account for the voltammetric redox peaks of 2-DMTHP observed at the PGE.

tetrahydropterin (6,7-DMTHP) and 6-methyl-5,6,7,8-tetrahydropterin (6-MTHP).[9,11] Thus tetrahydropterins substituted at C(6) and C(7) or substituted only at C(6) exhibit three electrooxidation peaks at the PGE. There is a fourth oxidation peak which occurs at relatively high positive potentials (E_p >1.2V) due to oxidation of the corresponding pterin. 6,7-DMTHP, 6-MTHP and 2-DMTHP give rise to an electrooxidation peak (peak I_a) to generate an intermediate dihydropterin which undergoes a pH-dependent chemical reaction. 2-DMTHP may form only one quinonoid-dihydropterin whereas the electrooxidation of both 6,7-DMTHP and 6-MTHP may result in the formation of up to five different forms of quinonoid-dihydropterins. Based on spectroelectrochemical studies and kinetic measurements it is clear that 6-MTHP or 6,7-DMTHP[9,11] may form the same quinonoid intermediate as 2-DMTHP. The observed first-order rate constants obtained show a different pH dependence. For example, 2-DMTHP forms a more unstable quinonoid than both 6,7-DMTHP and 6-MTHP. It is interesting to note that the cofactor activity of reduced diaminopterins is reported to be quite low. 6-MTHP has the highest cofactor activity towards phenylalanine hydroxylase followed by 6-DMTHP and then 2-DMTHP. It is possible that there is a direct correlation between the stability of the intermediate quinonoid-dihydro generated and the activity of the cofactor, i.e., the more stable the quinonoid the

higher the activity of the cofactor. In biological systems the quinonoid generated may be reduced back to the tetrahydro oxidation state in the presence of dihydropterin reductase and a reducing agent such as nicotinamide adenine dinucleotide (NADH). Therefore the more stable the intermediate quinonoid species the higher its chances of being converted back to the tetrahydro level, thus increasing the activity of the tetrahydropterin cofactor used. If the quinonoid-dihydro species is not very stable and rapidly reacts to form the 7,8-dihydro derivative it is not possible to get the tetrahydropterin back since the reductase enzyme will not reduce the 7,8-dihydro species.

The quinonoid generated in the primary electro-oxidation peak I_a process of 2-DMTHP is not very stable ($t_{1/2}$ = 6.5s at pH 7.3). Therefore it was not very easy to obtain a well defined spectrum of the intermediate species. However, a clearly defined U.V. spectrum of 5,8-dihydro-intermediate could be recorded during the reduction of 2-DMP. The 5,8-dihydropterin species generated by the electro-reduction of 2-DMP at peak II_c potentials appears to be more stable than the corresponding species obtained by electroreduction of 6,7-DMP.

By analyzing the electrochemical data it is clear that 2-DMDHP gives rise to two oxidation peaks which involve a transfer of two electrons. The species responsible for these two peaks seem to be in an equilibrium. Thus, as

was the case in the electrooxidation of 6-MTHP and 6,7-DMTHP the stable 7,8-dihydropterin formed by a rearrangement reaction of the quinonoid-dihydropterin hydrates, most likely across the C(5)=C(6) double bond, to form a covalently hydrated dihydropterin. The hydrated and nonhydrated dihydropterins are in equilibrium. The structure of the hydrated-dihydropterin is very similar to that of the tetrahydro derivative. Thus it is not very surprising that peak II_a peak potentials are close to peak I_a electrooxidation potentials. It would be interesting to study the cofactor activity of such covalently hydrated dihydropterins. Because of the similarity in structure it would be expected that these hydrated dihydropterins would be active cofactors in hydroxylation reactions. Enzymatic hydroxylation reactions reported which involve 7,8-dihydropterins as possible cofactors were carried out at physiological pH or higher.[12] It was observed that 7,8-dihydropterins showed no cofactor activity towards hydroxylase enzymes. Since the hydration of dihydropterins appears to be pH dependent these reported results are self-explanatory (i.e., 7,8-dihydropterins do not hydrate above ca. pH 5 thus are not active as cofactors). The same 7,8-dihydropterins used would be expected to show some cofactor activity in solutions of pH <5.

Cyclic voltammetric experiments indicate that two electrochemically active, short-lived species are generated

in the peak II_a electrooxidation process which can be reduced in peaks IV_c and IV'_c. Since the covalently hydrated dihydropterin species has a very similar structure to that of the tetrahydro derivative its oxidation would possibly result in the formation of a hydrated quinonoid species with structures such as (2-6) except with a hydroxyl group at C(6) adjacent to the methyl substituent.

Kinetic measurements obtained for reaction of the intermediate generated upon peak II_a electrooxidation of 6,7-DMDHP and 6-MDHP indicate that there are at least two unstable species generated. Comparison of cyclic voltammetric data obtained from 2-DMDHP with those obtained from 6,7-DMDHP suggests that there are also two intermediate species generated.

EXPERIMENTAL

Chemicals

2-Dimethylamino-3,6,7-trimethylpterin (2-DMP) was synthesized according to the procedures described by Pfleiderer.[13] Reported m.p. 157°-167°C, observed m.p. 162°-164°C. Calculated analysis: C 52.69%, H 6.77%, N 27.89%; found: C 53.18%, H 6.02% and N 28.21% with a molecular formula of $C_{11}H_{15}N_5O \cdot H_2O$. An I.R. spectrum and a direct insertion mass spectrum of 2-DMP are presented in Figs. 35 and 36, respectively. The observed molar absorptivity for 2-DMP was on the average about 20% higher

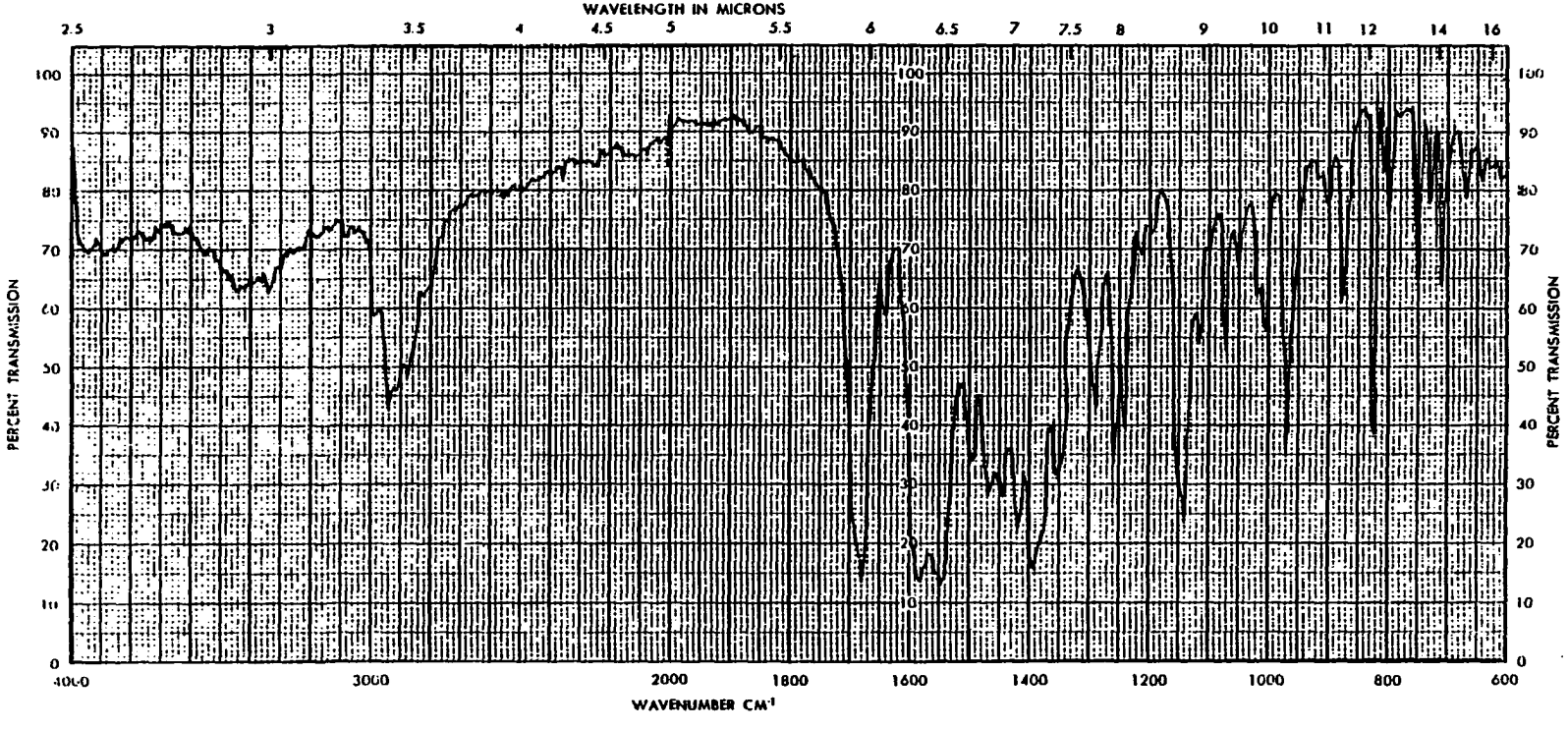

Figure 35. I.R. spectrum of 2-DMP, KBr pellet.

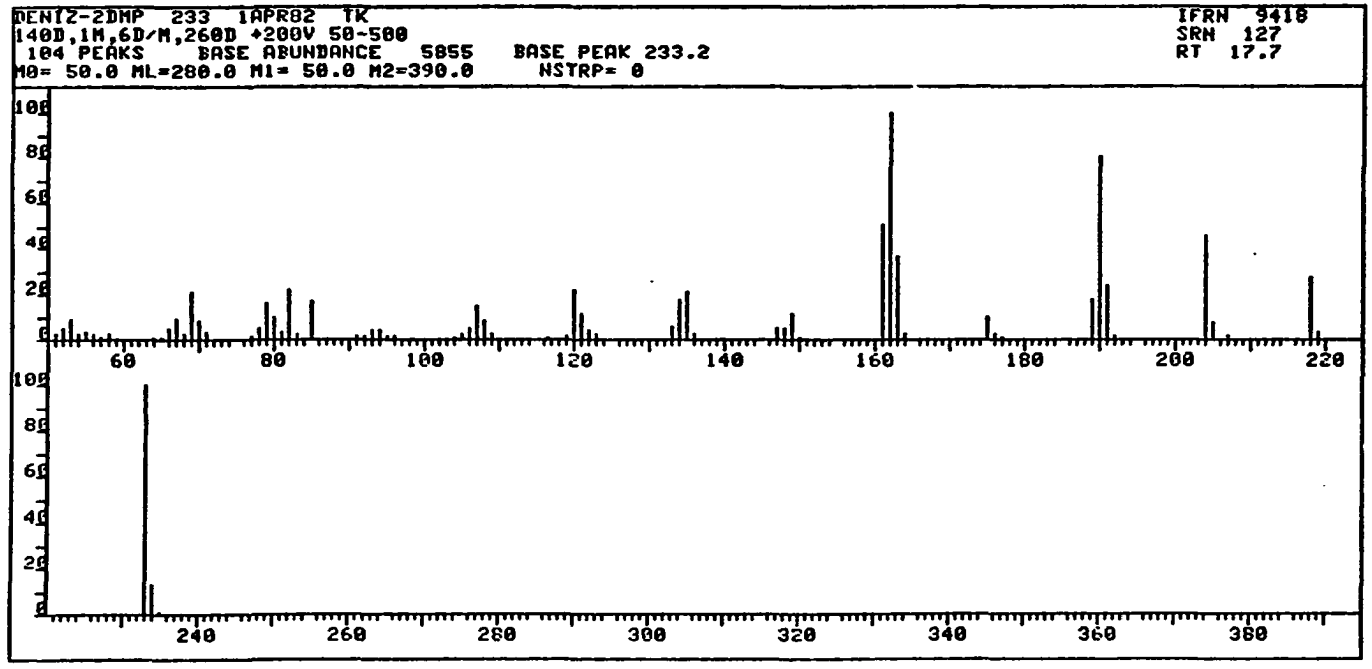

Figure 36. Direct insertion mass spectrum of 2-DMP.

than reported in literature[13] (Table 7). 2-Dimethylamino-3,6,7-trimethyl-7,8-dihydropterin (2-DMDHP) was generated electrochemically either by electrooxidation of 2-DMTHP using a large pyrolytic graphite electrode (PGE) or by electroreduction of 2-DMP using a mercury pool electrode. 2-Dimethylamino-3,6,7-trimethyl-5,6,7,8-tetrahydropterin (2-DMTHP) was prepared by hydrogenating 2-DMP over PtO_2 (Aldrich) using a hydrogenation apparatus at atmospheric pressure.[14] The hydrogenation was stopped when there was no longer H_2 uptake and approximately the required amount of hydrogen was consumed. The catalyst was removed by filtration under a nitrogen atmosphere with the aid of Filteraid (Fisher). The catalyst-free, colorless solution was transferred into another flask which contained deaerated concentrated HCl (the amount of HCl used changed with the size of sample to give a concentration of 5 m$\underline{M}$). The tetrahydro- compound was extremely air sensitive. Upon oxidation the solution turned clear yellow and in that case hydrogenation procedures were repeated. The reduced compound was freeze-dried after the addition of HCl. Upon freeze-drying, light yellow shiny crystals were obtained which were stored in a desiccator at 0°C. Calculated analysis: C% 40.24, H% 7.01 and N% 21.34; found: C% 39.81, H% 6.81 and N% 21.21 with a molecular formula of $C_{11}H_{19}N_5O \cdot 2HCl \cdot H_2O$. A direct insertion mass spectrum for 2-DMTHP is shown in Fig. 37. The isolation procedure for

Table 7. Comparison of absorbance[a] data for 2-DMP with literature values.

pH	λ_{max} obs.	λ_{max} rep.	$A_{obs.}$	$\varepsilon_{calc.}$[c]	$\varepsilon_{rep.}$[c]
1.13	407	407[b]	0.242	3248	2291
	326	325	0.623	8362	7244
	302	304	0.683	9168	7244
	257	257	0.990	13289	10965
4.60	245	238	1.000	13513	12023
	290	289	1.306	17650	14454
	351	351	0.458	6189	5495
	207		1.244	16811	n.r.

[a]Solutions having a concentration of 7.45×10^{-5} M at pH 1.13 and 7.40×10^{-5} M at pH 4.6 were used.

[b]λ_{max} reported was obtained at pH 0.

[c]Molar absorptivity $E = \frac{A}{cb}$.

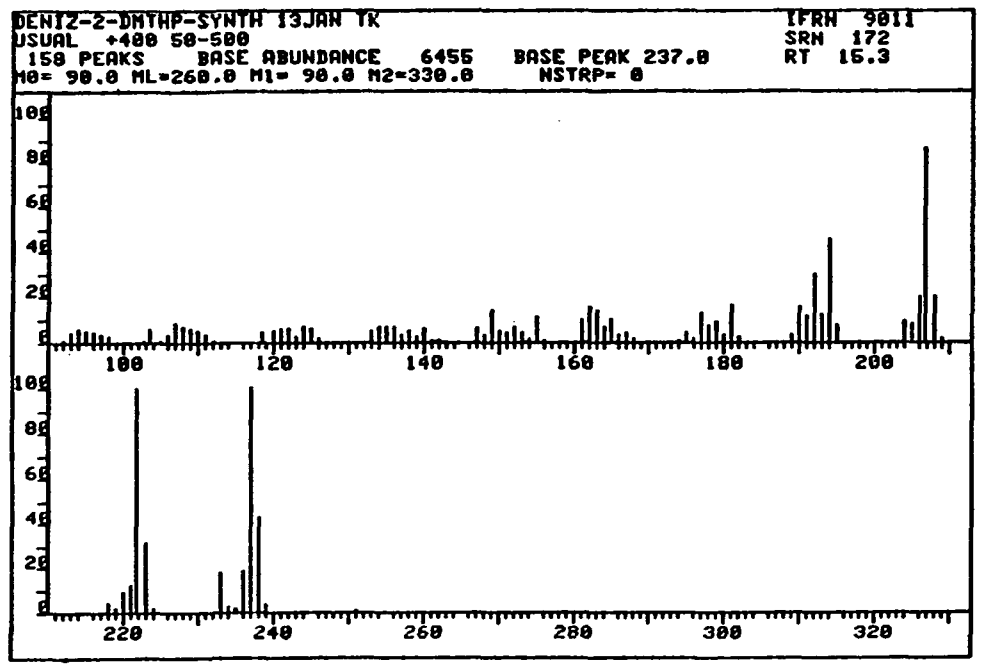

MASS	%	MASS	%
BIG 60		165.1	10.1
93.1	4.1	167.1	4.1
94.1	5.7	175.1	4.2
95.2	5.0	177.1	13.2
96.2	4.1	178.1	7.0
103.6	5.9	179.1	9.4
107.1	8.2	181.0	16.4
108.1	6.9	190.1	15.9
109.1	5.9	191.1	12.0
110.2	5.0	192.1	30.1
111.1	4.0	193.0	12.1
118.7	4.6	194.1	46.3
120.2	4.8	195.1	7.0
121.1	6.0	204.1	9.2
122.2	6.2	205.0	8.2
124.1	7.0	206.0	20.6
125.1	5.7	206.9	86.9
133.0	4.8	208.1	20.6
134.1	7.2	218.1	4.5
135.1	6.8	220.1	9.1
136.1	6.9	221.1	12.2
138.0	5.1	221.9	100.0
140.0	6.4	223.1	31.4
147.0	5.7	233.1	17.7
149.0	13.9	236.2	18.7
150.0	5.3	237.0	100.0
151.1	4.2	238.1	43.0
152.1	7.1		
153.1	4.7		
155.1	10.7	LAST 4	
161.0	10.3	254.0	.0
162.0	15.9	255.1	.0
163.1	13.8	256.1	.0
164.1	6.6	257.0	.0

Figure 37. Direct insertion mass spectrum of 2-DMTHP.

the tetrahydro compound is a modified version of that reported by Bailey and Ayling.[15] Deaerated phosphate buffers having an ionic strength of 0.5 M were used for all experiments.

Apparatus:

Equipment for electrochemical and thin-layer spectroelectrochemical measurements has been reported in Chapter 2. All potentials refer to the SCE at 25°C. Quartz cells containing optically transparent RVC electrodes (0.7 mm thick, 100 ppi, Fluorocarbon Co., Anaheim, Ca., or 0.5 mm thick, 100 ppi INF, Norman, Ind., Anaheim, Ca.) were utilized for spectroelectrochemical studies. The thin-layer cell made using 100 ppi INF was pretreated before use according to the procedure reported by Wang.[16] In order to exclude atmospheric oxygen a special cell was used which was described in Chapter 2. An air-tight 5 ml syringe (Hamilton) was used to introduce sample into the cell in order to prevent air oxidation of the sample solution.

A mercury (Bethlehem Instr., Hellertown, Pa.) pool electrode was used for the reduction of 2-DMP in a three compartment electrolysis cell separated by Nafion membranes (Du Pont). A Hewlett-Packard Model 5985B gas chromatograph-mass spectrometer was used for the analysis of electrolysis products and starting materials. U.V. spectra were recorded using a Hitachi Model 100-80 computerized spectrophotometer.

SUMMARY

2-Dimethylamino-3,6,7-trimethyl-5,6,7,8-tetrahydropterin (2-DMTHP) gives three voltammetric oxidation peaks (peaks I_a, II_a and III_a) at the pyrolytic graphite electrode. Peak I_a is a $2\underline{e}$-$2H^+$ quasi-reversible reaction due to oxidation of 2-DMTHP to a locked quinonoid-dihydro species. This quinonoid rearranges to form 2-dimethylamino-3,6,7-trimethyl-7,8-dihydropterin (2-DMDHP) in a pH-dependent first-order reaction. The rate of this reaction is much faster than that noted for the quinonoid-dihydropterins generated by electrooxidation of 6,7-dimethyl- or 6-methyl-tetrahydropterins. Peak II_a is due to a quasi-reversible electrooxidation of covalently hydrated 2-DMDHP (2-DMDHP·H_2O) to form two quinonoid-dihydro species which in turn chemically react to form 2-dimethylamino-3,6,7-trimethylpterin (2-DMP). Peak III_a is due to electrooxidation of nonhydrated 2-DMDHP to form 2-DMP. 2-DMP can be reduced in a $2\underline{e}$-$2H^+$ reaction to 2-dimethylamino-3,6,7-trimethyl-5,8-dihydropterin in the peak II_c process. This rearranges to 2-DMDHP in a pH dependent process. Peak III_c is due to electroreduction of 2-DMDHP to 2-DMTHP.

REFERENCES

1. S. Kaufman, Proc. Nat. Acad. Sci. USA, 50(1963) 1085.

2. P. Hemmerich in, Pteridine Chemistry, W. Pfleiderer and E. C. Taylor (eds.), Pergamon, London, 1964, pp. 143, 323.

3. S. Kaufman in, Pteridine Chemistry, W. Pfleiderer and E. C. Taylor (eds.), Pergamon, London, 1964, p. 307.

4. S. Kaufman, J. Biol. Chem., 239 (1964) 332.

5. M. Viscontini and A. Bobst, Helv. Chim. Acta, 48 (1965) 816.

6. M. C. Archer and K. G. Scrimgeour, Can. J. Biochem., 48 (1970) 278.

7. S. Kwee and H. Lund, Biochim. Biophys. Acta, 297 (1973) 285.

8. R. H. Wopschall and T. Shain, Anal. Chem. 39 (1967) 1514.

9. D. Ege-Serpkenci and G. Dryhurst, Bioelectrochem. Bioenergetics, 9 (1982) 175.

10. K. A. Connors, in Reaction Mechanisms in Organic Analytical Chemistry, John Wiley, N. Y., 1973, p. 90.

11. L. G. Karber and G. Dryhurst, J. Electroanal. Chem., 136 (1982) 271.

12. S. Kaufman, J. Biol. Chem., 234 (1959) 2677.

13. H. Rokos and W. Pfleiderer, Chem. Ber. 104 (1971) 739.

14. A. Bobst and M. Viscontini, Helv. Chim. Acta, 49 (1966) 875.

15. S. W. Bailey and J. E. Ayling, J. Biol. Chem., 253 (1978) 1598.

16. J. Wang, Electrochim. Acta, 26 (1981) 1721.

CHAPTER 4

COMPARISON OF ELECTROCHEMICAL AND SPECTRO-ELECTROCHEMICAL BEHAVIOR OF VARIOUS METHYLATED PTERINS

INTRODUCTION

For several years this laboratory has been investigating the electrochemical oxidation reactions of methylated pterins, some of which can act as pseudo cofactors for the enzyme phenylalanine hydroxylase. It was expected that such studies might lead to a better understanding of the biological redox reactions of the natural cofactor tetrahydrobiopterin in the hydroxylation of phenylalanine. There is significant evidence that an unstable quinonoid-dihydropterin intermediate is formed during enzymic, chemical and electrochemical oxidation of tetrahydropterins.[1-7] No conclusive evidence for the preferred quinonoid structure exists. It was believed that electrochemical and spectroelectrochemical studies of various methylated pterins, which may form locked quinonoid-dihydropterins (see Chapter 3 Introduction), would result in useful information concerning the structure of the putative quinonoid-intermediate.

Detailed electrochemical and spectroelectrochemical investigations involving some of the commonly used phenylalanine hydroxylase pseudo cofactors (6,7-dimethyltetrahydropterin (6,7-DMTHP), 6-methyltetrahydropterin (6-MTHP) and tetrahydropterin (THP)) have been reported.[4-6] In this chapter, the spectroelectrochemistry of various methylated pterins which may form only a single or locked quinonoid structure will be compared to the behavior of 6,7-DMTHP and 6-MTHP. Before any spectroelectrochemical experiments were carried out it was necessary to become familiar with the electrochemical behavior of these compounds. Therefore, the first part of this chapter will be devoted to a brief discussion of the electrochemistry of 3,6,7,8-tetramethyltetrahydropterin (3,6,7,8-TMTHP) and 2-dimethylamino-6,7,8-trimethyltetrahydropterin (2-DMTTHP). Detailed electrochemical studies of 2-dimethyl-3,6,7-trimethyltetrahydropterin (2-DMTHP) have been described in the previous chapter. The electrochemical behavior of eight different tetrahydropterins will be discussed in the final part of this chapter.

3,6,7,8-Tetramethyltetrahydropterin

3,6,7,8-TMTHP (1) is one of the reduced pterins which forms a "locked" quinonoid-dihydropterin upon a $2\underline{e}$-$2H^+$ electrooxidation process. Solutions of 3,6,7,8-TMTHP are very air sensitive. The susceptibility of the reduced compound to O_2 attack is high and this increases with

increasing pH. Totally reduced 3,6,7,8-TMTHP solutions were colorless but turned clear yellow upon air-oxidation. The pK_a of 3,6,7,8-TMTHP is about 6.2 as determined using spectrophotometric data (Fig. 1), corresponding to protonation at N(5).

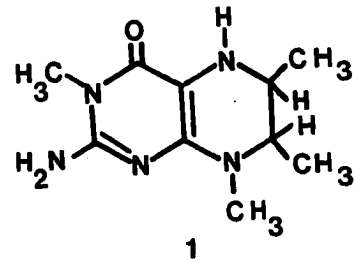

1

RESULTS

3,6,7,8-TMTHP gives rise to two electrooxidation peaks (peaks I_a and III_a) at the PGE. There are two additional electrooxidation peaks observed at more positive potentials than peak III_a. However, these additional peaks were also observed when solutions of 3,6,7,8-tetramethylpterin (3,6,7,8-TMP) were studied (Fig. 2). Therefore, they are believed to be due to oxidation of 3,6,7,8-TMP which forms during electrooxidation of 3,6,7,8-TMTHP. It has been reported that 3,6,7,8-TMP may exist in different ionic, hydrated and open-ring forms in aqueous solution depending on pH.[8] At least one of these forms, for

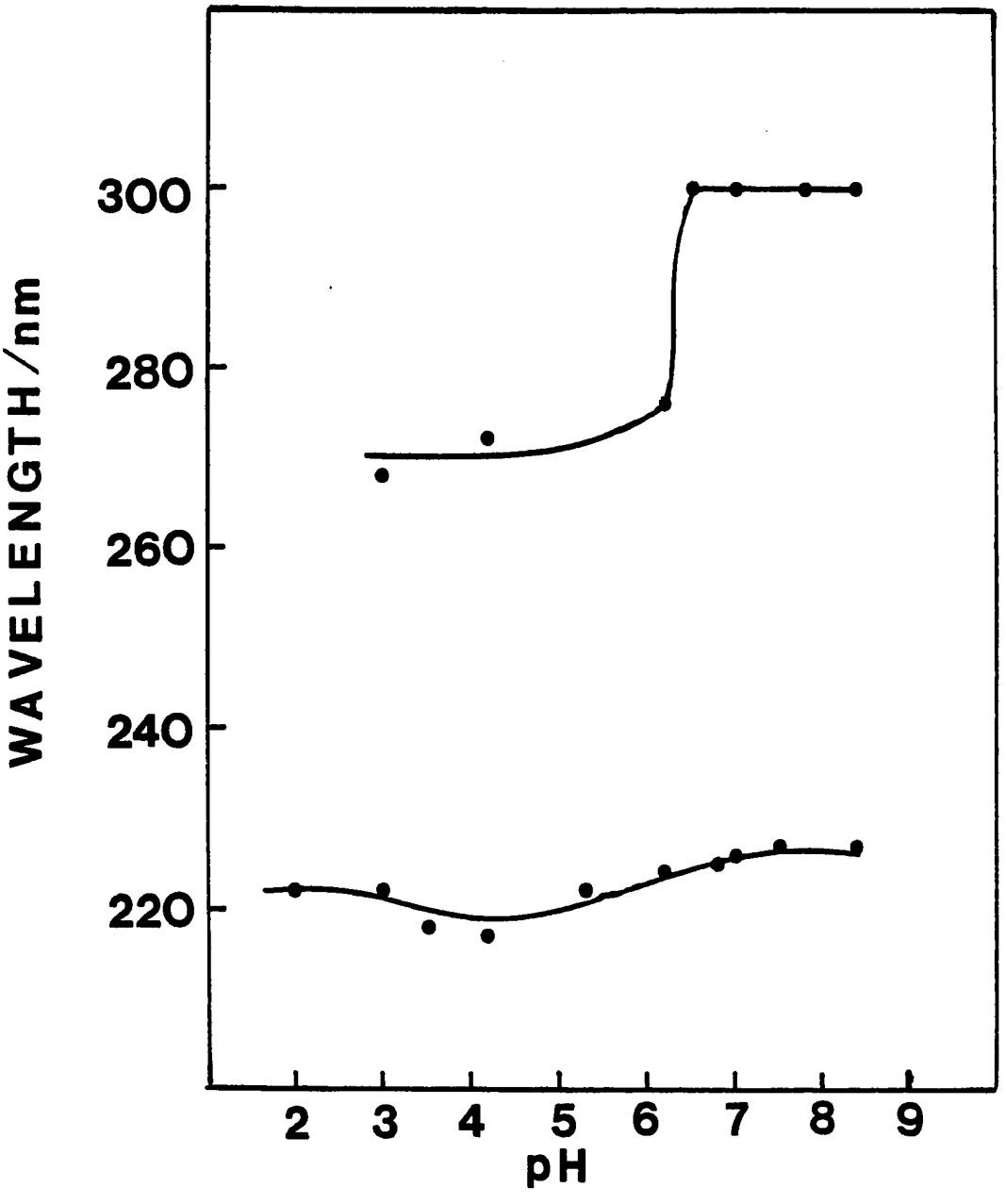

Figure 1. Change in λ_{max} for 3,6,7,8-TMTHP as a function of pH.

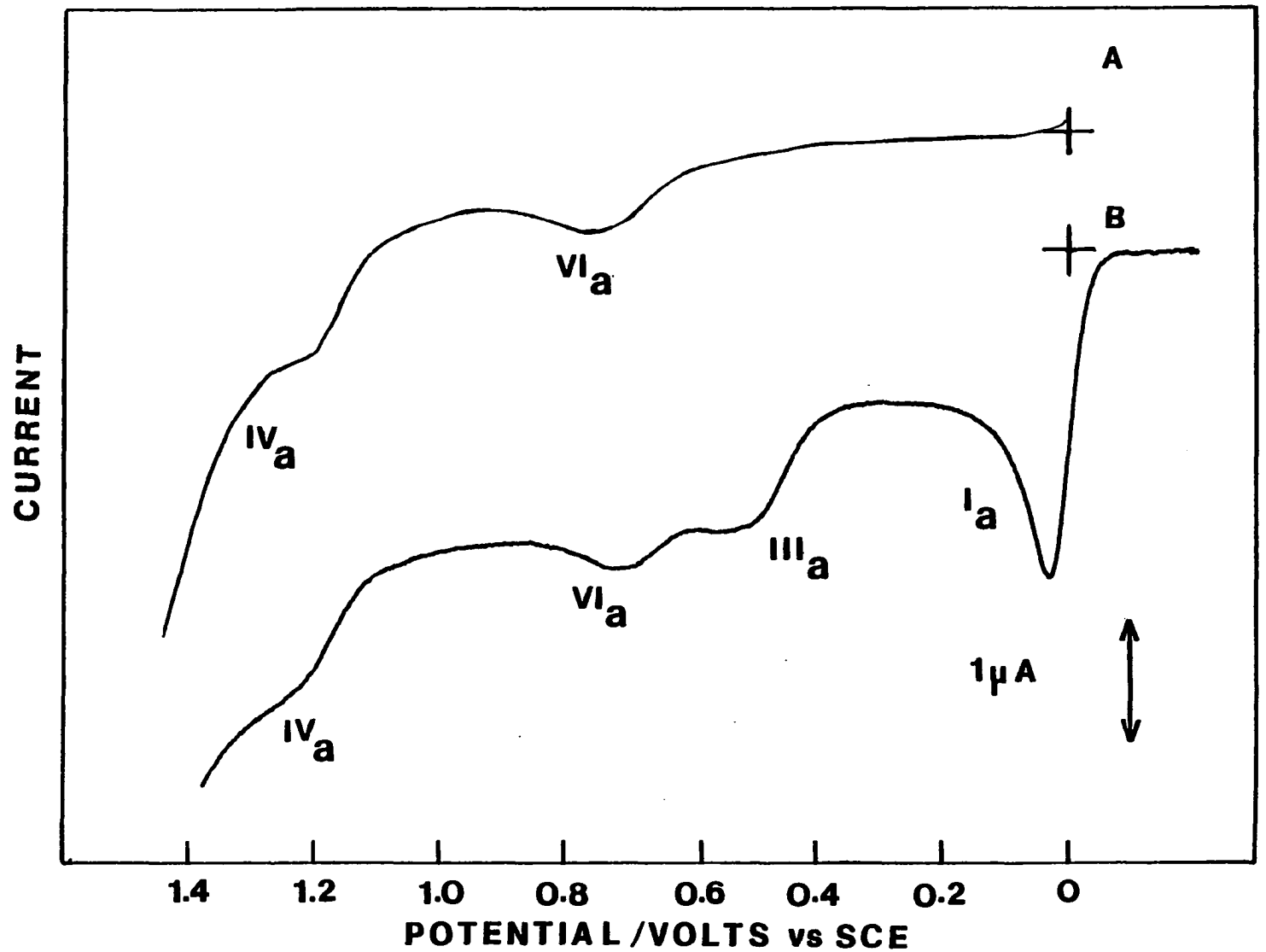

Figure 2. Single sweep voltammograms of (A) 1 mM 3,6,7,8-TMP at pH 4.0, (B) 1 mM 3,6,7,8-TMTHP at pH 4.2 at a sweep rate of 5 mV s^{-1}.

example, the cationic open-ring form is thought to be unstable.[8] Between pH 4.87 and 12.0, hydrated 3,6,7,8-TMP undergoes ring-opening and ring-closing reactions.[8] The equilibrium constants for the existence of different forms of 3,6,7,8-TMP in aqueous solution are given in Table 1.[8] Therefore, it seems possible that 3,6,7,8-TMP may exist in a variety of different forms which may undergo electrooxidation. It is also reasonable to assume that some of the voltammetric oxidation peaks observed may be due to some decomposition products of 3,6,7,8-TMP.

The dependence of the peak potential on pH for the voltammetric electrooxidation peaks of 3,6,7,8-TMTHP is given by the following equations:

Peak I_a $E_p = (0.26-0.050\ pH)V$
(pH = 2.9-9.0)

Peak III_a $E_p = (0.90-0.105\ pH)V$
(pH = 2.0-4.0)

(pH = 4.0-9.0) $E_p = (0.56-0.011\ pH)V$

Cyclic voltammograms of 3,6,7,8-TMTHP show two electrooxidation peaks (peaks I_a and III_a) between pH 2-9 when scanned initially in a positive direction (Fig. 3A). At low pH values, for example pH 2, and at a sweep rate of 20 mV s^{-1} two additional voltammetric peaks (peaks II_a and IV_c) may be observed if the potential is clipped at +0.5V (Fig. 4). Upon reversal of the sweep direction up to four

Table 1. Acid dissociation constants for 3,6,7,8-TMP in water at 20°C[a]

	pK_a	Equilibrium
3,6,7,8-TMP	8.25	cation $\rightleftharpoons$ hydrated neutral molecule[b]
	10.04	cation $\rightleftharpoons$ water-free neutral molecule
	4.60	ring-open cation $\rightleftharpoons$ ring-open neutral molecule
	13.72	ring-open neutral molecule $\rightleftharpoons$ ring-open anion[c]

[a]Data obtained from ref. 8.

[b]Mainly ring-open form.

[c]Additional equilibrium between the ring-closed forms.

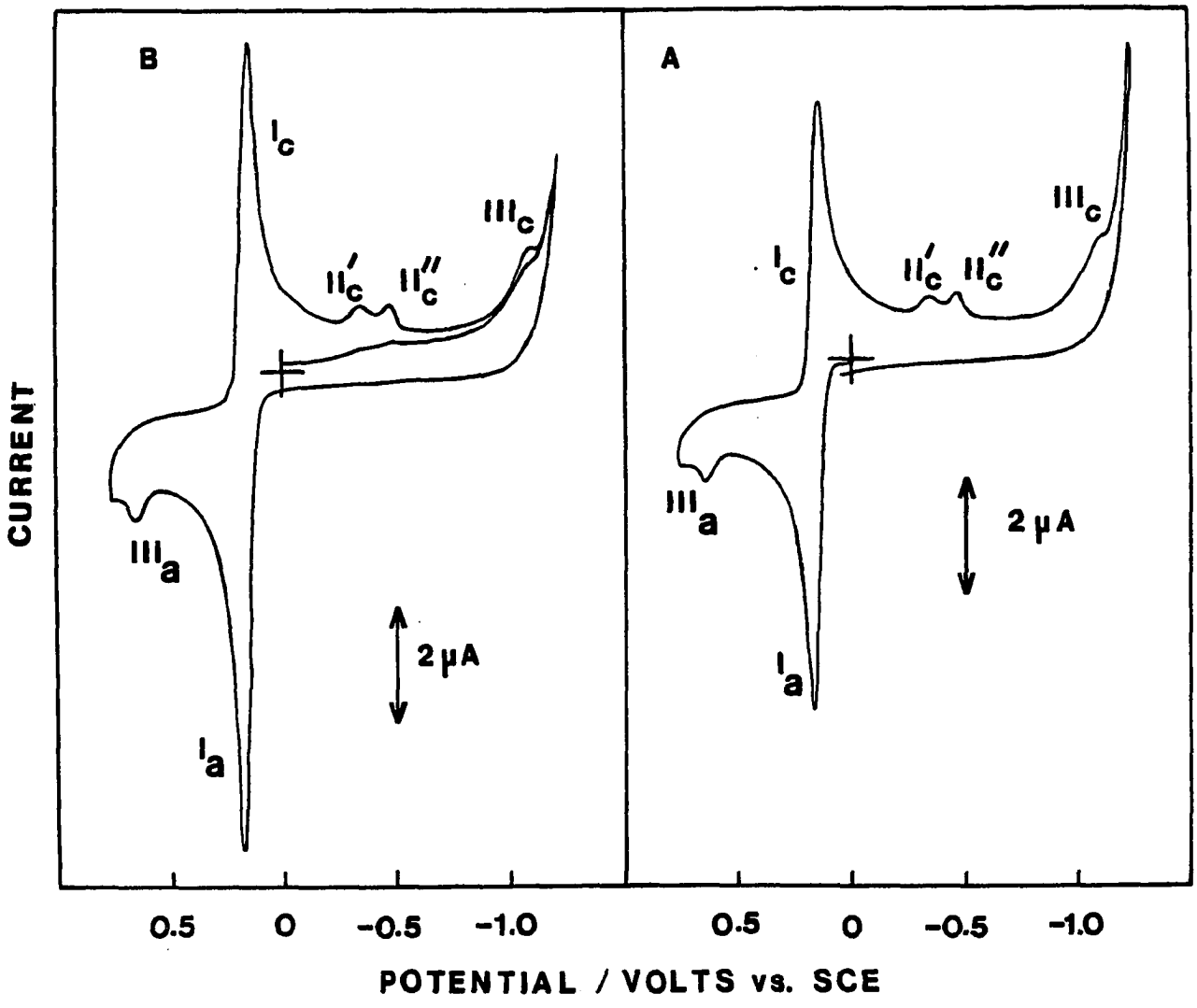

Figure 3. Cyclic voltammogram of 1 mM 3,6,7,8-TMTHP in phosphate buffer pH 2 (A) first sweep in positive direction (B) first sweep in negative direction at a sweep rate of 500 mV s^{-1}.

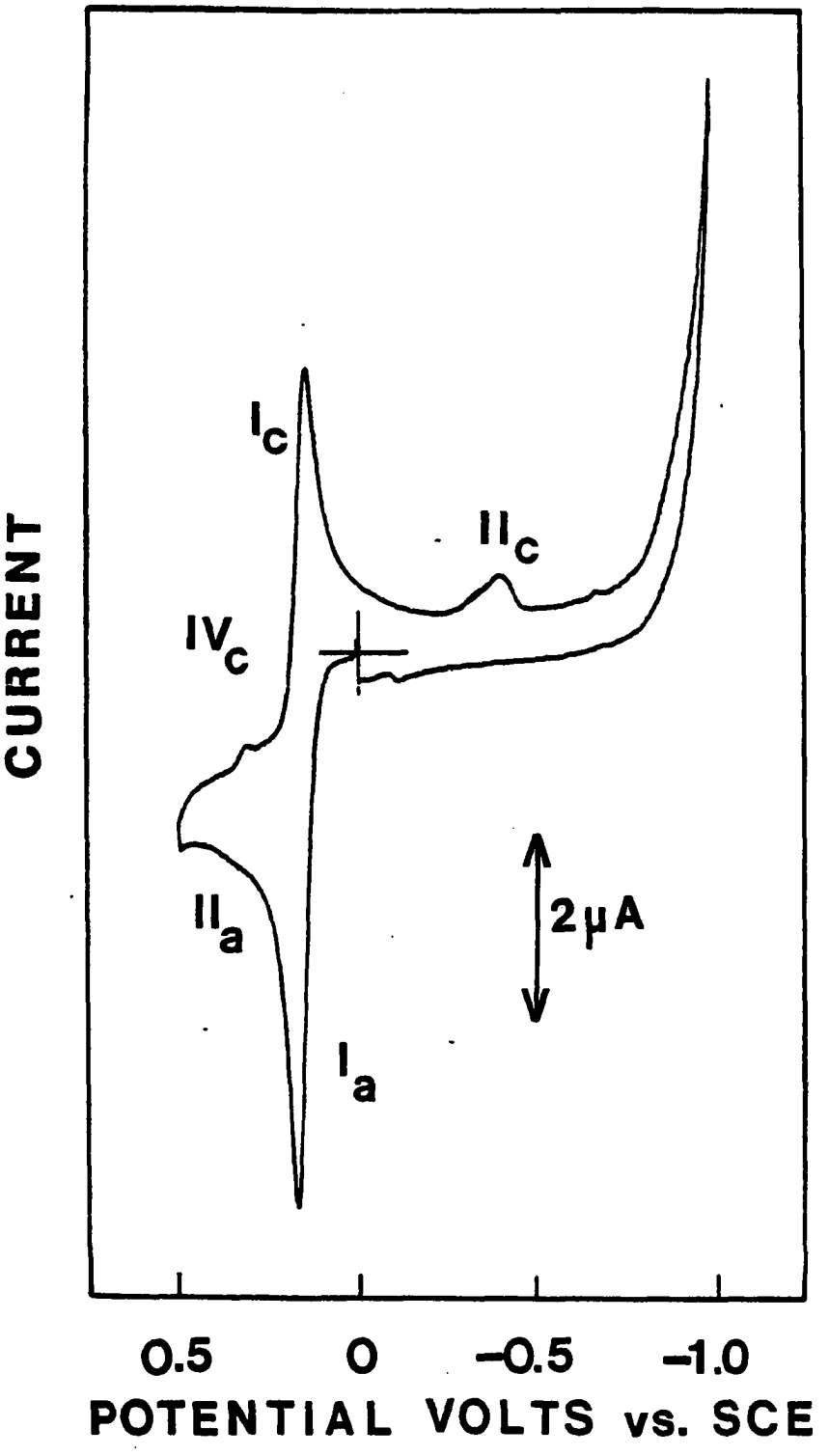

Figure 4. Cyclic voltammogram of 1 mM 3,6,7,8-TMTHP in phosphate buffer pH 2 at a sweep rate of 20 mV s^{-1}. Switching potential is +0.5V.

voltammetric reduction peaks may be observed (peaks I_c, II'_c, II''_c and III_c) (peak III_c is very close to the background current) (Fig. 3A). If the potential is initially scanned towards increasingly negative potentials no electroreduction peaks may be observed (Fig. 3B).

Peaks I_a and I_c form a quasi-reversible redox couple. The peak separation, ΔE_p, between peaks I_a and I_c averages 38±11 mV between pH 2-9 at a sweep rate of 200 mV s^{-1}.

Peak clipping experiments show that it is necessary to sweep past peak I_a in order to observe peaks I_c and III_c (Fig. 5A). If the potential is clipped past peak III_a, peaks I_c, II'_c and II''_c are observed (Fig. 5B). Additional electroreduction peaks appear if the potential is swept beyond peak III_a to potentials at which additional oxidation peaks may be observed and reversed (Fig. 6).

A careful study of the peak heights for peaks I_a and I_c reveal that with increasing pH the peak height for peak I_c decreases with respect to peak I_a at a fixed sweep rate, i.e., 200 mV s^{-1} (Table 2). A similar effect on relative peak heights may be observed when the sweep rate is decreased. At slow sweep rates peak I_c is much smaller than peak I_a and as the sweep rate is increased the ratio of the heights of peak I_c to peak I_a approaches unity (Table 2). The behavior described above indicates that the peak I_a electrooxidation product is not very stable and undergoes a chemical follow-up reaction.

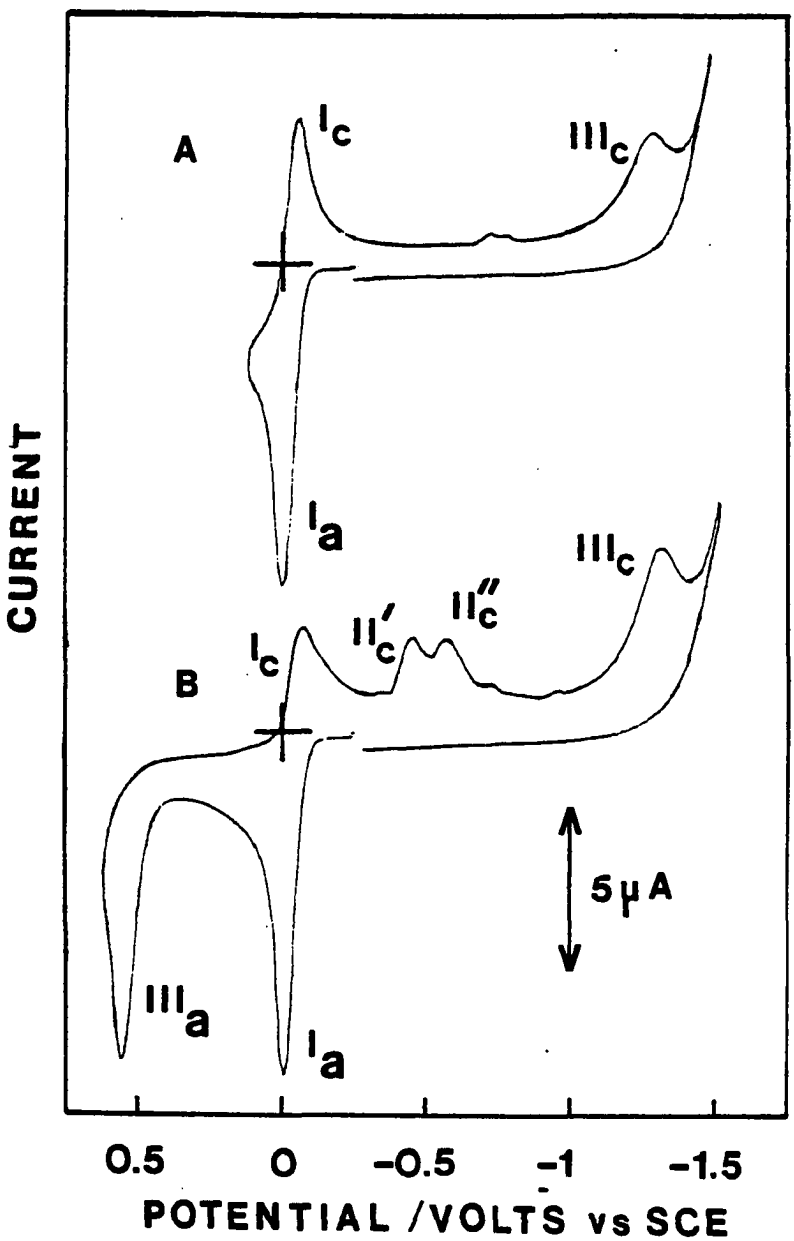

Figure 5. Cyclic voltammograms of 1 mM 3,6,7,8-TMTHP in phosphate buffer pH 5.6 at a sweep rate of 200 mV s^{-1} (A) switching potential past peak I_a, (B) switching potential past peak III_a.

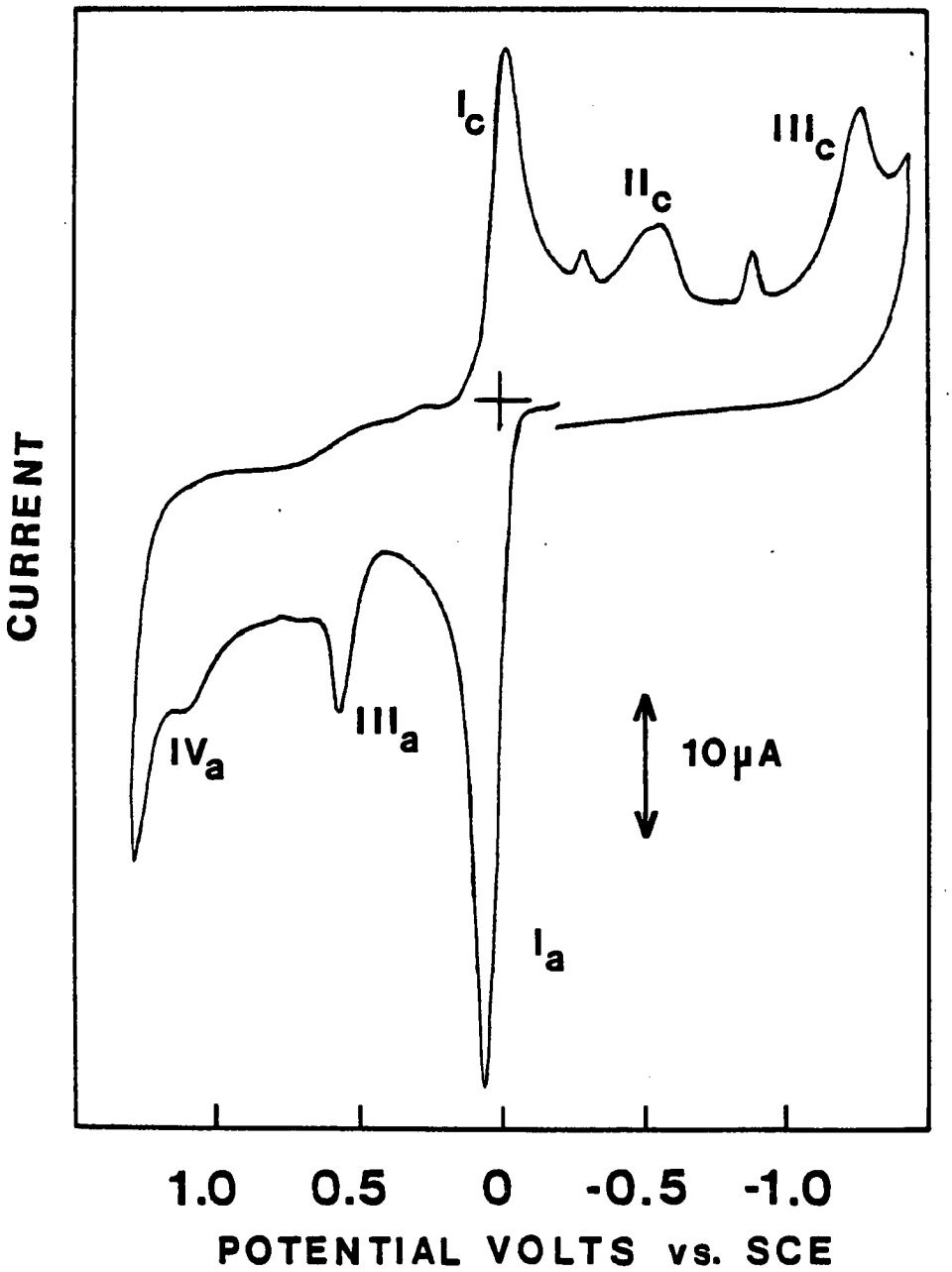

Figure 6. Cyclic voltammogram of 1 mM 3,6,7,8-TMTHP in phosphate buffer pH 4.2 at a scan rate of 200 mV s^{-1}.

Table 2. Comparison of the peak current ratio i_{p_c}/i_{p_a} for peaks I_c and I_a observed at a PGE as a function of sweep rate and pH[a]

pH	(i_{p_c}/i_{p_a})	scan rate (V s^{-1})	clipping potential[b]
2.0	0.64	0.020	II_a
	0.60	0.020	III_a
	0.84	0.100	II_a
	0.79	0.100	III_a
	0.87	0.200	I_a
	0.80	0.200	III_a
3.9	0.73	0.200	I_a
	0.67	0.200	I_a[c]
	0.52	0.200	III_a
	0.44	0.200	III_a[c]
4.6	0.63	0.200	I_a
	0.55	0.200	I_a[c]
	0.53	0.200	I_a[d]
	0.47	0.200	III_a
5.6	0.46	0.200	I_a
	0.32	0.200	III_a
	0.19	0.050	III_a
7.0	0.35	0.200	I_a
	0.17	0.200	III_a
8.0	0.14	0.200	I_a

[a]Phosphate buffers of ionic strength of 0.5 M were used.

[b]The potential was scanned past the peak indicated and then reversed to record the peak current for peak I_c.

[c]The potential was scanned 0.1V past the peak indicated and then reversed.

[d]The potential was scanned 0.3V past the peak indicated and then reversed.

Several 3 mg samples of 3,6,7,8-TMTHP were electrolyzed at pH 2 and pH 4 at potentials corresponding to peak I_a. Voltammograms of the electrolysis products showed only peak III_a when scanned initially in a positive direction, and peak III_c when scanned initially in a negative direction (Fig. 7A,B). U.V. spectra recorded before, during and after electrolysis at peak I_a potentials at pH 2 are shown in Fig. 8A and B. At pH 2 3,6,7,8-TMTHP shows two absorption bands at λ=221 nm and 268 nm (Fig. 8A). When a potential is applied corresponding to peak I_a a new absorption band starts to grow in at 359 nm, the band at 268 nm decreases in intensity and shifts to shorter wavelengths and a new highly intense absorption band starts to grow in at 257 nm. Furthermore, the absorbance at 221 nm decreases (curve 2, Fig. 8B). At the end of the electrolysis, three absorption bands at λ_{max} = 359 nm, 254 nm and 215 nm and a shoulder around 278 nm are observed (curve 3, Fig. 8B). If the same solution is further electrooxidized at peak III_a potentials, the absorption band at 359 nm decreases in intensity and shifts to longer wavelengths, the shoulder at 278 nm increases in intensity (curve 2, Fig. 9). The absorbance at 215 nm and 254 nm decrease. The final electrooxidation product exhibits λ_{max} = 210 nm, 258 nm, 281 nm and 394 nm (curve 3, Fig. 9) which corresponds to the absorption spectrum of 3,6,7,8-TMP at pH 2.

Controlled potential coulometric experiments were

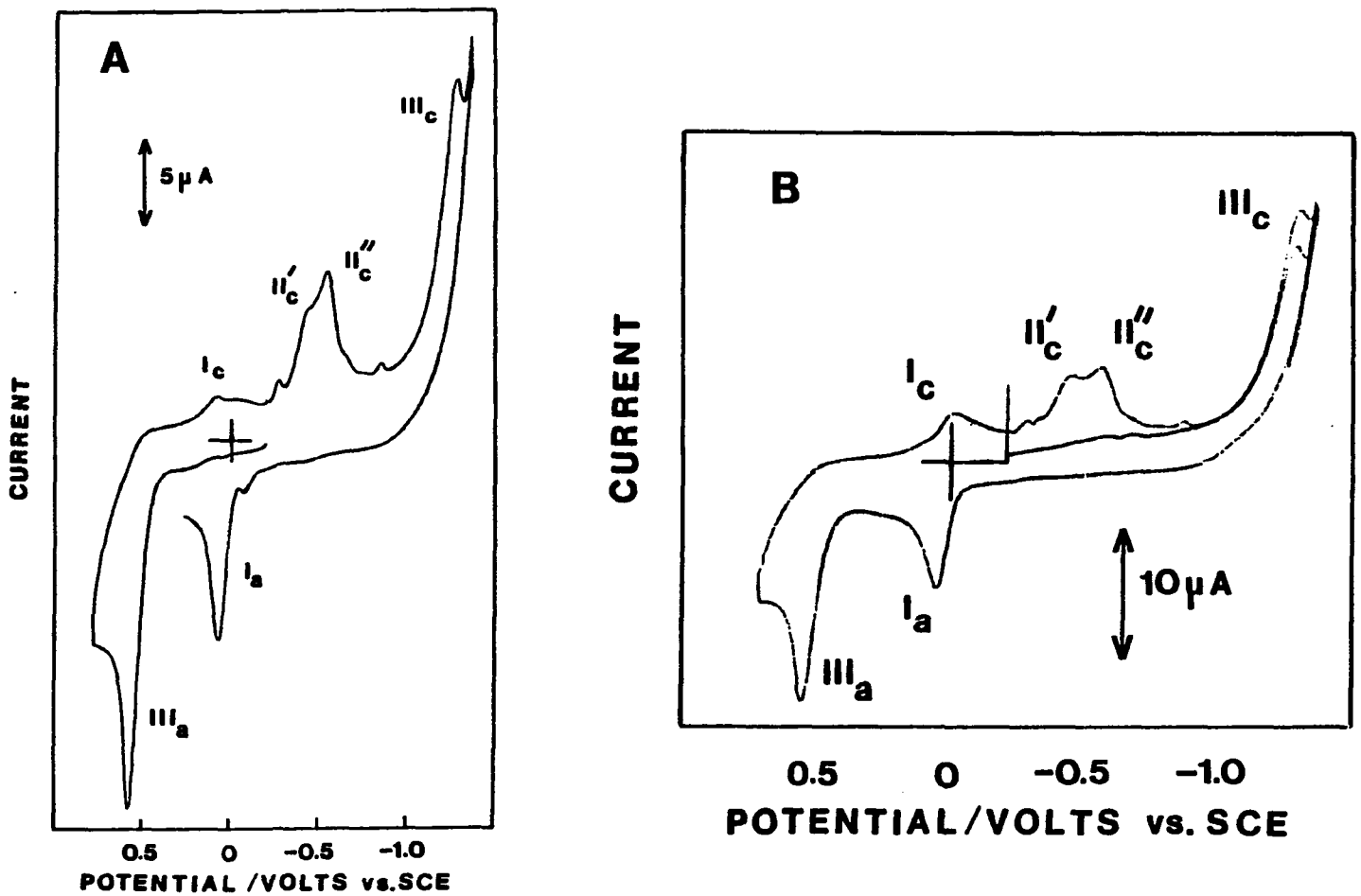

Figure 7. Cyclic voltammograms of 0.56 mM 3,6,7,8-TMTHP electrolyzed at +0.1V in phosphate buffer pH 4.2 (A) scanned positive first (B) scanned negative first, at a sweep rate of 200 mV s^{-1}.

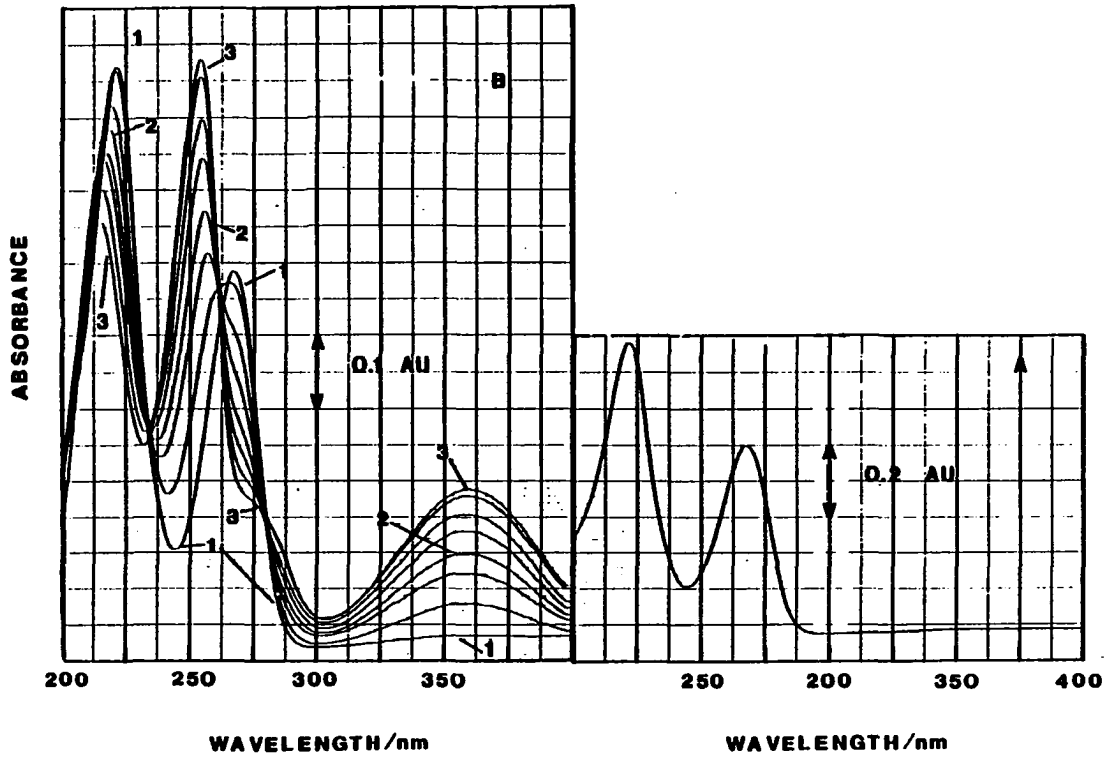

Figure 8. Spectra of 0.56 mM 3,6,7,8-TMTHP in phosphate buffer pH 2 (A) before electrolysis, (B) during electrolysis at +0.24V (Peak I_a) curve 1 corresponds to the initial spectrum, curve 2 is spectrum during the electrolysis, curve 3 corresponds to the final spectrum. 0.1 cm quartz cells were used at a scan rate of 200 nm/min, 0.5s response time.

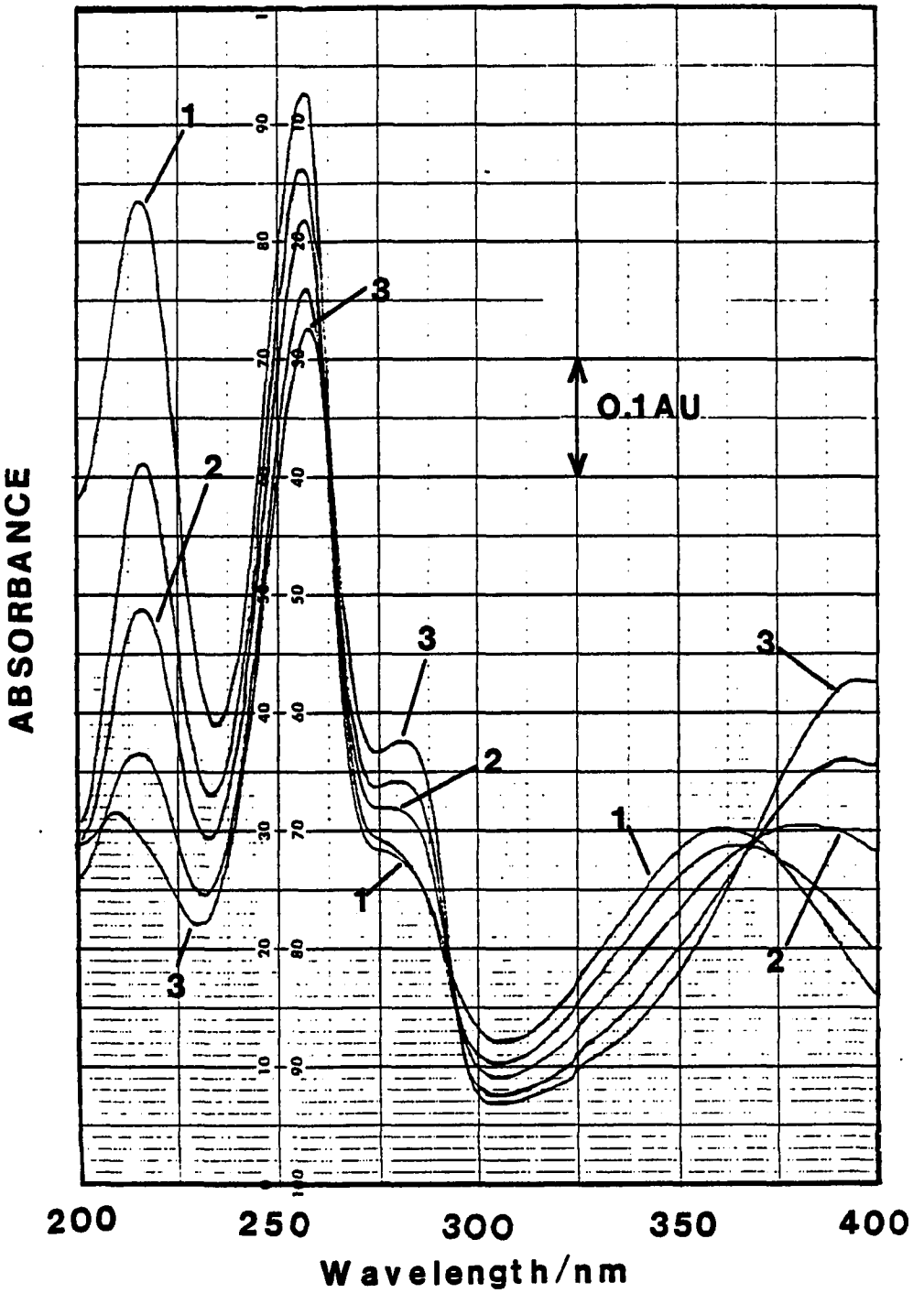

Figure 9. Spectra of 0.56 mM 3,6,7,8-TMDHP in phosphate buffer pH 2 (1) before applying a potential, (2) during application of peak III_a potentials, (3) final electrooxidation product.

carried out in a sealed thin-layer cell at an RVC electrode between pH 1.85-6.0. Application of a potential corresponding to peak I_a resulted in transfer of 1.6±0.3 electrons.

Controlled potential electrolyses carried out in low phosphate buffer (0.5 M NaCl and 0.005 M Na_2HPO_4) at pH 3 and pH 7 at peak III_a potentials resulted in formation of a product identified as 3,6,7,8-TMP in GC-MS experiments (see Experimental Section in Chapter two).

Electrochemical reduction of 3,6,7,8-TMP at a dropping mercury electrode (DME) has been studied by Pfleiderer, et al.[9] For purposes of comparison, electroreduction of 3,6,7,8-TMP was carried out at a PGE. The results obtained at the PGE are compared with those reported by Pfleiderer, et al.[9] in Table 3. The relationship between the observed peak potentials and pH at the PGE may be represented by the following equations:

Peak II_c E_p (-0.276-0.052 pH)V
(pH = 2-7.8)
Peak III_c E_p (-0.940-0.052 pH)V
(pH = 2-7.8)

It has been reported that the first reduction step (peak II_c') involves one electron and one proton to generate a radical species.[9] This radical may be reduced back to 3,6,7,8-TMP. The same radical may also be further electroreduced to give a 5,8-dihydropterin (Note that 5,8-dihydro-

Table 3. Comparison of peak potentials[a] observed for peaks II_c and III_c of 3,6,7,8-TMP at the PGE with values[b] obtained at a DME as a function of pH[c]

pH	E_p II_c[d] /V	E_p II[b] /V	E_p III_c[d] /V	E_p III_c[b] /V
2.0	-0.380	-0.41	-1.04	-0.92
3.0	-0.430	-0.45	-1.10	-0.98
4.0	-0.480	-0.49	-1.16	-1.04
4.7	-0.530	-0.53	-	-1.10
6.0	-0.585	-0.57	-1.23	-1.16
7.0	-0.610	-0.61	-1.32	-1.21
7.8	-0.680	-0.65	-	-1.27

[a] E_p values obtained from 1 m$\underline{M}$ solutions at a sweep rate of 5 mV s^{-1}.

[b] E_p values calculated from $E_{1/2}$ data $\underline{vs}$. Ag/AgCl obtained by Pfleiderer $\underline{et\ al}$.[9] using the formula[10]

$$E_p = E_{1/2} - \frac{0.029}{n} \quad n = 2,$$

these values were also corrected so that they are referred to the SCE.

[c] Phosphate buffers of ionic strength 0.5 $\underline{M}$ were used.

[d] Values obtained voltammetrically in this study.

nomenclature is used to indicate the oxidation state of the compound) in a second one electron, one proton reaction (peak II_c'').[9] The 5,8-dihydro derivative is not very stable and reacts to form a 7,8-dihydropterin derivative. The mechanistic information provided by Pfleiderer, et al. is based on wave-height analysis and no cyclic voltammetric evidence was given. Cyclic voltammograms obtained in this present study of 1 mM solutions of 3,6,7,8-TMP in phosphate buffer pH 2.4 at the PGE at high sweep rates (>5V s^{-1}) clearly demonstrate the two-step electroreduction of 3,6,7,8-TMP (Fig. 10). It may be observed from Fig. 10 that there are two electrooxidation peaks (peaks V_a' and V_a'') coupled to peaks II_c' and II_c''. With samples of 3,6,7,8-TMTHP electroreduction peaks II_c' and II_c'' could be observed as separate peaks throughout the pH range employed (pH 2.0-8.0) at sweep rates of 200 mV s^{-1} or higher. With samples of 3,6,7,8-TMP only one separate reduction peak (peak II_c) could be observed at slow sweep rates (Fig. 11). It is believed that two sequential one-electron, one-proton reduction steps are characteristic of the first electroreduction process of N(8)-methylated pterins. Other than comparing the electroreduction of 3,6,7,8-TMP as a function of pH with previous results reported in literature no further detailed study of 3,6,7,8-TMP was undertaken.

The main interest in 3,6,7,8-TMP was due to the fact that a $2e\text{-}2H^+$ electrooxidation at peak I_a potentials

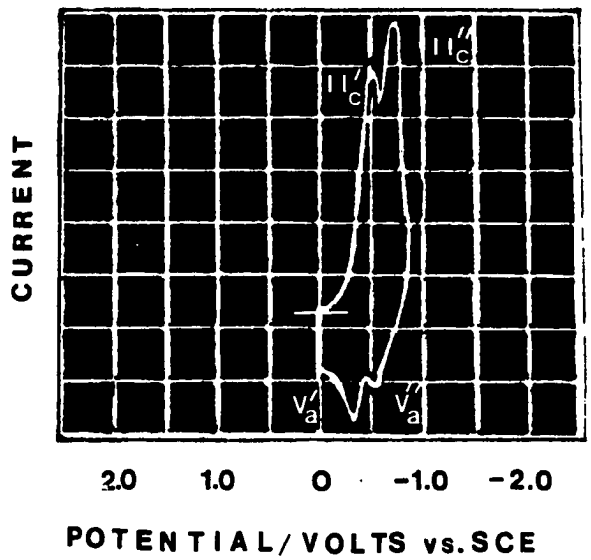

Figure 10. Cyclic voltammogram of 1 m$\underline{M}$ 3,6,7,8-TMP in phosphate buffer pH 2.4 at a sweep rate of 20 V s^{-1}.

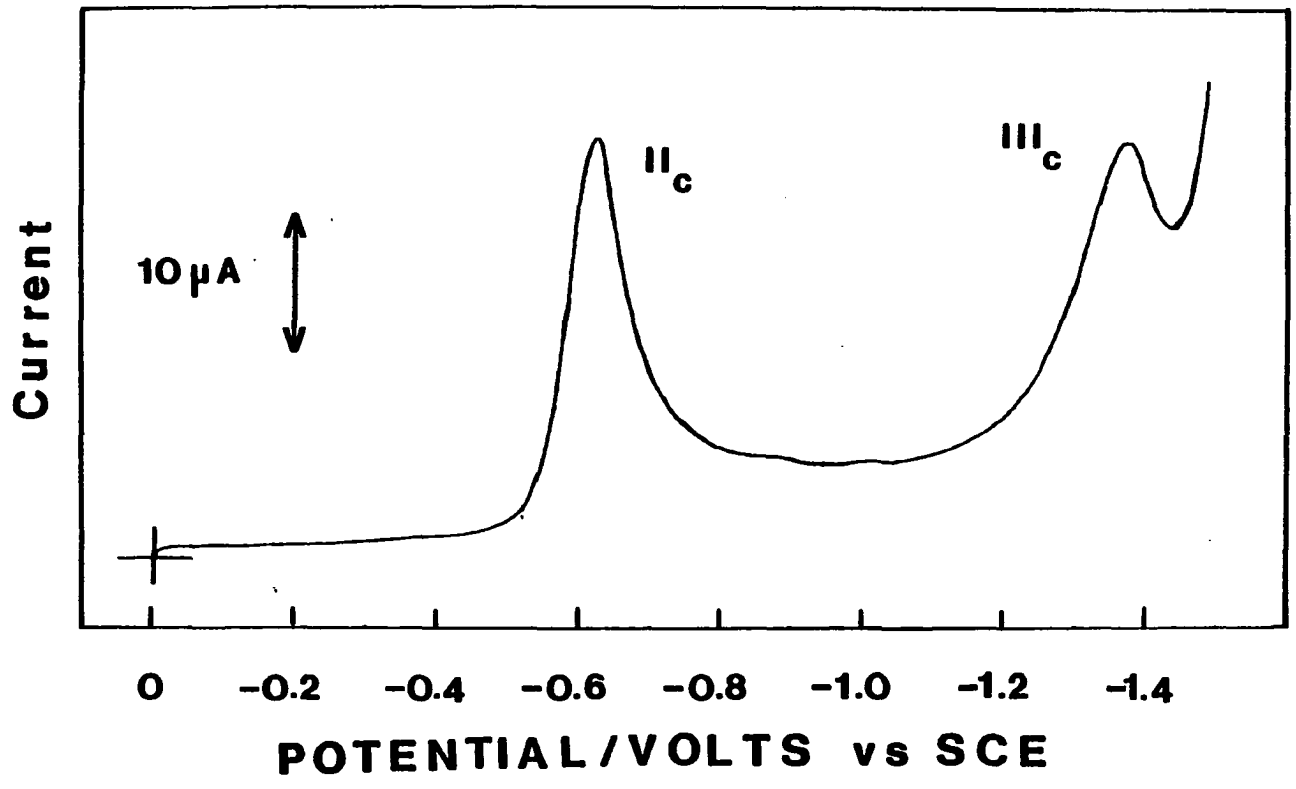

Figure 11. Single sweep voltammogram of 1 m$\underline{M}$ 3,6,7,8-TMP in phosphate buffer pH 6 at a scan rate of 200 mV s^{-1}.

would be expected to lead to formation of the "locked" quinonoid-dihydropterin (2).

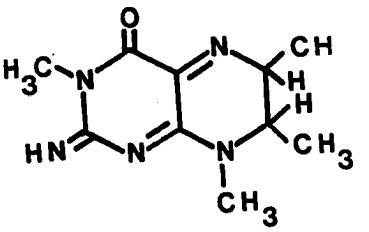

2

Therefore, more emphasis was placed on studying the spectroelectrochemical behavior of 3,6,7,8-TMTHP and determining the stability of the electrogenerated quinonoid-dihydropterin.

At pH 2.4 3,6,7,8-TMTHP exhibits two U.V. absorption bands (λ_{max} = 218 nm and 268 nm) (Fig. 12). When a potential was applied corresponding to peak I_a (as determined from cyclic voltammograms run in a thin-layer cell (TLC)), the absorbance of both bands goes down and the band at 268 nm shifts to shorter wavelengths. There is, correspondingly, an increase in absorbance at 256 nm and 352 nm (Fig. 12B). If the potential is kept on throughout the experiment to electrooxidize away all of the 3,6,7,8-TMTHP in the RVC electrode cavity, the resulting electrolysis product exhibits an U.V. spectrum with λ_{max} = 212 nm, 256 nm, 362 nm and a shoulder at about 280 nm. However, if the

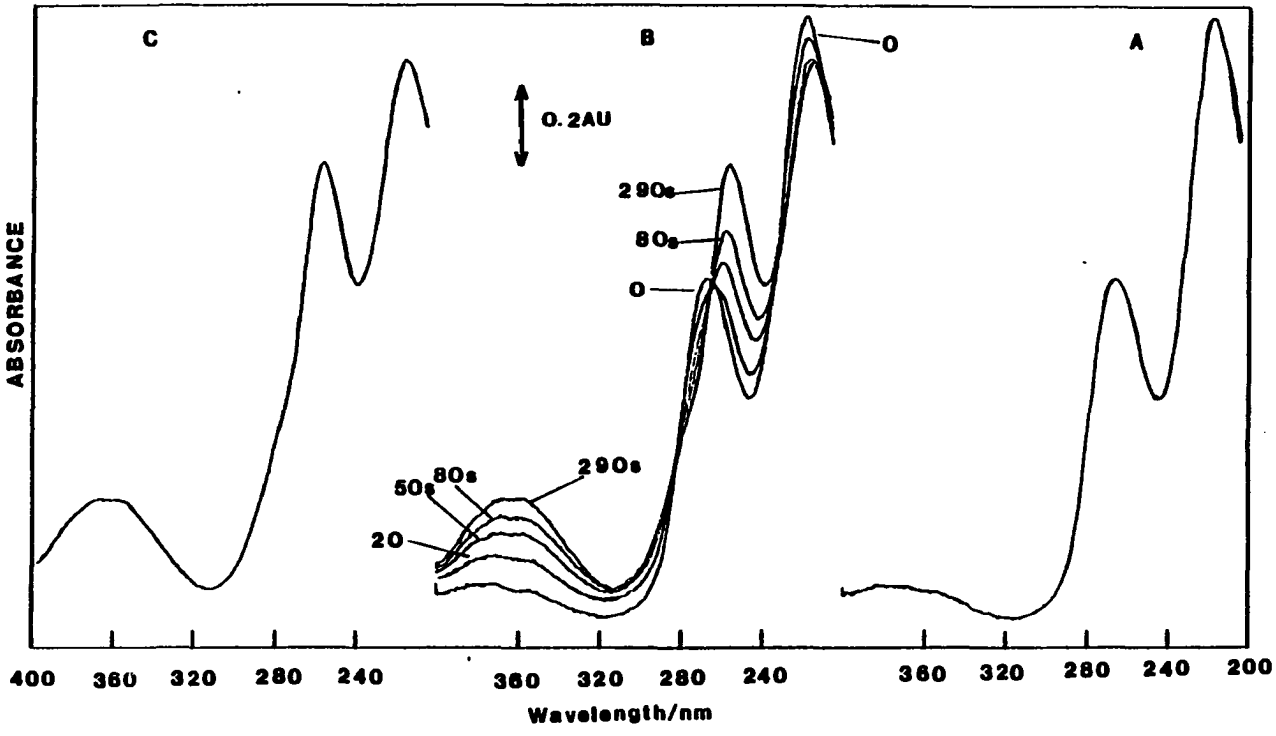

Figure 12. Spectra of 1 mM 3,6,7,8-TMTHP in phosphate buffer pH 2.4 electrolyzing at +0.25V at a reticulated vitreous carbon electrode in a thin-layer cell, (A) initial spectrum, (B) spectra obtained during the electrolysis. The potential was turned off at 30s, (C) spectrum obtained after turning off the applied potential.

potential is turned off when about 75% of the 3,6,7,8-TMTHP has been electrooxidized, the resulting absorption spectrum after the rearrangement reaction is slightly different (λ_{max} = 216 nm, 257 nm and 360 nm) (Fig. 12C). Since the absorbance changes even after the applied potential is turned off, formation of an unstable absorbing intermediate must occur.

At higher pH values, for example pH 8.8, the thin-layer spectroelectrochemical behavior of 3,6,7,8-TMTHP is somewhat different. At pH 8.8, 3,6,7,8-TMTHP absorbs at 231 nm and 306 nm (Fig. 13A). When a potential is applied corresponding to peak I_a, the absorbance at 306 nm and 231 nm goes down (Fig. 13B). An intermediate species absorbing at 312 nm is generated. When the potential is turned off, three new absorption bands at 236 nm, 290 nm and 328 nm may be observed (Fig. 13C).

A spectroelectrochemical method was used to determine the rate of the chemical follow-up reaction. The change in absorbance was monitored at preselected wavelengths as a function of time. The wavelengths chosen corresponded to wavelengths where the final electrolysis product or the intermediate generated had a significant absorbance. The change in absorbance with respect to time was exponential and first-order rate constants were obtained. At pH values greater than 6 occasionally two rate constants could be inferred from non-least-squares analysis of

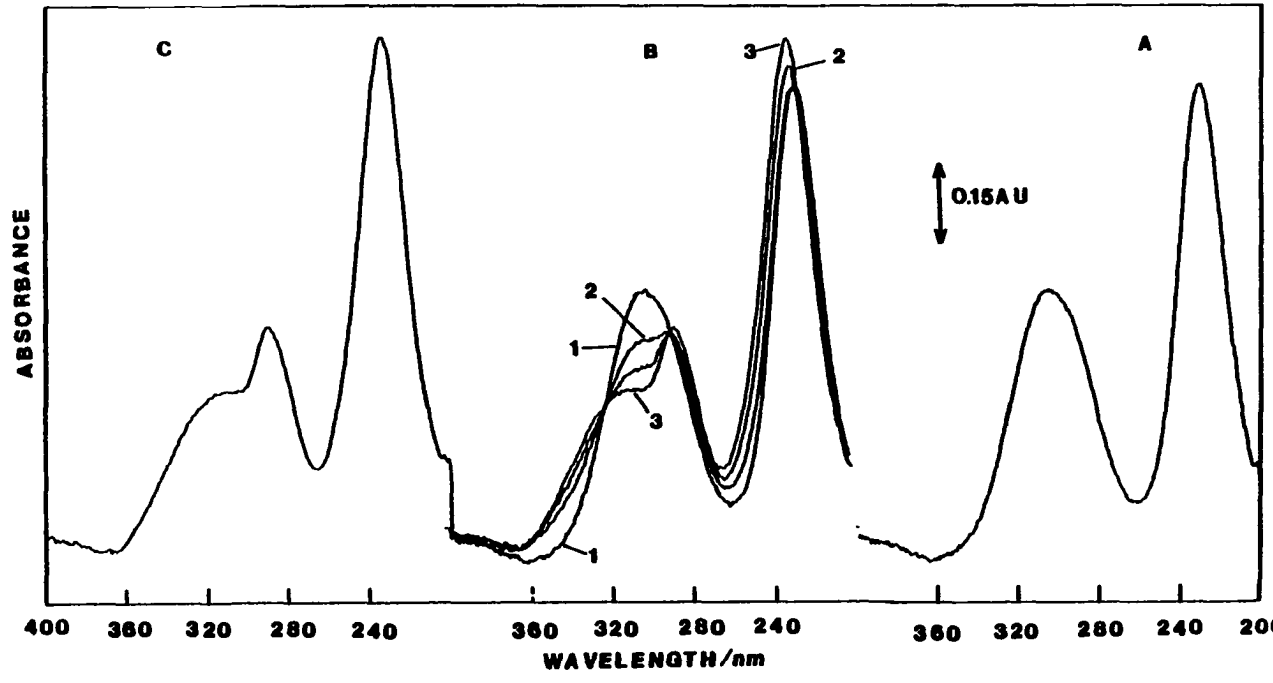

Figure 13. Spectra of 1 mM 3,6,7,8-TMTHP in phosphate buffer pH 8.8 electrolyzing at 0.05V at a reticulated vitreous carbon electrode in a thin-layer cell (A) initial spectrum, (B) spectra obtained during electrolysis, (1) initial spectrum, (2) spectrum of the intermediate, (3) final spectrum of the product, (C) final spectrum obtained after the applied potential is turned off.

Table 4. Observed first-order rate constants for rearrangement of the quinonoid-dihydropterin formed on peak I_a electrooxidation of 3,6,7,8-TMTHP[a]

pH[b]	$k_{obs} \times 10^3/s^{-1}$	$\sigma \times 10^3/s^{-1}$[c]	λ/nm[d]
1.9	14.3	0.6	244
1.9	18.2	1.6	256,356
2.6	22.7	1.4	256,360
3.2	19.1	1.6	260
3.7	19.5	1.2	244,260
3.7	20.2	2.2	256,360
4.7	28.3	1.8	260
5.3	35.4	5.1	228,326
5.8	50.7	12.5	226,320
6.0	32.2	2.5	234
6.3	120 and 18.1[e]	184 and 4.4[e]	228,282
6.6	35.6	8.3	230,284
7.0	134 and 15.0[e]	26.3 and 0.6[e]	236,290
7.8	208 and 16.1[e]	5.7 and 2.3[e]	230
8.4	8.0	3.0	238,290
8.8	10.9	1.2	236,290

[a]Measured by a thin-layer spectroelectrochemical method with electrolysis performed with an optically transparent RVC electrode.

[b]Phosphate buffers having an ionic strength of 0.5 M.

[c]Standard deviation.

[d]Wavelength used to monitor the change in absorbance with respect to time.

[e]Two rate constants were measured corresponding to a fast step followed by a slow one.

experimental absorbance vs. time curves corresponding to a fast and a slow reaction (the fast reaction appeared to be about 10 times faster than the slow one). The relationship between k_{obs} and pH is summarized in Table 4. The k_{obs} vs. pH data obtained gives a bell-shaped curve when plotted between pH 2-6.6. The maximum value of k_{obs} occurring at around pH 5.8 and dropping off suddenly at higher pH values. The fact that occasionally two rate constants were obtained is disturbing. However, a careful study of the cyclic voltammetric behavior of 3,6,7,8-TMTHP at pH values greater than 6 indicates that the intermediate generated in peak I_a process is not very stable which would explain the fast k observed. The peak height for peak I_c is much smaller than peak I_a (Fig. 14). If the slow rate constants are used, the observed rate constant profile as a function of pH is very similar to that observed with 6,7-DMTHP (see Chapter 2). But on the other hand, the cyclic voltammetric behavior of the two compounds at pH>6 do not compare. Therefore, it may be suspected that at pH>6 the intermediate generated may undergo more than one reaction.

It is not possible to propose a definitive reaction scheme for the electrooxidation of 3,6,7,8-TMTHP from the brief investigation reported above. However, it is clear that 3,6,7,8-TMTHP is electrooxidized in a $2e\text{-}2H^+$ quasi-reversible process to form one or possibly more unstable

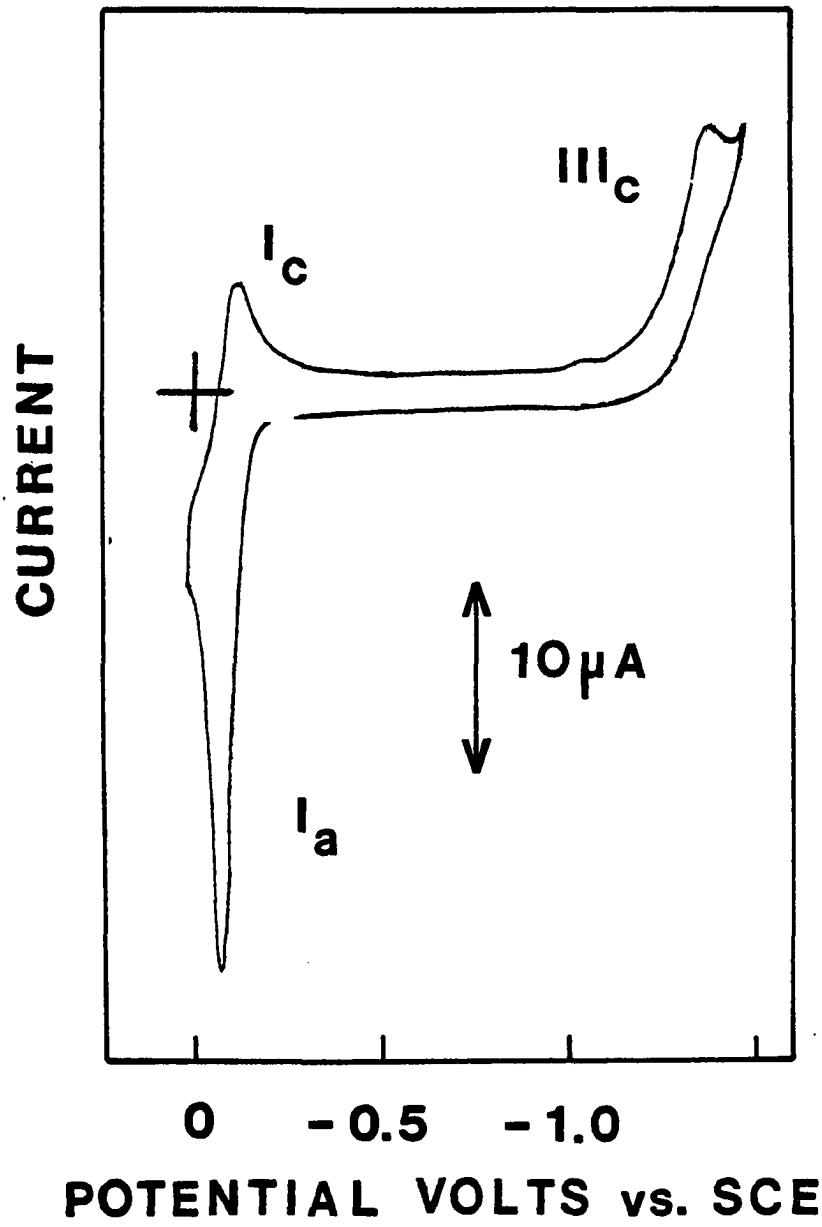

Figure 14. Cyclic voltammogram of 1 mM 3,6,7,8-TMTHP in phosphate buffer pH 7 at a sweep rate of 200 mV s^{-1}.

intermediates. The intermediate(s) apparently undergo a chemical reaction to form a more stable compound (k_{obs} $5.1x10^{-2}$ s^{-1} at pH 5.8). From what is already known about the electrooxidation of other tetrahydropterins[4-6] it is suspected that this stable product is a 3,6,7,8-tetramethyl-7,8-dihydropterin (3,6,7,8-TMDHP). The U.V. spectrum of 3,6,7,8-TMDHP in phosphate buffer pH 2.4 shows three absorption bands at λ_{max} = 217 nm, 257 nm and 362 nm and a shoulder at 280 nm. This spectrum is very similar to that observed for 6,7-DMDHP at pH 3 (λ_{max} = 213 nm, 252 nm, 352 nm and a shoulder at 272 nm). The absorption bands observed with 3,6,7,8-TMDHP are at slightly longer wavelengths probably due to the bathochromic shift caused by the electron-releasing effect of the additional methyl substituents. Pfleiderer et al.[11] have shown that 6,7-DMDHP has the following 7,8-dihydropterin configuration (3):

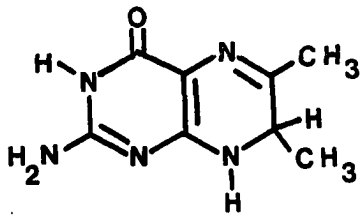

3

Since electrooxidation of 3,6,7,8-TMTHP at peak I_a potentials leads to formation of a relatively stable product (following rearrangement of the quinonoid) which has similar U.V. absorption characteristics to 6,7-DMDHP it may be concluded that this relatively stable product is also a 7,8-dihydropterin (4) (Note that 7,8-dihydro nomenclature is used to indicate that there is a single bond between C(7) and N(8) and not that there is an additional H on N(8)).

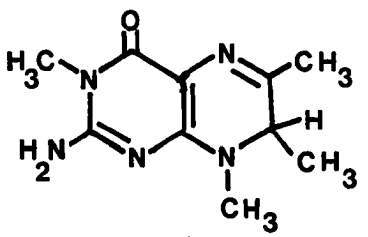

4

3,6,7,8-TMDHP absorbs at λ_{max} 235 nm, 291 nm and 312 nm in phosphate buffer pH 8.8. At the latter pH 3,6,7,8-TMDHP exists as a neutral molecule. It was noted that on going from a neutral molecule to a positively charged species there is a strong bathochromic shift (i.e., λ_{max} = 235, 291 and 312 nm at pH 8.8 and λ_{max} = 217, 257, (280), 362 nm at pH 2.4). The bathochromic shift observed by forming a positively charged molecule from a neutral one is one of the characteristics of the so-called "quasi-heteroaromatic" 7,8-dihydropterins.[11] 3,6,7,8-TMDHP is electrooxidized

in peak III_a process to give 3,6,7,8-TMP as evidenced by GC-MS product analysis of electrolysis solutions oxidized at peak III_a potentials in low phosphate buffers at pH 3 and 7. Peak I_c is due to electroreduction of the intermediate generated by the electrooxidation of 3,6,7,8-TMTHP. 3,6,7,8-TMP may be electroreduced in a two-step process giving rise to peaks II'_c and II''_c. At fast sweep rates it is possible to observe that two unstable species are formed in the peak II'_c, II''_c processes (Fig. 10). Peak V'_a is due to electroreduction of the radical species (6) formed in the peak II'_c electroreduction step back to 3,6,7,8-TMP (5). Peak V''_a on the other hand is due to the electrooxidation of the 5,8-dihydropterin derivative (7) back to the radical species (Fig. 10).

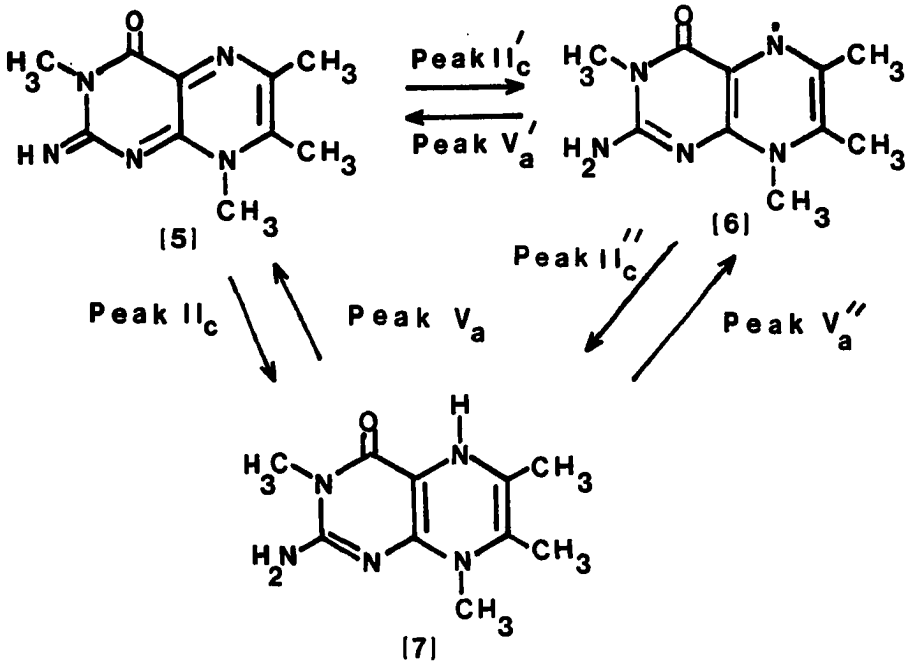

The 5,8-dihydro-derivative rearranges to form 3,6,7,8-TMDHP (3) which then may be reduced in the peak III_c process to form 3,6,7,8-TMTHP.

There is cyclic voltammetric evidence for the formation of a hydrated-dihydro derivative at low pH (e.g., pH $\leq$2, see Fig. 4) which may be oxidized at peak II_a potentials. Peak IV_c is coupled to peak II_a and is presumably due to reduction of the quinonoid-dihydro-hydrate intermediate(s) generated in peak II_a electrooxidation process. Figure 15 summarizes the proposed electrooxidation scheme for 3,6,7,8-TMTHP.

2-Dimethylamino-6,7,8-trimethyltetrahydropterin

2-DMTTHP is one of the five pterins discussed in chapter three which may form a "locked" quinonoid-dihydropterin (8) upon $2e^-2H^+$ oxidation. Solutions of 2-DMTTHP

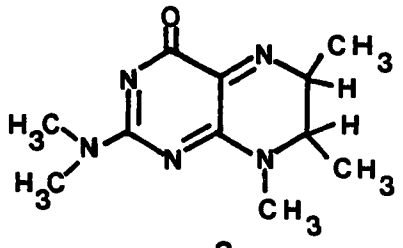

8

are air sensitive, especially at higher pH values. Air oxidation of 2-DMTTHP solutions may be observed very easily

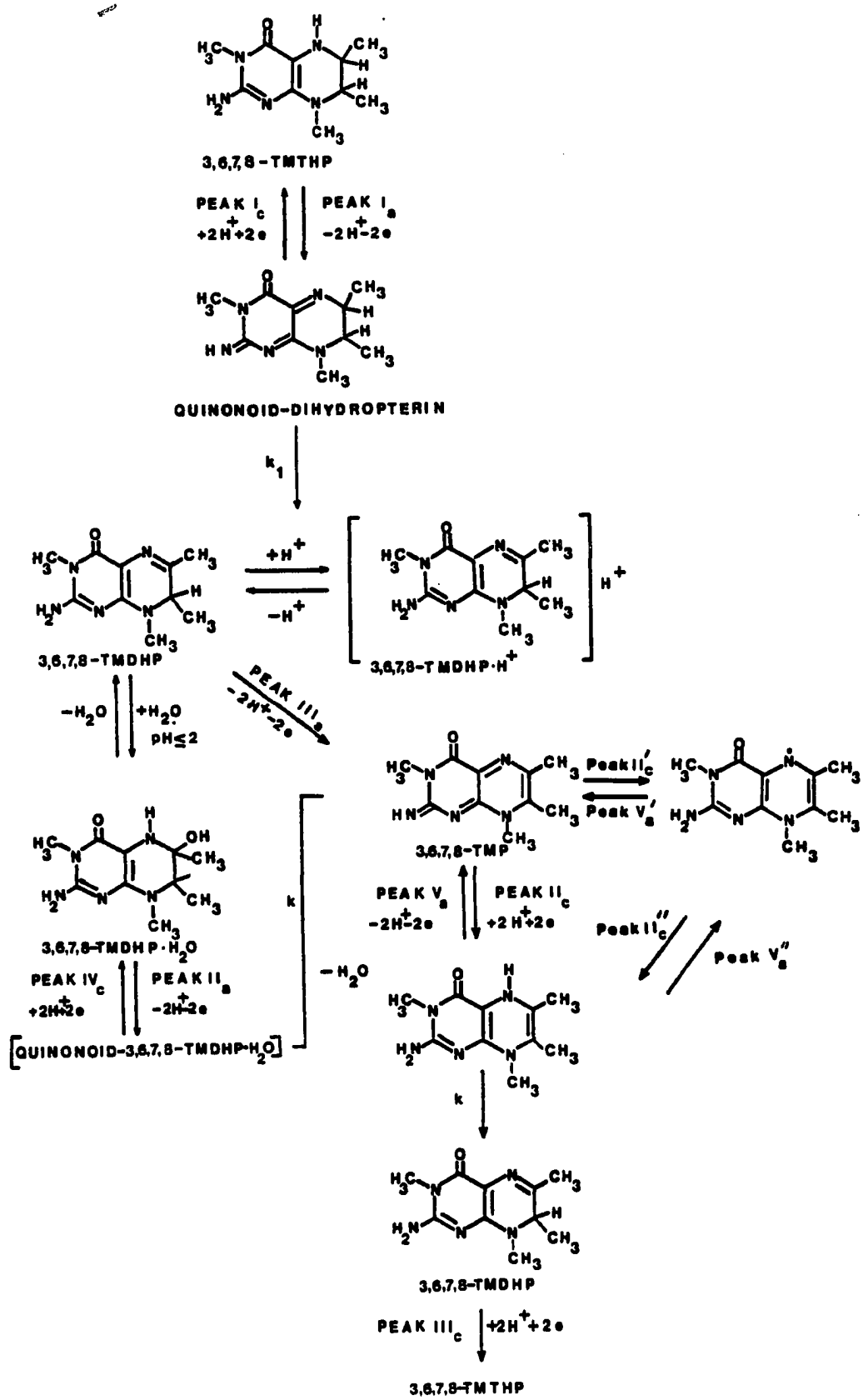

Figure 15. Proposed reaction scheme for the electrooxidation of 3,6,7,8-TMTHP at PGE.

and is indicated by the color of the solution changing from colorless to a clear yellow. The pK_a of 2-DMTTHP is 5.5 corresponding to protonation at the N(5) position. 2-DMTTHP gives rise to two electrooxidation peaks at the PGE between pH 2.9-10.3. The peak potential vs. pH dependence for these peaks may be represented by the following equations:

Peak I_a E_p = (0.275-0.062 pH)V
pH (2.9-10.3)
Peak III_a E_p = (0.695-0.040 pH)V
pH (2.9-10.3)

There is an additional electrooxidation peak, peak II_a, which may be only observed at low pH (e.g., pH 0.90).

Cyclic voltammograms of 2-DMTTHP exhibit two electrooxidation peaks (peaks I_a and III_a) when scanned in positive direction first. Upon reversal of sweep direction, four voltammetric electroreduction peaks appear (peaks I_c, II_c', II_c'' and III_c) (Fig. 16). Figure 17 shows a cyclic voltammogram of 0.53 mM 2-DMTDHP obtained by electrolyzing 2-DMTP at peak II_c potentials at a large PGE electrode in phosphate buffer pH 0.90. Cyclic voltammograms of 2-DMTTHP show no reduction peaks if scanned first in a negative direction (Fig. 18).

Peak clipping experiments show that no distinctive electroreduction peaks, other than peak I_c are observed if the potential is swept in a positive direction first and

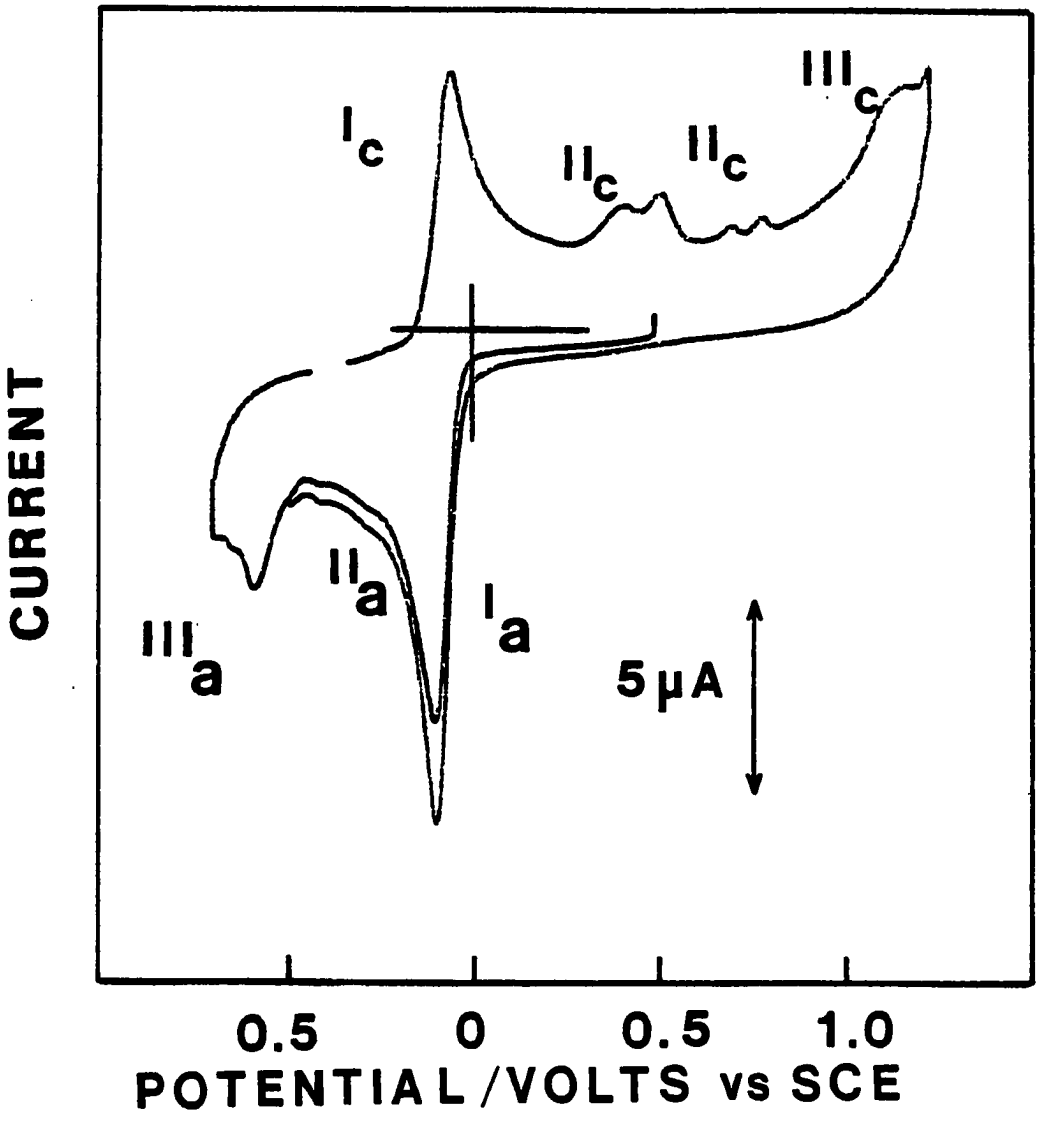

Figure 16. Cyclic voltammogram of 1 mM 2-DMTTHP in phosphate buffer pH 3.4 at a scan rate of 200 mV s^{-1}.

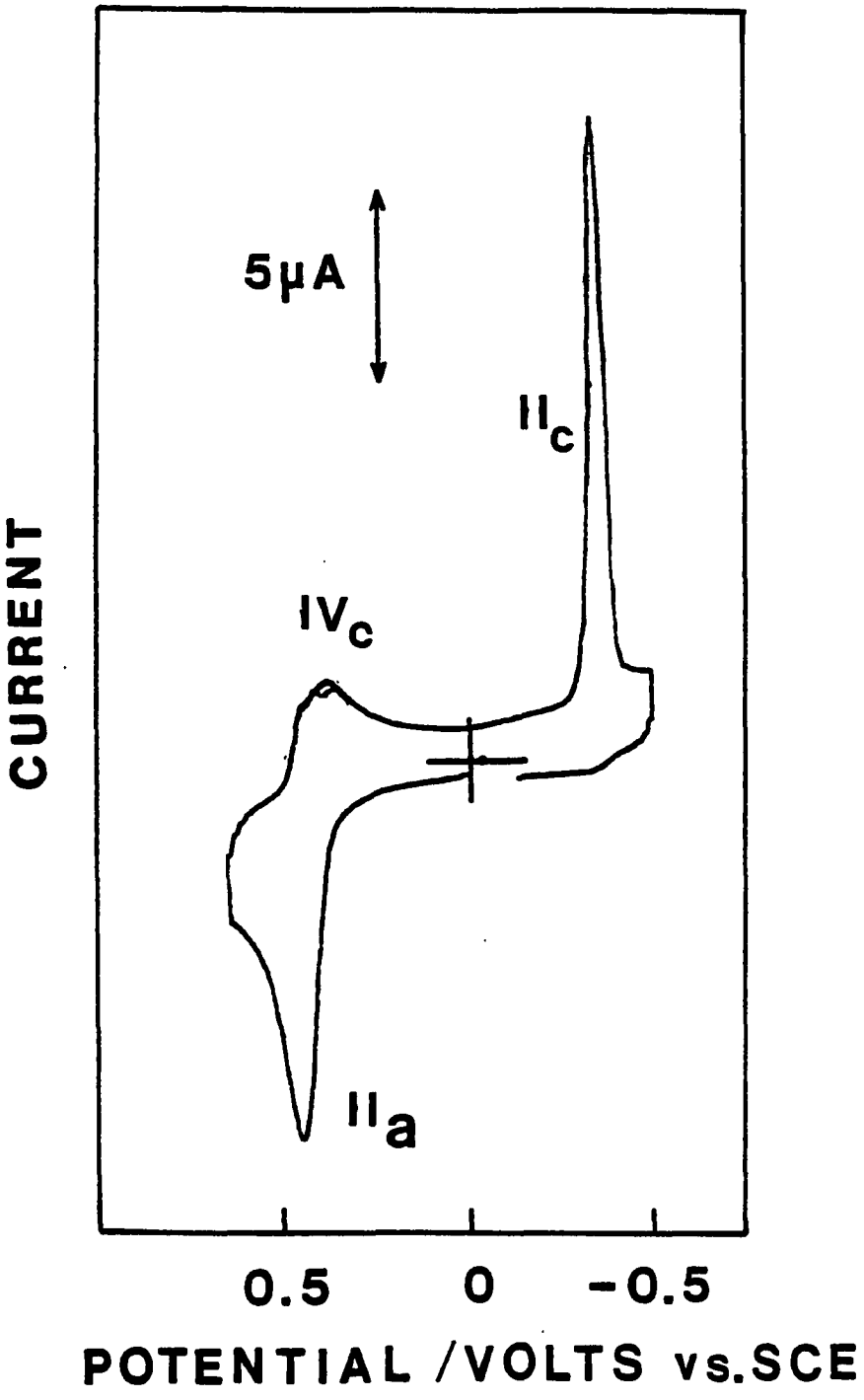

Figure 17. Cyclic voltammogram of 0.53 m$\underline{M}$ 2-DMTDHP obtained by electrolyzing 2-DMTP at peak II_c potentials in phosphate buffer pH 0.90 at a scan rate of 200 mV s^{-1}.

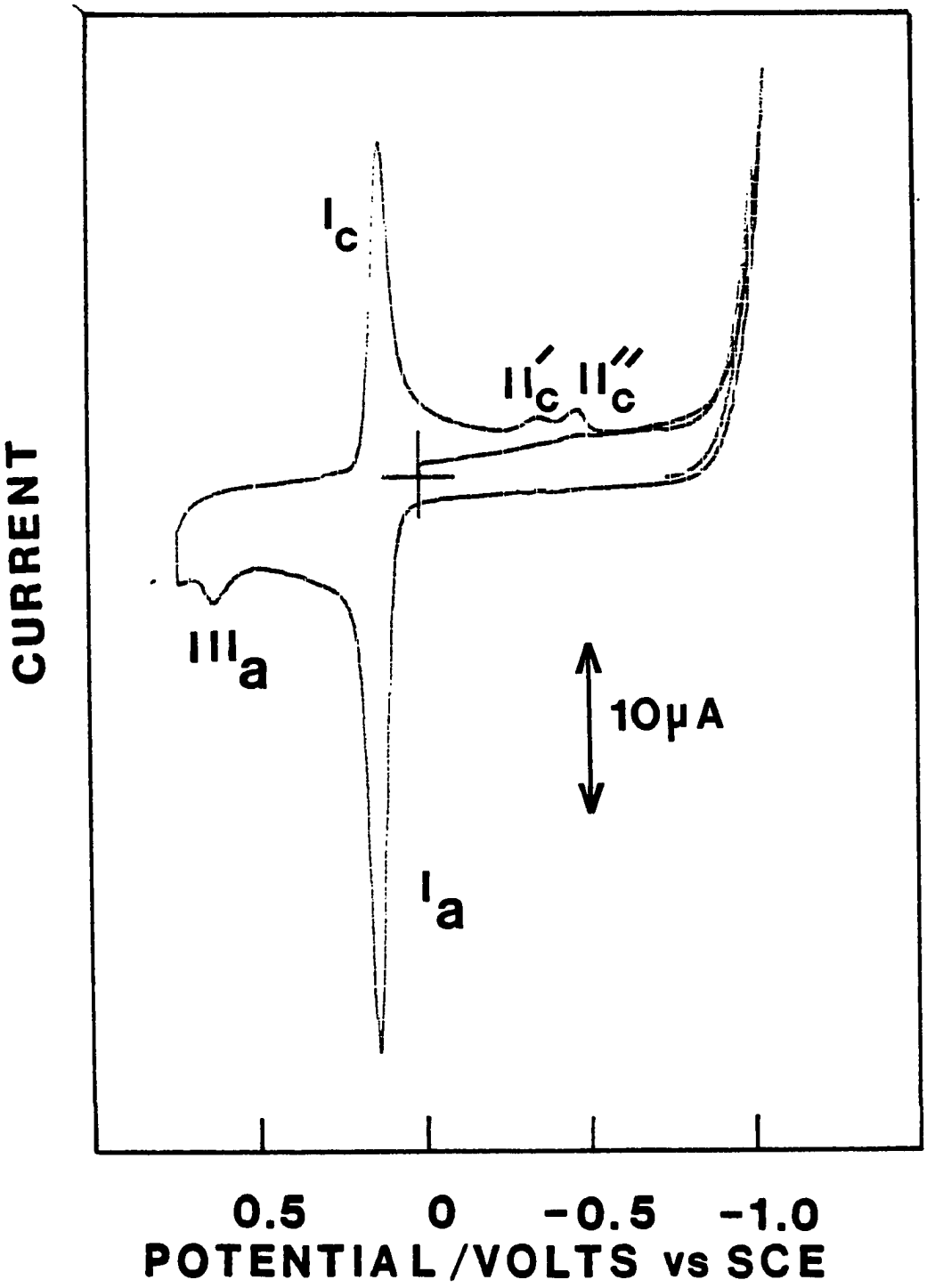

Figure 18. Cyclic voltammogram of 1 mM 2-DMTTHP in phosphate buffer pH 2 at a scan rate of 200 mV s^{-1}, initial scan in negative direction first.

clipped immediately past peak I_a (Fig. 19A). Peaks II_a and IV_c may be observed if the potential is clipped at more positive potentials (e.g., +0.45V, Fig. 19B). In this case a very small peak II_c may also be detected which may suggest that some 2-dimethylamino-3,6,7-trimethylpterin (2-DMTP) is being formed in the peak II_a process. If the potential sweep direction is changed past peak III_a, peaks I_c, II_c' and II_c'' may be observed (Fig. 19C). As the clipping potential is increased to about +1.0V, additional reduction peaks show up (Fig. 19D). These new peaks are probably due to reduction of electrooxidation products of 2-DMTP and they will not be discussed any further.

It was also observed that the peak height for peak I_c relative to that for peak I_a decreases as the clipping potential is shifted towards more positive potentials (Fig. 19). The peak height for peak I_c also changes as a function of sweep rate and pH. For example, the ratio of peak currents for peak I_c and I_a $(i_p)_c/(i_p)_a$ is 0.46, 0.60 and 0.70 at pH values of 7, 4.9 and 2, respectively, at a sweep rate of 200 mV s^{-1}. This behavior suggests that the primary peak I_a electrooxidation product undergoes a pH dependent chemical follow-up reaction.

Controlled potential electrooxidation of 2-DMTTHP at peak I_a potentials resulted in the transfer of 1.8±0.2 electrons between pH 2.9-10.3. The spectra of the resulting electrolysis product solution were the same as the spectra

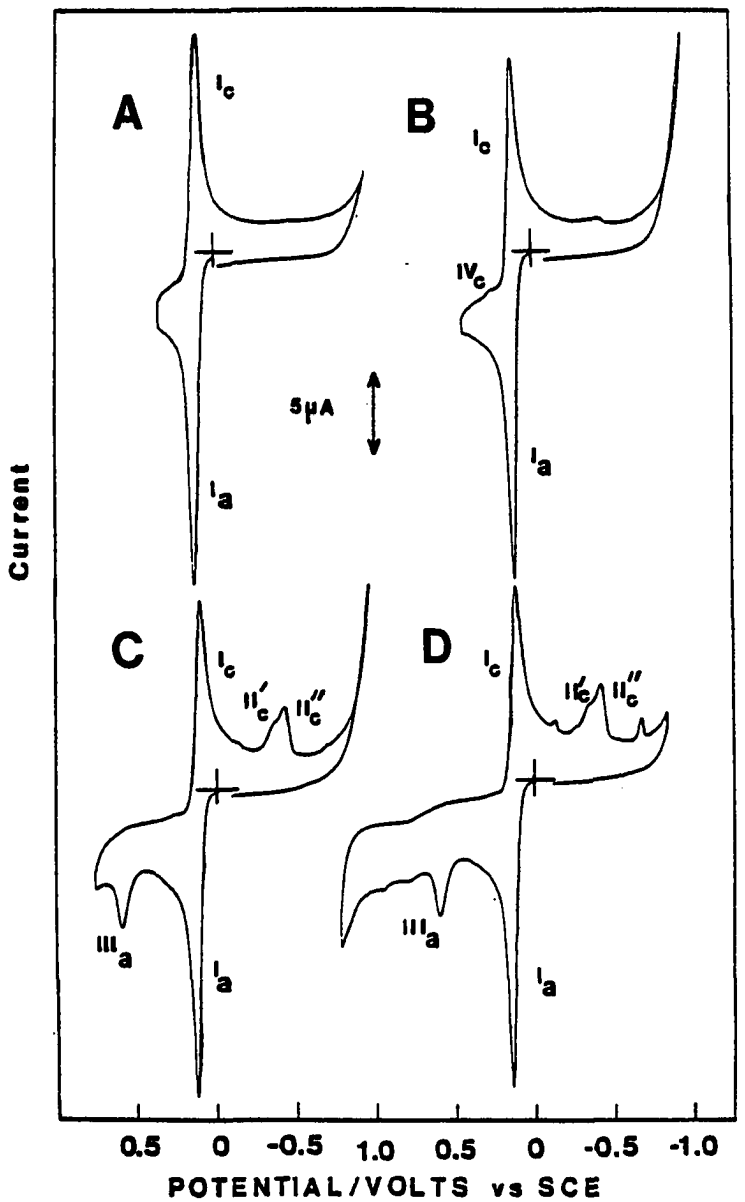

Figure 19. Cyclic voltammograms of 1 mM 2-DMTTHP in phosphate buffer pH 2 at a scan rate of 200 mV s^{-1}, (A) clipping potential past peak I_a, (B) clipping potential past peak II_a, (C) clipping potential past peak III_a, (D) clipping potential 0.6V past peak III_a.

of the electroreduction product of 2-DMTP at peak II_c potentials (i.e., 2-dimethylamino-6,7,8-trimethyl-7,8-dihydropterin (2-DMTDHP)). Electroreduction of 2-DMTP at peak II_c potentials involves the transfer of 2.0±0.13 electrons per molecule. It is believed that the peak I_a oxidation of 2-DMTTHP and peak II_c reduction of 2-DMTP results in formation of the same electrolysis product (i.e., 2-DMTDHP). Cyclic voltammetric experiments show that electroreduction of 2-DMTP at peak II_c potentials results in formation of an oxidation peak which occurs at the same potentials as peak III_a of 2-DMTTHP, and an electroreduction peak, peak III_c corresponding to peak III_c of 2-DMTTHP. Figure 20 shows cyclic voltammograms of a 0.5 mM solution of 2-DMTP in phosphate buffer pH 4.13 before electrolysis. Figure 20A shows that 2-DMTP gives rise to two reduction peaks, peaks II_c and III_c when scanned first in a negative direction. Upon reversal of the sweep direction three new oxidation peaks are observed (peaks V_a, I_a and III_a). Peaks I_a and III_a correspond to peaks I_a and III_a of 2-DMTTHP. If the potential is clipped past peak II_c, the only oxidation peaks observed are peaks V_a and III_a (Fig. 20B). Therefore peak II_c must correspond to reduction of 2-DMTP to give rise to a species which can be oxidized at peak III_a potentials (Fig. 21A). The product of the peak II_c process shows peak III_c when scanned first in negative direction. Upon reversal of the sweep direction

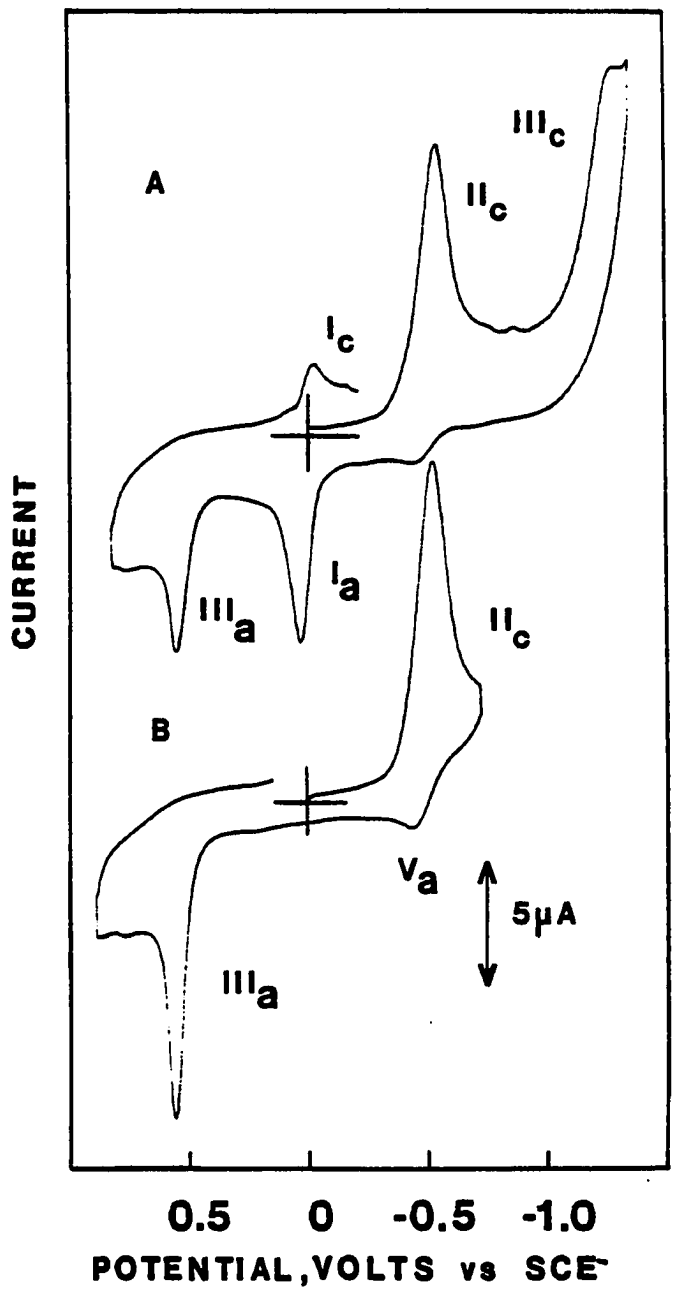

Figure 20. Cyclic voltammograms of 0.5 mM 2-DMTP in phosphate buffer pH 4.13 at a sweep rate of 200 mV s^{-1} before electrolysis (A) clipping past peak III_c, (B) clipping past peak II_c.

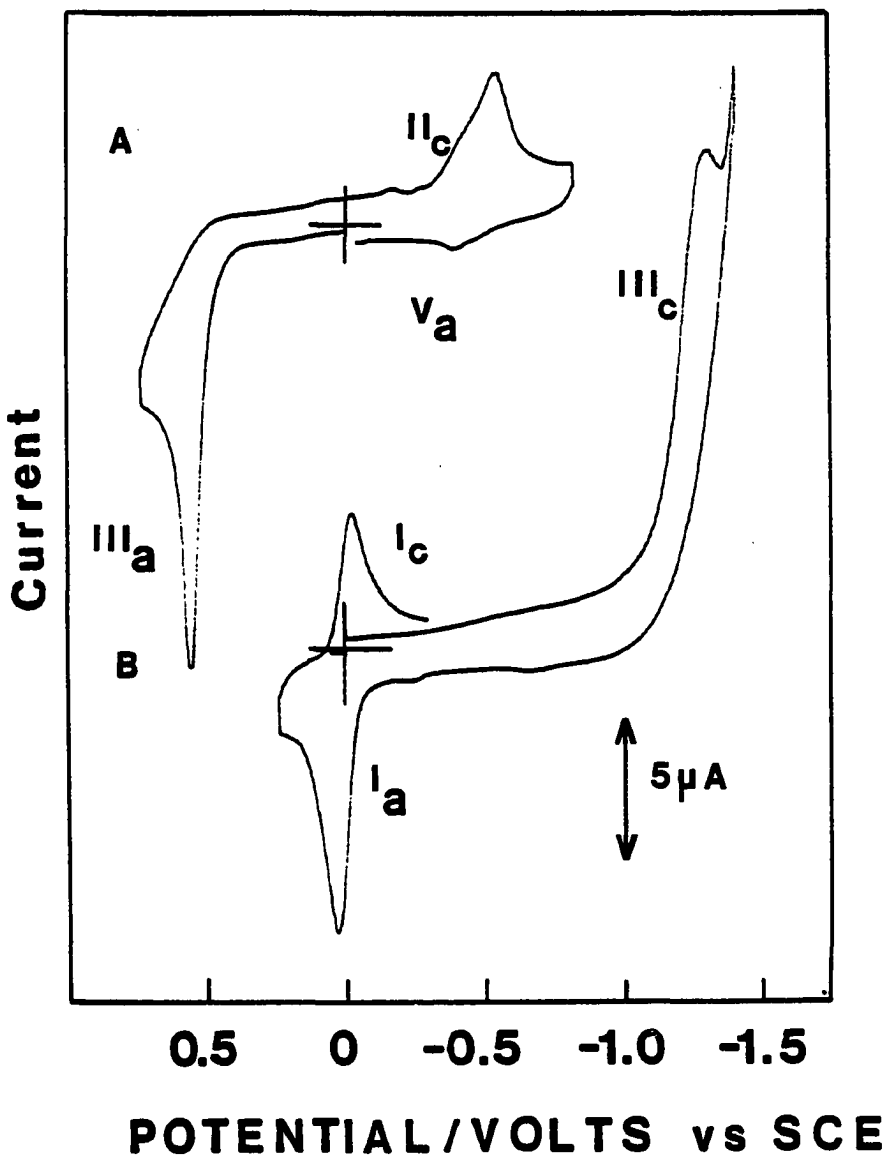

Figure 21. Cyclic voltammograms of 0.5 mM 2-DMTP in phosphate buffer pH 4.13 after electrolyzing at -0.7V (Peak II_c), (A) first scan in positive direction, (B) first scan in negative direction at a sweep rate of 200 mV s^{-1}.

peak I_a then appears at the same potentials as peak I_a of 2-DMTTHP (Fig. 21B). Therefore, it can be concluded that 2-DMTTHP is formed in the peak III_c process. Typical cyclic voltammograms of 2-DMTP at pH 7 are shown in Fig. 22. As seen in Figs. 20, 21 and 22, peak II_c may either be split into two peaks II_c' and II_c'' or observed as a single peak.

Based on the above observations and by comparison with other methylated pterins the electrochemical redox reactions of 2-DMTTHP may be summarized as shown in Fig. 23. The first electrooxidation step involves a 2e and $2H^+$ process to form an unstable quinonoid which then rearranges to form a more stable 7,8-dihydro-derivative (7,8-dihydro-nomenclature indicates that there is no double bond between C(7) and N(8)). The U.V. spectra obtained for 2-DMTDHP solutions between pH 0.9-8 confirm that a 7,8-dihydro-derivative is formed, when compared with U.V. spectra of 6,7-DMDHP solutions. The characteristic 7,8-dihydro batho-chromic shift is observed on going from a neutral to a positively charged molecule (e.g., at pH 3 2-DMTDHP has λ_{max} = 228 nm, 266 nm, (285 nm) and 360 nm, while at pH 8 λ_{max} = 240 nm, 287 nm and 329 nm). Peak III_a is due to electrooxidation of 2-DMTDHP to 2-DMTP. At lower pH values 2-DMTDHP may be hydrated across the N(5)=C(6) bond to give rise to peak II_a (Fig. 17). Peaks II_c' and II_c'' are believed to be due to two sequential one-electron, one-proton

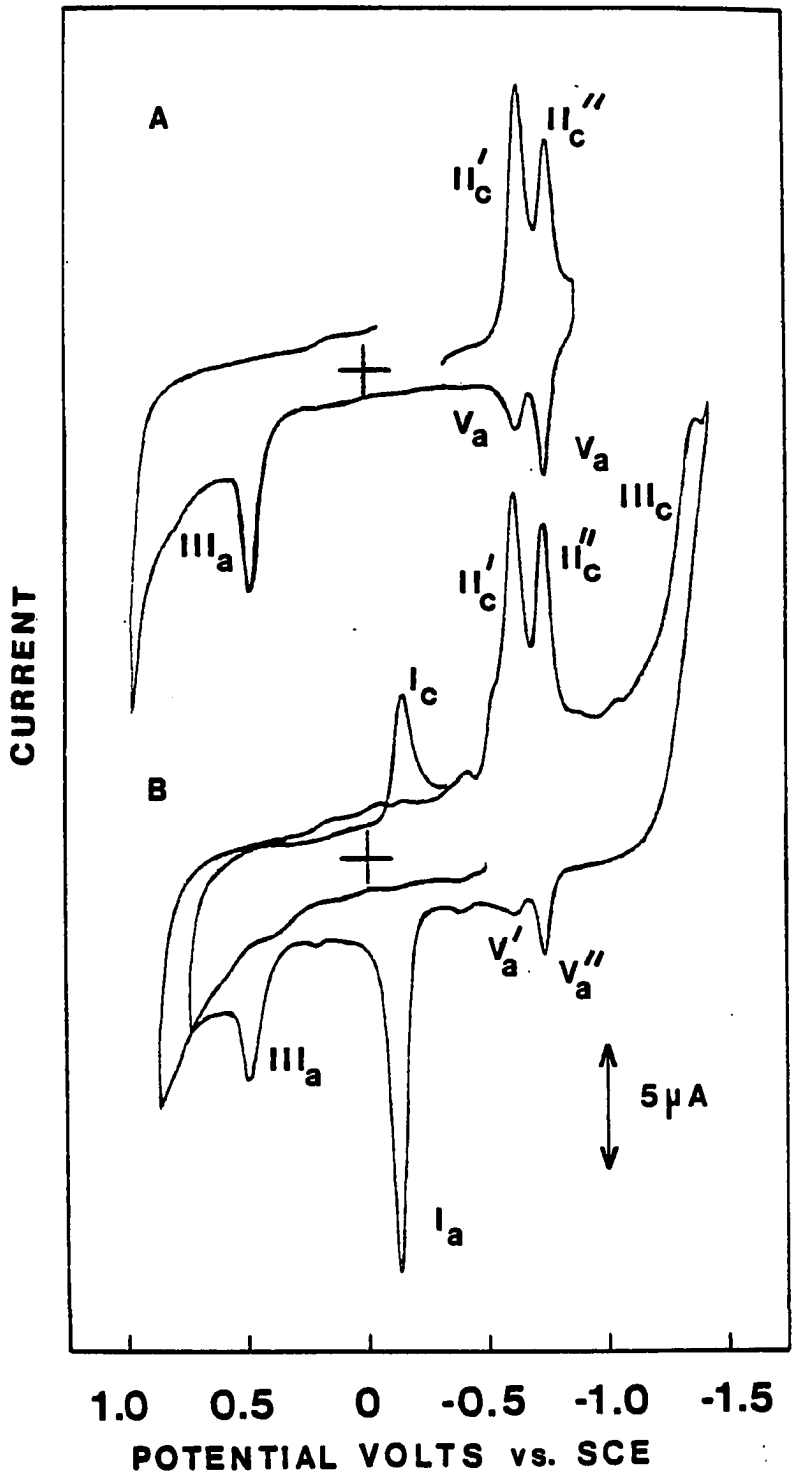

Figure 22. Cyclic voltammograms of 0.5 mM 2-DMTP in phosphate buffer pH 7.0 at a sweep rate of 200 mV s^{-1}, (A) first sweep in negative direction and clipped past peak II_c'', (B) first sweep in positive direction first and reverse scan clipped past peak III_c.

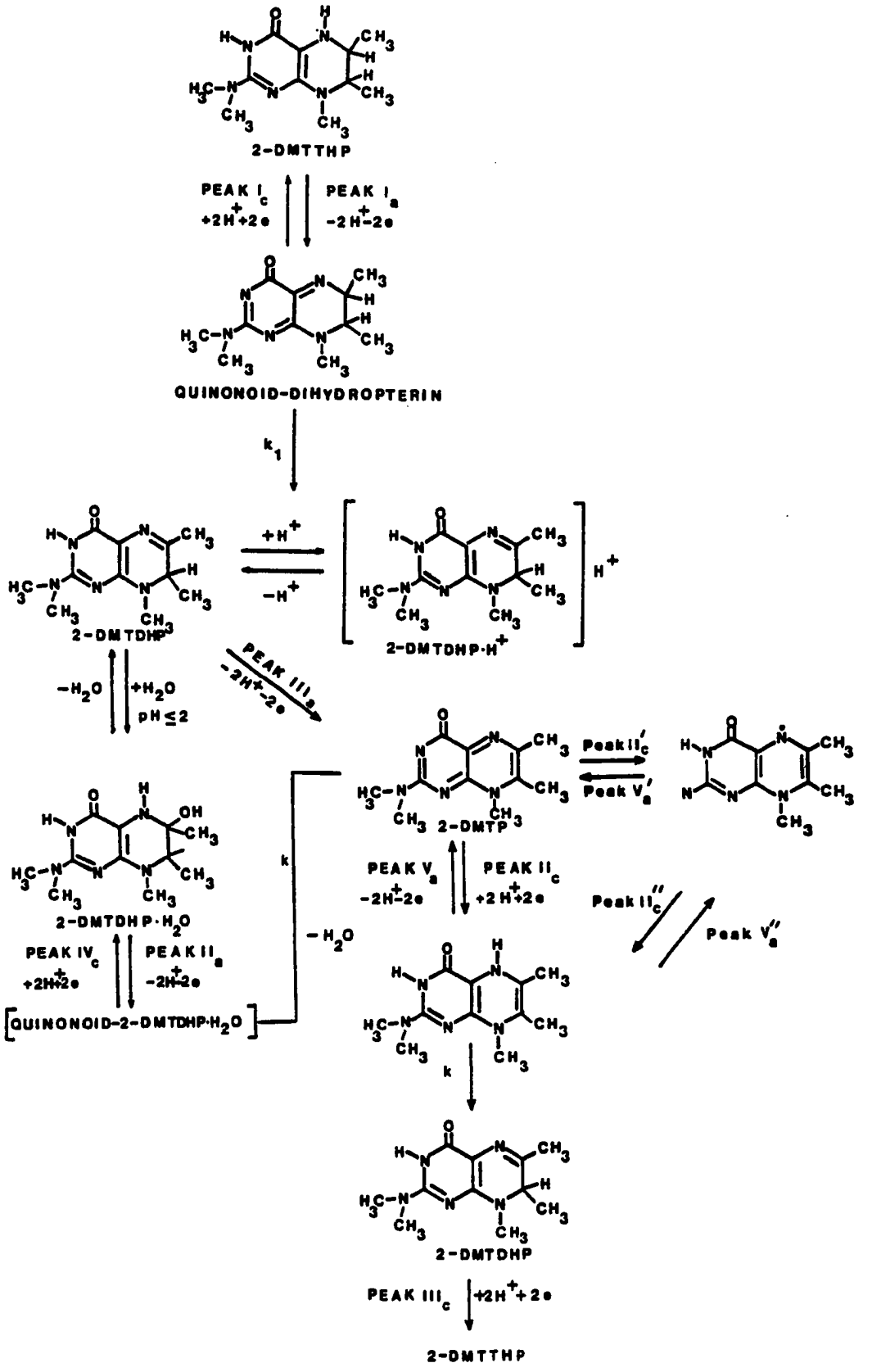

Figure 23. Proposed reaction scheme for the electrooxidation of 2-DMTTHP at PGE.

electroreductions of 2-DMTP to form first a free radical (peak II_c') and then a 5,8-dihydro-derivative (peak II_c''). The latter species then reacts chemically to form a 7,8-dihydro-derivative. Peak III_c is due to reduction of 2-DMTDHP to form 2-DMTTHP. This peak is not always observed in cyclic voltammograms because its reduction potential is very close to background reduction.

Because 2-DMTTHP may form only one quinonoid-dihydro species when electrooxidized at peak I_a potentials, its spectroelectrochemical behavior and the stability of the quinonoid formed was of great interest in terms of determining the structure of the putative quinonoid generated in the peak I_a electrooxidation process of 6,7-DMTHP.

At pH 3.08, 2-DMTTHP shows two absorption bands (λ_{max} = 236 nm and 275 nm, Fig. 24A, the band observed at longer wavelengths (~372 nm) indicates that 2-DMTTHP has already partially oxidized to 2-DMTDHP). When a potential is applied to an RVC electrode in a thin-layer cell the absorbance goes down at both wavelengths and new absorption bands appear at around 360 nm and 268 nm (Fig. 24B). The band at 236 nm shifts to slightly shorter wavelengths (λ_{max} = 233 nm) during the electrooxidation process. In addition a shoulder is formed around 288 nm. When the applied potential is turned off, the absorbance decreases at around 318 nm and increases at 364 nm, 268 nm and 233 nm (Fig. 24C). This spectral behavior is very similar to that observed

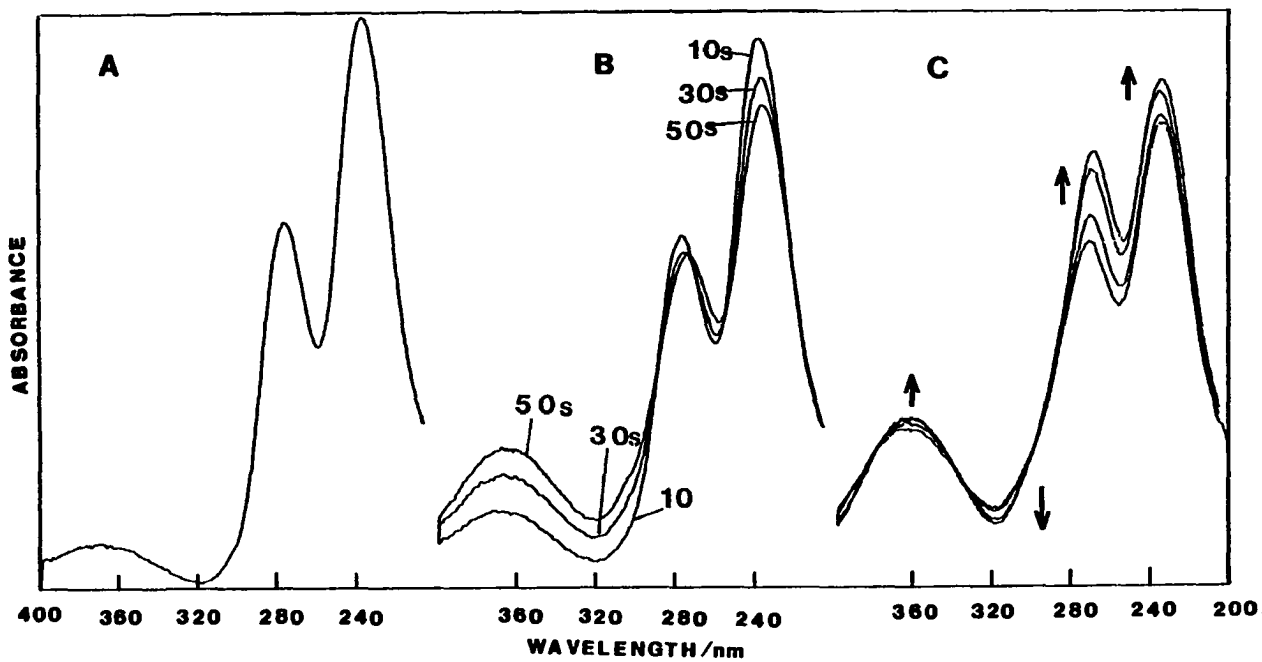

Figure 24. Spectra of 1 mM 2-DMTTHP in phosphate buffer pH 3.08 electrolyzing at +0.2V at a reticulated vitreous carbon electrode in a thin-layer cell (A) initial spectrum, (B) spectra obtained during electrolysis, (C) final spectrum obtained after the applied potential is turned off.

Table 5. Observed first-order rate constants for rearrangement of quinonoid-dihydropterin on peak I_a electrooxidation of 2-DMTTHP[a]

pH[b]	$k_{obs} \times 10^3/s^{-1}$	$\sigma \times 10^3/s^{-1}$[c]	λ/nm[d]
1.0	13.5	0.6	230
3.0	11.3	1.2	266
3.9	13.5	0.6	228
4.6	11.2	1.8	232
5.0	11.2	1.8	232,276
5.4	11.2	2.4	238,284,359
6.0	11.2	1.2	244,288,360
6.5	5.5	0.3	240,288,360
7.0	2.8	0.5	240,288,360
8.0	1.7	0.2	240,288

[a]Measured using a thin-layer spectroelectrochemical method with electrolysis performed at an optically transparent RVC electrode.

[b]Phosphate buffers having an ionic strength of 0.5 M.

[c]Standard deviation.

[d]Wavelength(s) used to measure k_{obs}.

when 6,7-DMTHP is electrooxidized in a thin-layer cell in phosphate buffer under the same conditions.

At higher pH values, for example at pH 8.8, 2-DMTTHP exhibits absorption bands at λ_{max} = 242 nm and 308 nm (Fig. 25A). When a potential is applied corresponding to peak I_a, the absorbance goes down at both wavelengths and a broad absorbance band appears between 320-400 nm along with another sharp band at λ_{max} = 216 nm (Fig. 25B, curve 2). When the potential is turned off, the absorbance decreases between 320-400 nm forming an absorption band at λ_{max} = 320 nm. Concurrently, the absorbance increases at around 292 nm and 246 nm and decreases at around 216 nm. The final product has an U.V. spectrum with λ_{max} = 246 nm, 292 nm and 320 nm (Fig. 25C). The rate of the chemical reaction at this pH characterized by these spectral changes after termination of the electrolysis is relatively slow, the intermediate formed having a half-life of about 6.6 min.

The rate constants for the chemical step were measured spectrally in a thin-layer cell as a function of pH and are summarized in Table 4. In contrast to the behavior observed with other methylated tetrahydropterins, the observed rate constant profile as a function of pH does not show a bell shape. Rather, the k_{obs} value is largest at lower pH values (1-6) and then drops off sharply at higher pH values (Fig. 26).

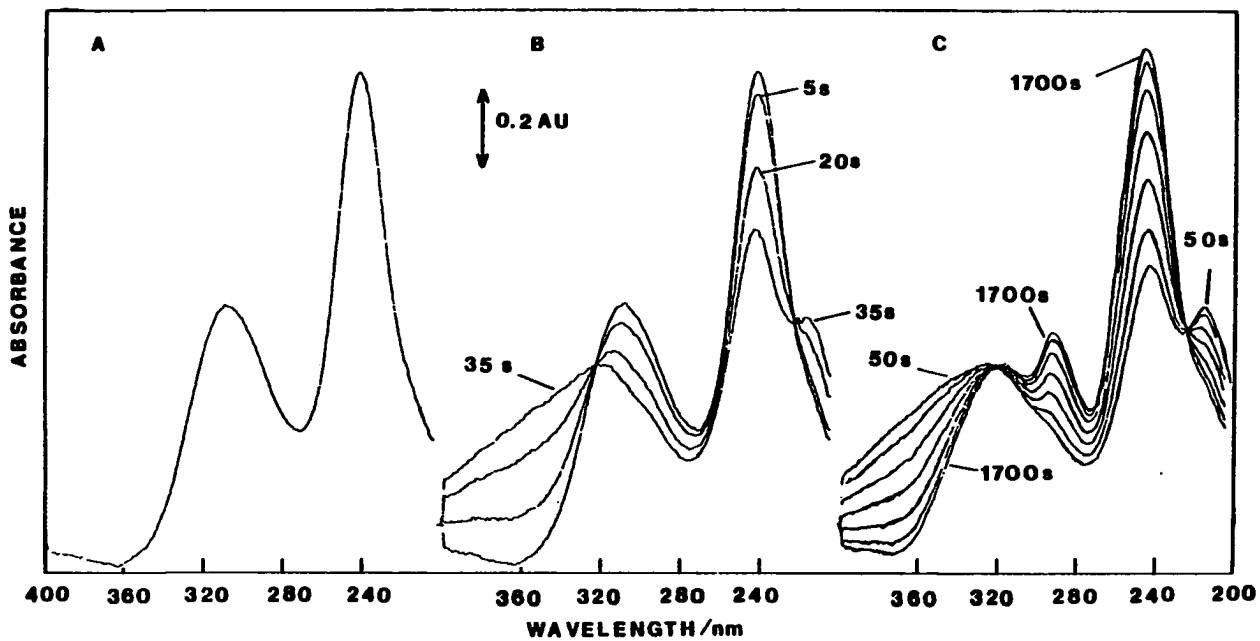

Figure 25. Spectra of 1 mM 2-DMTTHP in phosphate buffer pH 8.8 electrolyzing at -0.05V at a reticulated vitreous carbon electrode in a thin-layer cell, (A) initial spectrum, (B) spectra obtained during electrolysis. Spectrum at 35s corresponds to the spectrum of the intermediate generated, (C) spectra showing the decay of the intermediate generated.

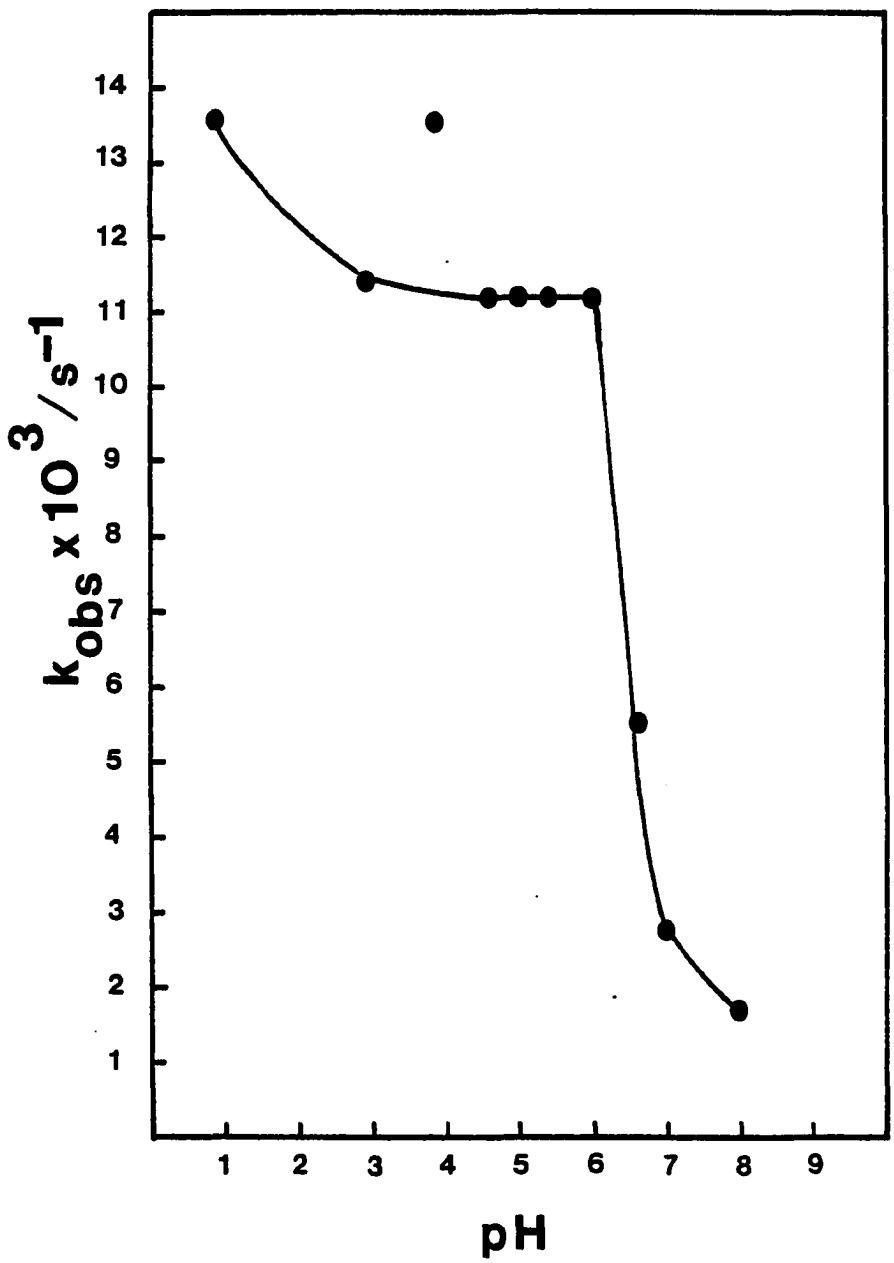

Figure 26. Variation of the observed first-order rate constant for the chemical reaction of peak I_a electro-oxidation product of 2-DMTTHP to give 2-DMTDHP as a function of pH.

Comparison of spectral properties of various methylated pterins

All the tetrahydropterins (13, 19, 21, 22) studied had a basic pK_a around 6. Generally, tetrahydropterins are reported to have three pK_a values, one acidic and two basic.[12] The lowest pK_a of each compound is reported to have a value between 0-1. The second pK_a is close to 6 and the third around 11[12] (see Table 6). The spectral properties of various methylated pterins (13, 15, 19, 21, 22) have been studied between pH 2-9.3. In the lower pH range, the tetrahydropterins studied exist as singly-charged cations, the site of protonation being at the N(5) position. At higher pH values these tetrahydropterins exist as neutral molecules. At pH 2 all methylated tetrahydropterins and tetrahydropterin (THP) show two U.V. absorption bands. For example, at pH 2, THP absorbs at λ_{max} = 216 nm and 265 nm. The U.V. absorption bands observed with methylated tetrahydropterins studied and others as reported in the literature are summarized in Table 6. It may be noticed that THP, 6-MTHP, 6,7-DMTHP and 5-methyltetrahydropterin (5-MTHP) have very similar λ_{max} values at pH 2. Owing to the electron releasing effect of methyl groups it would be expected that these absorption bands would shift to progressively longer wavelengths as the number of methyl substituents increases.

It is apparent, however, that methylation at N(5), C(6) and C(7) does not cause such a noticeable bathochromic

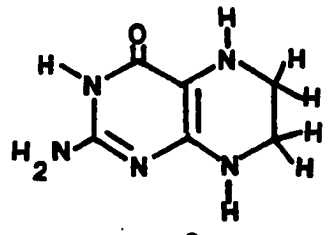

9
ss

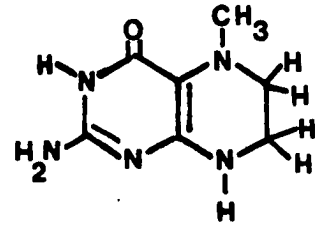

10
ss

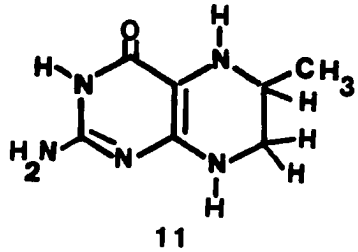

11
ss

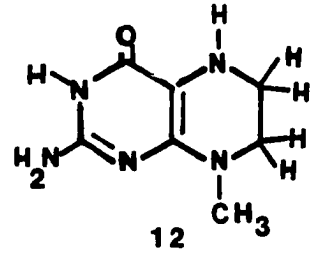

12
ss

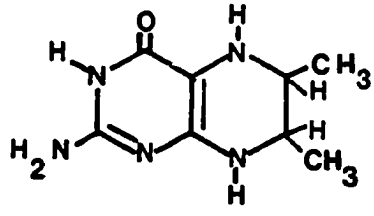

13
ss

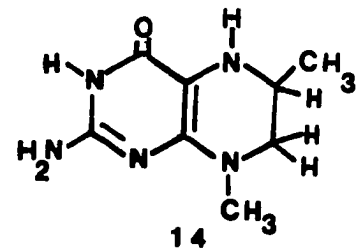

14
ss

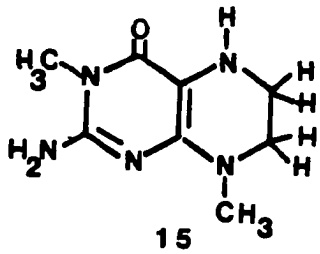

15
ss

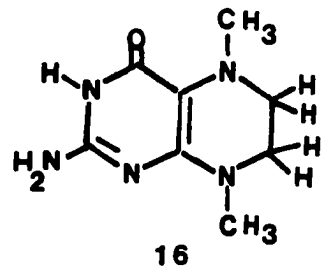

16
ss

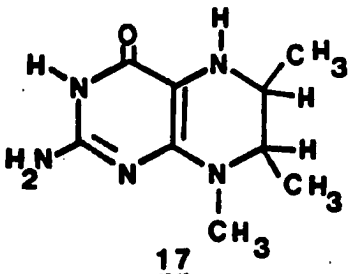

17

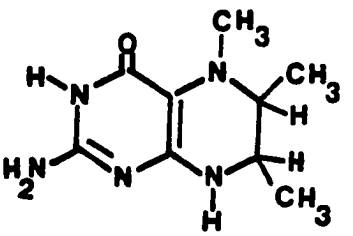

18

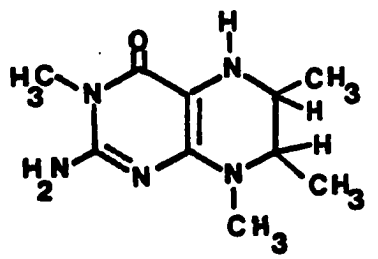

19

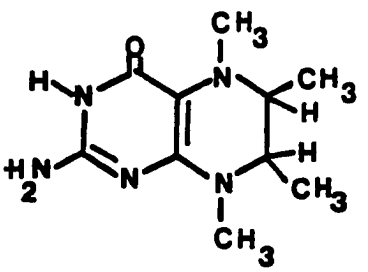

20

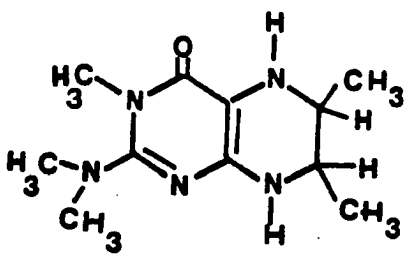

21

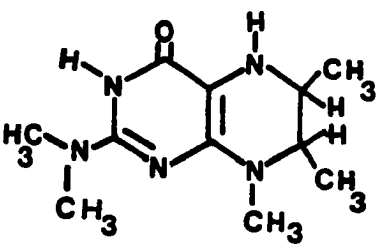

22

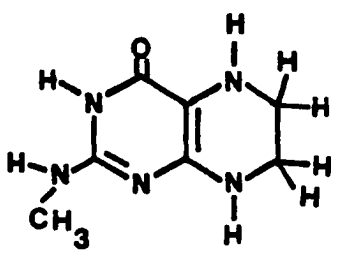

23

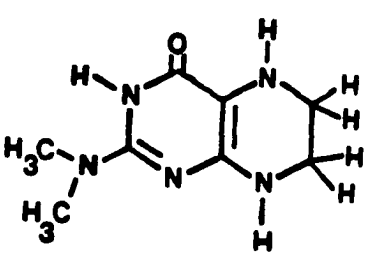

24

Table 6. Comparison of spectral properties of various methylated tetrahydropterins[a]

Tetrahydropterin	pK_a	pH	λ_{max}/nm
THP (9)		2.0	216,265
		7.0	220,300
5-MTHP (10)[b]	1.05,[b] 5.99[b]	3.5	215,265
	11.33[b]	8.5	215,287
6-MTHP (11)[c]		2.0	212,264
		7.0	218,302
8-MTHP (12)[d]	5.70[d]	3.0	223,271
	10.65[d]	9.0	227,(265),306
		13.0	219,289
6,7-DMTHP (13)	1.4,[e] 5,6[e]	2.0	217,265
	10.4[e]	7.0	220,298
6,8-DMTHP (14)[d]		3.0	223,270
		8.0	226,(270),307
3,8-DMTHP (15)		2.0	219,265
		7.0	225,281,300
5,8-DMTHP (16)[b]	0.50[b]	-2.0	270
	6.3[b]	2.0	225,270
	11.3[b]	8.5	293
6,7,8-TMTHP (17)[b]	0.62[b]	-1.5	272
	5.2[b]	3.5	224,271
		8.5	270,314
6,7,8-TMTHP (17)[d]	5.9[d]	3.0	224,270
	11.0[d]	8.0	227,(265),302
		13.0	286
5,6,7,-TMTHP[b] (18)	1.05[b]	-1.0	262
	6.23[b]	3.5	219,264
	11.43[b]	8.5	285

Table 6 (continued)

Tetrahydropterin	pK_a	pH	λ_{max}/nm
3,6,7,8-TMTHP (19)	6.2	2.0	224,269
		7.0	228,286,300
5,6,7,8-TMTHP[b] (20)	0.27[b]	-2.0	271
	6.34[b]	3.5	225,270
	11.32[b]	8.5	228,295
2-DMTHP (21)	7.0	2.0	234,274
		7.0	234,285,306
2-DMTTHP (22)	5.5	2.0	233,273
		7.0	236,306
2-MTHP[e] (23)		6.8	(270),300
2-DMATHP[f] (24)		6.8	(270),300

[a]Spectral data obtained in 0.1 cm quartz cells at a scan rate of 100 nm/min and 0.5s response time.

[b]Values reported in ref. 12.

[c]Values reported in ref. 5.

[d]Values reported in ref. 13.

[e]2-MTHP = 2-methylaminotetrahydropterin, ref. 14.

[f]2-DMATHP = 2-dimethylaminotetrahydropterin, ref. 14.
Values in parenthesis correspond to shoulders observed.

shift. However, when 2-DMTHP, 2-DMTTHP or 3,6,7,8-TMTHP are considered, a shift in the U.V. absorption bands towards longer wavelengths is observed. The same kind of behavior may be observed at higher pH values (e.g., Table 6) where the longest wavelength absorption bands are exhibited by 2-DMTTHP and 2-DMTHP.

Spectroelectrochemical studies of several methylated pterins were carried out in order to obtain information concerning the structure of the putative quinonoid-dihydropterin intermediate formed when 6,7-DMTHP is electrooxidized at peak I_a potentials. It was hoped that by comparing the spectroelectrochemical behaviors of 6,7-DMTHP and various methylated tetrahydropterins which give a locked quinonoid upon $2e^- - 2H^+$ electrooxidation at peak I_a potentials, it would be possible to decide upon the most probable structure for the quinonoid-dihydro intermediate structure. The spectroelectrochemical behaviors have already been discussed in this chapter, in Chapters two and three and elsewhere.[4-6] The U.V. absorption characteristics of the quinonoid-dihydropterins generated upon electrolysis at peak I_a potentials and of the 7,8-dihydropterins formed upon the resulting chemical follow-up reaction are summarized in Table 7.

Analysis of this spectroelectrochemical data reveals that at lower pH values (e.g., pH 3), the intermediates formed upon electrooxidation of the most commonly used

Table 7. Comparison of spectral characteristics of several quinonoid-dihydropterins generated electrochemically in a thin-layer cell at an RVC electrode at peak I_a potentials

pH	Compound	Tetrahydropterin λ_{max}/nm	Quinonoid λ_{max}/nm	7,8-Dihydropterin λ_{max}/nm
7.0	THP	220,300	300,∿326	232,281,332
3.1	6,7-DMTHP	212,264	300,336	210,248(276),350
9.3		218,300	∿308,320-400	226,280,340
3.1	6-MTHP[a]	212,264	300,328	
9.3		216,303	304,282,320-400	210,250,340 224,280,320
3.2	3,6,7,8-TMTHP	224,270	∿264	220,260,(280),356
8.8		231,306	∿300	235,290,310
			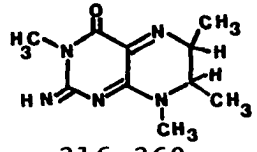	
3.1	2-DMTHP	236,278	316,360	233,(265),358
8.8		244,304	∿314,360-400	248,288,324
			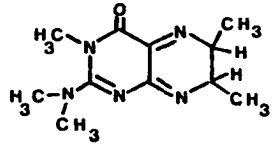	

Table 7 (continued)

pH	Compound	Tetrahydropterin λ_{max}/nm	Quinonoid λ_{max}/nm	7,8-Dihydropterin λ_{max}/nm
3.1	2-DMTTHP	236,275	268,360	233,268,364
8.8		242,308	216,320-400	246,292,300

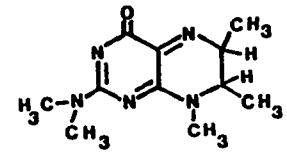

Values in parentheses indicate shoulders.

[a]Values obtained from reference 5.

pseudo cofactor, i.e., 6,7-DMTHP and 6-MTHP,[5] absorbs at 300 nm. The quinonoid generated from 6,7-DMTHP also absorbs at around 336 nm, whereas the quinonoid generated from 6-MTHP shows an additional absorption band around 328 nm. At pH 9.3 the intermediate generated from the same pseudo cofactors absorbs around 300 along with a broad band between 320-400 nm.

When the spectroelectrochemical behavior of three methylated pterins which form "locked" quinonoid structures are compared with that of 6,7-DMTHP or 6-MTHP it may be observed that the quinonoid derived from 2-DMTHP and 2-DMTTHP show similar U.V. absorption spectra. The quinonoid formed upon electrooxidation of 3,6,7,8-TMTHP has a different absorption spectrum than that generated from 6,7-DMTHP. 3,6,7,8-Tetramethylquinonoid-dihydropterin (3,6,7,8-TMQDHP) does not absorb at 300 nm at pH 3. 6,7-Dimethylquinonoid-dihydropterin (6,7-DMQDHP) absorbs at 300 nm since the absorbance at around this wavelength decreases when the thin-layer cell is open-circuited following the $2\underline{e}$-$2H^+$ electrooxidation of 6,7-DMTHP.

Figure 27 shows spectra obtained of 3,6,7,8-TMTHP and 6,7-DMTHP in a thin-layer cell being electrolyzed at peak I_a potentials at an RVC electrode in phosphate buffer pH 3.0. (3,6,7,8-TMQDHP) generated at higher pH values, for example at pH 8.8, also behaves in a different way than the quinonoid generated from 6,7-DMTHP which clearly absorbs between 320-400 nm in a broad band. At pH 8.8,

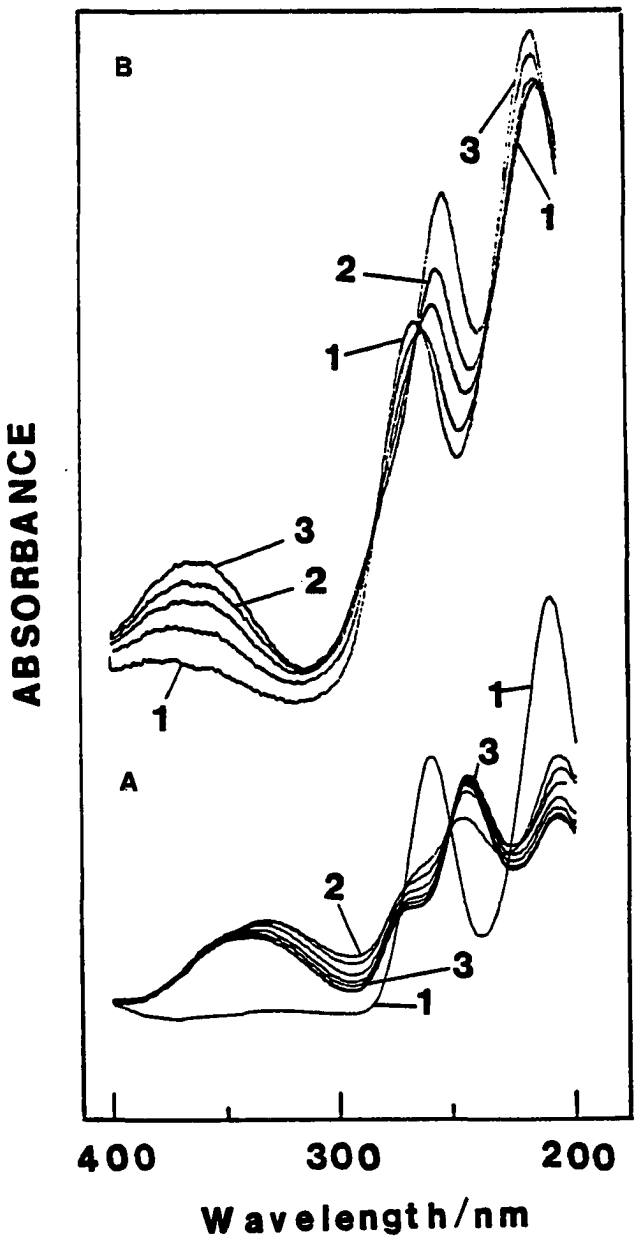

Figure 27. Spectra of (A) 1.36 mM 6,7-DMTHP electrolyzing at +0.3V at pH 3.1 and (B) 1 mM 3,6,7,8-TMTHP electrolyzing at +0.25V at pH 2.4 at an RVC electrode in a thin-layer cell. Curve 1 corresponds to the initial spectrum, curve 2 to the spectrum obtained when the potential was turned off and curve 3 to the final spectrum in both (A) and (B).

(3,6,7,8-TMQDHP) absorbs around 300 nm but does not show any absorbance between 320-400 nm (Fig. 28). 6-MTHP which has the highest activity among the various pseudo cofactors, forms an intermediate which also absorbs between 320-400 nm at pH 9.3 similar to 6,7-DMTHP. Spectroelectrochemical analysis of 2-DMTHP and 2-DMTTHP reveals that both 2-dimethylamino-3,6,7-trimethylquinonoid-dihydropterin (2-DMQDHP) and 2-dimethylamino-6,7,8-trimethylquinonoid-dihydropterin (2-DMTQDHP) absorb at 300 nm at pH 3. Figure 29 shows the spectra obtained when 2-DMTHP and 2-DMTTHP are electrooxidized in a thin-layer cell at pH 3, at peak I_a potentials and compares their spectra to the spectrum obtained when 6,7-DMTHP is electrooxidized at the same pH under similar conditions. At pH 3 the absorbances of both 2-DMQDHP and 2-DMTQDHP decrease at 300 nm when the applied potential is turned off. At higher pH values (8.8), however, 2-DMTQDHP absorbs between 320-400 nm and is relatively stable ($t_{1/2}$ = 6.6 min) whereas 2-DMQDHP absorbs only weakly between 360-400 nm. The half-life of the quinonoid intermediate generated from 6,7-DMTHP is about 2 min at pH 9.3, whereas the half-life for 2-DMQDHP is only about 0.3 min at pH 8.8. The stability of the 6-MTHP intermediate is higher at pH 9.3 ($t_{1/2}$ $\sim$4 min).[5] The proposed structures for the 2-DMQDHP ($\underset{\sim}{25}$) and 2-DMTQDHP ($\underset{\sim}{26}$) intermediates are shown on the next page:

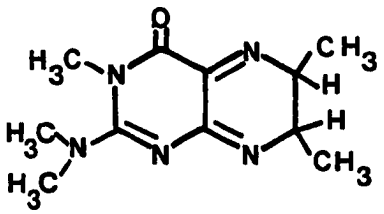

25
ss

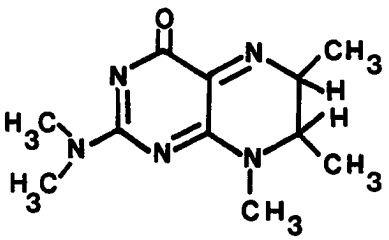

26
ss

Spectroelectrochemical data obtained in this study clearly suggest that the intermediate formed in the peak I_a electrooxidation of 6,7-DMTHP does not have a parallel-para configuration (27) based on the spectroelectrochemical behavior of 3,6,7,8-TMTHP which would form an intermediate having such a structure. It is believed that a parallel-para quinonoid-dihydropterin would probably be quite

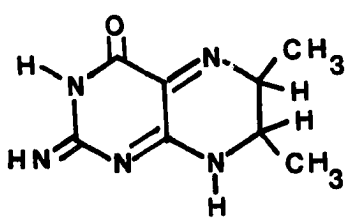

27
ss

unstable in aqueous solution possibly undergoing attack by H_2O molecules across the N(5)=C(4a) and/or N(1)=C(8a) double bonds to give an imine alcohol or a diol. 3,6,7,8-TMP (28)

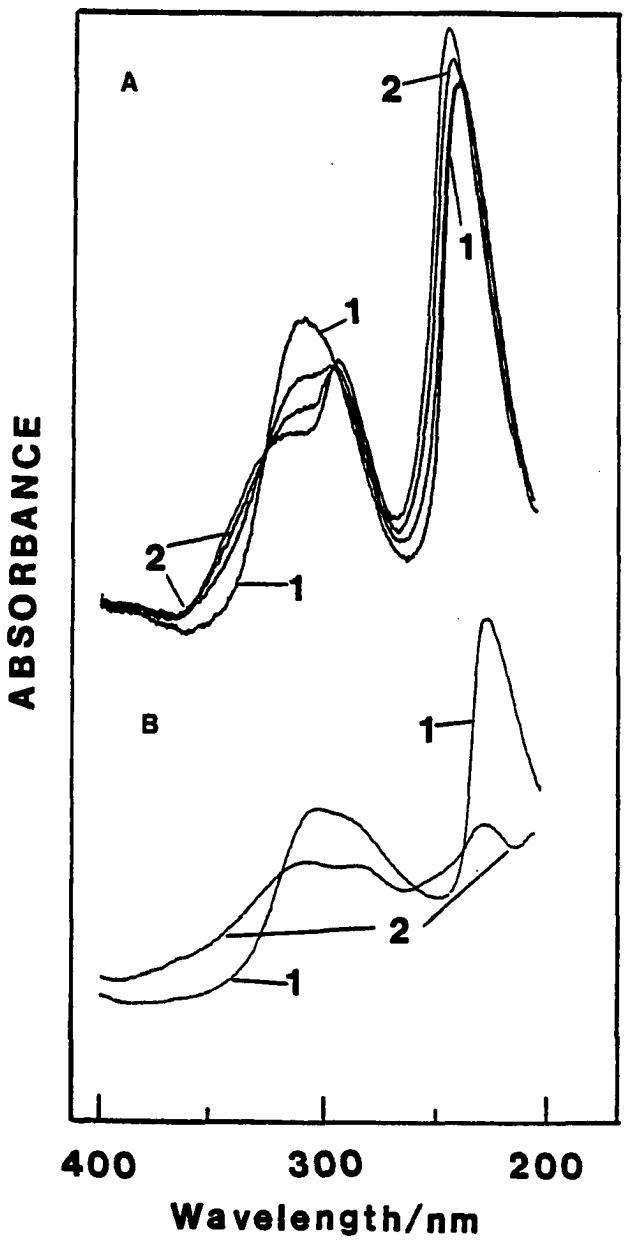

Figure 28. Spectra of (A) 1 mM 3,6,7,8-TMTHP electrolyzing at +0.05V at pH 8.$\overline{8}$ and (B) 1 mM 6,7-DMTHP electrolyzing at -0.3V at pH 9.$\overline{3}$ at an RVC electrode in a thin-layer cell. Curve 1 corresponds to the initial spectrum, curve 2 corresponds to the intermediate generated in both (A) and (B).

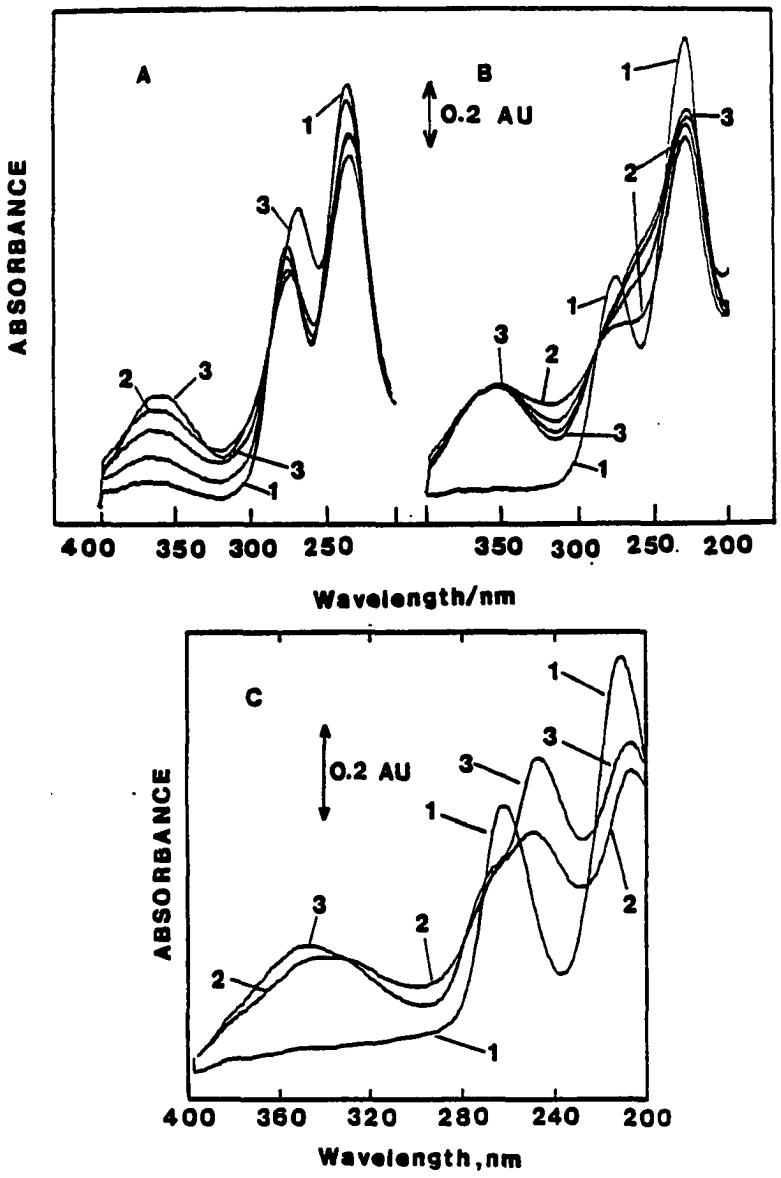

Figure 29. Spectra of (A) 1 mM 2-DMTTHP at pH 3.08 electrolyzing at +0.2V, (B) 1 mM of 2-DMTHP at pH 3 electrolyzing at +0.55V and (C) 3 mM of 6,7-DMTHP at pH 3.1 electrolyzing at +0.4V at an RVC electrode in a thin-layer cell. Curves 1 correspond to the initial spectrum, curves 2 correspond to the spectrum of the intermediate and curve 3 represents the spectrum of the final product.

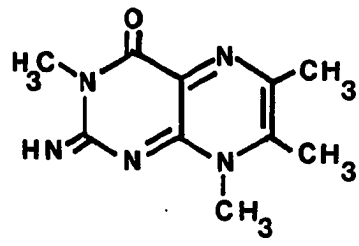

28

is reported to be unstable in aqueous solution[9] which may also suggest that (27) is not a preferred structure.

Quinonoidal compounds, such as p-benzo-quinone-mono and -diimine, are known to be unstable to light, water and acids.[15] It has also been reported that the diimine (30) formed upon oxidation of p-phenylenediamine (29) can undergo rapid hydrolysis to give the quinoneimine (31) which further hydrolyzes to produce p-benzoquinone (32) as shown in equation (1).[10]

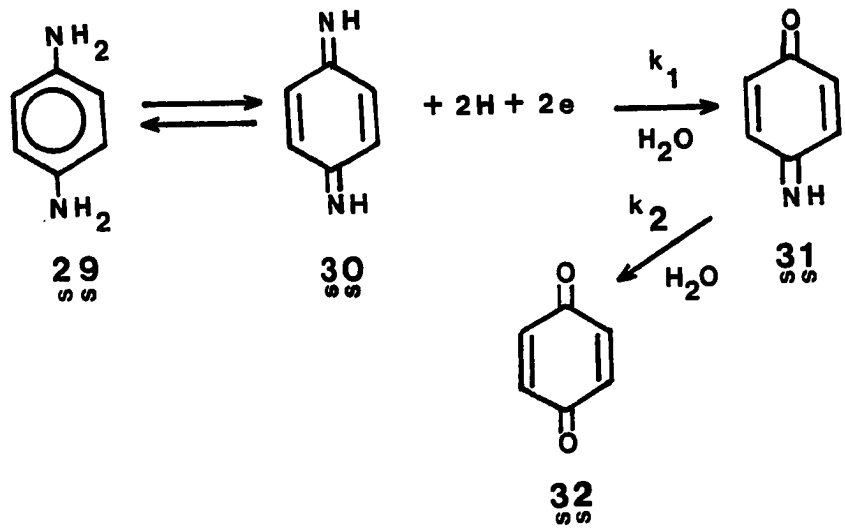

29 30 31 32

Accordingly, it is not very likely that a parallel-para quinonoid intermediate is formed during the electrooxidation of the most commonly used tetrahydropterin pseudo cofactors, 6,7-DMTHP or 6-MTHP. If formed, the parallel-para intermediate would be expected to be very unstable.

Based on the spectroelectrochemical data presented earlier, it appears likely that either the perpendicular-para (7) or the ortho (6) configurations may be the preferred quinonoid-dihydro structures.

In order to gain more information about the structure of the intermediate formed, rate constants for the chemical follow-up reactions were measured as a function of pH. It was believed that if rate constants were obtained from one of the tetrahydropterins that gives a locked quinonoid-dihydropterin were similar to that measured with 6,7-DMTHP, the assumption could be made that formation of a similar intermediate dihydropterin structure might be reasonable. Observed first-order rate constant profiles as a function of pH for 2-DMTHP, 2-DMTTHP, 3,6,7,8-TMTHP and 6,7-DMTHP are shown in Fig. 30. Inspection of these rate profiles indicates that all of the quinonoid-dihydropterins studied give bell-shaped curves for the dependence of k_{obs} on pH except for 2-DMTTHP. Bell-shaped curves for the variation of k_{obs} as a function of pH is common in biological systems and indicate acid-base catalysis of the chemical follow-up reaction. It can be observed that the rate profile for

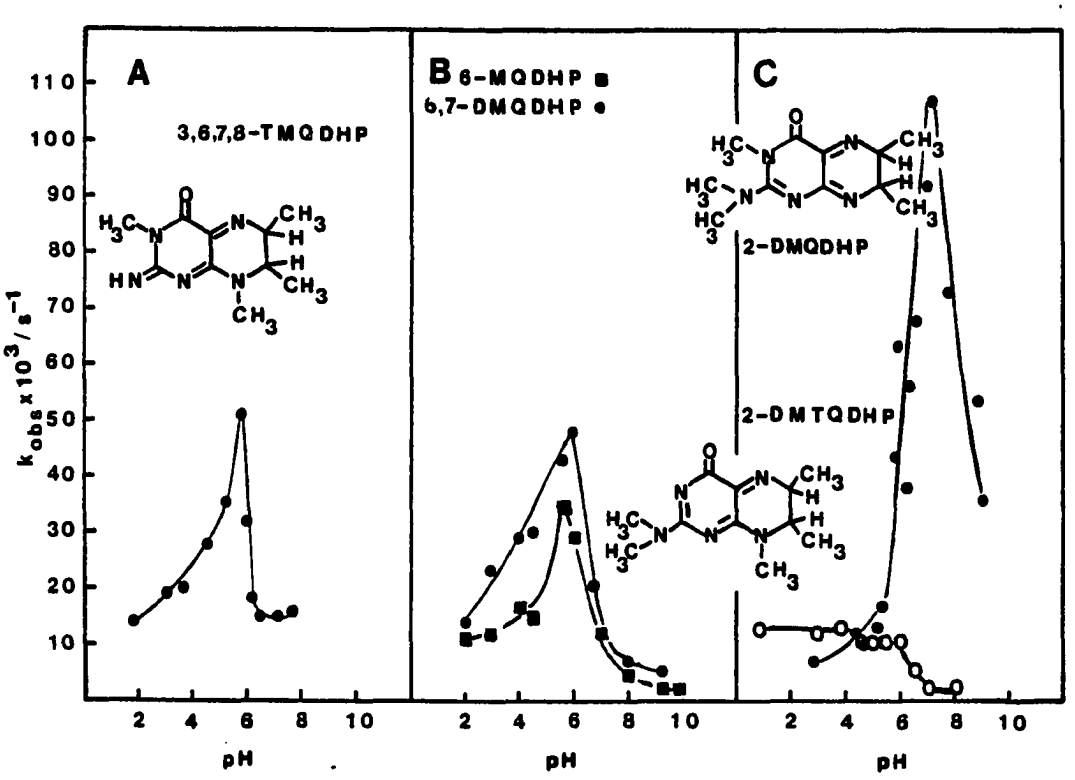

Figure 30. Variation of the observed first-order rate constant for the chemical reaction of peak I_a electrooxidation product of (A) 3,6,7,8-TMTHP, (B) 6,7-DMTHP and 6-MTHP, (C) 2-DMTHP and 2-DMTTHP.

3,6,7,8-TMQDHP and 6,7-DMQDHP are very similar up to about pH 6. Above pH 6 3,6,7,8-TMQDHP gives up to two rate constants as discussed earlier (p. 242). The rate constants obtained for 2-DMQDHP are somewhat higher than those observed for 6,7-DMQDHP. 2-DMTQDHP on the other hand does not show a bell-shaped k_{obs} vs. pH relationship (Fig. 26).

Based on kinetic measurements it may be concluded that the intermediate formed upon electrooxidation of 3,6,7,8-TMTHP and 6,7-DMTHP at peak I_a potentials have very similar structures. However, it is already known that the U.V. spectral properties of the intermediate formed from 3,6,7,8-TMTHP and 6,7-DMTHP are not the same. It would be expected, if the same or similar intermediates were formed, that the spectral properties would be similar. Therefore, based on the spectroelectrochemical behavior described previously, the parallel-para structure (27) for the quinonoid-dihydropterin may be ruled out. Considering the fact that 3,6,7,8-TMTHP has twice as many methyl groups as 6,7-DMTHP which may have a considerable effect on stability, the k_{obs} for 3,6,7,8-TMQDHP may not only be characteristic for a parallel-para quinonoid structure, but also characteristic for a quinonoid with methyl substituents at C(3), C(6), C(7) and N(8) (generally methyl substituents act as activating groups[16] and the stability of a compound with methyl substituents would be expected to be different than that without any substituents). It is believed that k_{obs} measured

for 3,6,7,8-TMTHP is not only representative of formation of a parallel para quinonoid intermediate but also indicative of a quinonoid intermediate with methyl substituents at C(3), C(6), C(7) and N(8).

Therefore, simply because the magnitudes for the rate constants observed for 3,6,7,8-TMQDHP and 6,7-DMQDHP are similar, it cannot be definitely concluded that the same intermediate species is formed. Since the observed rate constant vs. pH dependence for these compounds is similar one can only conclude that there is a possibility that similar intermediates are formed. It has been discussed earlier that 3,6,7,8-TMTHP and 6,7-DMTHP form intermediates which have different spectral properties. Therefore, the parallel-para quinonoid configuration may be ruled out as a possible structure for 6,7-DMQDHP. This leaves two other possibilities: formation of a perpendicular para or an ortho quinonoid dihydropterin intermediate. 2-DMTTHP must give a perpendicular-para quinonoid dihydropterin when electrooxidized at peak I_a potentials, and its spectral properties are very similar to those observed for 6,7-DMQDHP. However, the observed rate constant for rearrangement of the dihydro-quinonoid to the 7,8-dihydro derivative does not show a bell-shaped pH dependence. If 6,7-DMTHP were electrooxidized to a perpendicular para quinonoid it would be expected that both 2-DMTTHP and 6,7-DMTHP would show similar k_{obs} vs. pH relationships.

This leaves only the possibility of formation of an ortho quinonoid. 2-DMTHP which may form a locked ortho quinonoid dihydropterin has similar U.V. absorption characteristics to 6,7-DMTHP and its k_{obs} relationship gives a bell-shaped curve. Therefore, it may be concluded both on the basis of kinetic and spectral studies that the ortho quinonoid structure is preferred. When the electrochemical behavior of 6,7-DMTHP and 2-DMTHP are compared, it may be observed that these two compounds exhibit very similar electrochemical properties (see chapter two and chapter three).

Comparison of electrochemical oxidation of methylated pterins

Tetrahydropterin and all of its methylated derivatives studied give at least two well-defined voltammetric electrooxidation peaks at the PGE. Tetrahydropterin and all tetrahydropterins without methyl substituents at the C(6) and/or C(7) show very complex electrochemical behavior and exhibit up to five or more electrooxidation peaks. Generally, tetrahydropterins with methyl substituents at C(6) and C(7) give four electrooxidation peaks. The fourth voltammetric peak, appearing at relatively positive potentials (E_p>1.0V) is believed to be due to electrooxidation of the corresponding pterin. The first and major electrooxidation peak of all the tetrahydropterins (peak I_a) is pH-dependent and corresponds to an electron transfer process in which the same number of electrons and protons are involved, i.e.,

Table 8. Linear peak potential (E_p) *vs.* pH relationships for voltammetric oxidation peak I_a of tetrahydropterin and its methylated derivatives at the pyrolytic graphite electrode[a]

Compound[b]	pH range	E_p/ V *vs.* SCE	E_p at pH 7/ V *vs.* SCE
THP	3-5.4	0.38-0.070 pH	
	5.8-11	0.26-0.049 pH	-0.083
6-MTHP[c]	2-11	0.32-0.056 pH	-0.072
5-MTHP[d]	1.4-10.7	0.43-0.047 pH	0.101
6,7-DMTHP	2-11	0.309-0.053 pH	-0.062
3,8-DMTHP	2-7.6	0.23-0.058 pH	-0.126
3,6,7,8-TMTHP	2.0-6.0	0.29-0.059 pH	-0.123
2-DMTHP	1.5-9.2	0.30-0.048 pH	-0.036
2-DMTTHP	2.9-10.3	0.275-0.062 pH	-0.159

[a]Sweep rate 5 mV s^{-1}.

[b]Data obtained at a concentration of 1 m*M*.

[c]Data from ref. 5.

[d]Data from ref. 17.

$dE_p/d(pH)$ ≈-60 mV. Equations describing the variation in peak potential for peak I_a as a function of pH are presented in Table 8. The shift of peak I_a peak potential with pH for tetrahydropterin (THP) and its methylated derivatives averages 57±7 mV. This is in approximate accord with that expected for a reversible $2\underline{e}$-$2H^+$ electrode reaction. Since there is no obvious break in the E_p *vs.* pH plot for electrooxidation peak I_a for any of the tetrahydropterins studied (except THP) it may be concluded that both the monocation and neutral forms of the compounds are electrooxidized in quasi-reversible $2\underline{e}$-$2H^+$ reactions. The ease of oxidation with increasing number of methyl substitution in the pyrazine ring is clearly indicated in Table 8. Methyl substitution in the pyrimidine ring generally decreases the ease of oxidation (compare 2-DMTHP and 2-DMTTHP). It is interesting to note that methylation at N(5) increases the resistance of the tetrahydropterin towards electrooxidation. Viscontini *et al*. have shown that the sensitivity of tetrahydropterin to air oxidation is reduced significantly by methylation of the N(5) position.[18] The stability of 5-MTHP towards air oxidation was studied and compared with the air oxidation of THP. In pH 14 solution at 25°C, the tetrahydropterin anion decomposed within 15 min, whereas under the same condition 5-MTHP decomposed slowly over the course of 30 hours.[12] The same stabilizing effect of the N(5) methyl substituent was also observed for the neutral molecules.[12]

It is believed that the first electrooxidation step of tetrahydropterins involves the oxidation of the C(4a)-N(5)bond.[19] 5-MTHP has a methyl group at N(5) and oxidation of C(4a)-N(5) is not favored because the methyl substituent is not a good leaving group.[20] Therefore, it is believed that the first electrooxidation step of 5-MTHP involves oxidation of the C(6)-C(7) bond forming a 5,8-dihydropterin as shown in Eq. (2).

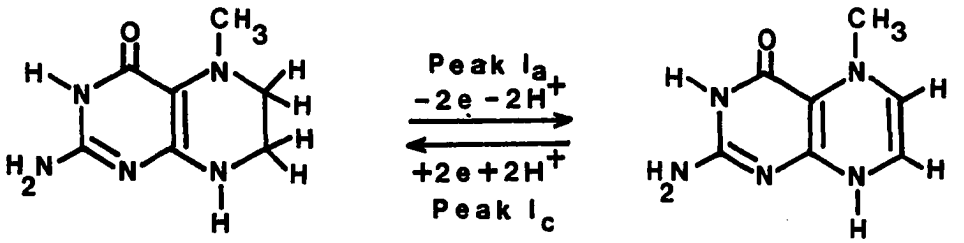

[2]

By comparing spectroelectrochemical data obtained during electrooxidation of 5-MTHP at peak I_a potentials, with spectra of 5,8-dihydro-species generated during electroreduction of pterins (at peak II_c potentials) it should be possible to verify formation of this species.

Controlled potential coulometric experiments at a large PGE or at an RVC electrode in a thin-layer cell reveal that electrooxidation at peak I_a potentials results in transfer of two electrons.

Cyclic voltammetric and spectroelectrochemical experiments indicate that an unstable intermediate species

Table 9. Variation of peak current ratio for peaks I_a and I_c of various methylated tetrahydropterins in phosphate buffer pH 7[a]

Compound[b]	(i_{p_c}/i_{p_a})[c]
THP	0.84
6,7-DMTHP	0.79
3,6,7,8-TMTHP	0.35
2-DMTTHP	0.63
3,8-DMTHP	0.30[d]
2-DMTHP	0.42

[a]Ionic strength of 0.5 M were used.

[b]Approximately 1 mM.

[c]Peak current data was obtained from cyclic voltammograms recorded at a sweep rate of 200 mV s^{-1}, the applied potential was clipped right past peak I_a.

[d]Value obtained at pH 7.6.

is formed in the peak I_a electrooxidation process. This species may then be reduced back to the corresponding tetrahydropterin in the peak I_c electroreduction process.

The peak height for peak I_c changes with respect to peak I_a as a function of pH and sweep rate. The ratio of peak heights for peak I_a and peak I_c for various methylated tetrahydropterins at pH 7 is shown in Table 9. Spectrophotometric and cyclic voltammetric evidence suggests that the final peak I_a product is a 7,8-dihydropterin.

All tetrahydropterins studied gave rise to an electrooxidation peak corresponding to peak II_a which only appeared at lower pH values and is well defined only at slow sweep rates (e.g., 5 mV s^{-1}) and low concentrations (<0.5 mM). The peak potential vs. pH relationships for this peak for various tetrahydropterins is summarized in Table 10. Cyclic voltammetric experiments reveal that the oxidation peak II_a process forms a quasi-reversible couple with reduction peak IV_c. It is believed that the peak II_a process is due to the electrooxidation of a covalently hydrated 7,8-dihydropterin. Upon electrooxidation such an hydrated dihydropterin may form up to five different unstable quinonoids. The structure of the hydrated 7,8-dihydropterin is very similar to that of a tetrahydropterin. Therefore, formation of similar quinonoid dihydropterins would be expected. There is cyclic voltammetric and kinetic evidence that at least four of the tetrahydropterins

Table 10. Linear peak potential (E_p) *vs.* pH relationships for voltammetric oxidation peak II_a of tetrahydropterin and its methylated derivatives at the pyrolytic graphite electrode[a]

Compound[b]	pH range	E_p/ V *vs.* SCE
THP	3-8	0.37-0.054 pH
6-MTHP[c]	2-5	0.42-0.055 pH
6,7-DMTHP	2-4.1	0.44-0.055 pH
3,8-DMTHP	2-5.6	0.32-0.046 pH
2-DMTHP	1.5-5	0.42-0.043 pH
2-DMTTHP	>2	not observed
3,6,7,8-TMTHP	>2	not observed

[a]Sweep rate 5 mV s^{-1}.

[b]Data obtained at a concentration of approximately 1 m*M*.

[c]Data obtained from ref. 5.

studied (6,7-DMTHP, 6-MTHP,[5] THP[6] and 2-DMTHP) form a hydrated 7,8-dihydro derivative which may form two unstable intermediates upon electrooxidation at peak II_a potentials. The final oxidation product of peak II_a is the corresponding pterin as a result of a $2\underline{e}$-$2H^+$ electrooxidation step.

The peak III_a process is believed to be due to electrooxidation of the appropriate 7,8-dihydropterin derivative to form pterin. This electrooxidation process again corresponds to transfer of $2\underline{e}$ and $2H^+$. In fact, the species responsible for peaks II_a and III_a are in an equilibrium. Cyclic voltammetric and controlled potential coulometric experiments give supporting evidence for this equilibrium. The peak potential *vs.* pH relationships for peak III_a for various tetrahydropterins is presented in Table 11.

With the exception of 6,7-DMTHP and 2-DMTHP, the curves representing the peak III_a peak potential dependence on pH have no breaks. This indicates that the electrooxidation of the dihydro species proceeds via the same route through different ionic forms. 6,7-DMTHP, however, shows two breaks at pH values corresponding to reported pK_a values (4.2 and 10.6[21,22]). 2-DMTHP shows one break at pH 5 possibly corresponding to the first pK_a of 2-DMDHP.

As discussed previously, THP and tetrahydropterins with no methyl substituents at the C(6) or C(6) and C(7) positions show very complex voltammetric behavior. Two cyclic voltammograms corresponding to the oxidation of THP

Table 11. Linear peak potential (E_p) *vs.* pH relationships for the voltammetric oxidation peak III_a of tetrahydropterin and its methylated derivatives at the pyrolytic graphite electrode[a]

Compound[b]	pH range	E_p/ V vs. SCE	E_p at pH 7/ V *vs.* SCE
THP	3-11	0.88-0.070 pH	0.39
6-MTHP[c]	3-11	0.73-0.051 pH	0.37
6,7-DMTHP	2-4.1	0.85-0.078 pH	0.30
	4.1-10.6	0.63-0.021 pH	0.48
3,6,7,8-TMTHP	2-4	0.900.110 pH	0.13
2-DMTHP	1.5-5	0.89-0.067 pH	
	5-9.2	0.66-0.018 pH	0.53
2-DMTTHP	2.9-10.3	0.695-0.040 pH	0.42

[a]Sweep rate 5 mV s^{-1}.

[b]Data obtained at a concentration of approximately 1 m*M*.

[c]Data obtained from ref. 5.

and 6,7-DMTHP are shown in Fig. 31 for comparative purposes.

The electrochemistry of THP has been studied carefully and the overall electrooxidation scheme elucidated.[6] According to this scheme the additional electrooxidation peaks (i.e., peaks II_a and IV'_a in Fig. 32) are due to oxidation of 7,8-dihydroxanthopterin (peak VI_a in Fig. 31) which is formed by electrooxidation of covalently hydrated 7,8-dihydropterin and xanthopterin (peak VII_a in Fig. 31). Comparing the voltammetric oxidation peaks observed for 3,8-DMTHP with those observed for THP suggest that similar kinds of electrooxidation processes may be taking place. The electrochemical reactions of 3,8-DMTHP have not been studied in great detail. However, preliminary voltammetric studies indicate that electrochemical oxidation of 3,8-DMTHP is complex and parallels may possibly be drawn between the electrochemical oxidation of 3,8-DMTHP and THP. A single sweep voltammogram of 3,8-DMTHP is shown in Fig. 33. The dependence of peak potentials on pH observed when 3,8-DMTHP is oxidized at PGE may be represented by the following equations:

Peak I_a $E_p = (0.28-0.058\ pH)V$
(pH 2-7.6)

Peak II_a $E_p = (0.32-0.046\ pH)V$
(pH 2-5.6)

Peak III_a $E_p = (0.48-0.044\ pH)V$
(pH 2-7.6)

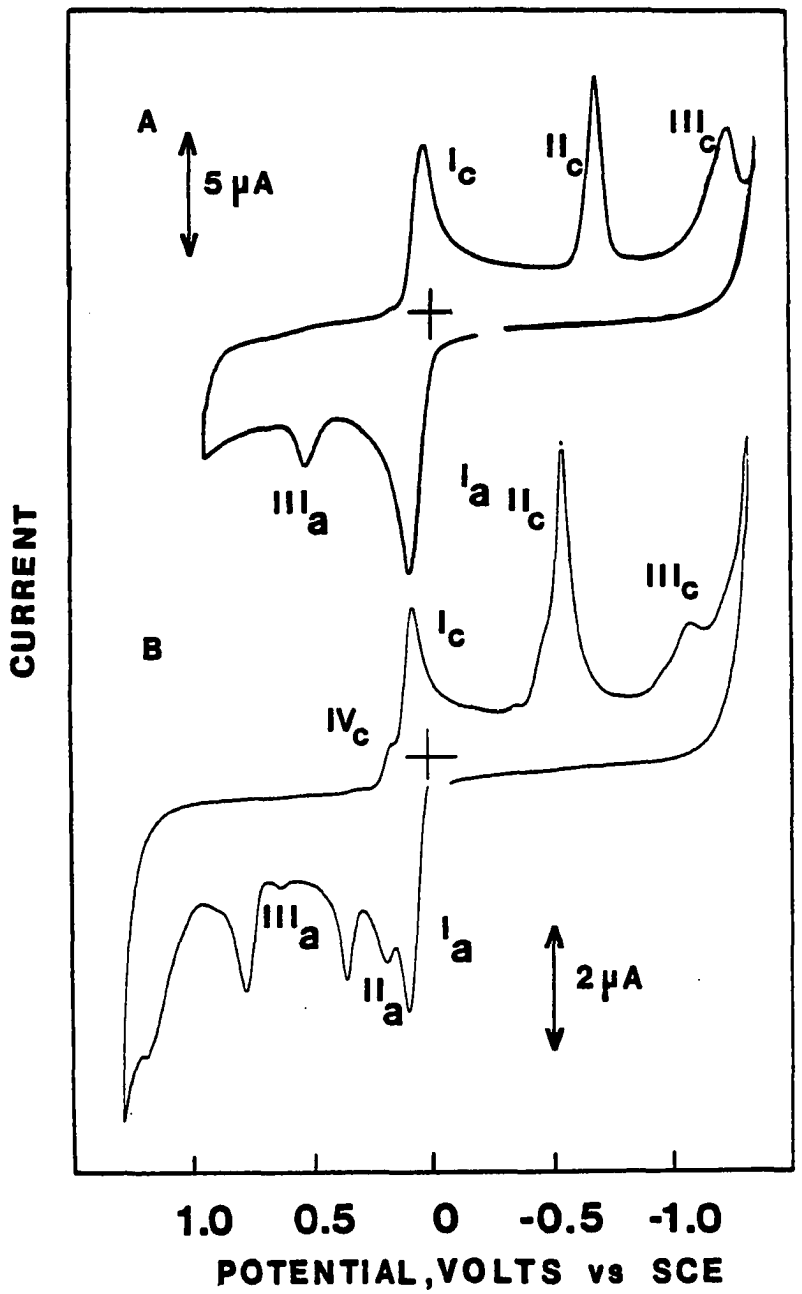

Figure 31. Cyclic voltammograms of (A) 0.5 mM 6,7-DMTHP at pH 4 at a scan rate of 200 mV s^{-1} and (B) 0.4 mM THP at pH 4.2 at a scan rate of 50 mV s^{-1}.

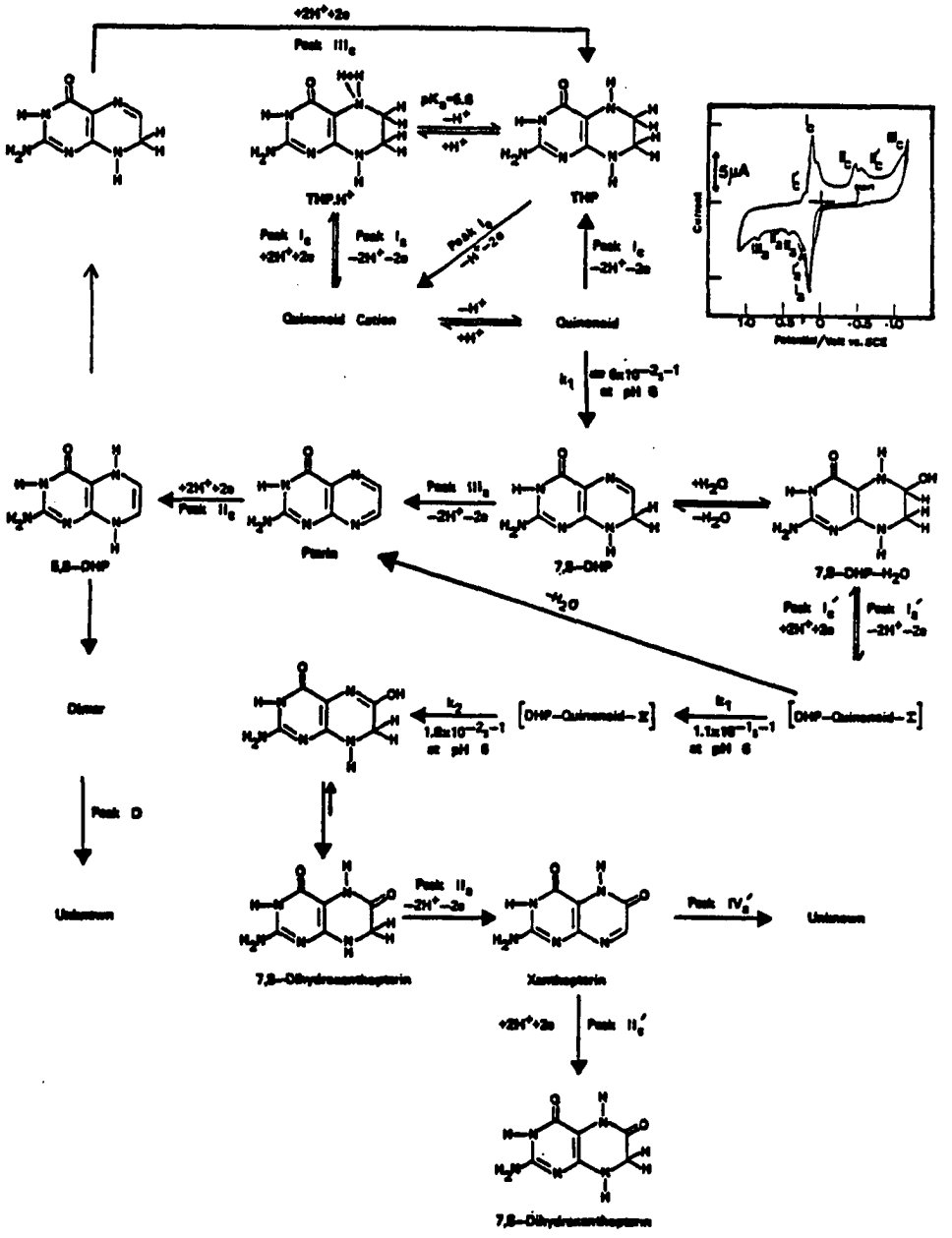

Figure 32. Proposed reaction scheme for the electrooxidation of THP at PGE.

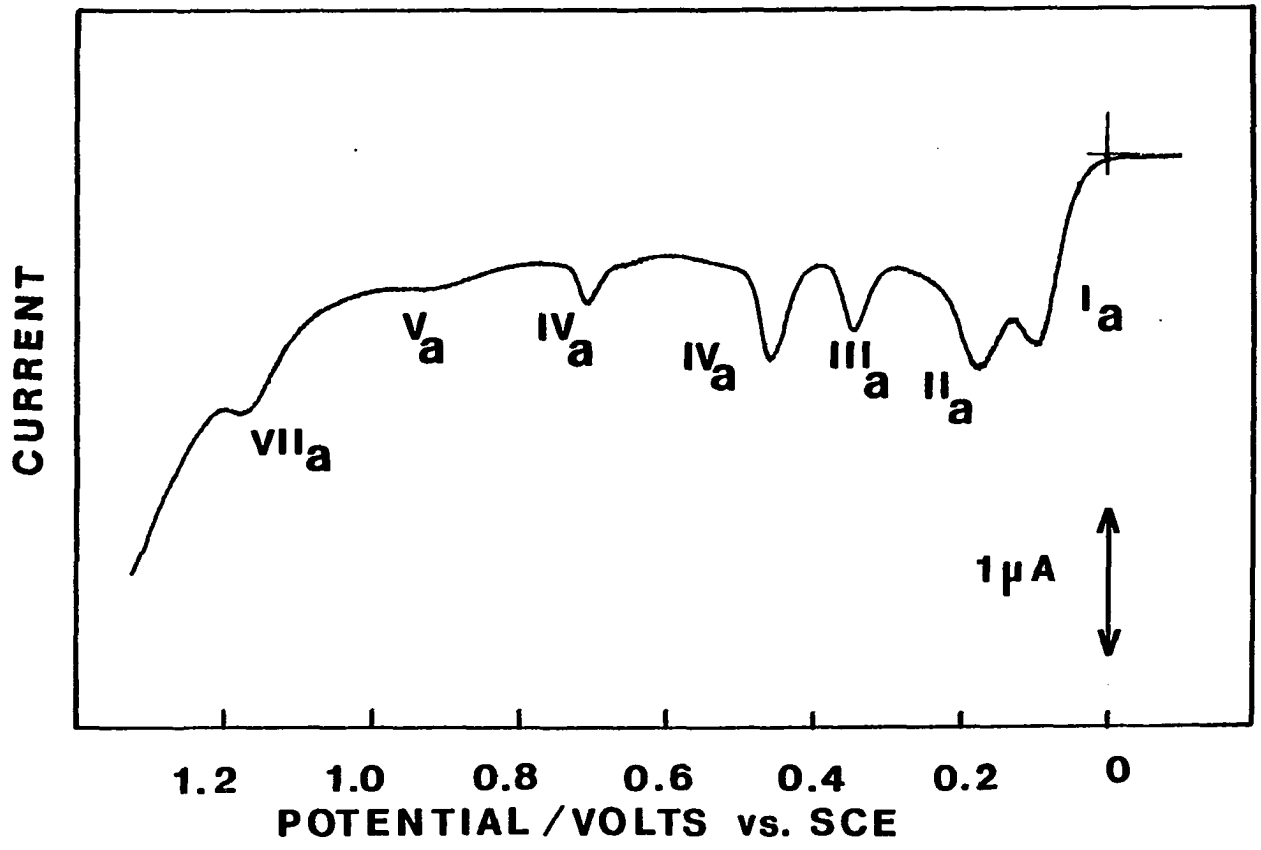

Figure 33. Single sweep voltammogram of 0.5 m<u>M</u> 3,8-DMTHP at pH 3.55 at a sweep rate of 5 mV s^{-1}.

Peak IV_a E_p = (0.61-0.046 pH)V
(pH 2-7.6)

In addition to the voltammetric peaks represented by the above equations, there are at least two more electro-oxidation peaks observed. The peaks referred to as III_a and IV_a in the above equations are not due to the same peak III_a or peak IV_a processes discussed before for compounds such as 6,7-DMTHP or 2-DMTHP.

All of the tetrahydropterins exhibit peaks II_c and III_c corresponding to electroreduction of the corresponding pterin first to a 5,8-dihydropterin and after rearrangement to a 7,8-dihydropterin further reduction to the corresponding tetrahydropterin. Tetrahydropterins with a methyl substituent at the N(8)-position exhibit two well defined, closely spaced electroreduction peaks for peak II_c. At fast sweep rates two well defined electro-oxidation peaks coupled to these peaks may also be observed. It is believed that electroreduction of N(8) methylated pterins can take place in two steps forming first a free radical. Detailed studies of the electroreduction of pterins have been reported by Kwee and Lund.[3] Therefore, no additional detailed studies of the electroreduction of pterins have been carried out. Generally, however, pterins are initially reduced to a 5,8-dihydropterin which is not very stable and which rearranges to form a 7,8-dihydropterin.

The stabilities of 5,8-dihydropterins are dependent upon pH, their stability increasing with increasing pH. Methyl substituted 5,8-dihydropterins seem to be more stable than their unsubstituted analogs. For example, 2-DMP forms a much more stable 5,8-dihydropterin derivative than does 6,7-DMP. The former species can be monitored spectrally (see chapter 3, thin-layer spectroelectrochemistry of 2-DMP).

All of the tetrahydropterins studied gave rise to an electroreduction peak III_c which corresponds to reduction of the 7,8-dihydropterin to the corresponding tetrahydropterin.

CONCLUSION

Based on the spectroelectrochemical, kinetic and electrochemical studies of the most commonly used pseudo cofactors (6,7-DMTHP and 6-MTHP) for phenylalanine hydroxylase and of a variety of methylated tetrahydropterins which are believed to form "locked" quinonoid-dihydropterin structures, it has been concluded that the common pseudo cofactors probably form an ortho quinonoid-dihydro intermediate. If this is in fact the case, the first step in the electrooxidation of the pseudo cofactors may be represented as follows:

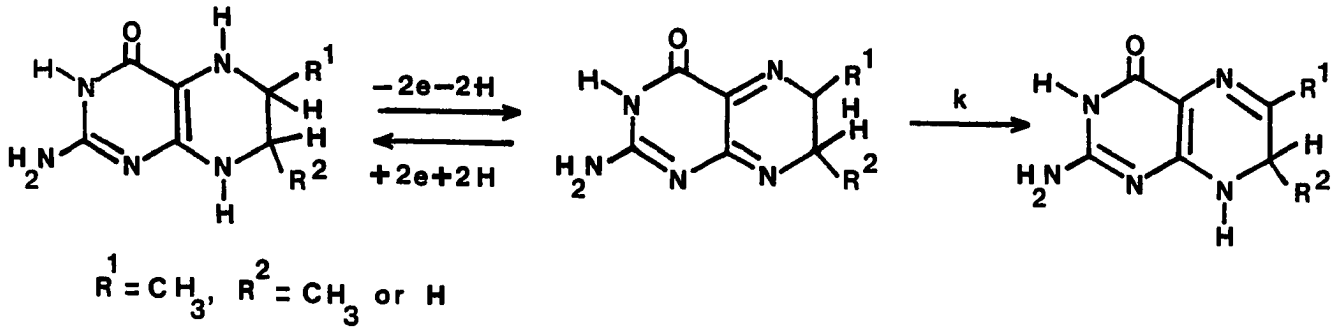

$R^1 = CH_3$, $R^2 = CH_3$ or H

2-DMTHP, which forms a "locked" ortho quinonoid intermediate has very similar electrochemical and spectroelectrochemical behavior to 6,7-DMTHP. Detailed electrochemical and spectroelectrochemical studies of 2-DMTHP are reported in Chapter three. 2-DMTHP is electrooxidized in a $2\underline{e}\text{-}2H^+$ peak I_a process to an intermediate ortho quinonoid. The linear peak potential vs. pH relationship for this process may be represented by the equation

$$E_p = (0.30\text{-}0.048\ pH)V$$

between pH 1.5-9.2. The same process for 6,7-DMTHP is represented by the equation

$$E_p = (0.31\text{-}0.053\ pH)V$$

between pH 2-11.0. The intermediates generated from both of these tetrahydropterins are not very stable and rearrange to form 7,8-dihydro derivatives. Kinetic studies based on

spectroelectrochemical methods reveal that the chemical rearrangement reactions of the putative quinonoids is first order and dependent on pH. 2-DMTHP and 6,7-DMTHP both show a bell-shaped k_{obs} *vs.* pH relationship. However, the magnitudes of the observed rate constants are somewhat different. The maximum k_{obs} for 6,7-DMTHP is observed at pH 6 having a value of 4.8×10^{-2} s^{-1}. 2-DMTHP shows a maximum k_{obs} at pH 7.2 having a value of 11×10^{-2} s^{-1}. The spectral properties of the intermediates generated are very similar at pH 3 (Fig. 29B,C). At higher pH values, for example at pH 8.8, the observed spectra for the intermediates also show considerable similarities. 6,7-DMTHP absorbs at λ_{max} = 244 nm and 304 nm) at pH 8.8. The absorption bands observed with 2-DMTHP are shifted to longer wavelengths because of the bathochromic effect caused by the methyl substituents. The intermediates generated from both compounds absorb between 360-400 nm. The quinonoid-dihydropterin intermediate generated from 6,7-DMTHP also absorbs at λ_{max} = 308 nm (pH 9.3) and the quinonoid electrogenerated from 2-DMTHP absorbs at λ_{max} = 314 nm (pH 8.8).

It has been reported on the basis of electrochemical studies carried out using several methylated pterins that formation of an ortho quinonoid is favored.[3] Theoretical molecular orbital calculations do not support a perpendicular para configuration. Viscontini *et al.*[23] have studied the chemical oxidation of several methylated tetrahydropterins

and (based on kinetic and spectral data) have concluded that a parallel para quinonoid intermediate is formed during the oxidation of tetrahydropterin. The kinetic and spectral data they obtained did not support formation of a perpendicular para configuration. Our studies show that there is no spectral evidence for the formation of a parallel para quinonoid. It has been pointed out that the electrochemical behavior of the tetrahydropterins studied here and the analogous 5,6-dihydropyrazine/1,4,5,6-tetrahydropyrazine system are similar.[3] In the 5,6-dihydropyrazine/1,4,5,6-tetrahydropyrazine system the oxidized form possesses an ortho quinonoid structure[24] which would support the formation of an ortho quinonoid-dihydropterin in the oxidation reactions of tetrahydropterins. No conclusive statement can be made concerning the structure of the intermediate formed when tetrahydrobiopterin is oxidized. However, it would be expected that tetrahydrobiopterin would be electrooxidized in a $2\underline{e}\text{-}2H^+$ step to form an ortho quinonoid-dihydropterin.

EXPERIMENTAL

Chemicals

3,6,7,8-Tetramethylpterin (3,6,7,8-TMP) was synthesized according to the procedures described by Pfleiderer *et al.*[8] Reported m.p. 228°C; observed m.p. 220°C. Calculated analysis for 3,6,7,8-TMP: C 38.68%, H 5.48%, N 22.57%,

Table 12. Comparison of absorbance data for 3,6,7,8-TMP with literature values[a]

pH	λ_{max} obs	λ_{max} rep	A_{obs}	log ε_{calc}[b]	log ε_{rep}
5[c]	400	400	0.430	4.09	4.10
	284	284	0.323	3.96	4.01
	261	261	0.529	4.19	4.24
11[d]	365	365	0.222	3.71	3.68
	311	311	0.836	4.29	4.30
	245	245	0.805	4.27	4.29

[a]Values reported in reference 8.

[b]Molar absorptivity was calculated using the formula $E = \frac{A}{Cb}$.

[c]Solutions at a concentration of 3.5×10^{-5} M were used.

[d]Solutions at a concentration of 4.29×10^{-5} M were used.

found: C 39.92%, H 5.37%, N 22.90% with a molecular formula of $C_{12}H_{13}N_5O$, $2\cdot HCl\cdot H_2O$. An I.R. spectrum and a direct insertion mass spectrum of 3,6,7,8-TMP are presented in Figs. 34 and 35, respectively. Table 12 summarizes the reported and the observed spectral properties of 3,6,7,8-TMP.

3,6,7,8-Tetramethyltetrahydropterin (3,6,7,8-TMTHP) was prepared by hydrogenating 3,6,7,8-TMP over PtO_2 (Aldrich) using a conventional hydrogenation apparatus at atmospheric pressure. The procedure for hydrogenation is described in the Experimental section of Chapter three. Calculated analysis: C% 38.22, H% 6.68, N% 22.28; found: C% 38.08, H% 5.74, N% 21.67 with a molecular formula of $C_{10}H_{17}N\ O\cdot 2HCl\cdot H_2O$.

2-Dimethylamino-6,7,8-trimethylpterin (2-DMTP) was prepared in four steps as shown below:

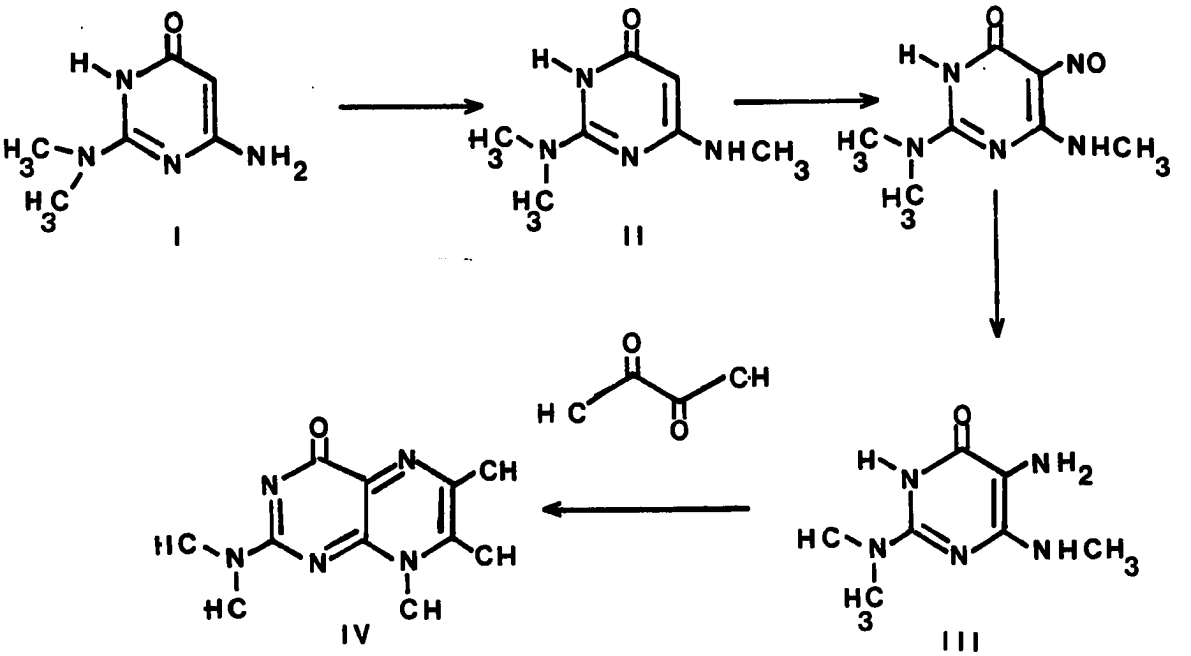

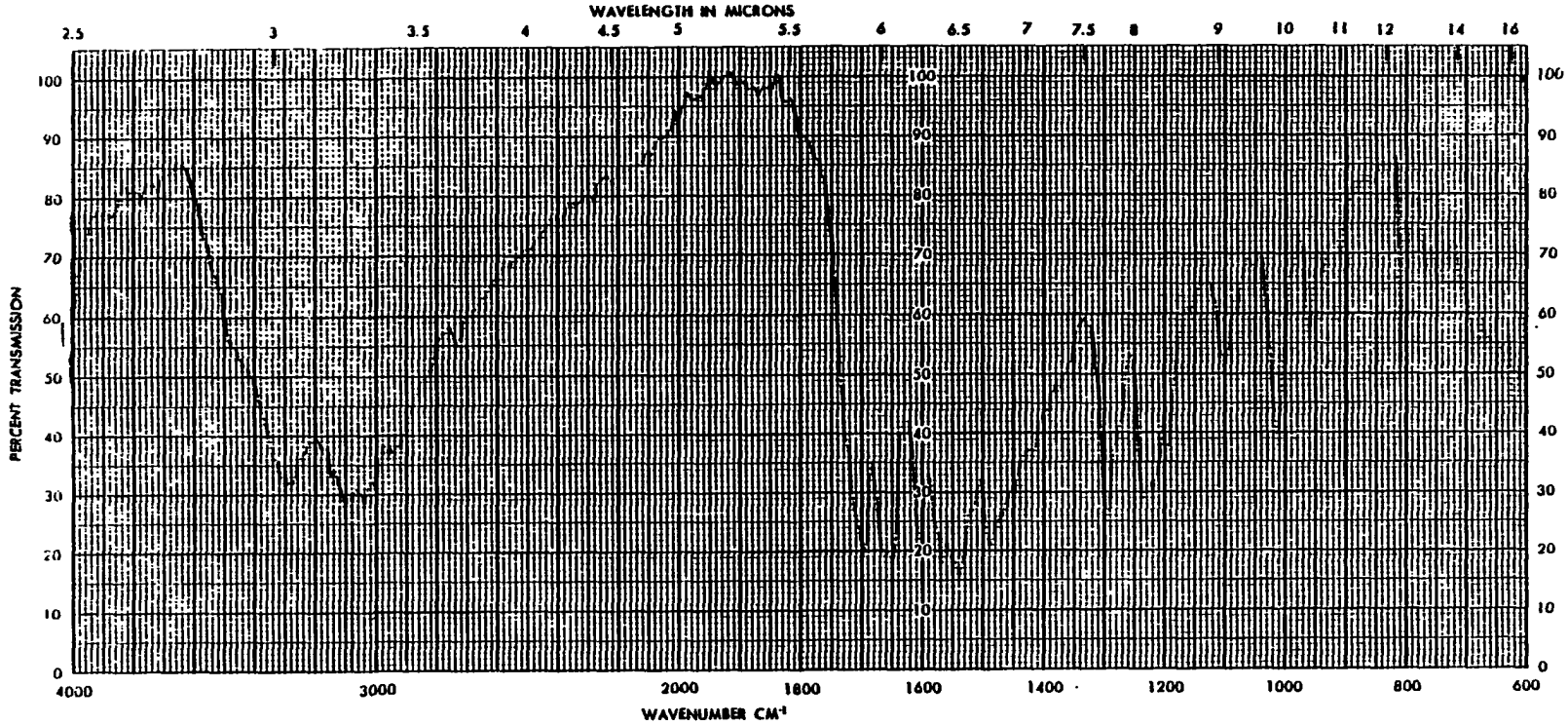

Figure 34. I.R. spectrum of 3,6,7,8-TMP.

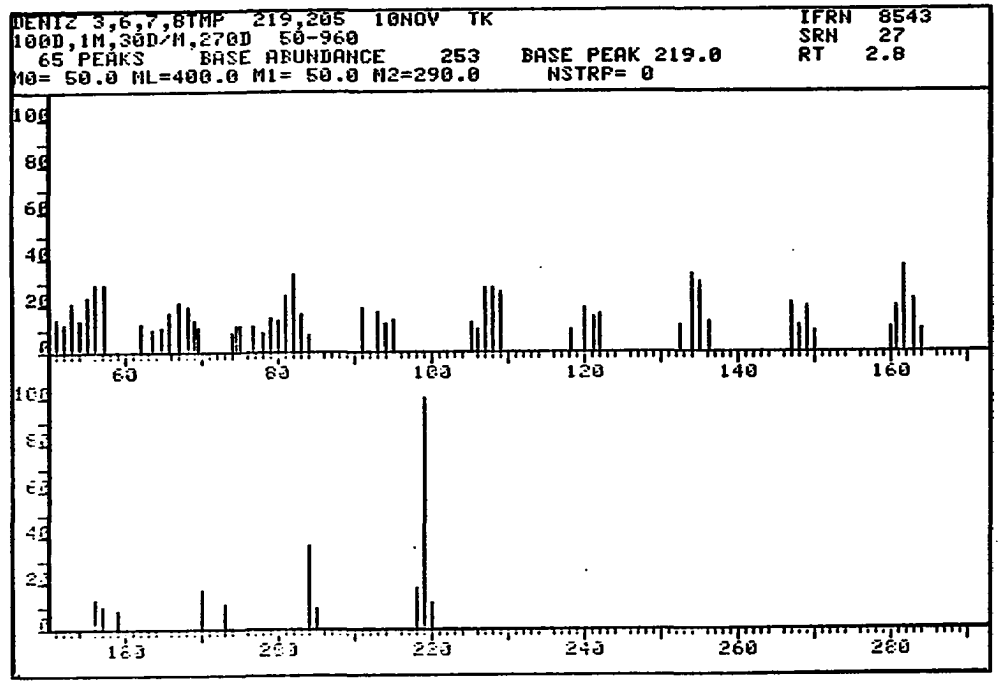

MASS	%	MASS	%
BIG 60		109.1	25.7
50.0	13.4	118.3	10.3
51.1	15.8	120.2	18.6
52.0	12.6	121.3	15.0
53.1	21.3	121.4	15.4
54.0	14.2	122.1	16.6
55.2	23.3	132.7	11.5
56.2	29.2	134.1	33.2
57.3	28.9	135.1	30.0
62.1	12.3	136.3	13.0
63.6	9.9	147.2	20.9
64.8	10.7	148.0	11.9
65.9	17.0	149.2	19.8
67.1	20.9	160.2	11.1
68.3	19.8	160.9	19.4
69.1	14.2	161.9	37.2
69.5	10.7	163.1	22.9
69.7	10.3	164.0	10.3
74.7	11.5	176.0	13.0
75.1	11.5	177.1	10.3
76.9	11.9	189.1	17.0
79.0	14.6	193.0	11.1
80.1	14.2	204.1	36.8
81.0	24.1	205.1	9.5
82.2	32.8	218.0	18.2
83.0	16.6	219.0	100.0
91.1	19.0	220.0	11.9
93.1	17.0		
94.2	12.3		
95.1	13.8	LAST 4	
105.4	13.4	215.1	9.5
106.2	9.9	218.0	18.2
107.1	27.3	219.0	100.0
108.1	27.7	220.0	11.9

Figure 35. Direct insertion mass spectrum of 3,6,7,8-TMP.

Compounds I-III were synthesized according to the procedures described in references 24, 25, and 26, respectively. The synthesis for IV was not reported in the literature. For the preparation of IV similar procedures were followed which were reported for the synthesis of 6,7,8-trimethylpterin.[8] The observed m.p. of the product was 228-230°C. U.V. spectrum in pH 7 phosphate buffer: λ_{max} = 279 nm, 429 nm, log ε 4.24 and 4.05, respectively; NMR in trifluoroacetic acid: C-2-NMe_2 3.58, 3.52 (singlet), N(8)-Me 4.40 (singlet), C-6-Me 2.84 (singlet), C-7-Me 3.03, (all δ values vs. TMS). 2-Dimethylamino-6,7,8-trimethyltetrahydropterin (2-DMTTHP) was synthesized by the catalytic hydrogenation procedure described in Chapter three. 2-Dimethylamino-6,7,8-trimethyl-dihydropterin (2-DMTDHP) was obtained electrochemically by either oxidizing 2-DMTTHP at peak I_a potentials at a PGE or reducing 2-DMTP at peak II_c potentials at a large PGE. All other chemicals used were the same as reported in previous chapters.

Apparatus

The apparatus used for voltammetry, spectroelectrochemistry and coulometry have been described in previous chapters.

SUMMARY

3,6,7,8-TMTHP and 2-DMTTHP give three voltammetric electrooxidation peaks (peaks I_a, II_a and III_a) at the pyrolytic graphite electrode. Peak I_a is a $2\underline{e}$-$2H^+$ quasi-reversible reaction due to the oxidation of the reduced tetrahydropterin involved. It is believed that $2\underline{e}$-$2H^+$ peak I_a electrooxidation of 3,6,7,8-TMTHP results in formation of a parallel-para dihydro-quinonoid intermediate while 2-DMTTHP gives a perpendicular-para quinonoid-dihydro pterin. These then chemically rearrange to form the corresponding 7,8-dihydropterin. The quinonoid-dihydroprerin derived from 3,6,7,8-TMTHP shows a bell-shaped first-order observed rate constant (k_{obs}) *vs.* pH relationship which is very similar to that observed with the quinonoid derived from 6,7-DMTHP up to pH 6. The quinonoid derived from 2-DMTTHP shows a sigmoidal k_{obs} *vs.* pH dependence. Peak II_a is due to a quasi-reversible electrooxidation of covalently hydrated 3,6,7,8-TMDHP and 2-DMTDHP to form at least one unstable quinonoid which in turn chemically reacts to form the corresponding pterin. Peak II_a may be observed only at low pH. Peak III_a is due to the irreversible electrooxidation of nonhydrated 3,6,7,8-TMDHP and 2-DMTDHP to the corresponding pterin. 3,6,7,8-TMP gives rise to several oxidation peaks which are believed to be due to electrooxidation of some of its decomposition products. 3,6,7,8-TMP and 2-DMTP

may be reduced in two $1e^{-}$-$1H^{+}$ reversible electroreduction steps to give the corresponding 5,8-dihydropterins. The 5,8-dihydropterins formed are not very stable and rearrange to the corresponding 7,8-dihydropterin in a pH dependent chemical reaction. Peak III_c is due to electroreduction of the corresponding 7,8-dihydropterin to form the corresponding 5,6,7,8-tetrahydropterin.

The spectral properties of methylated tetrahydropterins are very similar. The only difference observed in their spectra is due to the methyl substituents which cause a bathochromic shift. The electrochemistry of C(6) and C(7) substituted tetrahydropterins is very similar. Tetrahydropterins without any substituents at the C(6) and C(7) positions show very complex voltammetric behavior.

Based on the spectroelectrochemical and electrochemical information gathered, it has been concluded that the quinonoid structure favored in the oxidation of the pseudo-cofactor tetrahydropterins is the ortho structure.

REFERENCES

1. S. Kaufman, J. Biol. Chem., 239 (1964) 332.

2. M. C. Archer and K. G. Scrimgeour, Can. J. Biochem., 48 (1970) 278.

3. S. Kwee and H. Lund, Biochim. Biophys. Acta, 297 (1973) 285.

4. D. Ege-Serpkenci and G. Dryhurst, Bioelectrochem. Bio- 9 (1982) 175.

5. L. G. Karber and G. Dryhurst, J. Electroanal. Chem., 136 (1982) 271.

6. R. Raghavan and G. Dryhurst, J. Electroanal. Chem., 129 (1981) 189.

7. J. Pradác, J. Pradácová, D. Homolka, J. Koryta, J. Slavik, J. Weber and R. Cihar, J. Electroanal. Chem., 74 (1976) 205.

8. W. Pfleiderer, J. W. Bunting, D. D. Perrin and G. Nübel, Chem. Ber., 101 (1968) 1072.

9. H. Braun and W. Pfleiderer, Liebigs Ann Chem., 1973, 1099.

10. R. N. Adams in, Electrochemistry at Solid Electrodes, Marcel Dekker, N.Y., 1969.

11. W. Pfleiderer and H. Zondler, Chem. Ber., 99 (1966) 3008.

12. S. Matsuura and T. Sugimoto in, Chemistry and Biology of Pteridines, K. Iwai, M. Goto, M. Akino and Y. Twanami (eds.), Int. Acad. Print. Co., Tokyo, 1970, p. 35.

13. W. Pfleiderer and R. Mengel, Chem. Ber., 104 (1971) 2293.

14. R. L. Blakley in, The Biochemistry of Folic Acid and Related Pteridines, A. Newberger and E. L. Tatum (eds.), North-Holland, Amsterdam, 1979, p. 66.

15. K. T. Finley and L. K. J. Tong in, The Chemistry of the Carbon-Nitrogen Double Bond, S. Patai (ed.), Interscience, London, 1970, p. 664.

16. Organic Chemistry, J. B. Hendrickson, D. J. Cram and G. S. Hammond, (3rd edn.), McGraw-Hill, N.Y., p. 654.

17. L. G. Karber and G. Dryhurst, unpublished results.

18. M. Viscontini, H. Leidner, G. Mattern and T. Okada, Helv. Chim. Acta, 49 (1966) 1911.

19. M. C. Archer, D. J. Vonderschmitt and K. G. Scrimgeour, Can. J. Biochem., 50 (1972) 1174.

20. Organic Chemistry, J. B. Hendrickson, D. J. Cram and G. S. Hammond, (3rd edn.), McGraw-Hill, N.Y., p. 397.

21. W. Schwotzer, J. H. Bieri, M. Viscontini and W. von Philipsborn, Helv. Chim. Acta, 61 (1978) 2108.

22. R. G. Kallen and W. P. Jencks, J. Biol. Chem., 241 (1966) 5845.

23. J. Pinson and J. Armand, Bull. Soc. Chim. France (1971) 1764.

24. B. Roth, J. M. Smith and M. E. Halquist, J. Am. Chem. Soc., 73 (1951) 2869.

25. H. V. Curran and R. B. Angier, J. Org. Chem., 28 (1963) 2672.

26. W. Pfleiderer and K. Deckert, Chem. Ber., 95 (1962) 1602.